UNIVERSITY OF BIRMINGHAM

PARTICULATE MATTER (PM) CHARACTERISTICS FROM COMPRESSION IGNITION DIESEL ENGINES OPERATED BY RENEWABLE FUELS

By
Name

MOHAMMED ALI FAYAD

A thesis submitted to
The University of Birmingham
For the degree of

DOCTOR OF PHILOSOPHY

The University of Birmingham
School of Engineering
July 2017

Abstract

Diesel engine emission of particulate matter (PM) is probably one of the most critical issues which have a large impact on the environmental and human health. The concern increases with the increasing number of vehicles on the roads and leads to greater attention being paid to the control and understanding of PM characteristics.

The use of renewable fuels (biodiesel and butanol blend) and aftertreatment systems in diesel engines are the main requirements for reducing and controlling the pollutant emissions. Decoupling the dependences between emission reduction technologies and engine fuel economy in order to improve them both simultaneously has been proven as a major challenge for the vehicle research communities. To understand the effect of alternative fuels on PM characteristics and a diesel oxidation catalyst (DOC), rapeseed oil methyl ester (RME) biodiesel and an alcohol blend (butanol-diesel blend) were used for various engine operating conditions (engine load, speed, injection strategies). The platinum:palladium (Pt:Pd)-based DOC was used during this study to understand the effect of promotion/inhibition of tailpipe emissions (gas and solid) on its activity at lower exhaust gas temperatures and to meet the strict emissions' legislation.

Particulate matter emission reduction cannot be achieved without improved understanding of the PM's characteristics (size distribution, morphology, and microstructure) in the diesel engine. This thesis presents a method to calculate the soot particle morphology (number of primary particles (n_{po}), the radius of gyration (R_g), and the fractal dimension (D_f)) and microstructure parameters (interlayer spacing (d_{002}), and the thickness (L_c) and width (L_a) of the graphene layer) from the combustion of renewable fuels compared with diesel fuel. High-resolution transmission electron microscopy (HR-TEM) and subsequent image processing was used to analyse the soot samples, as well as to obtain the key parameters such as the morphology and structure of the soot particles.

The first work of this research was focused on the influence of a DOC on the engine-out particulate matter (PM) characteristics (morphology and structure) from the combustion of alternative fuels (including butanol blends and RME) in single fuel injection diesel engine. The results revealed that the combustion of alternative fuels produces lower emissions of unburnt hydrocarbons (UHC), carbon monoxide (CO), and PM number concentration, which enhanced the catalyst activity at lower temperatures.

In the second part, the experimental work was carried out on a common rail diesel engine equipped with a DOC. By studying the effect of oxygenated fuel and fuel injection strategies on the combustion characteristics and PM characteristics, and hence the catalyst's performance, can unveil synergies that can benefit vehicle emissions and fuel economy, as well as guide the design of the next generation of sustainable fuels. It was found that post-injection incorporation with a butanol blend produced lower PM concentration and modified the soot's morphological parameters by reducing n_{po}, R_g and D_f.

Finally, the research continued with work on a modern single cylinder experimental diesel engine to demonstrate how insignificant changes in the commonly used aftertreatment system architecture and the small addition of oxygenated fuels in the diesel fuel (butanol in this case) can provide meaningful low temperature catalyst activity improvements. Lower temperature catalyst light-off and higher conversion efficiencies with the combustion of the diesel-butanol blend were achieved.

ACKNOWLEDGEMENTS

Words are not enough to express my appreciation and thanks to all the people who support, encouragement, and helped me throughout this PhD study.

The primary person whom I would like to acknowledge is my thesis supervisor, Professor Athanasios Tsolakis for his full support, guidance, and patience, invaluable advice during these years at the University. I would also like to thank to my co-supervisor, Dr. Karl Dearn for his support, advice and welcome during course of this research. Thanks are also to Dr. Jose Martin Herreros for his constructive comments, technical and moral support.

Special thanks go to the Iraqi Government and Ministry of Higher education and scientific research (MOHER) in Baghdad/Iraq for the provision of the PhD scholarship and maintenance grant for the duration of my study. In addition, I express my appreciation to the Iraqi Cultural Attaché in London and University of Technology in Baghdad for their support throughout my study.

I would like to thank all my colleagues and friends (I cannot account their), who, with their presence and kind attention, made this whole PhD experience so fruitful in learning. I also want to thank Dr. Francisco J. Martos (University of Málaga), Dr. Magin Lapuerta, and Mr. David Fernández-Rodríguez (University of University of Castilla-La Mancha) for their help during my work.

Finally, I would like to thank my parents for their prayers to me, and moral support despite the distance, and for always cheering me up throughout my study. Last but not least, this thesis could not have been able to complete my thesis without the love, support, and patience of all my family member.

MOHAMMED FAYAD

JULY 2017

DEDICATION

This document is dedicated to my family, for always believing in me and supporting me every step of the way.

My parents

My Sisters and brothers

My wife

My son

My daughters

TABLE OF CONTENTS

LIST OF FIGURES

LIST OF TABLES

LIST OF NOTATIONS

Symbol	Units	
A_c	[m^2]	Area of piston head
C_p	[J/(kg·K)]	Specific heat capacity at constant pressure
C_v	[J/(kg·K)]	Specific heat capacity at constant volume
d	[nm]	Particulate diameter
L	[m]	Stroke length
m_f	[kg]	Mass of fuel burned
$\dot{m}_f$	[kg/s]	Mass flow rate of fuel
n	[-]	Number of cylinder
N	[rps]	Engine speed
P	[Pa]	In-cylinder pressure
P_i	[kW]	Engine indicated power
R	[kJ/(kmol·K)]	Universal gas constant
t	[s]	Time
t	[m]	Wall thickness
T	[K]	Temperature
V	[m^3]	Displaced cylinder volume
γ	[-]	Ratio of specific heat
θ	[deg]	Crank angle

LIST OF ABBREVIATIONS

Symbol	Definition
A/F	Air to fuel ratio
aTDC	After top dead centre
B20	Butanol 20%, and diesel 80%
B16R15	Butanol 16%, RME 15%, and diesel 69%
BN	Base number
bTDC	Before top dead centre
BTE	Brake thermal efficiency
BSFC	Break specific fuel consumption
CAD	Crank angle degree
CI	Compression ignition
CN	Cetane number
CO	Carbon monoxide
CO_2	Carbon dioxide
CPC	Condensation particle counter
Cpsi	Cell per in^2
EPA	Environmental protection agency
DES	Department of education and science
DI	Direct injection

DMA	Differential mobility analyser
d_{002}	Interlayer spacing
d_{po}	Size of primary particles
DOC	Diesel oxidation catalyst
D_f	Fractal dimension
DPF	Diesel particulate filters
EGR	Exhaust gas recirculation
EGT	Exhaust gas temperature
EOC	End of combustion
EOI	End of injection
GHSV	Gas hourly space velocity
FAME	Fatty acid methyl ester
GTL	Gas-to-liquid
HFID	Heated flame ionisation detector
HC	Hydrocarbons
HR-TEM	High resolution transmission electron microscopy
HSV	High space velocity
IC	Internal combustion
IMEP	Indicated mean effective pressure
L_a	Graphene layer width
L_c	Graphene layer thickness

LPM	Liquid particulate matter
LSD	Low sulphur diesel
LSV	Low space velocity
NO	Nitric oxide
NO_2	Nitrogen dioxide
NO_X	Nitrogen oxides
n_{po}	Number of primary particles
PAH	Polycyclic aromatic hydrocarbon
P_b	Brake power
Pd	Palladium
PM	Particulate matter
ppm	parts per million
PSD	Particulate size distribution
PI	Post-injection
Pt	Platinum
RME	Rapeseed methyl ester
R_g	Radius of gyration
ROHR	Rate of heat release
SCR	Selective catalytic reduction
SI	Spark ignition
SMPS	Scanning mobility particle sizer

SOC	Start of combustion
SOF	Soluble organic fraction
SOI	Start of fuel injection
SPM	Solid particulate matter
SV	Space velocity
TEM	Transmission electron microscopy
TDC	Top dead centre
TEM	Transmission electron microscope
THC	Total hydrocarbons
UHC	Unburnt hydrocarbons
ULSD	Ultra low sulphur diesel
WPM	Water particulate matter
w/w	Weight per weight
M-I	Main injection
W/O PI	Without post-injection

LIST OF DEFINITIONS

Name	Definition
Agglomeration	The process in which primary soot particles stick together to form large groups of primary particles (agglomerates)
Air-fuel Ratio	Mass ratio of air to fuel present in an internal combustion engine
Amorphous	Solid which does not exhibit crystalline structure
Catalyst	Compounds or elements that take part in speeding up the rate of a chemical reaction and lowering the activation energy
Coagulation/Coalescence	Collisions between particles during their random motions resulting in decreasing the number of particles, holding the combined mass of the two particles and larger sized particles
Condensation Particle Counter (CPC)	Measures particle number concentration
Decarbonisation	Remove carbon from an internal combustion engine
Decomposition	Separation of a substance into simpler substances or basic elements
Differential Mobility Analyser (DMA)	Classify particles depending on electrical mobility which can be related to the particle size
Equivalence Ratio	Ratio of fuel to oxidiser divided by the same ratio at stoichiometric conditions
Flame Ionisation Detection (FIM)	To measure concentrations of hydrocarbons within a sampled gas by burning it in an air-hydrogen flame, producing high levels of ionisation which is

	proportional to the number of single carbon atoms within the sample
Particle Inception	Formation of particles from gas-phase reactants. Chemical and physical growth of soot precursors resulting in the formation of particle nuclei with diameters around 1-2 nm
Permeability	The ability of a substance to allow another substance to pass through it
Porosity	A measure of the void (empty) space in a material
Pyrolysis	Process of thermal decomposition of organic material
Regeneration	Process of removing accumulated soot from a diesel particulate filter, either passively or actively
Sintering	Process of forming a solid or porous mass by heating a metallic powered material without melting
Soot Precursors	Fuel pyrolysis reactions result in the formation of these compounds (e.g. acetylene ‘C_2H_2’, polycyclic aromatic hydrocarbons ‘PAH’) further forming the first soot particle
Substrate	Consisting of multiple compounds that need to react together-Are essentially chemical reactants

LIST OF CHEMICAL FORMULA DEFINITIONS

Chemicals formula	Definition
Al_2O_3	Alumina
CH_4	Methane
C_2H_2	Acetylene
C_2H_4	Ethylene
C_2H_6	Ethane
C_3H_6	Propylene
CH_2O	Formaldehyde
H_2O	Water
H_2	Hydrogen
HO_2	Hydroperoxyl
SO_2	Sulphur Dioxide
SO_4	Sulphuric acid

CHAPTER 1
INTRODUCTION

1.1 OVERVIEW

Diesel engines have been used for over one hundred years and have penetrated daily life. Definitely, all commercial products and everything over the oceans, such as cargo, are transported by at least one machine powered by a diesel engine. Practically, diesel engines offer many advantages over gasoline fuelled spark ignition (SI engines), for example, they are perceived to be more durable and do not require an external ignition system. However, the level of particulate matter (PM) and nitric oxide (NOx) emissions produced by diesel engines are higher than those from conventional gasoline fuelled engines; which makes it more difficult to meet the strict emissions standards. The main motivations behind modern diesel engine design are the desire for lower exhaust gas emissions and noise, and for improved fuel economy. These desires are often conflicting and it is believed that they can be satisfied through the application of biofuel in diesel engines, as well as the implementation of exhaust aftertreatment technologies and optimum matching of fuel injection and air motion in the cylinder. Recent research also focuses on how the combustion processes can improve catalyst aftertreatment systems in diesel engines and how they affect the goals of low emissions and optimum operation. The reduction or oxidation of particulate matter (PM) emissions from compression ignition (CI) diesel engines is a major contemporary research challenge. Recently, the role of alternative fuels in meeting engine emissions and performance targets has become more widely recognised [1].

With a view to improve air quality standards, new engine and vehicle systems and technologies are under development in order to reduce pollutants emitted to the atmosphere especially in the very challenging transportation sector [2, 3]. In road transport, replacing fossil fuels with greener fuels such as biofuels (biodiesel and alcohol blends) also provides cleaner combustion and consequently, improves the efficiency of the catalytic aftertreatment systems; which in turn helps vehicle manufacturers to achieve the emissions' legislative limits such as the EURO 6 and CARB (LEV III) [4]. The fuel for better efficiency such as bioalcohol, biodiesel and other oxygenated fuels are a promising option for reducing emissions in diesel engines. More recently, these cleaner fuels have been studied as a substitute for diesel fuel [5] and the presence of oxygen-born fuel contributes in the reduction of the engine-out emissions such as CO, UHC (unburned hydrocarbons), total PM emissions and sometimes NO_X (nitrogen oxides) emissions [6]. It is reported that the hydroxyl group present in alcohols is more efficient in reducing diesel engine PM than other functional groups with the same oxygen content, especially at high engine loads [7-9]. The combustion of diesel-ethanol blends for example has been widely reported to reduce PM emissions [5, 10]. Butanol in diesel has shown more promising characteristics as an alternative fuel than ethanol [5] due to the higher cetane number and better solubility in diesel fuel as a consequence of being less polar than other alcohols with a shorter chain. Furthermore, it has a higher heating value, lower volatility and less hydrophilic character [11, 12].

Due to the recent popularity of diesel-powered vehicles, increased particulate matter (PM) emissions have become a major concern to human health and the environment. Solid soot particulates make up the majority of the content of diesel PM; they are carbonaceous particles with sub-micron scales [1, 13, 14]. Particulate emissions from compression ignition (CI) engines are variable in size and morphology, making their

control challenging. It is reported that the small size of the soot particles causes various diseases by penetrating deep into the respiratory system (Figure 1.1 and Figure 1.2) and they can reach the vital organs [15-17]. The reduction of soot particles emissions is essential to meet the stringent regulations on pollutant emissions through the consideration of three aspects: (1) improve fuel quality with additives (e.g. oxygenated fuels); (2) high pressure common-rail injection systems; (3) and using advanced aftertreatment technologies (e.g. Diesel Particulate Filter -DPF, Diesel Oxidation Catalyst (DOC), and Exhaust Gas Recirculation (EGR)). The development of catalysts in vehicles started from 1975 after it was found that they made a significant contribution to the removal of poisonous lead contained in gasoline. The first application of a diesel oxidation catalyst to reduce CO and HC in automotives (1989) was the diesel Volkswagen Golf "Umwelt" (German for "environment").

Modern engine aftertreatment systems consist of different components such as the DOC and DPF. The number of publications on this subject has continuously grown due to the increase in the emissions legislation which can help to minimize the adverse health and environmental impacts of air pollutants from different power sources. The main focus of the stringent regulations for diesel engines has been to reduce PM and NOx as well as to control hydrocarbon (HC) and CO emissions. The DOC is considered the first type of diesel catalyst and has been commercially established in a number of light and heavy duty applications. It is able to enhance a wide range of oxidation reactions' (chemically convert all emissions' components to CO_2 and water vapour) emissions through the diesel exhaust emissions under all engine operating conditions. DOCs have a honeycomb monolith shape with high cell density (large surface area) and with suitable loading of a catalyst material, such as platinum and/or palladium, is able to almost eliminate CO, HC and much of the particulate organic fraction [18, 19]. A DOC can also oxidise NO to produce NO_2 that can

then be utilised in the DPF to passively oxidise soot at low temperatures [20, 21]. The DOC's activity depends on the exhaust gas temperature, the residence time of the exhaust gas in the catalyst, the level and nature of the gaseous and particulate matter exhaust species and the inhibition/synergies between the different species contained in the exhaust gas [21, 22]. In the same way, the DPF's performance is also influenced by the size and morphology [fractal dimension (D_f), radius of gyration (r_g), and number of primary particles (n_{po})] of soot particles, making the understanding of their control challenging [23]. Therefore, understanding PM characteristics is likewise necessary for the design of control technologies such as particle traps.

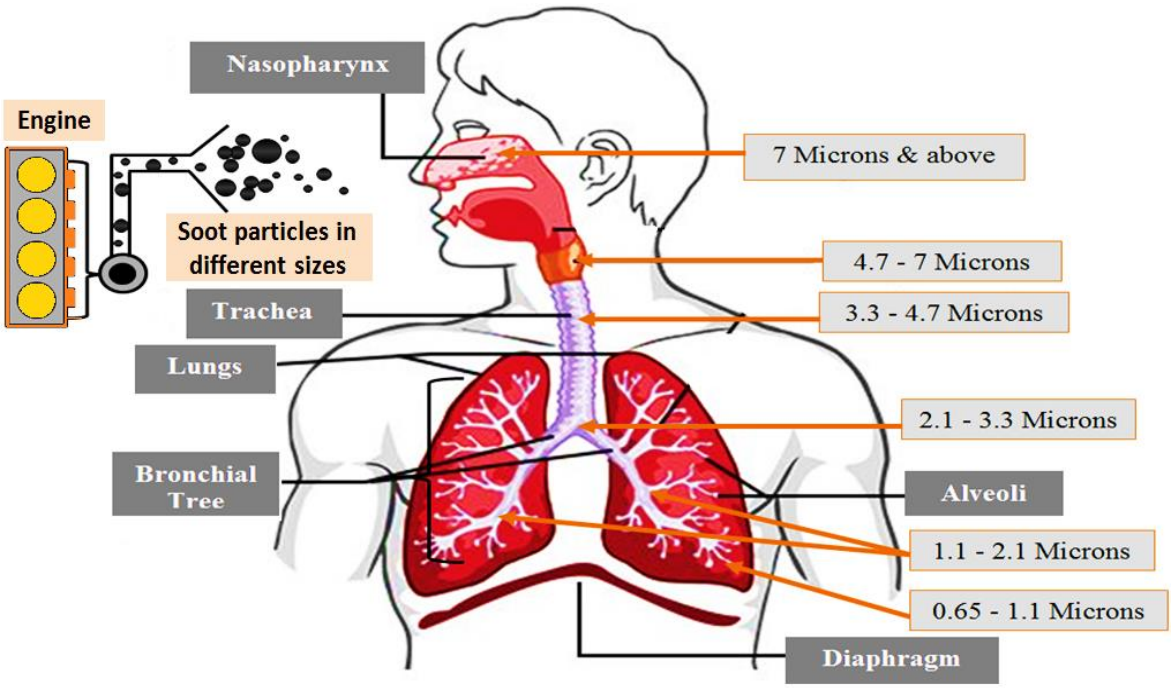

Figure 1.1: Transport of the diesel soot particles in the respiratory system according to their size [24]

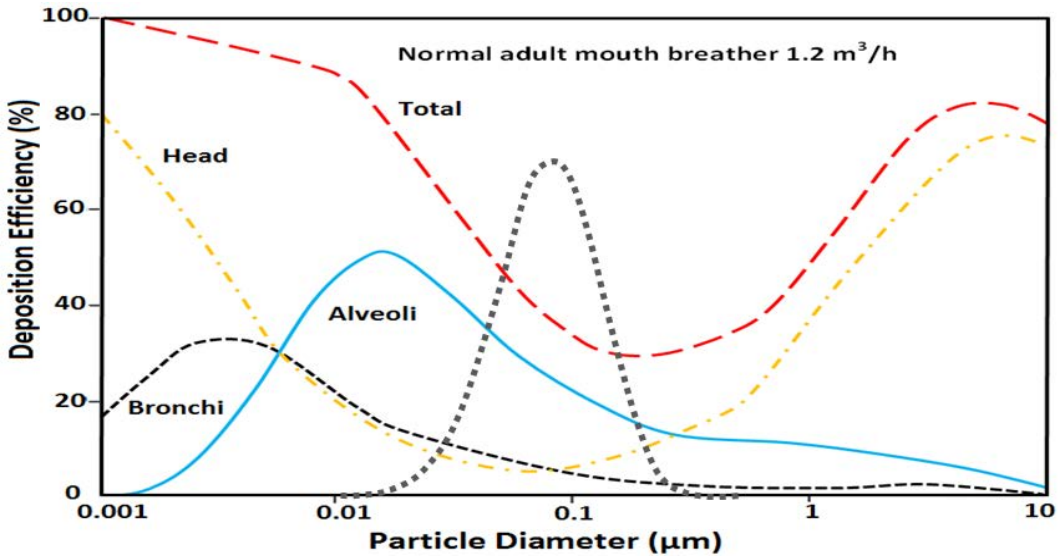

Figure 1.2: Particle size and their deposition rate in the human body location, fitted with a typical PSD (particulate size distribution) from the engine [24, 25].

Previous experimental studies have corroborated that the presence of oxygen in fuels contributes a significant reduction in soot formation and this is in agreement with both experimental [7, 26-31] and numerical [32, 33] studies. More recently bioalcohols and other oxygenated fuels have been studied as substitutes for diesel fuel to reduce engine emissions [5, 34, 35] and improve aftertreatment systems' (e.g. DOC's performance) [20]. It is reported in some studies that the soot emissions reduction also depends on the molecular structure of the oxygenated fuel and not only on the oxygen content. It is important to understand the impact of combustion chemistry in soot formation towards the smart selection of the next generation of alternative fuels [36]. The effect of combining oxygenated fuels and aftertreatment systems is essential in order to fulfil the stringent emissions regulations and also to help in decoupling mutual dependences between pollutant control and fuel economy. Most of the studies on alternative fuels combustion published in the literature are focused on the influence of fuel properties on the engine combustion performance and on the engine emissions; including PM characteristics [37] which influence passive and active DPF regeneration [18] as well as DPF trapping

efficiency [38]. Meanwhile, a few studies have documented work on the influence of gaseous emissions' interaction [20] and also on trapping/oxidising the volatile component of PM over a DOC. Furthermore, the majority of those studies are performed only for conventional diesel fuel [39, 40] and the issues associated with PM characteristics (morphology, size and microstructure) in a DOC have not been addressed in depth. Therefore, the PM characteristics have been addressed during this thesis from the combustion of different fuels over a DOC in more detail.

Combined advances in alternative fuels and engine operating parameters such as injection settings (number of injection, injection timing, injection pressure, injection quantity), are required to be understood in order to improve not only the engine performance (power/torque) characteristics but also the function of the aftertreatment system [41]. Several studies have shown that post-injection in combination with the DOC is commonly used to increase the exhaust gas temperature (EGT) in order to aid the DPF regeneration (i.e. active regeneration) [42]. It has also been documented that post-injection contributes in an increasing of soot oxidation in the combustion cycle, due to the enhancement of the gas mean temperature and air/fuel mixing, which leads to a reduction in PM (number and diameter) [43, 44]. However, there is still scarce information regarding the effect of alternative fuels (e.g. alcohol blends) on both PM characteristics and DOC activity with simultaneous use of a fuel post-injection strategy; that required in diesel vehicles for catalyst heat-up in active and DPF regeneration.

Broday et al. [15] and Zhang et al. [45] stated that the morphological parameters have a significant effect on the size and shape of soot particles. The morphology of soot particles is characterized by the size and the shape, and quantified by the fractal dimension; while the microstructure is quantified by interlayer spacing (d_{002}), and the thickness (L_c)

and width (L_a) of the graphene layer. The size of the soot particles of the engine's exhaust influences the environment in several ways; such as optical properties of the particles, resident time of the particles, surface area and ability of particles to participate in atmospheric chemistry and the health effects of the particles [13].

1.2 DIESEL ENGINE COMBUSTION AND SOOT FORMATION

Direct injection diesel engines depend primarily on different parameters such as fuel properties, engine operating conditions, combustion chamber design and the fuel injection system; it is considered as an unsteady process. The ignition and combustion processes in a diesel engine are controlled by the fuel injection timing and rate. The typical direct injection (DI) diesel engine combustion with one injection per cycle is shown in Figure 1.3 [1] and can be described in four distinct phases. The first phase (A-B) is ignition delay; defined as the period between the start of fuel injection (SOI) into the combustion chamber and the start of combustion (SOC). This can be determined from the analysis of rate of heat release (ROHR), which can be used to describe the overall diesel combustion process from the pressure against crank angle data. The second phase (B-C) is premixed combustion; defined as the fuel combustion that has been mixing with air during the ignition delay period, which occurs rapidly in a few crank angle degrees (CAD). This is because the mixture achieves its flammability limit, it begins to auto-ignite and burn, leading to the high ROHR characteristics of this phase. Subsequently, the diffusion combustion phase (C-D) occurs in a short time, when the fuel-air pre-mixture during the ignition delay has been consumed. The ROHR can only be controlled at this point by the rate at which the mixture becomes available to burn. Finally, there is the late combustion phase (D-E). In this phase the combustion extends into the expansion stroke and heat release continues at a lower rate. This is due to a small amount of fuel remaining unburned

and also to incomplete combustion products. The end of the diffusion phase and the beginning of late combustion represent the end of injection (EOI). The end of combustion (EOC) occurs when the ROHR reaches to lower levels as the pressure and temperature inside cylinder reduces due to the expansion of the stroke.

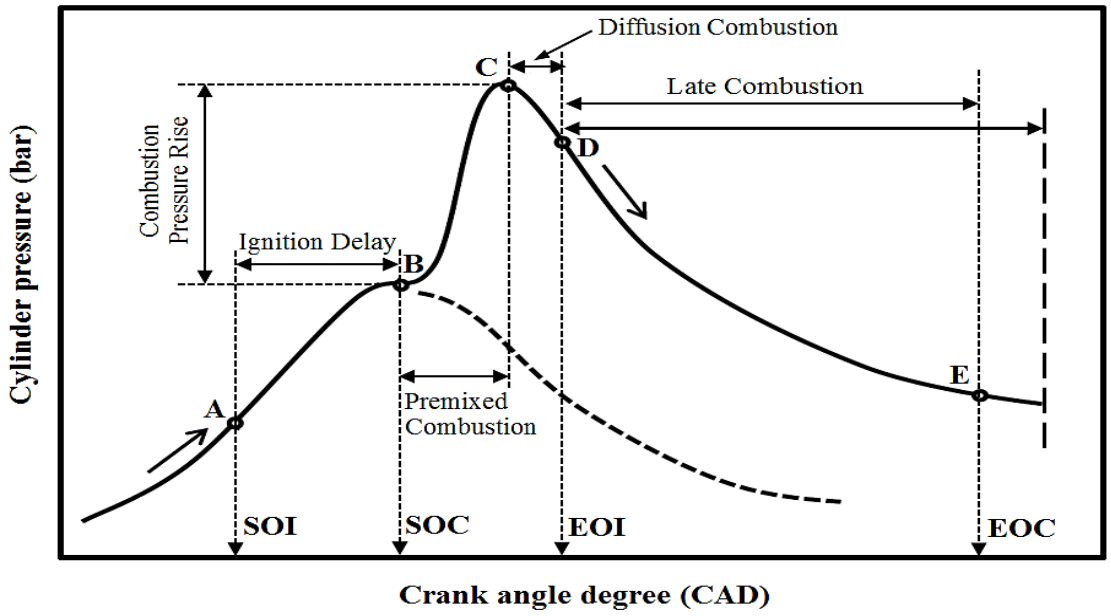

Figure 1.3: Pressure-crank angle (timing) diagram of the combustion phases in a direct injection diesel engine [1]

The formation of soot starts through pyrolysis of unburnt aromatic HC during the extreme heat produced during the combustion of fuel in a diesel engine, as described by Dec's conceptual model [46]. Figure 1.4 provides an understanding of the description of the reacting diesel jet structure, soot formation and oxidation processes from the model during the "quasi-steady" period, which occurs between autoignition and the end of fuel injection. The lift-off is the axial distance from the nozzle exit to the diffusion flame. Within the jet interior, the net soot formation is strongly affected by mixing upstream of the lift-off length. The cross-sectional slice describes the soot formation of a diesel fuel jet, taken between the end of the premixed-burn phase until the end of fuel injection. The flame

occurs through the injection fuel as a number of high velocity jets into the engine cylinder, towards the end of the compression stroke, forming a liquid jet. The fuel atomizes into small droplets (rich fuel/air vapour), it vaporises and is mixed at temperatures from 700-900 K for diesel fuel and high pressure cylinder gases. The fuel breaks down and large quantities of PAH (polycyclic aromatic hydrocarbons) are formed during the premixed phase at temperatures from 1300-1600K (pale blue) [32]. Within Dec's model, an exothermic reaction occurs around several stages which are depicted and the oxygen available is consumed which lead to the start of soot formation. Stone [47] reported that the PAHs are a strong function of temperature and formed during the combustion process. The soot particles take root and grow through the turbulent fuel jet as they move down towards the head vortex. They increase in soot size and concentration at the jet periphery from the injector nozzle and continue increasing to reach their highest (black) at the centre of the jet plume [48]. As plenty of oxygen is present in the air, an orange coloured diffusion flame develops around the fuel jet's periphery, which further increases the local temperature [48, 49]. These conditions are very suitable for NO formation (green) on the lean side of the diffusion flame and nearby soot is oxidised inside the peripheral flame.

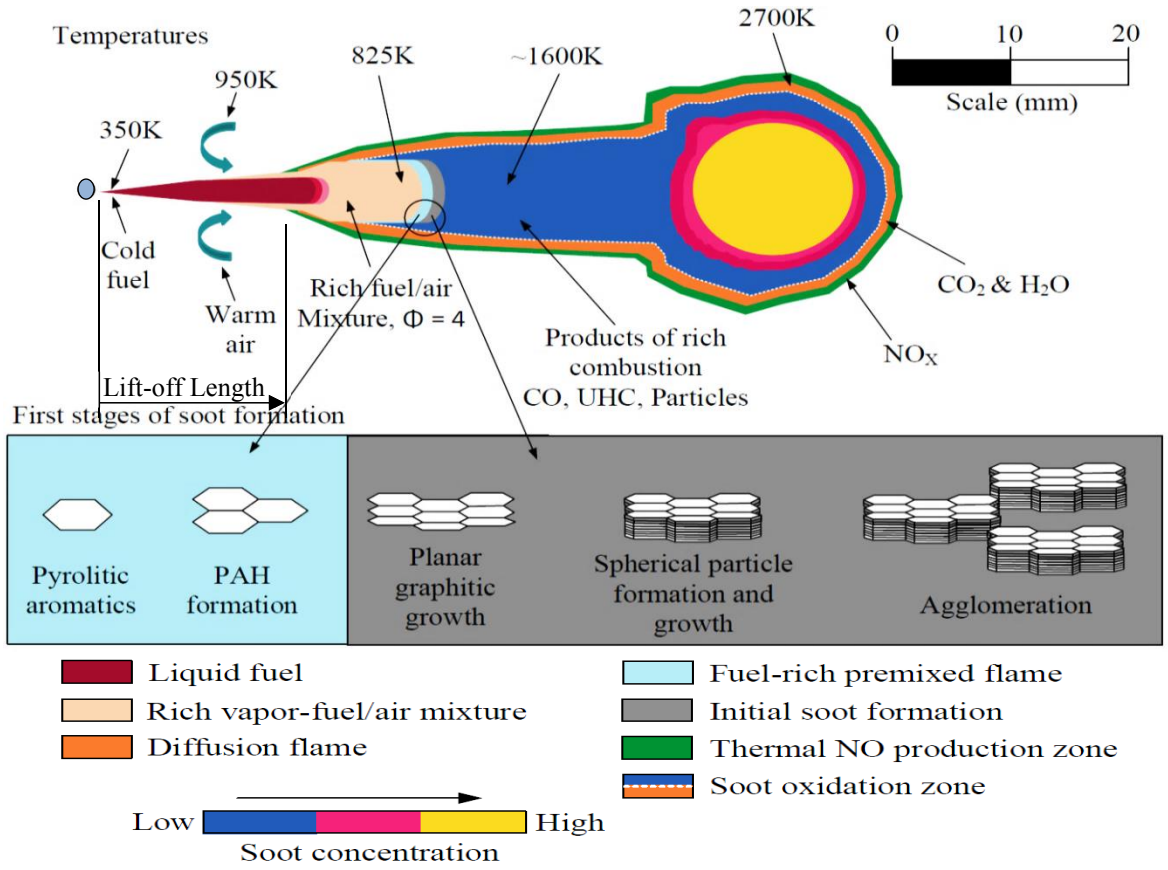

Figure 1.4: Dec's conceptual model of DI diesel combustion during the quasi-steady period related to the soot formation within the premixed flame [32, 46, 50]

Diffusion flame (mixing controlled) combustion as suggested by Dec's model occurs between the products of the fuel rich premixed combustion and air. A large quantity of soot is first formed during the diesel diffusion burning process, just downstream of the lift-off length. During the diffusion burn phase, it is thought that the soot particles start oxidation along the outside of the flame where oxygen is present and there is a high temperature to enhance the pyrolysis reactions. During the final stage of combustion, the particulate matter (PM) leaves the engine to go into the exhaust as soot particles form.

Physical properties such as density, vaporisation range and viscosity are among the important factors that have a significant impact on diesel combustion. All processes described above are dependent on the mixing of the injected fuel with air and some of

residual gases present in the cylinder. Furthermore, it is necessary to enhance the fuel properties or to have consistent properties of the fuels such that the engine performance (combustion characteristics) and emissions do not suffer. In the case of the ignition characteristics of a fuel, the chemical composition of a fuel is considered more important than the physical properties [51]. The useful property which indicates the ignition quality is the cetane number (CN). More discussion about soot formation and oxidation are provided in Chapter 2.

1.3 RESEARCH AIM AND OBJECTIVES

The aim of this thesis is to gain a deeper understanding of the particulate matter (PM) characteristics (morphology and microstructure) from a diesel engine fuelled with alternative fuels. The work presented in this thesis focuses on the proposing various strategies to control and reduce pollutant emissions through using the diesel oxidation catalyst, oxygenated fuels and injection strategies. The specific objectives of this thesis are to:

a) Investigate the effect of renewable fuels (e.g. biodiesel (RME) and butanol blends) on PM characteristics (morphology and microstructure) and gaseous emissions over a diesel oxidation catalyst.
b) Study the impact of combined fuel injection strategy and oxygenated fuel blending on particulate emissions and environmental catalysts' performance in modern diesel engines.
c) Study the effect of exhaust gas composition, temperature and reactant residence time on a diesel oxidation catalyst's light-off performance.
d) Examine the effect of the absence solid particles in the exhaust gas on a diesel catalyst light-off temperature and oxidation rate of gaseous emissions over DOC.

The outcomes of these objectives should provide a better understanding about the PM characteristics in an exhaust system and over a diesel oxidation catalyst. This will make it possible to identify the comprehensive characterisation of soot particulates in order to expand the knowledge about the effect of soot characteristics (number and size) on human health and the environment.

1.4 THESIS OUTLINE

Figure 1.5 describes the structure of this thesis based on a single cylinder diesel engine (one fuel injection event) and a new common-rail diesel engine (three fuel injection events). This thesis is categorised into seven chapters and a brief description of the remainder of this thesis will be organized as follows:

Chapter 1: Introduction

Chapter one introduces the overview on particulate emissions, oxygenated fuels and diesel exhaust aftertreatment systems. This chapter also provides the fundamentals of the diesel engine, which includes combustion and soot formation. In addition, it gives outlines of the research motivation and presents research objectives.

Chapter 2: Literature Review

In chapter two a literature review of diesel emissions legislation as prescribed by European standards is presented. This chapter also provides the background and literature review related to the diesel exhaust aftertreatment systems and soot formation and oxidation mechanism including soot morphology and microstructure parameters. Finally, an overview of using alternative fuels (e.g. biodiesel and alcohol blends) in diesel engines is also presented. The motivation for reducing the particulate emissions through the use of oxygenated fuel and an efficient environmental catalyst is also explained in this chapter.

Finally, there is a brief overview on injection strategies (pre, main, and post-injection) in a diesel engine including injection timing, and pressure.

Chapter 3: Experimental Facilities Set-up and Materials

This third chapter presents the experimental set-up including the engine test rig, the fuels used and their properties, engine instrumentation, gaseous and particulate emissions' analytical equipment and the diesel oxidation catalyst (DOC) characteristics. Furthermore, the details of the MATLAB code used in the analysis of the physical properties of the soot particles are also provided in this chapter.

Chapter 4: Role of Alternative Fuels on Particulate Matter (PM) Characteristics and Influence of the Diesel Oxidation Catalyst

This section of the research covers the characteristics of soot morphology and microstructure emitted from the combustion of biodiesel: in this case rapeseed (RME) and alcohol fuel blends with ultra low sulphur diesel (ULSD). The first part of this study focuses on the impact of the DOC (light-off and conversion efficiency) on PM reduction and oxidation, as well as the PM characteristics (size distribution, morphology and structure). The second part of this chapter focuses on understanding the interaction (promotion/inhibition) between various gaseous emissions (CO, HC, THC, and NO to NO_2) and the influences on the DOC's activity. The outcomes from this chapter provide a better understanding of exhaust species interaction within the catalyst and how they affect the catalyst's activity.

Chapter 5: Manipulating Modern Diesel Engine Particulate Emission Characteristics Through Butanol Fuel Blending and Fuel Injection Strategies For Efficient Diesel Oxidation Catalysts.

In Chapter five presents a study of the influence of the combined effect of fuel injection strategies and butanol blending on particulate matter (PM) characteristics (size distribution, morphology and structure) and performance of the DOC in a modern common rail diesel engine. The outcomes of this study provide cleaner exhaust gas from the combustion of oxygenated fuel which helps in decoupling dependences between emission reduction technology and engine fuel economy, i.e. will lead to reduced requirements for active control and enhance catalyst activity.

In this chapter, the changes in the fuels' properties from the incorporation of butanol into diesel fuel, led to cleaner combustion that eased species (i.e. HCs/fuel and engine-out emissions) oxidation in the DOC. These trends will favour the active control strategies in the aftertreatment systems and will positively impact on their performance (i.e. increase activity, improve durability) and overall engine fuel economy.

Chapter 6: Interactions Between Aftertreatment Systems Architecture and Combustion of Oxygenated Fuels in Diesel for Improved Low Temperature Catalysts Activity

In this chapter, the effects of the PM/soot and post-injection strategy on the oxidation efficiency of the DOC in a modern common rail diesel engine fuelled with a butanol blend (B20) are examined. This chapter shows how potentially insignificant changes in the common rail fuel injection system and aftertreatment systems architecture and/or small additions of oxygenated fuel in diesel fuel, can provide meaningful low temperature aftertreatment systems and catalyst activity improvements. Furthermore,

investigate the combination of a filtration (DPF) upstream oxidation (DOC) within aftertreatment at various space velocities to evaluate the risk of soot accumulation within the catalyst and how this affects the diesel oxidation catalyst's activity.

The results from this chapter help to understand the potential effects of PM/soot accumulation on the DOC's light-off performance. This study gives guidelines to design more efficient compact aftertreatment systems architecture and cleaner fuels. The absence of solid particles in the exhaust gas and the control of some of the HC species played a key role in improving catalyst light-off temperature and enhancing the oxidation rate of gaseous emissions.

Chapter 7: Conclusions and Recommendations

Finally, a summary of the most important conclusions from the research are discussed and recommendations are outlined for future work, to continue improve the understanding of soot emissions characteristics and catalyst performance for future research.

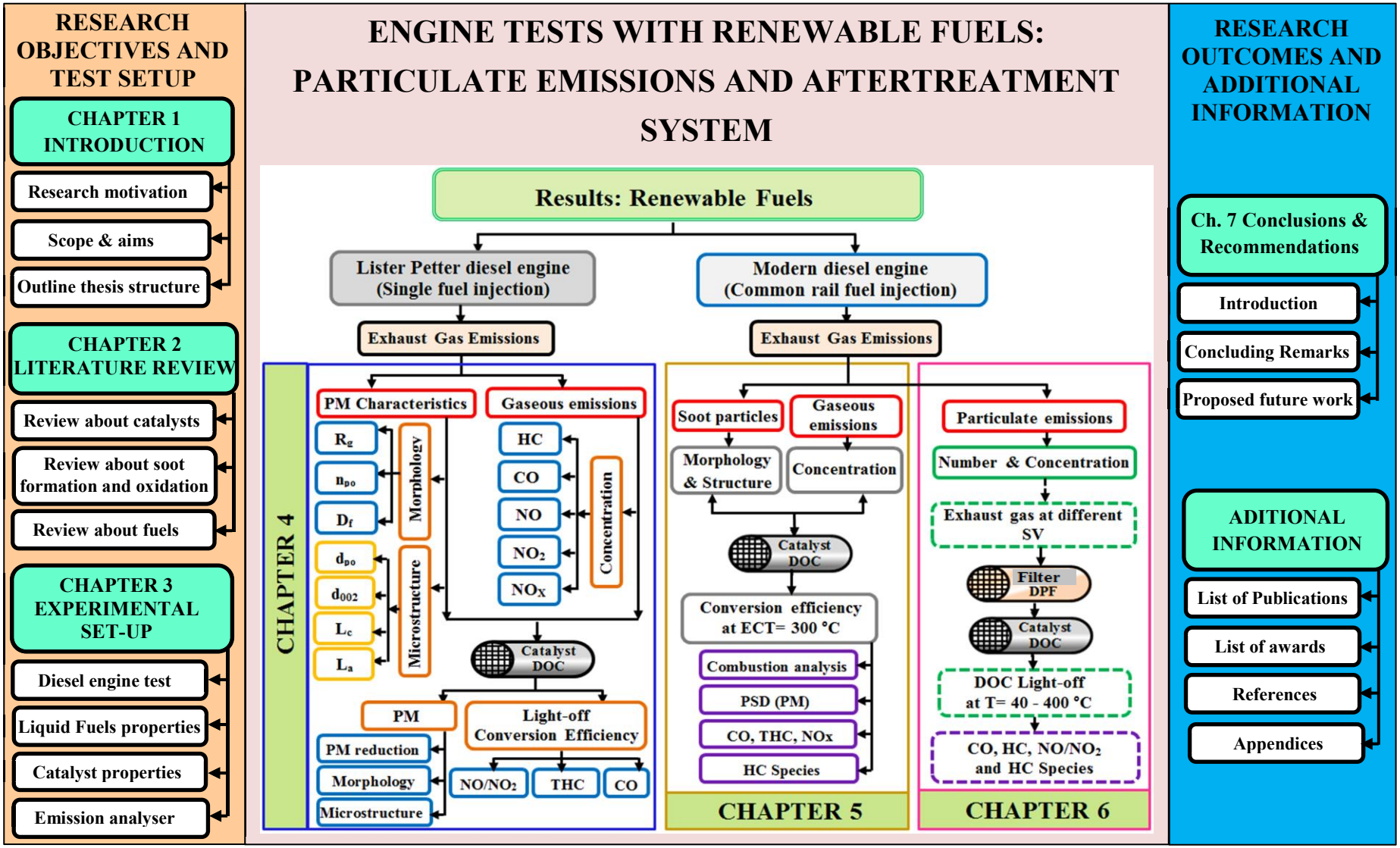

Figure 1.5: Thesis outline

CHAPTER 2

LITERATURE REVIEW

2.1 EXHAUST GAS EMISSIONS LEGISLATION

With a view to improve air quality, new engine and vehicle systems and technologies are under development in order to reduce pollutants emitted to the atmosphere, especially in the very challenging transportation sector [2, 3]. During many decades vehicles have been the subject of continued interest due to environmental and health concerns. Exhaust emissions (THC, CO, NO_X, and PM) are responsible for the majority of pollutants and are becoming the major driving factor in diesel engine development; where vehicles produce several pollutants such as combustion products and losses from evaporation (evaporative emissions, refuelling emissions). Therefore, emissions' legislation is becoming more and more stringent, as stipulated by the relevant governing bodies. The legislation of emissions has been led by some countries (e.g. Euro and Japan emissions' standards) in order to fulfil the standard of future emission regulations. There are different levels of European emission standards for NO_X and PM for both light and heavy duty diesel engines, as shown in Figure 2.1.

The current pollution levels have led to the appearance of laws and regulations which are employed to control the environmental and health impacts from the petroleum industry and engine emissions. The EPA (environmental protection agency) has developed rigid guidelines for both the petroleum industry and for the engine emissions that are allowed from combustion products. Recently, the relationship between the particle size and health effects has been the focus of much public debate. The legislation is going to

get tougher and tougher as shown in Figure 2.1; therefore countries will try to minimize local problems (smog, toxins etc.) and global problems to work towards the tighter and tighter emission levels. To meet these new levels, new technologies will be required with consideration to the efficiency, cost effectiveness and durability of the technology.

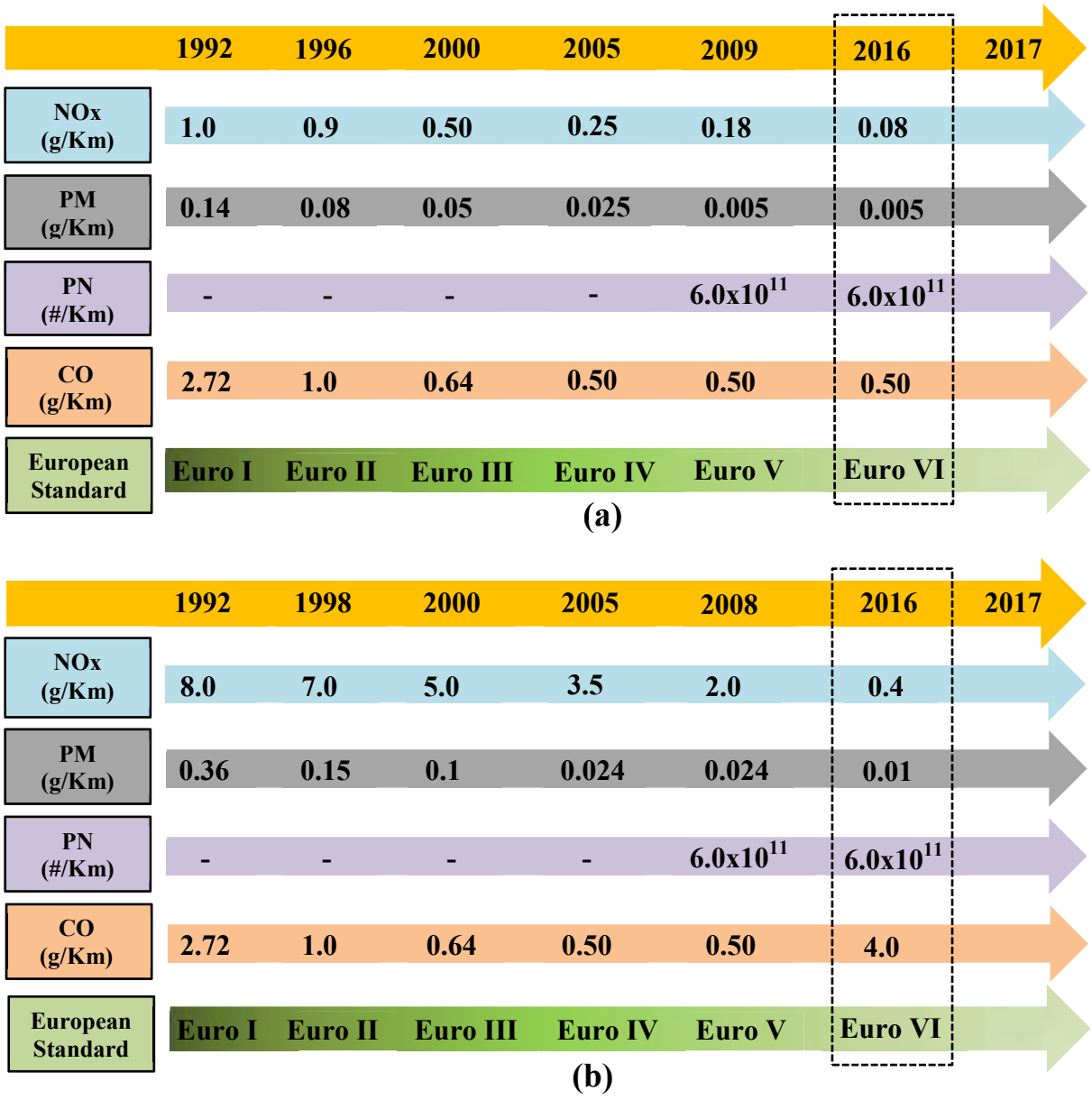

Figure 2.1: European emission standards for (a) light diesel commercial vehicles (b) heavy-duty diesel vehicles over a time period [52, 53]

2.2 TAILPIPE EMISSIONS FROM COMPRESSION IGNITION (CI) DIESEL ENGINES

Tailpipe emissions emitted by internal combustion (IC) engines for both compression ignition (CI) diesel engines and spark ignition (SI) engines are a main concern for both human health and the environmental. Compression ignition engines have base emission levels, which are prescribed by the European Union (EU). Diesel engines produce different levels of raw exhaust gas due to various conditions (heterogeneous mixtures non- and stoichiometric fuel-air ratios), such as total hydrocarbons (THC), nitrogen oxides (NO_X), carbon monoxide (CO) and particulate matter (PM) [1]. Some of these emissions are the result of the incomplete combustion of the fuel [54].

Presently, THC, NO_X, CO, and PM are the source of concern for the environment when these emissions react with smog and ozone levels. Particulate matter emissions have a chemical complexity that makes them a serious issue for engine emissions. Attention has been drawn to the soot particles in exhaust emissions, which has led to the introduction of controls on smoke and particulates in diesel engines due to their associated health risks [55]. The generation of small particles is initiated via the pyrolysis of unburnt hydrocarbon during the combustion process of the fuel. They are products that are difficult to eliminate, as they are of a small size about 10 µm or less. The smaller size of particle is more active than large size and stay for a long time in the atmosphere. Most of the soot particles can contaminate lubricant oil as a result of blow-by gases when reacts with engine oil [56, 57].

The soot particle sizes and their distribution inside the engine combustion cycle are affected during the steps of the soot particles' formation (growing from nucleation to agglomeration) and oxidation; hence its influence the size of the soot particles at the exhaust tailpipe. Further understanding about the size and structure of soot particles and their formation and oxidation mechanism becomes an urgent necessity to find the ways to reduce or control the harmful effects of soot emissions. This thesis will completely focus on the evolution of PM characteristics (size and structure) under different engine conditions and with renewable fuels (e.g. biodiesel (RME) and butanol-diesel blends). The morphological and structure analysis was carried out based on MATLAB programming code which will be explained in greater detail in this thesis (Chapter 3).

2.2.1 Carbon Monoxide (CO)

Carbon monoxide (CO) emissions are odourless, tasteless, colourless, poisonous, and noncorrosive. The formation of CO is as a consequence of incomplete combustion from oxygen deficient combustion and is mostly prominent in the fuel-rich combustion regions. Therefore, CO formation can be controlled by the air/fuel (A/F) equivalence ratio as a result of incomplete combustion (there is not enough available oxygen to burn all the fuel). This CO formation is usually accompanied from the progressive combustion mechanism of HC radicals ($\dot{R}$), which is represented by the reaction shown below [58]:

$$\dot{R}H \rightarrow \dot{R} \rightarrow \dot{R}O_2 \rightarrow \dot{R}CHO \rightarrow \dot{R}CO \rightarrow CO \qquad (2.1)$$

The formation of CO emissions is low or negligible during lean burn combustion due to the ratio of air/fuel always being lean ($\lambda>1$). In diesel combustion engines, may be

the temperature is high enough for oxygen and carbon monoxide to form carbon dioxide (CO_2), following the principal of CO oxidation as described below:

$$CO + OH \leftrightarrow CO_2 + H \quad (2.2)$$

The oxidation of CO emissions cannot take place in the exhaust system without the use of a diesel oxidation catalyst (DOC) due to the low temperature of diesel exhaust gas. Miles et al. [59] presented a depiction of CO emission formation conditions from a diesel engine. However, CO is strongly associated with both human health problems and environmental pollution. Strauss et al. [60] reported that CO can accumulate in red blood cells and drastically reduce their capability to carry oxygen to the cells, resulting in asphyxiation. In the environmental case, CO can contribute to low-level ozone and global warming through reactions with other gases in the low atmosphere.

2.2.2 Hydrocarbons (HCs)

Hydrocarbon emissions are formed from unburned fuel or partially burned fuel and recombined intermediate compounds, which result from the incomplete combustion of hydrocarbon fuel that is emitted from diesel engines. The fuel composition can determine the quantity and composition of the HC emissions, when fuel containing a high percentage of olefins and aromatics produces relatively higher concentrations of reactive HC [1]. However, THC emissions do not have a great effect on the overall pollutant emissions. A heated flame ionisation detector (HFID) is used to measure hydrocarbon emissions of exhaust gaseous. The HC remains in the vapour phase when the temperature is set at 190 °C in the heated sampling line. The total hydrocarbon (THC)

formation mechanism has two critical sources in a diesel combustion engine: fuel injected during the combustion cycle and fuel injected late (timing aTDC) during the combustion cycle [1, 61].

Lubricant oil is a source of HC emissions, a small amount of lubricant film on the cylinder wall can dissolve in the expansion stroke to participate in THC formation [62]. Mjewaski and Khair [63] stated that the shorter carbon chain hydrocarbons are produced from hydrocarbon fuel in exhaust emissions, while the heavier, longer hydrocarbon emissions generate from lubricant oil. Ferguson et al. [64] exhibited that some of the vaporised fuel that has a lower equivalence ratio than the lean limit of combustion (over-mixing between air and fuel more than ($\phi \simeq 0.3$), upsets the main combustion process. In general, a low level of HCs is produced from the lean burn combustion in diesel engines. The HCs cause a variety of negative effects on ozone levels when they react with NOx [63].

2.2.3 Nitrogen Oxides (NO_X)

Emissions of NO_X are toxic and produced from diesel combustion; they are considered as one of the most critical emissions [1]. They mainly consists of nitric oxide (NO) and nitrogen dioxide (NO_2) specifically in automotive aftertreatment, contributing to 90% and 10 of the total NO_X emissions respectively. The reaction of nitric oxide with molecular oxygen to form nitrogen dioxide was explained in Equation (2.3). The NO formation is considered the main component of the total NO_X emissions in CI diesel engines. The NO can be formed at a high combustion temperature (2000 K) [47]. The oxidation of atmospheric nitrogen (N_2) is a source of NO formation. The main source of

NO formation is the thermal NO mechanism which can be explained through the extended Zeldovich mechanism [1].

$$2NO + O_2 \rightarrow 2NO_2 \quad (2.3)$$

The primary pathway of NO formation is explained by the extended Zeldovich mechanism in which the hydroxyl radicals, atomic oxygen, and N_2 are all in equilibrium. The reaction of NO formation is shown below:

$$O + N_2 \rightarrow NO + N \quad (2.4)$$

$$N + O_2 \rightarrow NO + O \quad (2.5)$$

The reaction of the hydroxyl radicals with nitrogen can be explained by the thermal NO mechanism [65].

$$N + OH \rightarrow NO + H \quad (2.6)$$

The formation of NO_2 is the final reaction of the NO_X emissions; however, it can be formed at low temperature through the reaction of NO and HO_2 (hydroperoxyl radicals) through this reaction:

$$NO + HO_2 \rightarrow NO_2 + OH \quad (2.7)$$

Although after NO_2 formation, it is followed by conversion back (destruction) to NO at high temperatures, as shown in the reactions below:

$$NO_2 + O \rightarrow NO + O_2 \quad (2.8)$$

$$NO_2 + H \rightarrow NO + OH \quad (2.9)$$

Bowman Craig [58] explained that the NO_2 formation occurs at lower peak combustion temperature, while the destruction of NO_2 at high combustion temperature. Soot emissions can be oxidised by NO_2 at temperatures as low as 250 °C, NO_2 is present at very low concentration in a diesel raw exhaust (5-15% of total NO_X), thus this is are not sufficient to provide the required reaction rates. The reaction of NO with excess oxygen in the exhaust via diesel catalyst technology can facilitate NO_2 formation. Normally, NO_X is created depending on the nitrogen content in the fuel components, for example diesel fuel has a very low concentration of nitrogen.

2.2.4 Diesel Particulate Matter

Particulate matter (PM) emissions are emitted from diesel engines as a result of the incomplete combustion of hydrocarbon fuel because some of the fuel droplets do not burn and are vaporised inside cylinder. The PM from diesel fuel combustion consists of soot and other liquid or solid phase substances from the fuel or lubricant oil [13, 14]. Then, they become partly burned fuel droplets in the combustion cycle and subsequently they will be found in the exhaust gas as heavy liquid droplets or solid carbonaceous matter. In addition, some of the PM produced from partially burned lubricating oil is exhausted in

form of the soluble organic friction (SOF). Particulate matter sizes vary from several nanometres to several hundred microns; which is strongly linked to human health issues [66]. For example, the size distribution of particulate materials range from 20 nm to 10 µm and the diameters of particle in the range of 50 nm and 1000 nm (mostly less than 100 nm) from the combustions of diesel fuel [67, 68]. Based on the aerodynamic diameter of particles in the exhaust, the distribution of size and mass (Figure 2.2) can be classified into three main categories: firstly, nuclei-mode when the diameter ranges from 5-50 nm (usually formed from volatile precursors). Secondly, accumulation mode when the range is in the diameter from 50-100 nm; finally, coarse mode (accumulation particles deposited on cylinder and exhaust system surfaces) where the particles' diameter in this mode is larger than 1000 nm [13]. The atmospheric particle size distributions (PM_{10}) are also identified in Figure 2.2 as particles smaller than 10 µm. PM is a complex type of emission that includes many components (Figure 2.3), which include three categories:

1) Solid Particulate Matter (SPM) (Solid Fraction)

    a) Carbonaceous soot

    b) Ash (including metallic)

2) Liquid Particulate Matter (LPM) (Soluble Organic Fraction)

    a) Organic material derived from the fuel

    b) Organic material derived from the engine lubricating oil

3) Water Particulate (WPM)

    a) Water

    b) Sulphuric acid SO_4 (when fuel sulphur is present)

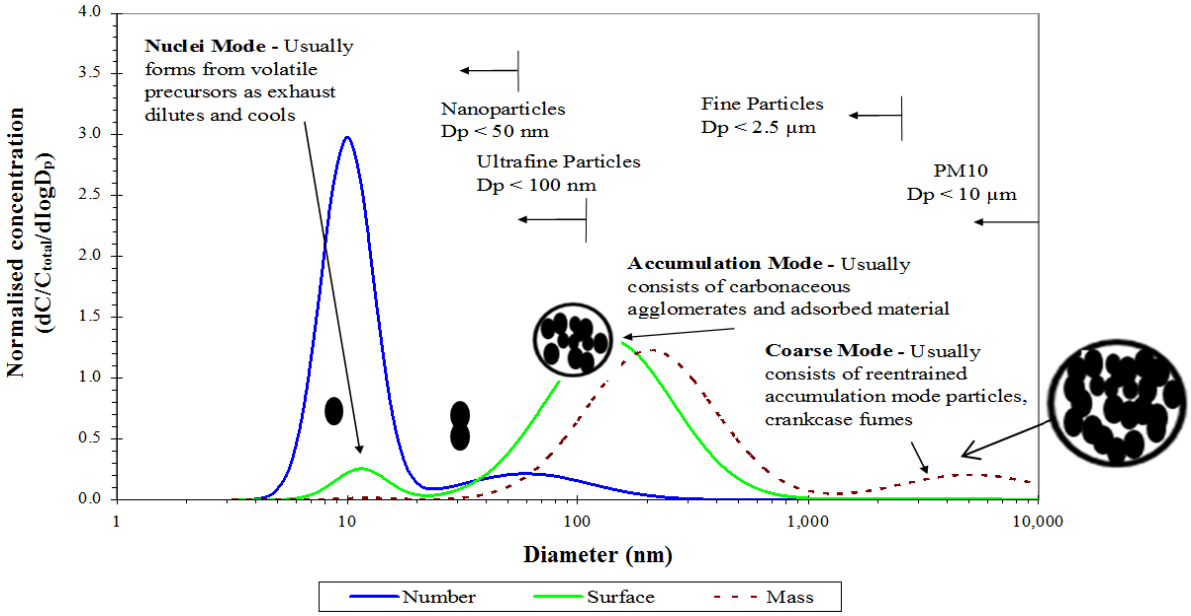

Figure 2.2: Schematic of mass and number based particle size distributions from combustion of diesel engines [24, 69]

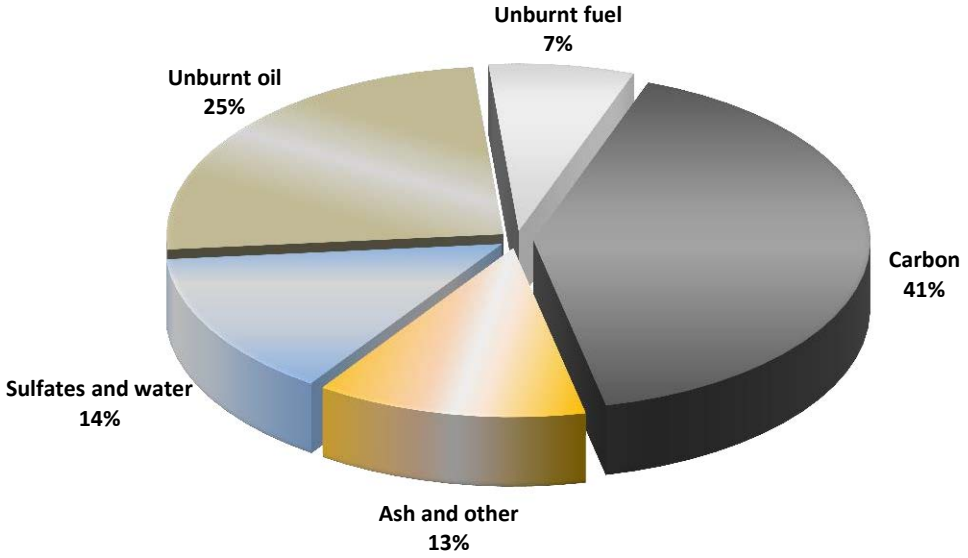

Figure 2.3: Illustrate representative composition of diesel particulate matter during combustion cycle [70]

Numerous research groups have described that the size distribution of particulates and their composition in a diesel engine depend on the combustion process and

the exhaust process. The source of particulates is a combination of two parameters which are soot and other products from the exhaust gas, such as liquid or solid phase materials [71-73]. To describe soot formation in DI engines, compression ignition combustion and commonly identified processes involve in six steps: fuel pyrolysis, PAHs (polycyclic aromatic hydrocarbons), solid nucleation, surface growth (coalescence), coagulation of primary particles, and agglomerates, as shown in Figure 2.9 (these steps will be discussed in more detail through this chapter). Krahl et al. [74] and Smith [75] adds that the PAH (polycyclic aromatic hydrocarbons) are a heavy organic compound and are easy to find in particulate matter (PM); it increases the carcinogenic potential when PAH are combined together with soot, compared to the effect of each component alone. In general, diesel fuel combustion emits many toxic ultrafine particles in different sizes, some of a diameter less than 100 nm; most of these small sized particles can be easily deposited in the human respiratory system [68, 76]. Carbonaceous soot is one of the main components of particle composition, its location upstream of the catalyst can directly effect on the oxidation catalyst activity by accumulating soot particles on the front face and in the catalyst channels. This could obstruct the exhaust emissions from accessing the coated catalyst material, which can reduce the oxidation rate over the catalyst and decrease the conversion efficiency of the catalyst [3, 20, 77].

Solid carbon particles and other chemical species agglomerate together to form particles of PM. In the high combustion temperature, the carbon particles agglomerate and mix with condensed heavy hydrocarbons, nitrogen oxides, sulphur oxides and metallic ash formed and moving through the exhaust pipe. The schematic diagram of the resulting particles (soot particles) is shown in Figure 2.4.

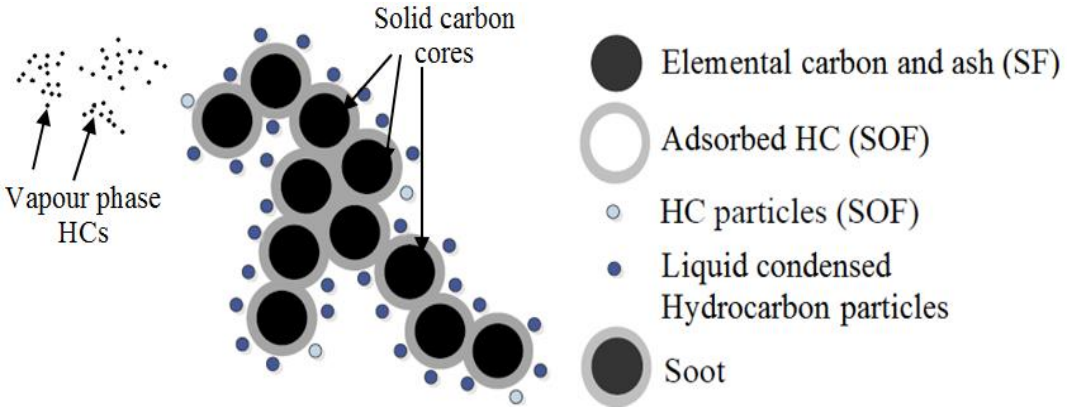

Figure 2.4: Schematic representation of diesel PM [78, 79]

2.3 EXHAUST GAS EMISSIONS CONTROL (AFTERTREATMENT SYSTEMS)

Driven mainly by tightening emission regulations, current emissions' control strategies and aftertreatment technologies are rapidly advancing with the aim to clean-up the gaseous and PM emissions from diesel engines. To meet the diesel emission' regulation there is a required improvement in fuel properties and the incorporation of aftertreatment systems. In this chapter, the details of the role of catalysts technologies used in CI engines will be explained and how these technologies clean-up the exhaust emissions.

2.3.1 Diesel Oxidation Catalyst (DOC)

The purpose of using a diesel oxidation catalyst (DOC) is to control engine emissions (e.g. HC and CO, and PM), several HC-derived emissions (aldehydes or PAHs and organic fraction of PM) and unpleasant odours of a diesel exhaust [63, 80]. The internal form of a DOC is similar to a monolith honeycomb substrate coated by Platinum (Pt): Palladium (Pd) and zeolite washcoat, with high cell density (large surface area) and

suitable loadings of a catalytic material, such as platinum (Pt) and/or palladium (Pd) that is able to almost eliminate CO, HC and much of the particulate organic fractions depicted in Figure 2.5. The DOC also oxidises NO to produce NO_2 that can then be utilised in the DPF to passively oxidise soot at low temperatures [18, 19, 77].

Several exhaust species can be oxidised by contact with the catalytic active sites coated on the channel walls in the DOC. Its activity depends on the exhaust gas temperature, the residence time of the exhaust gas in the catalyst, the level and nature of the gaseous and particulate matter exhaust species and inhibitions/synergies between the different species contained in the exhaust gas [20, 21]. Diehl et al., Al-Harbi et al., Patterson et al., Voltz et al. and Yao et al. [81-85] documented and modelled the interactions between several exhaust species within a catalyst by using synthetic mixtures of gases to represent engine exhaust gas to understand the DOC's activity, and the outcome from these studies are agreement with role of the catalyst that used in this thesis.

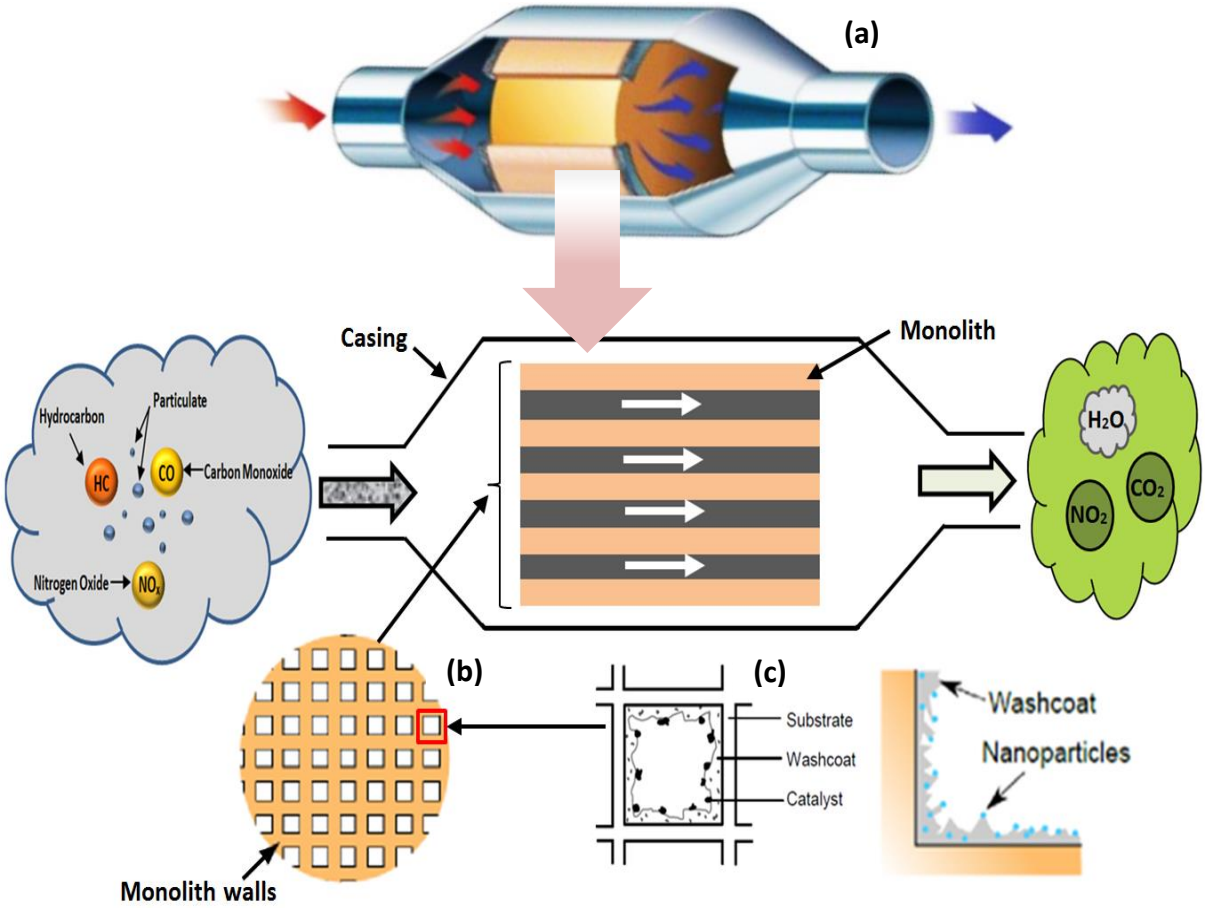

Figure 2.5: Schematic diagram of diesel oxidation catalyst: a) a typical diesel oxidation catalyst; b) a larger segment of the top view of DOC; c) a cross section of a square monolith channel [24]

A DOC with high suitable loadings of a catalytic material, such as platinum and high cell density, could also physically trap and oxidize the volatile component of PM [20, 39, 86]. The majority of the studies are performed only for conventional diesel fuel [39, 40, 87] and the issues associated with particulate matter oxidation/reduction in a DOC have not been addressed in depth. The pollutant removal could still take place when the exhaust temperature is limited, which leads to a reduction in the DOC's activity during engine operation. Additionally, the conversion efficiency could be affected from different compounds of gaseous exhaust and soot particles. A DOC reduces the particulate matter

(PM) through the oxidation of the soluble organic fraction (SOF) of PM [88]. In the case of solid soot particles, the oxidation catalyst can directly suffer from the soot emissions (produced by diesel engines) that could accumulate in the catalyst channels. The catalyst's monolith channel and surface interaction with the soot particles is still the major problem with regards to the catalyst's efficiency reduction [89]. Consequently, the soot particles could obstruct the access to the coated catalytic material (loose contact between catalyst and soot) and reduce the active sites in the catalyst; which leads to reduce the catalyst's efficiency and possibly increase the backpressure.

As the hot gaseous emissions pass through an oxidation catalyst, different exhaust pollutants will be oxidised and controlled as well as converted into harmless substances (carbon dioxide and water) during chemical oxidation for these emissions. The processes of chemical reactions for these emissions over the active catalytic sites can be described by the following oxidation reactions [63]:

$$\mathrm{HCs} + \mathrm{O_2} \rightarrow \mathrm{CO_2} + \mathrm{H_2O} \qquad (2.10)$$

$$CO + \frac{1}{2}\, O_2 \rightarrow CO_2 \qquad (2.11)$$

As described in reaction (2.10) and (2.11), the heat is generated (exothermic) during the oxidation of CO and HCs. In many modern diesel emission control systems, oxidation of NO to NO_2 through a catalyst is considered an essential for the engine operation and the chemical oxidation is illustrated in equation (2.12). Furthermore, DOC systems are specifically designed for the generation of high NO_2 in modern diesel engines

to support the regeneration of the diesel particulate filter (DPF) and enhance the performance of selective catalyst reduction (SCR) at low temperature.

$$NO + \frac{1}{2} O_2 = NO_2 \quad (2.12)$$

At low diesel exhaust temperatures (about 200 °C), the oxidation rate of some of the exhaust gases are reduced and may pass through the catalyst without oxidation. At the exhaust gas temperatures (250-300 °C), the light-off (conversion efficiency) can reach the maximum value and the HC and CO species catalytic combustion takes place (Figure 2.6). The DOC light-off temperature, defined as 50% conversion, is usually located at temperatures higher than 200 °C. A new technology of a Pt:Pd catalyst with a new state of the art washcoat type was proposed for use by Johnson Matthey [90] to improve the catalyst oxidation activity (thermally durable) for unburned diesel fuel at low exhaust temperature.

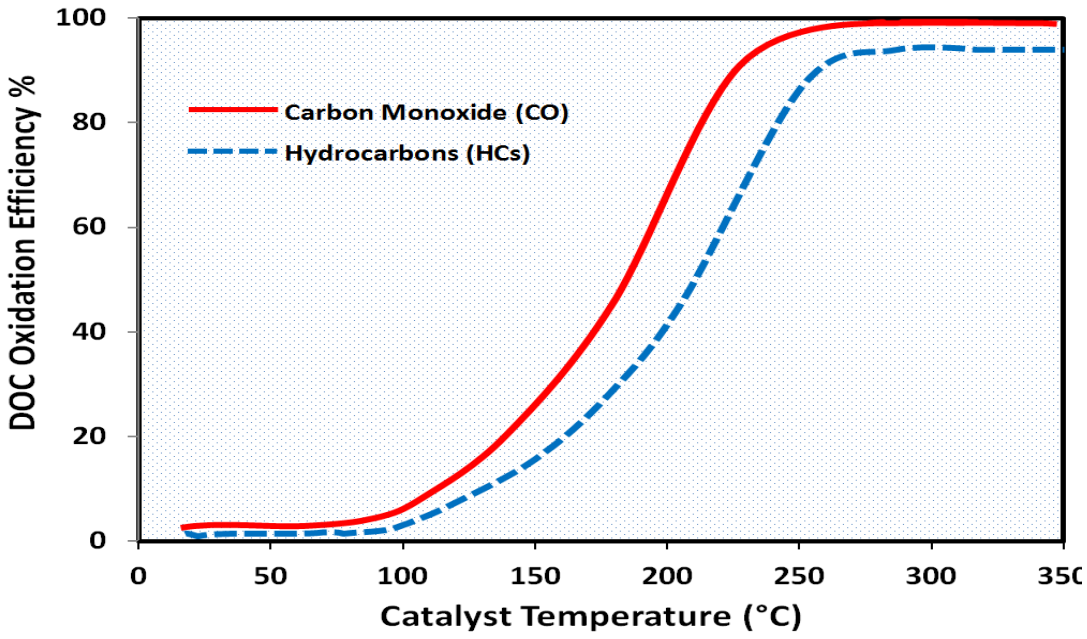

Figure 2.6: Catalytic conversion efficiency (light-off) of carbon monoxide and hydrocarbons [20]

In practical applications, the activity of the catalyst is reduced due to simultaneous thermal and chemical deactivation. There are many sources of catalyst deactivation such as sintering, reaction between catalytic species and the carrier, washcoat losses, poisoning and fouling. However, the chemical deactivation occurs when substances (derived from the fuels' components, soot emissions, and lube oil components) present in the exhaust gases from internal combustion and chemically deactivate the catalytic sites. In contrast, thermal deactivation is caused due to reactions between catalytic species and the carrier, or by loss of active catalytic sites as well as catalyst sintering (changes in the structure of the catalytic component with high temperature). Furthermore, the temperatures between 300-700 °C can be used to decrease the rate of catalyst sintering by producing less mobile particles on the catalyst surface and thus allowing it to provide large active sites. The conversion efficiency versus temperature curve of a new catalyst is changed by deactivation of the catalyst. The trend of the curve can be shifted towards higher temperature ((delay) as shown in Figure 2.7 [91]. This is due to various deactivation modes that affect the conversion profile of the catalyst, such as loss of active sites, increased pore diffusion and masking ((pore blocking).

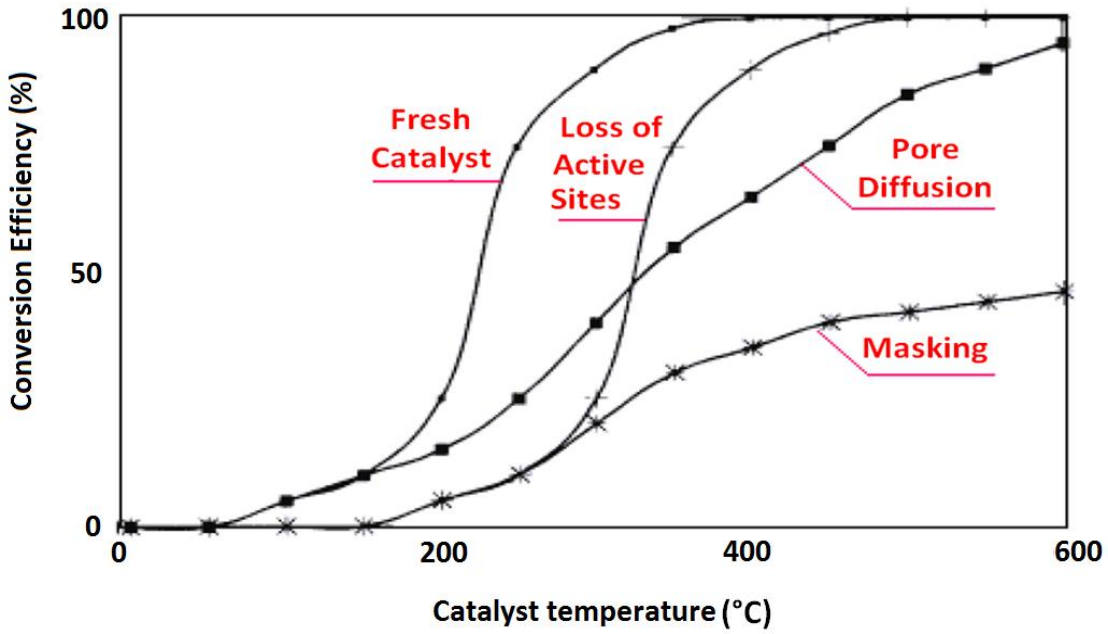

Figure 2.7: Effect of various deactivation modes on conversion efficiency [91]

2.3.2 Diesel Particulate Filter (DPF)

The DPF is the principle technology used to reduce/remove soot (solid PM) contained in diesel exhaust gas flow. The accumulation of the PM within the filter walls during the trapping process causes an increase in back-pressure. The most popular DPFs are the wall-flow monolith with alternately plugged inlet and outlet channels (Figure 2.8). This device forces the exhaust gas flow to enter the filter from the left (Figure 2.8) through porous walls, thus the exhaust cannot exit the cell directly. In addition, the soot particles are gradually reducing the pore porosity and permeability of the filter; which leads to plugging the filter pores (accumulated soot particles in the inlet channels of the DPF). This process leads to an increase in the backpressure and fuel penalty. Johnson Matthey have successfully designed the CR-DPF (catalysed continuously regenerating technology) which has shown high efficiency in removing 99% of PM by mass and 85-99% by PM number from the combustion of diesel fuel [76]. In Chapter 6 of this thesis DPF technology (not the

focus of this thesis) will be applied to remove the soot before the DOC, in an attempt to assess the role of soot particles on the DOC's performance from the combustion of different fuels.

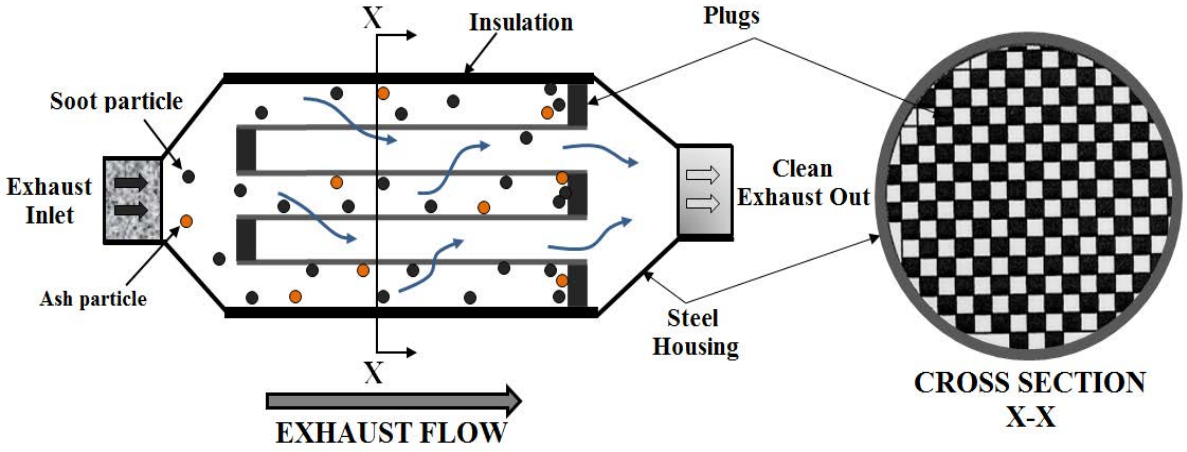

Figure 2.8: Schematic diagram of soot particles through a diesel particulate filter (DPF) [92]

2.4 SOOT FORMATION PROCESSES AND OXIDATION IN CI ENGINES

The transition from the gaseous to the solid phase is known as a soot formation process during fuel combustion. Soot formation and oxidation begins in the fuel-rich premixed zone [93] due to the high-temperature of liquid fuel pyrolysis which causes the decomposition of fuel molecules [94]. Therefore, soot is formed from unburned fuel and defined as a solid substance (solid graphite) mainly consisting of around eight parts of carbon with a minor part of hydrogen. Choi et al. [95] reported that the density of soot is 1.84±0.1 g/cm^3. The complex phenomenon of the soot process (soot formation and oxidation) can be divided into several steps: pyrolysis, formation and precursors, nucleation, particle surface growth, particle coagulation, particle agglomeration and particle oxidation, as shown in Figure 2.9. The soot particles have different shapes and

sizes (varying from nanometres to several hundred microns). This issue has a negative impact on both the environment and human health and has initialised studies aiming at the reduction of soot generation and improvement of soot oxidation. Active soot oxidation (conversion carbon or hydrocarbons to combustion products) can take place at any time during the soot formation process and depends on the process and state of the mixture at the time. Furthermore, the formation and oxidation of soot are affected by in-cylinder temperature, when the temperature inside the cylinder reduces the soot formation and a significant increase in the rate of soot oxidation [14].

2.4.1 Pyrolysis

Pyrolysis is the process of decomposition of organic material (such as fuels) in high temperatures without oxidation. During this process, fuels change their molecular structure and produce species such as unsaturated hydrocarbons, polycyclic aromatic hydrocarbons (PAH), and acetylene. In the first process, the molecular structure of the fuel is changed by exposure to the high temperatures. This process can be considered as pyrolysis of fuel since a significant oxidation does not occur, but may present some oxidation species. It is reported that the soot formation reduces with decreasing the residence time in the pyrolysis zone [96]. Glassman et al. [97] adds that during pyrolysis, radicals are formed and larger molecules increase the radical pool size. Pyrolysis increases at elevated temperatures in the absence of oxygen and this explains why soot is form in diffusion flames (no oxygen present in the pyrolysis region). Some species are produced such as precursors or building blocks for soot results from fuel pyrolysis.

2.4.2 Formation and Precursors

The soot precursor particles' stage in the diffusion flame region of ethane, methane, and acetylene was observed by Dobbins et al. [98]. The competition between both pyrolysis and oxidation rates (rate of pure fuel pyrolysis and precursor oxidation) by the hydroxyl radical (OH) is called soot precursor formation. The rates of soot precursors' production and oxidation is largely depends on the reaction temperature (increase with temperature) during fuel pyrolysis, but the oxidation rate increases faster. At the high temperature region of the flame, the soot precursor particles underwent conversion to carbonaceous soot by the process of carbonization. Furthermore, the remarkable changing in both chemical and physical properties of precursor particles leads to their transformation to mature soot. However, the precursors are easier to oxidise than mature soot; it was suggested that soot particle formation is more reactive when maintaining low combustion temperature [99]. Through the reactions of PAH-PAH and the addition of acetylenes onto PAH molecules, the small molecules grow to form larger PAH molecules. Furthermore, two-dimensional PAHs are formed from a combination of larger PAH molecules which will be the precursors for soot nucleation. Richter et al. [94] and other studies have generally agree that heavy polycyclic aromatic hydrocarbons (PAHs) of molecular (weight 500-1000 molecular amu) are the primary molecular precursors of soot particles.

The formation and evolution of the first aromatic ring from the small aliphatic compound is the main part in the soot precursors' formation, which has been established by several studies [94, 100]. It is reported that there is less soot precursor formation from the combustion of oxygenated fuels because of the remarkable effect on short chain fuel [66, 101, 102]. Westbrook et al [33] developed a chemical kinetic model to study the detail of reducing the amount of soot by adding n-heptane to different oxygenated groups (ester,

ether and alcohol). Soot emissions are reduced from the combustion of oxygenated fuels and this is attributed to the decreasing of the formation of soot precursor species due to the carbon atoms attached to an oxygen atom which inhibiting precursors from forming. Pepiot-Desjardins et al. [103] simulated the effectiveness of the reduction of soot formation (via the reduction of the formation of precursors) in mixtures of various oxygenated fuels, with a base fuel comprising n-heptane and 30% by volume toluene. Later, Cheng et al. [101] concluded that the effectiveness of alcohol is greater than that of ether in inhibiting the formation of precursors.

2.4.3 Nucleation/ inception of Particles

The nucleation process is defined as transitions of gas-phase precursors to the first particles (soot particle growth) which can occur at flame temperatures higher than 1300 K [14, 104]. The process of particle inception starts from the smaller fuel molecules after oxidisation and pyrolysis of the fuel [96]. The nuclei step is the process of the condensation reactions of gas phase species which lead to the first recognizable soot particles. This process generally involves the addition of small hydrocarbon radicals (acetylene and other precursors in the gas phase) to aromatic large molecules until they reach sufficient size to become a core particle with a diameter in the range of 1-2 nm [96] and 1000 amu [56]. The study presented by D'Anna et al. [105] proposed a model to describe the chemical growth for soot nuclei formation. Aromatics are rapidly formed in the main flame region according to the D'Anna model and they grow up to 2-, 3-rings attaining a concentration level in flames. The nucleation is still a complex process in the soot formation development and remains the least understood step during soot formation.

The particle core contains a large proportion of hydrogen (rate carbon/hydrogen) and later in the stage of surface growth will gradually decline (to about eight parts of carbon and hydrogen) [14]. Furthermore, the small size of these particles will not contribute significantly to the total soot mass [96], but they have a very significant influence on the final production of soot, as they act as nuclei for further growth surface. The nucleation occurs near the primary reaction zone where the temperature and the concentration of radicals and ions are maximum, for both premixed flames and diffusion [14]. Only nucleation rates are different depending on the amount of fuel-rich regions, and the amount of formed particle species in the previously mentioned processes (formation of precursors, formation of the first aromatic ring and growth PAHs). The nucleation particles are dependent on growth PAH and attached together with other PAHs to form nuclei particles. The nucleation/inception of particles (formation of precursor and involved in the growth of PAH species) from the oxygenated fuels is lower during the combustion process than for conventional diesel fuel.

2.4.4 Soot Particle Surface Growth

In this process, the soot mass is added to the surface of nucleated soot and the majority of soot mass (solid phase material) is generated in this step. Therefore, surface growth involves the attachment of gas phase species to the surface of the particles which comprises their incorporation into the particulate phase [94]. It is suggested by Harris and Weiner [106] that acetylene is the dominant growth species which makes the main contribution to increasing the soot mass. The general agreement in this process is that the major species in hydrocarbon flames is acetylene (C_2H_2); surface growth occurs by reactions of certain compounds in the gas phase through the reactive sites on the surface of

soot particles, which appear to be mostly acetylenes [56]. Hence, the soot mass is increased in this process, while the trend of the number of primary particles remains constant.

This stage usually occurs simultaneously to nucleation and in reality, the two processes are concurrent, as there is not clear distinction between the end of the nucleation and start of surface growth. Therefore, the length of the particles formation is important at this stage to determine the mass and volumetric amount of soot; whereas the number of particles is not affected by this process [96]. The surface growth rates of smaller particles is higher than the larger particle size because they have more active radical sites per unit mass [14].

Frenklach et al. [107] employed a simulation model to study the growth of PAHs and soot formation and also to calculate the growth rate of soot particles. They used the Monte Carlo method (or Monte Carlo simulation) to simulate collisions between the reactive species H, H_2, and C_2H_2 with the surface of the soot particles [51].

2.4.5 Soot Particle Coagulation

The growth of the primary particle can be produced by surface or by coagulation growth. Coagulation or coalescence occurs after collision between two approximately spherical primary particles to yield a larger single spherical particle via the physical process of coagulation [14, 108]. Therefore, the collisions between particles leads to a reduction in the numbers of soot particles, but an increase in the size of the particles, while maintaining a constant total of soot mass [96]. The particles are usually assumed to be spherical in this regime because they collide and coalesce to form new spherical particles. Regarding the fuel effect in this process, it is reported that the fuels with no aromatic content such as those obtained by the Fischer-Tropsch process and oxygenated fuels,

produced lower core soot, and therefore the rate of coagulation between particles is less than that for conventional diesel.

2.4.6 Soot Particle Oxidation

This process can be occurring at any time during the soot formation, the process of soot particle and PAH oxidation process is parallel to the surface growth. Soot oxidation starts from fuel pyrolysis to the agglomeration process and takes place when the temperature is higher than 1300 K. During fuel combustion, most carbon or hydrocarbon is converted to combustion products through the post-oxidation process; which generally become CO (partial oxidation), CO_2 (full oxidation), and H_2O. [14]. The oxidation process is divided into stages; (1) chemical oxygen with the attached fuel component (absorption); (2) desorption of the oxygen with the attached fuel component. The potential oxidation reactants of soot are molecular oxygen (O_2), radical (OH), and under fuel-rich and stoichiometric conditions. Furthermore, OH is mostly the largest contributor to the soot oxidation process under fuel-rich conditions via oxidative destruction of precursors; while soot is oxidised by both OH and O_2 under fuel-lean conditions [14, 94]. In addition, Haynes and Wagner [96] stated that about 10-20% of all OH collisions with soot could be effective at gasifying a carbon atom. Kennedy et al. [56] pointed out that other oxygenated species included O atom, H_2O, and CO_2 under some conditions probably have a vital role in soot oxidation. The time required for soot oxidation is highly dependent on two main factors: the mixing rate and temperature mixture. It is mentioned by Glassman et al. [109] that the temperature required for particulate oxidation is higher than 1300 K. According to the previous reports, soot formation rate reduces significantly with higher temperature during post-oxidation while increasing the oxidation rate [110].

Puri and Santoro [111] concluded that OH is an important for soot oxidant, particularly in areas of high temperature and low ratio A/F diffusive flame. Also, it is mentioned that the OH radical appears to be the main oxidant in stoichiometric and rich fuel conditions [14]. The use of oxygenated fuels leads to the reduction of the formation of precursors' soot and it also has a beneficial effect for the soot oxidation process. For example, the work by Cheng et al. [101], they studied the effect of various oxygenated groups on soot particle production; it was concluded that the use of oxygenated fuels increases the production of radicals such as O, OH and HCO, which enhances the oxidation of precursors and aromatic compounds. This leads to decreasing rates of nucleation and surface growth of soot particles. A phenomenon that should be considered in the oxidation is the aggregation or agglomeration.

Several documents [77, 101, 112] reported that combustion of oxygenated fuels (e.g. biodiesel and butanol blends) improved the oxidation of the soot particles more than the combustion of conventional diesel fuel (without oxygen content in the fuel molecule). It is anticipated that better oxidation is related to the greater amount of oxygen found in the surface of the primary particles, which makes them form a capsule type structure with an inner hole in the outer surface of the primary particle, and allows faster access of oxygen into the particle. Consequently, the soot particles are oxidized at a lower temperature and in less time.

2.4.7 Soot Particle Agglomeration and Aggregation

Although the concepts of agglomeration and aggregation are slightly different, both processes occur by particles combining into a single bigger spherical particle.

Furthermore, an aggregation is a combination of two roughly spherically shaped particles; while agglomeration occurs when primary particles stick together to form a cluster of soot (large group of primary particles) which may not be spherical. Agglomeration is the extension of the soot particle coagulation process. The soot particles may form a chain of discrete spherules (spherical agglomerate of particles) at a final stage of agglomeration, which is likely to be due to electrostatic activity [113]. In most situations, the terms aggregation (aggregate) and agglomeration (agglomerate) are used interchangeably to refer to the result of collisions and coalescence between particles.

The soot particles combine together to form chain-like structures; it has been observed in some cases that they have a clumping form. It is reported that the primary particles have a spherical shape from the diesel engine, which then agglomerate to form long chain-like structures [14]. The size of the primary soot particles depends on the operating condition, injection type and injection conditions. It ranges between 20 to 50 nm with an average diameter of about 30 nm as documented by Lee et al. [114] and Bruce et al. [115]. The shape of the particles' agglomeration is seen to be chain-like at the end of combustion and typically ranges in size from 100 nm to 2 μm [116]. Once the primary particles have formed, larger compounds of several sizes of primary particles collide together to forming agglomerates. Hence, the collisions between the primary particles and agglomerates and then collisions between agglomerates together may occur. This is depending on the relationship between the particles' distance, size of the particle, agglomerates between successive collisions, pressure and temperature. There are different types of agglomeration shape depending on the fractal dimension (D_f) [117].

In most of the references, the values of the fractal dimension are obtained from two-dimensional images by using a TEM (Transmission Electronic Microscope). The

values of the fractal dimension depend on the engine type, mode of operation and fuel used; the type of the majority of the collisions was found from the final shape of the agglomerates [114, 118]. A brief literature review will be presented in this chapter which will show and discuss the fractal dimension values.

The fuel properties can exert some effect on the agglomeration according to the size and number of the primary particles. For example, the combustion of oxygenated fuels produces a lower number of primary particles than conventional fuels and a smaller size of primary particles, as well as the agglomerates also being less [77, 119]. It is believed that for diesel combustion the enhanced net formation rate of particles increases the likelihood of collisions and further aggregation, leading to a higher number of primary particles.

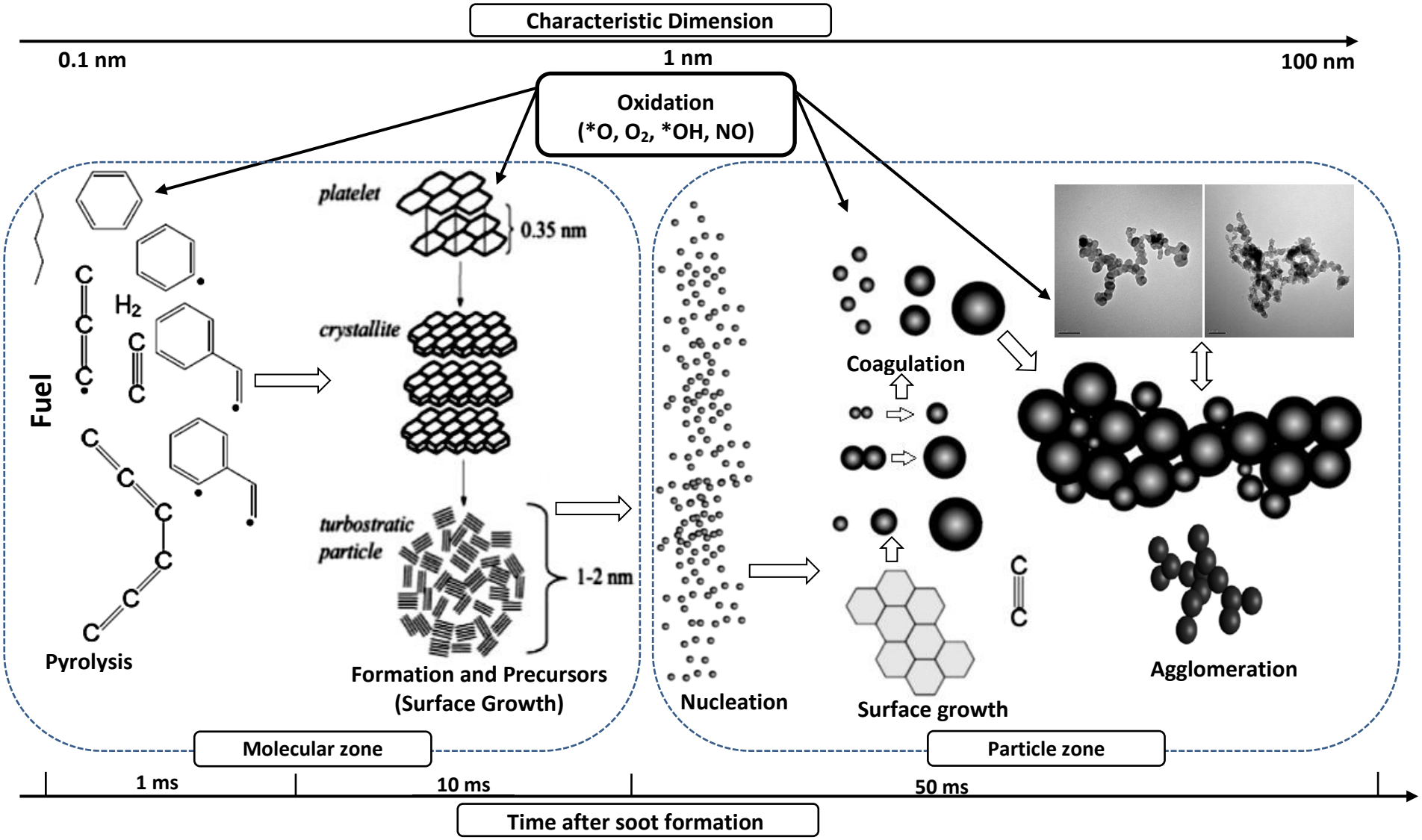

Figure 2.9: Schematic representation of the fundamental formation and oxidation mechanism of diesel soot particle in combustion [94, 120]

2.5 SUMMARY OF SOOT FORMATION PROCESS

Figure 2.9 displays an indication of the changes that occur in soot formation processes with time from the pyrolysis process to soot agglomeration, within the diesel combustion process. Amann et al. [113] indicated that a complex series of chemical and physical processes represent the steps of soot formation and oxidation which may occur concurrently in a given elemental mixture packet. Under a normal operating condition, the elementary soot particles from various combustion processes do not show much variation in size within the range of 20-40 nm. The size of soot particles (primary and agglomerated) from different combustion systems are listed in Table 2.1 with different measuring methods. For example, the average size of primary soot particles and agglomerated soot from engine-out can be in the range of (10 to 70 nm) and (100 to 300 nm) respectively as shown in Table 2.1.

Table 2.1: Size of primary and agglomerated soot particles from different combustion systems using different measuring methods

Type of combustion	Method of measurement	Soot primary size (nm)	Soot agglomerate size	Ref.
In-cylinder	Optical diagnostic (scattering/extinction, & radiation/scattering)	10-40 nm		[121]
	Optical diagnostic (scattering/extinction, & radiation/scattering)	10-40 nm		[122]
	Laser-induced incandescent (LII)	30-100 nm		[123]
	Time-resolved laser-induced incandescent (TR-LII)	25-80 nm		[124]
Engine out	Transmission Electron Microscopy (TEM)	17.5-32.5 nm		[125]
	Scanning Mobility Particle Analyser (SMPS)		10-400 nm Peaks around 50-60 nm	[125]
	Scanning Mobility Particle Analyser (SMPS)		7-250 nm Peaks around 50-90 nm	[126]
	Scanning Electron Microscope (SEM)	35-45 nm (SMD)		[127]
	Centrifugal sedimentation analysis		120 nm	[127]
	Scanning Mobility Particle Analyser (SMPS)		10-500 nm	[127]

	Transmission Electron Microscopy (TEM)	10-45 nm (mean 25 nm)		[55]
	Scanning Mobility Particle Analyser (SMPS)		10-120 nm	[128]
	Transmission Electron Microscopy (TEM)	10-50 nm		[124]

2.6 SOOT PARTICLE MORPHOLOGY AND NANOSTRUCTURE

Due to the stringency of the forthcoming emissions' regulations, engine manufacturers have focused more attention on diesel exhaust particles (mass and number) because it's now considered a serious problem in diesel engines [129]. The physical properties of soot particles can be described by the measurement of the total mass, number concentration and size distribution through the exhaust gas pipe. A scanning mobility particle sizer (SMPS) is used to measure the particle size distribution (PSD). More detailed information can be obtained by collecting soot particles by inserting a TEM (Transmission Electron Microscopy) compatible grid (copper grids) into the tailpipe flow of an engine and then analysing them by HR-TEM (high resolution transmission electron microscopy) imaging [55, 125, 130]. Hence, TEM analysis is considered the best method for analysis of soot particles and it has been widely used to better understand soot particle morphology. However, the TEM image technique has been improved by the increase in the level of the magnification of the microscope, which reveals the structure of soot particles along the axis of tailpipe emissions during the combustion process. Furthermore, it shows the shape and

internal structure (with high magnification) of the primary particle composed from an agglomerate of soot particles (see Figure 2.10 a-c).

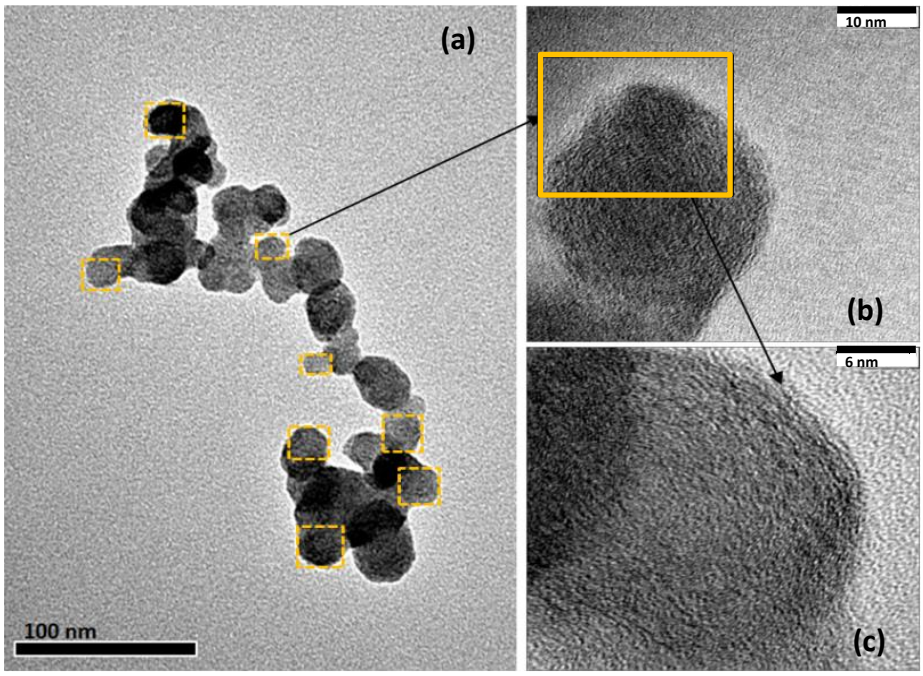

Figure 2.10: Sizing method of primary soot particles from diesel fuel combustion [77, 117]

2.6.1 Soot Particle Morphology

As discussed above, the fractal dimension parameter is used to quantify the irregularity of particles. This section provides a brief literature review on the effect of the mode of operation and fuel on parameters related to the morphology of the soot agglomerates (see equation (2.13)), such as fractal dimension (D_f), the average number of primary particles (n_{po}), and radius of gyration (R_g). Lapuerta et al. [117] presented a method to obtain the morphological parameters (e.g. D_f , R_g, and n_{po}) of individual agglomerates. Soot particles generated from diesel combustion have a fractal structure that

can be characterised based on the following power law relationship, as shown in equation (2.13).

$$n_{po} = K_f \left(\frac{R_g}{d_{po}} \right)^{D_f} \quad (2.13)$$

Where n_{po} is the number of primary particles; R_g is the radius of gyration of the agglomerate; K_f is the dimensionless prefactor of the power law relationship; and d_{po} is the average diameter of the primary particles. It reported that the fractal dimension decreased with the increasing of both air/fuel ratio and exhaust gas recirculation (EGR) [68]. On the other hand, the fractal dimension increases with a higher engine load. The distance between the centroid of the aggregate and the centre of primary particles is defined as a radius of gyration. It is reported that the overlapping factor should provide variations (0-0.8488) depending on the number of primary particles and fractal dimension of the soot agglomerate [117]. Medalia and Heckman [131] proposed the overlapping effect by means of another type of expression as explained below.

$$n_{po} = \left(\frac{A_p}{A_{po}} \right)^{z'} \quad (2.14)$$

Where *z'* is the overlapping through a potential expression and also defined as an overlapping exponent. The overlapping exponent has different values according to the literature; for example, Medalia and Heckman [131] proposed that *z'* = 1.15, while it is coincidentally obtained by many authors [132-134] that *z'* = 1.09 from different

experimental procedures. Finally, Meakin et al. observed that for a fractal dimension higher than 2, the exponent appeared as $z' = D_f / 2$.

$$K_f . \left(\frac{d_g}{d_{po}}\right)^{D_f} = \left(\frac{A_p}{A_{po}}\right)^{z'} \quad (2.15)$$

The size and morphological characteristics of the soot particles is studied via a heavy engine by Lee [114, 135] and a light engine by Zhu et al. [136] in different modes of operation. Lee et al. [114, 135] analysed the effect of engine speed on morphological parameters, and they concluded that the dominant factor on the primary particles is the pressures and temperatures reached in the cylinder. Lapuerta et al. [68] presented results on the effect of the air/fuel (A/F) ratio, EGR, and engine speed on the number of primary particles that make up the agglomerates. They found that the number of primary particles decreases exponentially with the increasing of the A/F relationship; while it increased with the increasing of the EGR. Also, there was an increase in engine speed resulting in a slight decrease in the number of primary particles, because the less time available for collisions between particles resulted in a lower number of collisions and therefore agglomerates were formed by a smaller number of primary particles. Ishiguro et al. and Al-Qurashi et al. [130, 137] showed that the physical properties of the soot were strongly influenced by exhaust gas recirculation (EGR), which leads to enhanced soot oxidation rates [130]. The oxidation behaviour of the diesel soot decreased as the time of regeneration increased during the regeneration process of a DPF [138].

The fractal dimension can be calculated from the soot agglomerates that collect from the exhaust gas (see the methodology in Chapter 3). It is stated that the values of the fractal dimension of the agglomerates from a light engine are consistently lower than those

of a heavy engine [136]. The D_f is calculated by a method published in [117] (the same used in this thesis) from the radius of gyration and projected agglomerates using TEM micrographs for the area and the number of primary particles.

Luo et al. [139] calculated the D_f of soot agglomerates that collected in diluted conditions from different vehicles, characterized by having a different number of cylinders. In addition, the values of the fractal dimension were obtained in the range between 1.64 and 1.77, matching values with those obtained in a study where agglomerates were collected in an undiluted condition. Furthermore, it was found in the same work that the fractal dimension is approximately constant with the same number of cylinders; while if increasing the number of cylinders, the volume of each cylinder leads to increases in the fractal dimension. This is due to greater volume per cylinder which results in more power, higher temperature, producing more efficient combustion, and increased oxidation.

Park et al. [140] also calculated the fractal dimension and density of agglomerates effectively emitted by a diesel engine in different modes of operation. The fractal dimension is calculated from the relationship between the diameter and mass mobility, by a SMPS system and APM (Aerosol Particle Mass Analyser), as well as obtained from TEM micrographs using an agglomerate in diluted conditions. In operating modes tested, it concluded that fractal dimension decreases with the increasing of the degree of loading and this is in agreement with Maricq et al. [141]. In fact, Virtanen et al. [112] obtained fractal dimensions between 2.6 (high load) and 2.8 (low load) and these are larger than the other studies presented. However, the decrease of the fractal dimension with the degree of loading is justified because a higher degree of load implies an increase in fuel consumption and a decrease in the air/fuel relationship. This results in an increase in the number of primary particles and the agglomeration produces irregular particles with

less fractal dimension. In the case of oxygenated fuels, Song et al. [142] and Fayad et al. [77] indicated that the combustion of oxygenated fuels produced a lower number of primary particles, radius of gyration, and fractal dimension of the soot agglomerate than in the diesel fuel combustion.

2.6.2 Soot Particle Nanostructure

Both the size of the primary particles and the microstructure are the result of formation processes of precursors, nucleation, surface growth and oxidation, and therefore monitoring or observing these features leads to obtaining information about how were these processes. Over the years, knowledge and interpretations related to the microstructure/nanostructure of the primary particles have changed and there have been new techniques incorporated along with micrographs obtained by TEM to discover more information about soot particles. The structure of soot particles emitted from the combustion of diesel engines can be analysed from high resolution TEM images (see Figure 2.10-(b) & (c)) by using HR-TEM. Usually, the soot agglomerate particles consist of tens to hundreds of primary particles agglomerated together, forming chain-like structures. The primary particles are considered to be the fundamental unit of the soot agglomerates with diameters of 10-50 nm (composed of elemental carbon). The nanostructure of primary soot particles is formed from long fringes arranged concentrically at the edges and short fringes randomly oriented in the centre [143]. A significant amount of the soot formed is subsequently oxidized in the diesel combustion process. The varied oxidation rates that were observed in the literature from using HR-TEM images can be attributed partly to the differences in nanostructure between the soot particles. The end of soot's nanostructure develops during the inception and growth events. Also, it was found that the interlayer spacing of the carbonaceous soot was in the range of 0.365 nm and this

value is higher than graphite at a value of 0.3354 nm. Many of the studies have been devoted to investigating the effects of fuel composition with additives and engine operating conditions on soot formation, through experiments and soot models [56, 144, 145]. Meanwhile, less attention has been given to the impact of these parameters on soot's nanostructure.

Lipkea, et al. [146] and Kawaguchi, et al. [147] proposed some basic information about the microstructure of primary particles. The fundamental structure of the primary particle is atomic, forming carbon networks of a multitude of hexagonal cells, which in turn are joined together to form graphene sheets (Figure 2.11-(a)). Furthermore, these graphene sheets join together to form crystals (Figure 2.11-(b)), which in turn bind with different orientations to form primary soot particles (order of 10^3- 10^4 crystals and 10^5-10^6 carbon atoms per primary particle) (Figure 2.11-(c)).

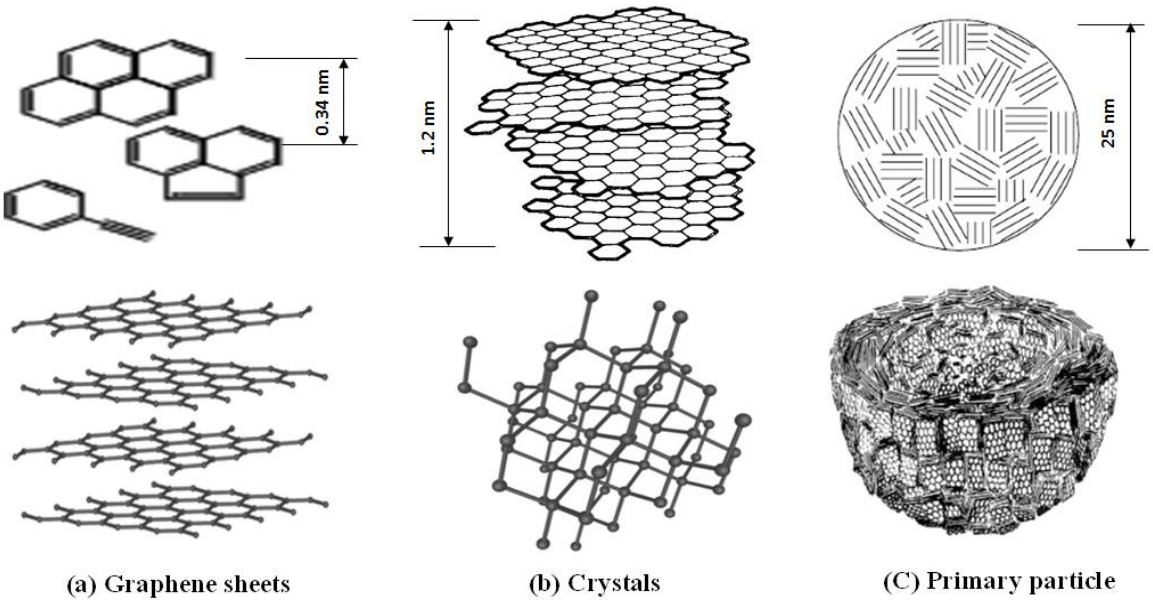

Figure 2.11: Schematic of primary soot particle formation (strucure); adopted from [148]

The platelet represents the basic unit of the crystallites which is a hexagonal face-centred array of carbon atoms. The HR-TEM image shows the internal structure of a

soot particle; which includes the outer shell and inner core as shown in Figure 2.12. The structure of the outer part of the spherule is rigid, more than the inner core and for this reason the inner core is considered structurally less stable.

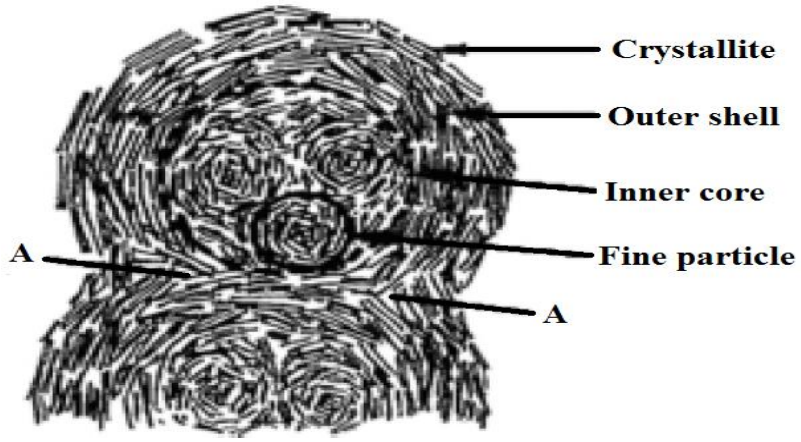

Figure 2.12: HR-TEM shows the diesel particle with finer resolution [149]

The parameters of size, orientation, and organization of the graphene layers represent soot nanostructure. In another common study related to soot nanostructure, Lee et al. [135] analysed the nanostructure properties of diesel soot by using HR-TEM and Raman spectroscopy. Al-Qurashi et al. [130, 150] showed that the nanostructure of soot particles (average number of graphene layers) changed according to the rate of soot oxidation. The nanostructure parameters of soot particles (Figure 2.13) such as interlayer spacing (d_{002}), thickness of the graphene layer (stacking height) (L_c) and the crystalline basal plane diameter (L_a) are derived from an HR-TEM image [151-153]. High-resolution transmission electron microscopy provides direct information on the graphene layers of soot particles [130, 154, 155].

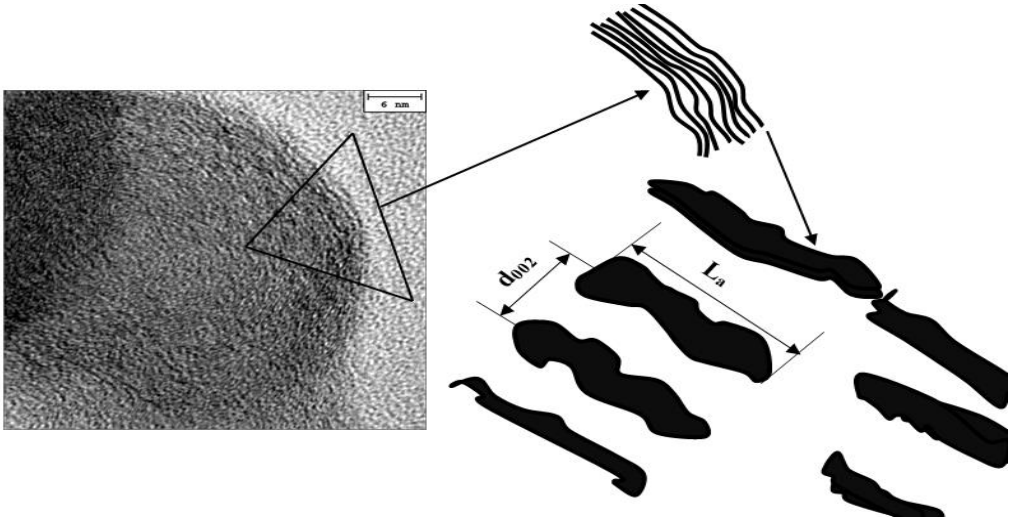

Figure 2.13: Schematic diagram of magnified extracted structure showing example measurement of microstructure parameters (diesel combustion): interlayer spacing (d_{002}) and lattice length (L_a) [77]

The microstructure of the primary particles is similar to that of graphite, in which the crystal lattice is formed as hexagonal structures which are defined as graphene sheets. In the case of the diesel particulate, some authors agree that the diesel soot inter-layer distance is similar to that of graphite structures [156], and also have stated by others that the different heat treatments of particles can change the internal structures (number of layers, length and alignment) [157]. When the crystal orientation is random and unsystematic it will lead to a different form of soot structure such as onion-like morphology, which proposed by [154, 158, 159] as shown in Figure 2.14-(a). Lipkea et al. [146] observed that some soot structure occurs less frequently than others (turbostratic graphite structure) and is formed by small plates of undefined orientation (see Figure 2.14-(b)). Crookes et al. [160] and Zhu et al. [161] suggested that soot structure has purely turbostratic layers (see Figure 2.14-(c)); while other authors observed that primary particles from diesel engines have two distinct regions (inner core and outer shell) [73, 154, 162-

164] (see Figure 2.14-(d)), which are formed by multiple spherical nuclei surrounded by several graphite layers (multi core structure).

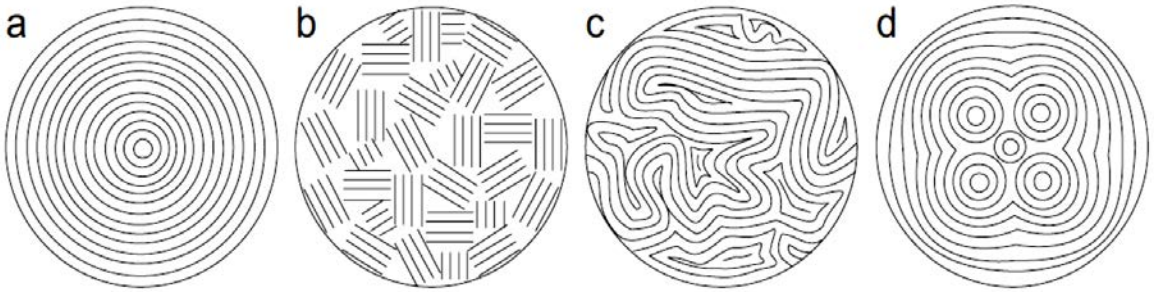

Figure 2.14: Types of internal structures (microstructure) of the soot primary particles: (a) onion type structure, (b) turbostratic graphitic structure, (c) purely turbostratic structure, and (d) multi core structure [55]

The interlayer spacing and internal structures of primary soot particles are measured from TEM images with high magnification (Figure 2.13, left), which allows the assumption that the particles are formed by spherical layers. The interior layers of soot particles are easily oxidizable; whereas the outer region has a rigid structure [165]. This seems to indicate that the primary particles can be easily oxidized at the beginning of their formation (before this structure becomes more rigid) [166]. Vander Wal et al. [163] studied the microstructure of the particles that collected in a DPF; it has been found that particles have a crystalline structure in the outer region, while the inner region appears to be hollow. The inner and outer regions of the crystalline structure are greater or lesser extent structure depending on the degree of oxidation (oxidation rate), which it has been subjected in the DPF. Therefore, the microstructure of the diesel primary particles may be different in terms of the distance between the sheets forming the crystals; while the orientation can determine the degree of crystallinity of the particles. Additionally, all these aspects seem to present

more variation depending on the fuel and modes of engine operation, which defines the orientation of the crystals. This can provide information on how they have been through the processes of particle formation among other things such as oxidation/reactivity of soot. Most studies find that particles produced from a low load of engine operation are more reactive than at high load [167]. The reactivity of soot particles depends on the temperature and time necessary to oxidize the soot [142, 158, 168, 169]. For example, a microstructure with a high degree of organization would be more difficult to oxidize due to lower temperature and shorter time for soot oxidation [142, 158].

Soot planar graphitic layers are less reactive than soot and are more curved and disorganized. It is reported that there is a great difference in soot structure derived from different fuels [169]. The different organisation of soot from different fuels is a feature of the crystallite structure of soot particles. It was found by Vander Wal and Tomasek et al. [169] that there is a remarkable difference in soot microstructure and correspondingly oxidation rates from pyrolysis of benzene, ethanol, and acetylene under the same operating conditions. Soot nanostructure from benzene fuel combustion has a lesser degree of curvature than that for acetylene soot.

Boehman et al. [168] studied the effect of oxygenated fuels (mixture of 20% biodiesel with diesel) on soot oxidation and reactivity. The authors concluded that the particles' oxidation was emitted from the combustion of biodiesel more easily than to the diesel fuel combustion. In other work by Fayad et al. [77], it was established that the particles emitted from the combustion of a butanol blend were easier to oxidise than those emitted from the combustion of biodiesel and conventional diesel. The oxygenated fuels begin by the oxidation of the outer surface of the primary particles (which is in contact with oxygen). This outer part of soot particles usually has an onion type structure and

therefore is difficult to oxidize. The oxygen molecules' content in oxygenated fuels can reach inside the primary particle that have structure which is more disordered than the external layer (more rigid) in which approximately 75% is reached by oxidation. The characteristic of particulates from butanol blend reach this stage of the oxidation process before those issued by diesel fuel, due to groups as many oxygenates present on the surface of the particles. Also, Raman spectra have showed that the butanol-diesel blend (20% and 100) produces soot with of more disorder than soot produced from diesel fuel combustion. Therefore, the oxidation stage of the inner part of the particle leads to a large decrease in the mass of particles but not the diameter. Subsequently, coalescence occurs between the surfaces of the various primary particles at the last step of oxidation and takes minimum energy for configuration.

2.7 RENEWABLE FUELS IN DIESEL ENGINES

A renewable fuel is defined as a fuel synthesized from a sustainable source (from biomass source) with no adverse effects on engine operation and maintenance. It is more attractive and has a lower environmental impact [170] in terms of exhaust emissions than the other potential energy sources because it delivers a similar performance to the diesel fuels. Biofuel production is derived from various sources and can be considered as a short/medium term alternative to diesel fuel in the future energy chart. Nowadays, bioalcohol and biodiesel are receiving wide attention as well as having the largest production and consumption rate in the world fuel market in terms of the transport sector. The European Union market targets for biofuels to be available in the transportation sector by up to 10% by 2020. Biofuel production statistics in European countries in 2014 are shown in Figure 2.15 and there is a high level of production in Germany and Spain compared with the rest of Europe. Furthermore, the transformation of vegetable oils is the

most common process to produce biofuel by the transesterification process; while bioalcohol can be produced via the alcoholic fermentation of sugar rich cereal crops. The first generation biofuels (biodiesel and bioalcohols) are generally obtained from edible feedstock. To increase the amount of biofuel, new technologies are being developed to produce second-generation biofuels which can be achieved by utilising non-edible feedstock (waste cooking oil, jathropa, castor oil and grease tallow) to reduce the competition with food production.

COUNTRIES		Production [Ml/yr]
AT	Austria	495
BE	Belgium	741
BG	Bulgaria	378
CR	Croatia	55
CY	Cyprus	20
CZ	Czech Republic	502
Dk	Denmark	250
EE	Estonia	35
FI	Finland*	400
FR	France	2445
DE	Germany	4655
EL	Greece	702
HU	Hungary	158
IE	Ireland*	74
IT	Italy	1837
LV	Latvia	156
LT	Lithuania	147
LU	Luxemburg	20
MT	Malta	5
NL	The Netherlands	2505
PL	Poland	1269
PT	Portugal	590
RO	Romania	407
SK	Slovakia	158
SI	Slovenia	108
ES	Spain	4194
SE	Sweden	282
UK	United Kingdom	505
EU-28	**TOTAL**	**23,093**
CH	**Switzerland**	**8**

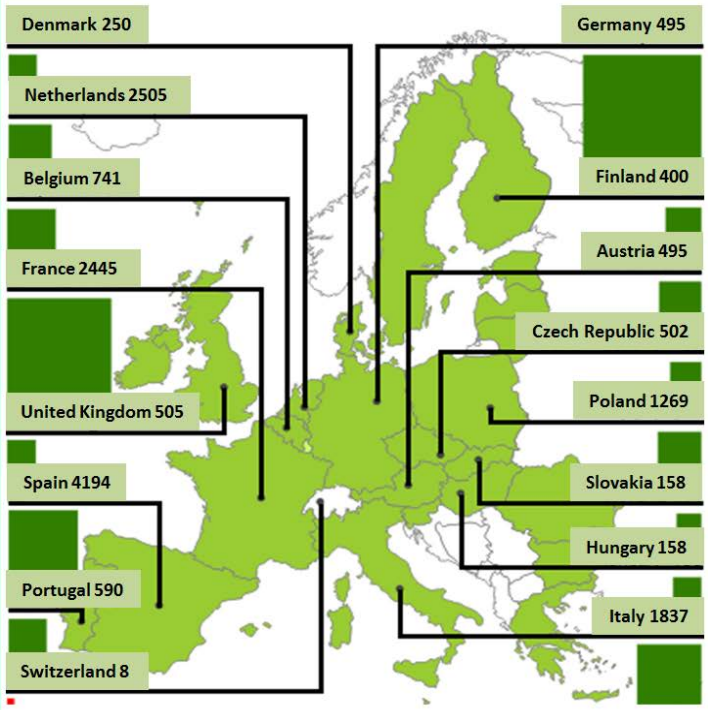

Figure 2.15: Biofuel production statistics in European countries in 2014, [171]

2.7.1 Butanol as a biofuel in diesel engines (production and combustion)

Butanol (first-generation fuel) is a competitive candidate to be used in engines and can be produced from fermentation of renewable feedstock [5, 172]. It can be produced

from maize, sugar cane, sugar beets and conventional production processes. Furthermore, a lignocellulosic process can be used to produce butanol through the fermentation because it has the ability to diversify potential feedstocks for bioalcohols enormously. In diesel engines, butanol has also been considered as a feasible fuel for use due to its higher energy density, higher miscibility in diesel fuel and better blending stability than ethanol [12, 173]. A ternary blend alcohol-diesel-biodiesel is considered to compensate for the low cetane number and lubrication properties of the alcohol fuels. On the other hand, the engine performance, exhaust emissions, lubricity and fuel miscibility are affected by variations in butanol composition in fuel blends [174, 175]. Some properties of butanol fuel such as its short chain and oxygen content can provide a significant reduction in unburnt hydrocarbons (HCs), PM and carbon monoxide (CO) emissions [12, 176].

In particular, butanol has good indissolubility (alcohol molecules contain alky, hydroxyl, and length of carbon chains) with diesel fuel and it can be blended with diesel without co-solvents. Yao et al. and Dogan [177, 178] studied the performance and emissions of a direct injection diesel engine fuelled with different butanol percentages (0%, 5%, 10%, 15%, and 20%) in diesel fuel. However, the butanol showed similar thermal efficiency when used in compression ignition engines [11, 179] compared to that of diesel fuel, due to the presence of the oxygen content in the molecule fuel and the high burning velocity of butanol [180]. Furthermore, more oxygen content in butanol allows cleaner and more complete combustion, which enhances soot oxidation, as well as more premixed and lower C/H; which can be another reason used to support the soot emissions' reduction. As a consequence, it is reported that a butanol blend produces lower PM (number, concentration, size) in an internal combustion engine than conventional diesel fuel [77]. Likewise, oxidation rates inside the crucial zones increase with higher temperature and lower C/H ratio [12].

Also it is reported that the THC emissions level is higher from the combustion of ethanol blends than butanol blends, due to the higher heat of vaporization of ethanol [5]. Furthermore, it is indicated that ethanol blends' combustion produces lower carbon monoxide (CO) emissions than diesel fuel combustion and higher than butanol blend [181, 182]. On the other hand, regarding to the CO, it is suggested that butanol blends in some cases increase the CO emissions due to the heat of vaporization [183].

The NO_X in the exhaust is considered as one of the most difficult substitutes to be reduced in IC engines. Butanol blends have conflicting effects on NOx emissions in diesel engines as suggested by some researchers [10, 12, 184]. However, the temperatures inside cylinder, oxygen concentration and residence time for the reaction to take place are significant parameters which can affect NO_X formation. Also, the relatively low cetane number of butanol has a potential to increase the ignition delay which results in increasing the combustion temperatures (premixed combustion mode) and this leads to higher NO_X emissions. Additionally, the oxygen content in butanol could be another reason it assists in the NO_X formation inside the combustion cycle. Another work by Xing-cai et al. and Li et al. [10, 184] documented that the high heat of vaporization of butanol tends to decrease the flame temperature, which results in lower NO_X emissions.

2.7.2 Butanol- diesel blends

Butanol has excellent properties (including good stability, higher energy density, good indissolubility, reduced ignition related problems, and provides easy distribution through existing pipelines) and is thought to be an important future fuel [185, 186]. Higher miscibility of butanol in diesel fuel at any percentage without a blend stability problem over a wide range of temperatures and water content when compared with ethanol [187].

The physical and chemical properties (cetane number, heating value, and bulk modulus related to the density) which have a direct noticeable effect on emissions and combustion characteristics of a diesel engine are listed in Table 3.3 (in Chapter 3). However, biodiesel can be added to the blend (alcohol-diesel blends) to avoid any problems caused by the density of fuel blends.

To define the percentage of butanol in diesel fuel, B factor is commonly used to classify the blend, such as B20 which composed of 20% butanol and 80% conventional diesel. The low cetane number in some of alcohols will reduce the total cetane number of the fuel blends and this is not recommended for use directly in an engine without modification. He, et al. [183] recorded that ethanol reduced the cetane number by 10% when blended more than 10% with diesel fuel. A consequence of that, the longer carbon chain and high cetane number of butanol, can be more attractive than the shorter carbon chain of ethanol for use in diesel engines.

2.7.3 Biodiesel

2.7.3.1 Biodiesel production and motivation

Biodiesel is a fuel produced from straight vegetable oil, waste cooking oil, animal (oil/fats), tallow and renewable resources; it can be considered an environmentally friendly alternative fuel. Also, it is the most important biofuel in European countries and represents around 80% of the total transport biofuels market. In the EU, biodiesel was the first biofuel used as a fuel in the transport sector in the 1990s. Figure 2.16 shows how the biodiesel production increased in the EU, mainly in Germany, Spain, and Benelux.

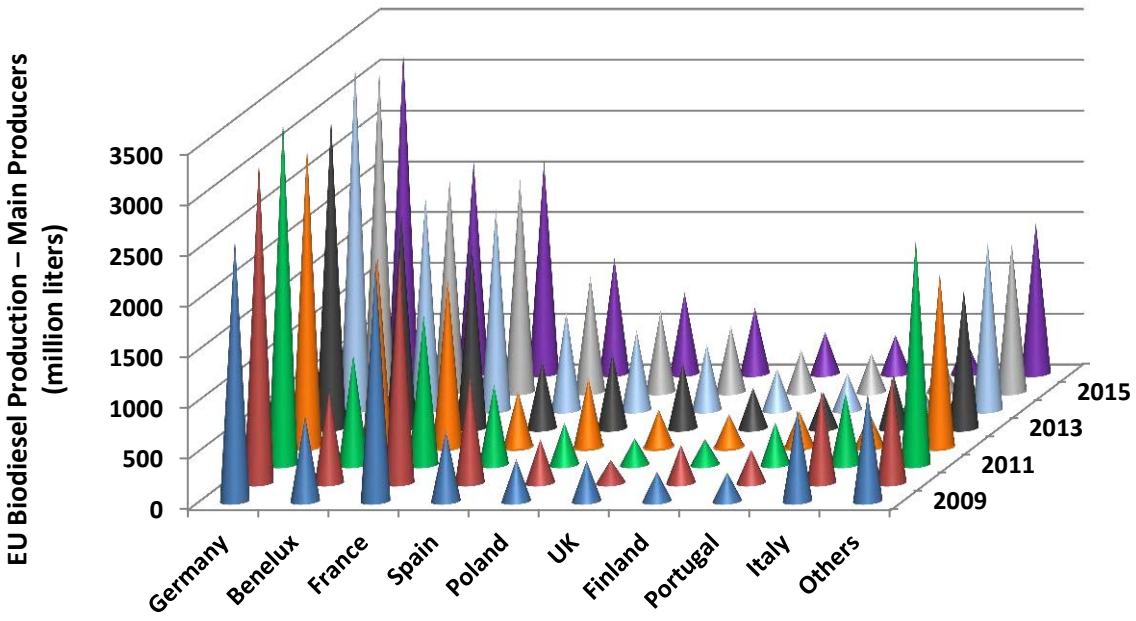

Figure 2.16: Biodiesel production in the EU from 2009 to 2016 [188]

The production of a sample form of biodiesel is outlined in Figure 2.17. Renewable feedstock in the form of triglycerides reacts with an excess of alcohol in the presence of a catalyst to yield biodiesel with a high oxygen content, which reduces the viscosity and degradation of renewable feedstock in the form of triglycerides [189]. The biodiesel supply and demand in the EU are illustrated in Figure 2.18.

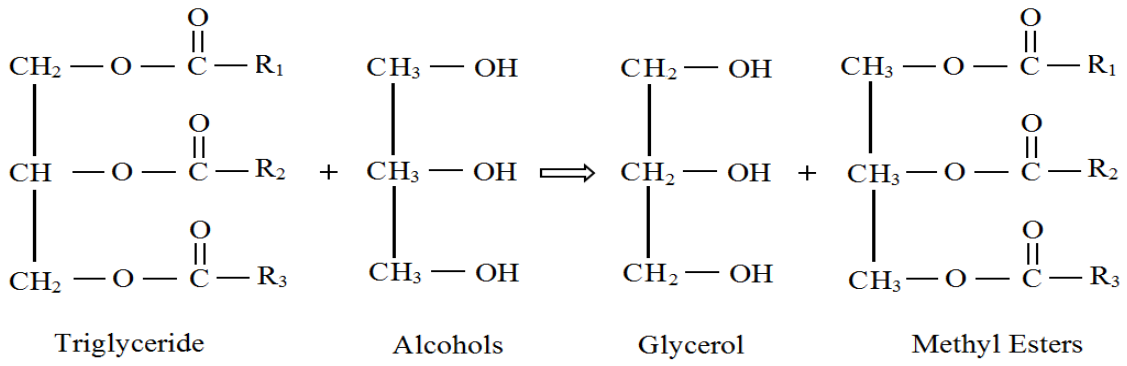

Figure 2.17: Transesterification reaction [190]

Biodiesel can be used directly in compression ignition (CI) engines or by being blended with petroleum diesel at any percentage level to create a biodiesel blend with little or no modifications [191]. To meet the European standard EN 14214, a pure form of biodiesel (R100) or neat biodiesel (rapeseed crop) is used as an automotive fuel. Table 2.2 presents the specific fatty acid profile of rapeseed methyl ester, reference [192] is from a recent work (RME used in Chapter four). The physical and chemical properties of neat RME and the blend are detailed in Chapter 3 (Table 3.3). In addition, biodiesel is simple to use and has advantageous properties (high oxygen content, biodegradable, nontoxic, good lubricating properties) which can be a benefit for complete combustion in diesel engines [5, 32]. The chemical composition of biodiesel depends on the source of feedback which is a mixture of saturated and unsaturated methyl esters.

Table 2.2: Fatty acid profiles of Rapeseed Methyl Ester (RME)

Fatty Acid	**RME**				
	Structure	**References**			
		[193]	[194]	[195]	[192]
Myristic acid	C14:0	0.0	-	0.1	-
Palmitic acid	C16:0	5.0	3.3-6.0	4.4	4.51
Palmitoleic acid	C16:1	-	0-3.0	-	-
Stearic acid	C18:0	3.0	4-6	1.5	1.47
Oleic acid	C18:1	59.0	52-65	63.4	63.12
Ricinoleic acid	C18:1 OH	-			-
Linoleic acid	C18:2	21.0	18-25	19.9	19.85
Linolenic acid	C18:3	9.0	10-11	7.9	9.03
Gadoleic acid	C20:1	1.0	-	-	0.55
Erucic acid	C22:1	1.0	-	-	1.47

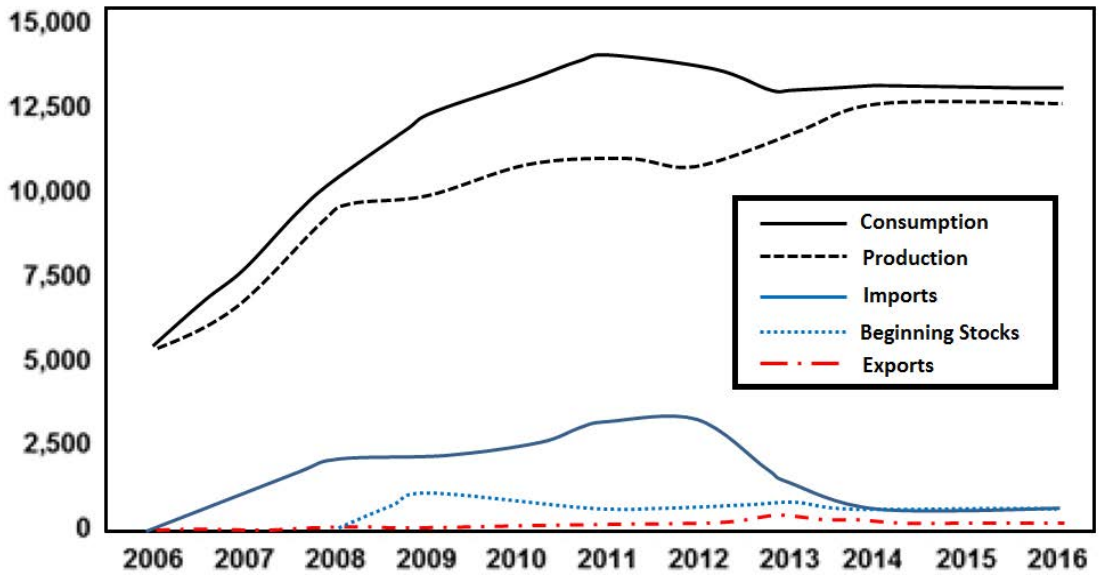

Figure 2.18: Development of biodiesel trend for supply & demand EU (Million Liters)' [188]

2.7.3.2 Engine emissions from first generation biodiesel combustion

Biodiesel (RME) combustion and emissions in direct injection CI engines have been studied by many authors in the case of pure biodiesel or blends with petroleum derived diesel [77, 182, 196-198]. Higher fuel consumption was recorded with biodiesel compared to diesel, to produce the same power output due to the lower heating value [199, 200]. Furthermore, biodiesel has a higher cetane number and higher bulk modulus which can improve the combustion process due to an advance in the start of combustion.

It is reported in the majority of the publications that biodiesel contributes to reduce gaseous emissions (THC and CO) and to produce less soot emissions but gives a minor increase in NO_X emissions [196, 201-203]. Additionally, many researchers have reported that the higher oxygen content of biodiesel is an important factor contributing to a reduction of THC and CO emissions, compared to diesel fuel operation. On the other hand,

there are some works which disagree and show no reduction in CO emissions [204, 205]. Numerous researchers have documented that significantly lower solid emissions (soot/carbon) are produced from biodiesel combustion with a higher portion of unburned fuel in the soluble organic fraction (SOF) [32, 74, 206]. Schaberg et al., Lapuerta et al., and Tsolakis, et al. [55, 198, 207] reported that the properties of biodiesel such as higher density and higher bulk modulus can affect the engine operating conditions (start of injection timing, injection pattern and the amount of injected fuel). However, it has been shown that there is no difference recorded in injection timing in a high pressure common rail diesel engine between biodiesel and diesel fuel [208].

2.8 EFFECT OF FUEL INJECTION STRATEGY ON SOOT EMISSIONS IN DIESEL ENGINES

The common rail fuel injection system is widely used in diesel engines, due to its capability of controlling the injection parameters (injection pressure, timing, duration and number of injections). Therefore, this system is able to inject fuel at high pressures, select the number of injections as well as splitting the injections, which can effectively control the spray characteristics and the combustion process [47]. A wide range of injection pressures can be used in common rail systems and this expands the potential for reducing exhaust emissions and improving combustion efficiency [209]. At high injection pressure and advanced injection timing conditions, they have been shown to produce lower levels of soot or smaller particle sizes in diesel engines fuelled with diesel fuel [144, 210, 211]. Previous reports also stated that the maximum pressure inside the combustion chamber improved combustion performance and reduced the particulate emissions [212, 213].

It is previously known that the fuel injection parameters are significantly impact on the engine-out soot emissions. It is reported that optimisation injection timing and

increasing the injection pressure leads to lower soot levels or smaller particle sizes [144, 211]. Furthermore, advanced fuel injection timing has caused a significant impact on soot formation in diesel engines because of the main combustion event moving backwards towards TDC during the expansion stroke which results in improvement of thermal efficiency [214]. To explain, a greater fraction of the fuel would be burned with high temperature as well as soot oxidation being increased [97]. Advanced injection timing makes a significant impact on soot formation because a greater fraction of the fuel would be burned with higher ambient temperature. It is reported by Pickett and Siebers [210] that increased temperature results in reducing soot formation, as well as increased soot oxidation. Another important parameter in diesel engines is injection pressure, which has a significant influence on soot formation and oxidation. Several studies have been published highlighting the influence of the advanced injection timing [215] and high injection pressure [212, 213] on reducing the soot emissions. This occurs because of enhanced fuel-air mixing, shorter combustion duration (faster time to reach the maximum pressure), shorter residence time for soot to form and grow [210, 211].

To get a better understanding of size and structure of soot particles in diesel engines under different injection strategies, researchers have conducted TEM [55, 118, 125, 161, 216] to measure soot characteristics with different injection timings and pressures [217].

2.8.1 Post-injection Emission Reduction

Post-injection or secondary injection is originally used in diesel engines for the purpose of diesel particulate filter regeneration, which starts after the main injection and takes place during the expansion or 200° after TDC. Kong et al. [218] proposed many methods on temperature control for the DPF regeneration. Common rail fuel injection systems in modern diesel engines provide good flexibility by multiple injection strategies (pilot, main and post-injection), which can be interesting for better combustion and emissions. Many studies have been reported that the multiple injections reduce the peak cylinder pressure, combustion noise and pollutant emissions in a single cylinder diesel engine [1, 219]. Yamamoto et al. [41], Chen et al. [44] and Benajes et al. [220] stated that the injected fuel late in the cycle leads to an increase in hydrocarbon (HC) emissions and slightly increased fuel consumption, due to a proportion of the fuel not being combusted. In addition, it is found that the exhaust gas temperatures (EGT) increased with late combustion caused by post-injection [221]. The impact of fuel post-injection on engine out gaseous emissions and PM has also been investigated [44, 222, 223]. The temperature increase late in the combustion cycle due to the post-fuel injection, which can enhance soot oxidation, was produced during the main combustion event [44, 224-227]; but this is reported to be dependent on the engine calibration and operation conditions. Some studies have reported PM increase with post-injection at high engine loads and speeds [222]. In some cases post-injection also contributes in the reduction of engine-out NO_X due to the formation of nitrated-hydrocarbons through the reactions of NOx with HC radicals [228, 229]. It is reported that CO and THC are reduced with post-injection and sharply increased with later post-injection timing (after 70 CAD ATDC) [42]. Late combustion caused by post-injection increases the level of THC emissions as the late injected fuel is not burnt in

the combustion chamber [41, 221, 223]. In this way, HCs are oxidized in the DOC, increasing considerably the temperature of the exhaust upstream of the DPF and trapping a high proportion of the soot flowing in the exhaust stream [42, 230, 231]. It is documented that the main-post-injection increases the rate of soot oxidation in the combustion cycle due to the enhancement of the gas mean temperature and air/fuel mixing; this leads to the reduction in number and diameter of the primary particles [43, 232]. Storey et al [233] studied the effect of post-injection on hydrocarbon speciation from 40° crank angle (CA) to 100° CA after top dead centre (ATDC). They observed that delayed post-injection timing increases the light hydrocarbons; while the change in heavy hydrocarbons was negligible. In addition, it was more beneficial for the production of light and reactive hydrocarbons (e.g propylene) for NO_X aftertreatment.

Some universal conclusions can be drawn from studies reported on the benefits of post-injection on PM reduction. There are four main theories that are used to define this trend: first, small amount of fuel quantity (10%) is injected after the main injection event (10-40 °CA) leading to an increase in the temperature late in the combustion cycle, which in turn starts to promote the soot oxidation [223, 234]. Secondly, there is improved combustion by late fuel injection in the cycle and this is due to the enhancing of air-fuel mixing [44, 223]. Thirdly, a reduced main injection duration leads to reduction of the soot emissions, as can often be done when using post-injection [220, 223]. Finally, post-injection can accelerate the main combustion according to the combustion acceleration phenomenon which in turn leads to reducing soot emissions [235].

2.9 LITERATURE SUMMARY

In this chapter, mainly concerns the impact of diesel engine emissions (mainly particulate emissions) on human health and the environment and methods for their reduction/oxidation have been reviewed. More advances systems will need to be developed to meet the long-term emission targets, even though significant advances for control of diesel exhaust gas emissions which have been reviewed during this chapter.

Firstly, many studies have focusing on the PM emissions' phenomenon, but still a gap in the literature on the PM characteristics (morphology and microstructure) needs to be understood. Therefore, the knowledge contained in the soot particle characteristics was highlighted to further understand about soot formation and oxidation from different fuels operating in a diesel engine. Secondly, improve diesel oxidation catalyst (DOC) activity and faster light-off was highlighted at low exhaust gas temperatures through individual or a combination of oxygenated fuels and injection strategies, while keeping a good compromise between efficiency, cost and emissions. Consequently, particulate matter (PM) is one of the main problems currently faced the catalyst; however there are still obstacles that need to be solved and understand, the methods to implement these on-board the vehicle need to be made practical.

Finally, the oxygenated fuels improve the combustion and reduce engine emissions without impairing engine performance. The oxygen content in the fuels molecules can provide major reduction in the PM as well as change the shape and structure of soot particles. However, investigate the incorporation between oxygenated fuels and aftertreatment systems were presented to increase the catalyst activity and reduce the dependence on active regeneration.

CHAPTER 3

EXPERIMENTAL FACILITIES SET-UP AND MATERIALS

This chapter describes the experimental procedure and tests and facilities (instrumentation and equipment) that have been used within this research. The information about the diesel engine specifications, instruments, emissions' analysers and fuel properties are introduced in this chapter. The engines' instruments, the various test criteria, emissions' analysers, diesel catalysts and the analytic sampling methods for PM collection will be explained.

3.1 RESEARCH DIESEL ENGINE TESTS AND INSTRUMENTATION

Two research diesel engines are presented in this chapter, their details and specifications will be explained via this experimental study. The first engine (Lister Petter) is a single fuel injection diesel engine and was used for the first experimental test discussed in Chapter 4; while the second engine is a common rail modern diesel engine used for the experimental tests presented in Chapters 5 and 6.

3.1.1 Experiments with Single Fuel Injection Compression Ignition (CI) DI Diesel Engine

The first experiments (section 4.1) were carried out on an air-cooled single cylinder, DI CI engine that has been designed for petroleum diesel combustion, as shown

in Figure ß3.1, with engine parameters listed in Table ß3.1. The pump-line-nozzle DI fuel system is used in this engine and located at the top of the combustion chamber; which enables directly fuelling into the piston crown bowl and provides a 180 bar of injection pressure. The test engine consists of a thyristor-controlled DC electric dynamometer coupled with a load cell, which provides the engine with various load conditions. The variable engine conditions (speed and loads) were fed via electric sensors which are set by the control panel and the signals of the actual running conditions. A Romet G65 rotary air flow meter was used to measure the intake air flow. A K-type thermocouple was used to record the engine oil temperature as well as to check that the engine was fully warm as a means to reduce the engine condition. The engine was equipped with various standard engine test rig instrumentation to measure and monitor the engine temperatures (oil, inlet manifold and exhaust gas temperature), intake air, exhaust gas recirculation (EGR) and pressures. To change the exhaust gas temperature, flow rate and composition, the engine was essentially used as an exhaust generator and operated at different conditions (engine load, speed, EGR rate, type of fuel). To monitor the engine operating parameters on the computer, LabVIEW code-based software interface was used. The engine load was maintained at a constant level when changing between different fuels.

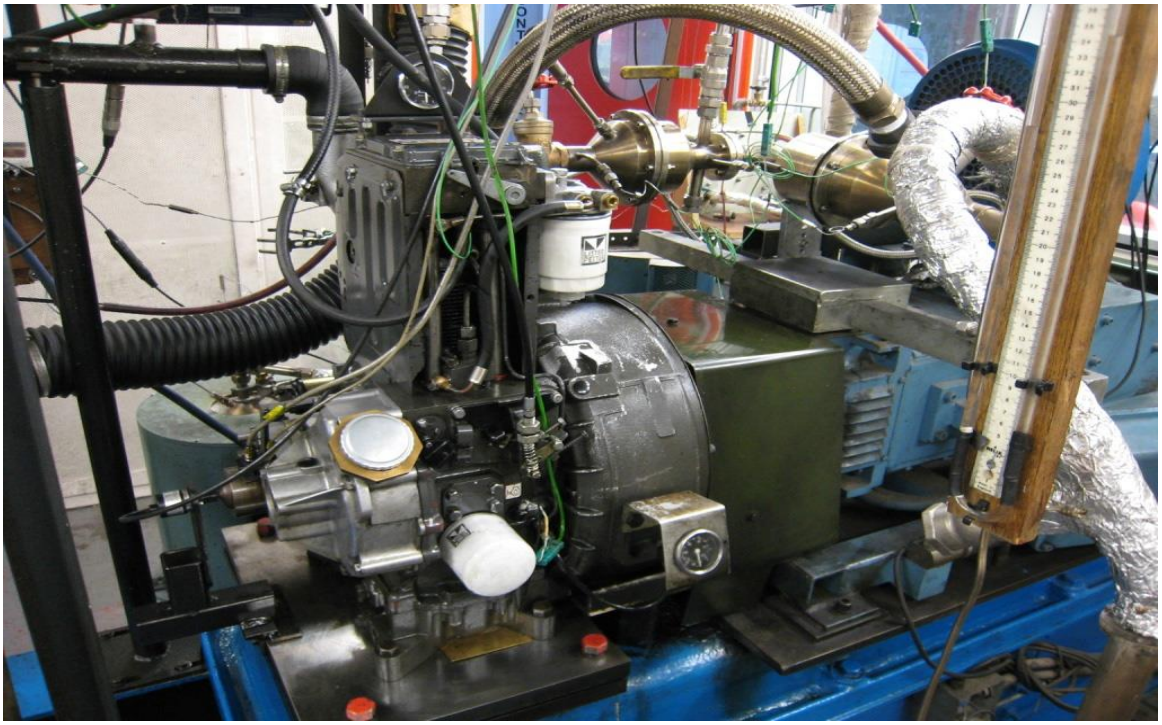

Figure 3.1: Lister Petter TR1 single cylinder diesel engine instrumented with a dynamometer

Table 3.1: Engine Specifications

Diesel engine parameter	Specifications
Type	One-cylinder
Maximum power	8.6 (kW @ 2500 rpm^{-1})
Maximum torque	39.2 (Nm @ 1800 rpm^{-1})
Bore/Stroke (mm)	98.4/101.6
Displacement (cm^3)	773
Compression ratio	15.5:1
Injection timing (^{o}bTDC)	22
Maximum injection pressure (bar)	180
Injection system	Three holes pump-line-nozzle
Injection system diameter	Ø 0.25 mm
Engine piston	Bowl-in-piston

3.2.1 Experiments with a Common Rail Direct Injection (DI) Modern Diesel Engine

The second and third experimental parts of this thesis (sections 5.1 and 6.1) were implemented with a modern single-cylinder, water cooled, common rail fuel injection system, four-stroke experimental diesel engine (Figure 3.2), fuelled by diesel fuel and a butanol-diesel blend (butanol blend). The main specifications of the test research diesel engine can be found in Table 3.2. The combustion characteristics and emissions (CO, THC, NOx and PM) of the diesel engine were measured. An AVL GH13P was used to record the in-cylinder pressure [236]. The charge from the pressure transducer (mounted in the cylinder head) was amplified by an AVL FlexiFEM 2P2 Amplifier [237] as well as monitored and stored on a PC for processing. A digital shaft encoder producing 360 pulses per revolution was used to measure the crank shaft position. The data from the crank shaft position and pressure was combined to create an in-cylinder pressure trace. A bespoke LabVIEW based code was developed to control, collect and monitor the additional data acquisition and combustion analysis based on external sensors. During all test, the engine load was maintained at a constant level when changing both fuels and injection strategies.

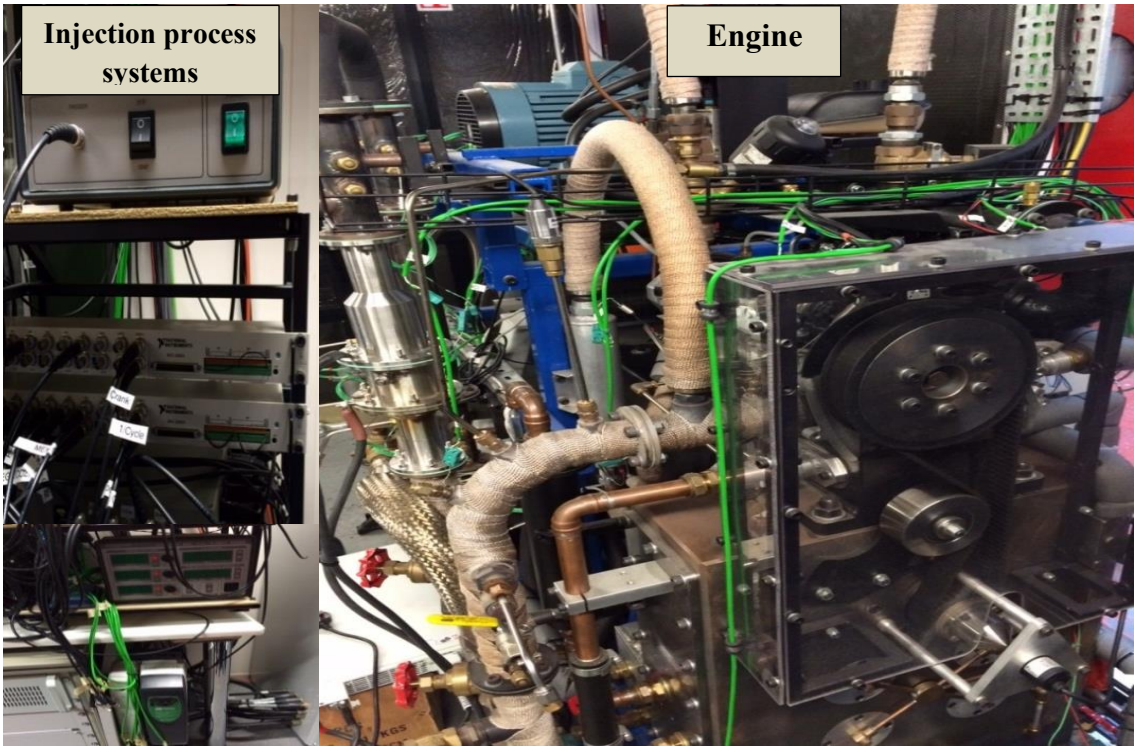

Figure 3.2: Single cylinder diesel engine equipped with common-rail fuel system

Table 3.2: Research engine specifications

Engine parameters	Specifications
Engine type	Diesel 1- cylinder
Stroke type	Four-stroke
Cylinder bore x stroke (mm)	84 x 90
Connecting rod length (mm)	160
Compression ratio	16.1
Displacement (cc)	499
Engine speed range (rpm)	900 – 2000
IMEP range (bar)	< 7
Fuel pressure range (bar)	500 – 1500
Number of injections	3 injection events

The flow chart of engine lines equipped with a common rail fuel injection system is presented in Figure 3.3. The common rail fuel system allows the control of three injections events per cycle (pre, main, and post fuel injection) and provides 1200 bar maximum rail pressure. The injection parameters and exhaust gas recirculation (EGR) valve are controlled and monitored on a PC by the engine's ECU (electronic control unit) as shown in the flow chart of Figure 3.3. The high-pressure fuel rail is measured by a sensor (see component 5 in Figure 3.3) through the signal which is controlled by the ECU. The amount of injected fuel in the combustion chamber by the common rail system can be regulated via a solenoid valve. The ECU illustrated in Figure 3.3 has the ability to open each injector electrically and control the amount of fuel injection. It can reduce the engine noise by injecting a small amount of diesel fuel before the main injection event; this can reduce the vibration, as well as optimising injection timing and quantity. Much effort has been made in the industry sector to control and monitor the amount of fuel injected in the common rail system of a diesel engine. Combustion characteristics and emissions are influenced by the rate of fuel injection in a diesel engine.

This kind of system gives the opportunity to go into the control computer's software and adjust injection timing, amount of fuel, or number of injections. The injection strategy is maintained at a constant desired pressure, and then distributed to the injector. Furthermore, the common rail injection system offers split injection (fuel volume injected into multiple injections) which can improve the fuel economy, engine torque, engine combustion, noise and exhaust gas emissions [238, 239]. Regarding these benefits, Mahr stated that one or two pilot injection resulted in reduced noise and NOx emissions at low injection pressure. Soot emissions reduced with coupled post-injection and high injection pressure. Late post-injection contributes by increasing considerably the temperature of the

exhaust upstream of the DPF and trapping a high proportion of the soot following in the exhaust stream [41, 223]. The injection strategies (pilot, main and post) were found to be very effective in reducing soot emissions and increasing the soot oxidation. The injection timing and amount of injected fuel are controlled by the ECU via signals controlling the valve in the injector.

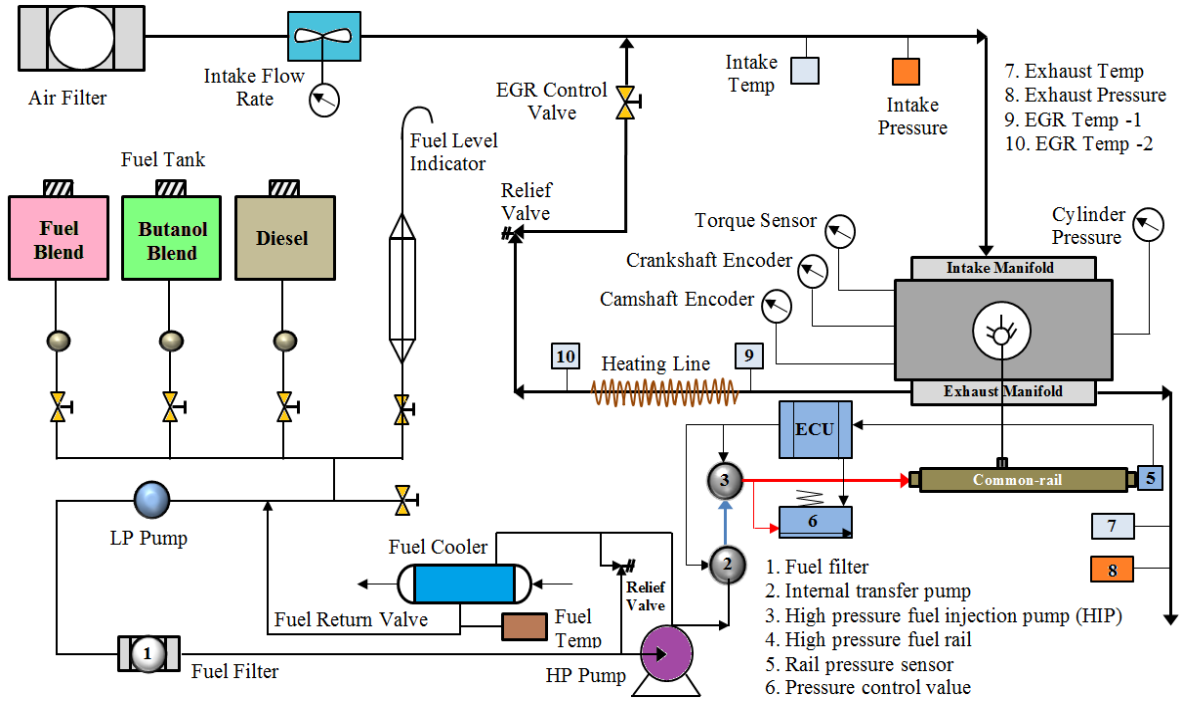

Figure 3.3: Flow chart of common-rail DI diesel engine with lines and a common rail fuel injection system

The engine's fuel consumption rate can be calculated under steady-state engine conditions. The indicated specific fuel consumption (ISFC) is calculated from the ratio that compares the fuel used by the engine to the amount of power the engine produces (the mass flow rate per unit power output) and can be calculated by using the following equations (3.1) and (3.2) (Equation (3.1 correct for 4-stroke engines):

$$P_i = \frac{IMEP \times A_c \times L \times n \times N}{120} \qquad (3.1)$$

Where P_i (Pa) is the indicated engine power; N (rpm) is the engine speed; Ac is the area of the piston head; L (m) is the stroke length; and n is the number of cylinders.

$$ISFC\ (kg/kWh) = \frac{\dot{m}_f\ (kg/h)}{P_i\ (kW)} \quad (3.2)$$

Where $\dot{m}_f$ is the mass flow rate of fuel consumption.

The brake specific fuel consumption (BSFC) can be calculated by the fuel consumption divided by the brake power (P_b) using the equation below:

$$P_b = T \times w \quad (3.3)$$

Where w is the engine speed ($w = {}^{2\pi N}/_{60}$); and T is the engine torque.

$$BSFC\ (kg/kWh) = \frac{\dot{m}_f\ (kg/h)}{P_b\ (kW)} \quad (3.4)$$

Engine brake thermal efficiency (BTE) is defined as the brake power developed by combustion of fuel in the engine cylinder. It is used to evaluate how an engine converts the heat from a fuel to mechanical engineering and can be expressed by the equation as shown below:

$$BTE = \frac{P_b\ (kW)}{\dot{m}_f \left(\frac{kg}{h}\right) \times CV(kJ/kg)} \quad (3.5)$$

Where CV is the calorific value of a kilogram of fuel.

The data of the cylinder pressure is recorded for 200 consecutive cycles under stable engine operating conditions. It is recorded with higher resolution used for the analysis of steady state engine tests. The evaluation of combustion characteristics is based on individual analyses of the pressure trace for each engine cycle. A MATLAB code was used to analyse the average in-cylinder pressure inside the engine for 200 cycles. The overall diesel combustion process can be described by analysis of the rate of heat release (ROHR). The ROHR is calculated from the filtered cylinder pressure traces. The model used to expression and calculated for ROHR in this research is presented by the following equation:

$$\frac{dQ}{d\theta} = \frac{\gamma}{\gamma - 1} p \frac{dV}{d\theta} + \frac{\gamma}{\gamma - 1} V \frac{dp}{d\theta} \qquad (3.6)$$

Where p is the instantaneous cylinder pressure; γ is the ratio of specific heats (C_p/C_v); and V is the instantaneous cylinder volume at crank angle θ.

3.2. LIQUID FUELS

The fuels and fuel blends used (Figure 3.4) were ultra low sulphur diesel (ULSD), biodiesel derived from rapeseed oil (RME) and was supplied by Shell Global Solutions UK. Butanol used in blending with diesel and RME and was purchased from Fisher Scientific. The physical and chemical properties of the pure components of the fuel and fuel blend were calculated or obtained from the Company or publications (Table 3.3 and Table 3.4). In the first test (Chapter 4) of this thesis, the alternative fuel was operated with the fixed fuel injection timing in order to produce a variety of exhaust gases and not the optimisation of the combustion. In the second and third tests of this thesis (Chapter 5

and 6) common rail fuel injection system was used in order to study the effect of injection strategies particulate emissions with alternative fuels. The particular diesel fuel used in the second and third investigation as a reference fuel was selected without any biodiesel (thereby with zero oxygen content) in its composition (Table 3.4); in order to study the effect of the oxygen in the combustion process when diesel fuel is blended with butanol.

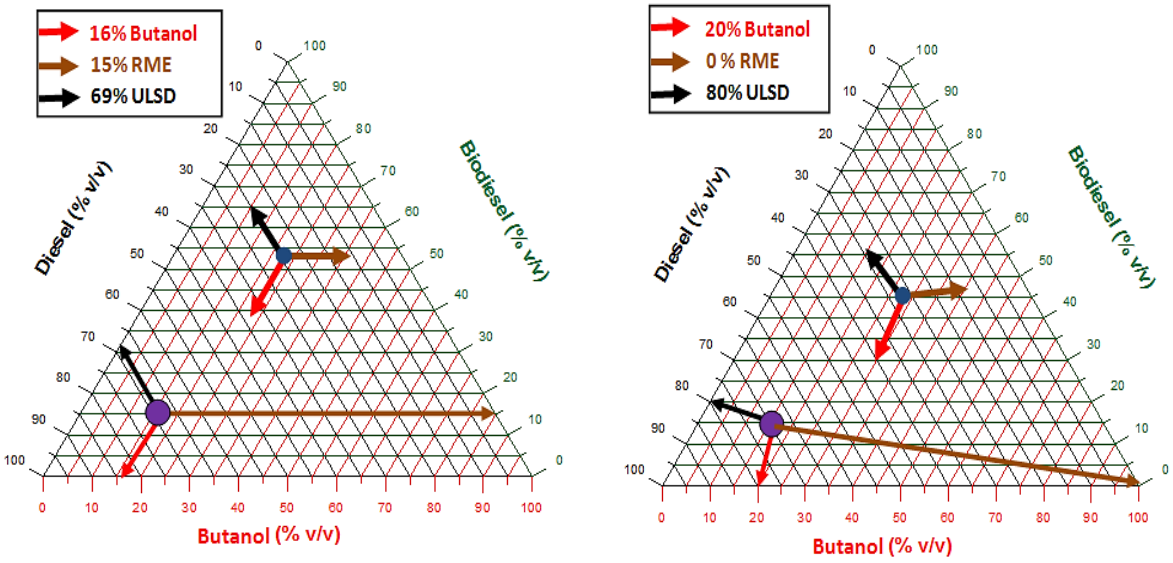

Figure 3.4: Ternary diagrams representing the test blends

Table 3.3: Specification of tested fuels [5, 77]

Properties	ULSD 100%	RME 100%	Butanol	B16R15D
Chemical formula	$C_{14}H_{26.1}$	$C_{19}H_{35.3}O_2$	C_4H_9OH	$C_{11}H_{21.4}O_{0.5}$
Cetane number	53.9	54.74	17	
Latent heat of vaporization (kJ/kg)	243	216	585	
Bulk modulus (MPa)	1410	1553	1500	
Density at 15 °C (kg/m^3)	827.1	883.7	809.5	835.2
Kinematic viscosity at 40 °C (cSt)	2.70	4.53	2.23	2.54
Lower calorific value (MJ/kg)	43.11	37.80	33.12	39.97
Lubricity at 60 °C(μm)	312	205	620	405
C (wt %)	86.44	77.09	64.78	81.56
H (wt %)	13.56	12.07	13.63	13.34
O (wt %)	0	10.84	21.59	5.08
O from OH group (wt %)	0	0	21.59	3.36
Boling point (°C)	-	-	117.5	
50% distillation (°C)	264	335	117	
90% distillation (°C)	329	342	117	

Table 3.4: Specification of tested fuels with particular diesel fuel (without any biodiesel in its composition) [5, 77]

Properties	Method	ULSD	Butanol	B20D80
Cetane number	ASTM D7668-14	50.2	17	41.98
Latent heat of vaporization (kJ/kg)		243	585	-
Bulk modulus (MPa)		1410	1500	-
Density at 15 °C (kg/m^3)	EN 12185	840.4	809.5	833.2
Upper heating value (MJ/kg)		45.76	36.11	43.5
Lower heating value (MJ/kg)		43.11	33.12	40.91
Water content by coulometric KF (mg/kg)	EN 12937	40	170	389.4
Kinematic viscosity at 40 °C (cSt)	EN ISO 3104	2.564	2.23	2.27
Lower Calorific Value (MJ/kg)		43.11	33.12	39.95
Lubricity at 60 °C(μm)	EN ISO 12156	424	571.15	444.5
Fatty acid methyl ester % (v/v)	NF EN 14078-A	<0.05		
Cold filter plugging point (CFPP)	ASTM D-6371	-18	<-51	-18
C (wt %)		86.44	64.78	81.56
H (wt %)		13.56	13.63	13.35
O (wt %)		0	21.59	4.318

3.3 ENGINE EXHAUST AND AFTERTREATMENT SYSTEM

3.3.1 Exhaust System and Instrumentation

The exhaust gas properties were measured at different positions along the exhaust line by using thermocouples and pressure sensors in different sampling points. The diesel oxidation catalyst studies were carried out using a one inch in diameter monolith catalyst that was placed in a reactor inside a furnace and was fed with real engine exhaust gas. During this research work, two engines were used for the same DOC catalyst which was located in the exhaust line as shown in Figure 3.5. The temperature and the engine exhaust gas flow can be controlled by a thermocouple (located upstream of the catalyst) and a flow meter respectively. The engine is used for this research as a source of exhaust gas, in order to obtain a diverse spectrum of exhaust gas compositions from different fuels (diesel, RME, alcohol blends). The temperature upstream and downstream of the DOC was monitored using K-type thermocouples. The temperature of the mini-reactor inside a tubular furnace (Figure 3.6) was set at a rate of 2 °C/min during every test. The oxidation catalyst was subjected to different exhaust gas space velocities of 35000 h^{-1} (Chapter 4 and 5), 25 000/h^{-1} and 50 000/h^{-1} (Chapter 6). To ensure consistency between the gas hourly space velocity GHSV (exhaust gas divided by the volume of the monolith catalyst) for all tests, calibrated flow meters were used to control the exhaust gas volumetric flow rate over the DOC. To avoid any changes in the exhaust gas composition during the test, the engine-out exhaust species' concentrations were measured at the beginning and at the end of each experiment. The exhaust gas concentration after the DOC was continuously recorded during the test to calculate the conversion efficiency based on the inlet emissions' concentration. To measure the emissions from the engine exhaust directed towards the aftertreatment, the exhaust gas sampling line at a temperature of 200 °C was made to limit

any water and hydrocarbon condensation, as well as preventing any reaction between the exhaust gas species in the sampling line.

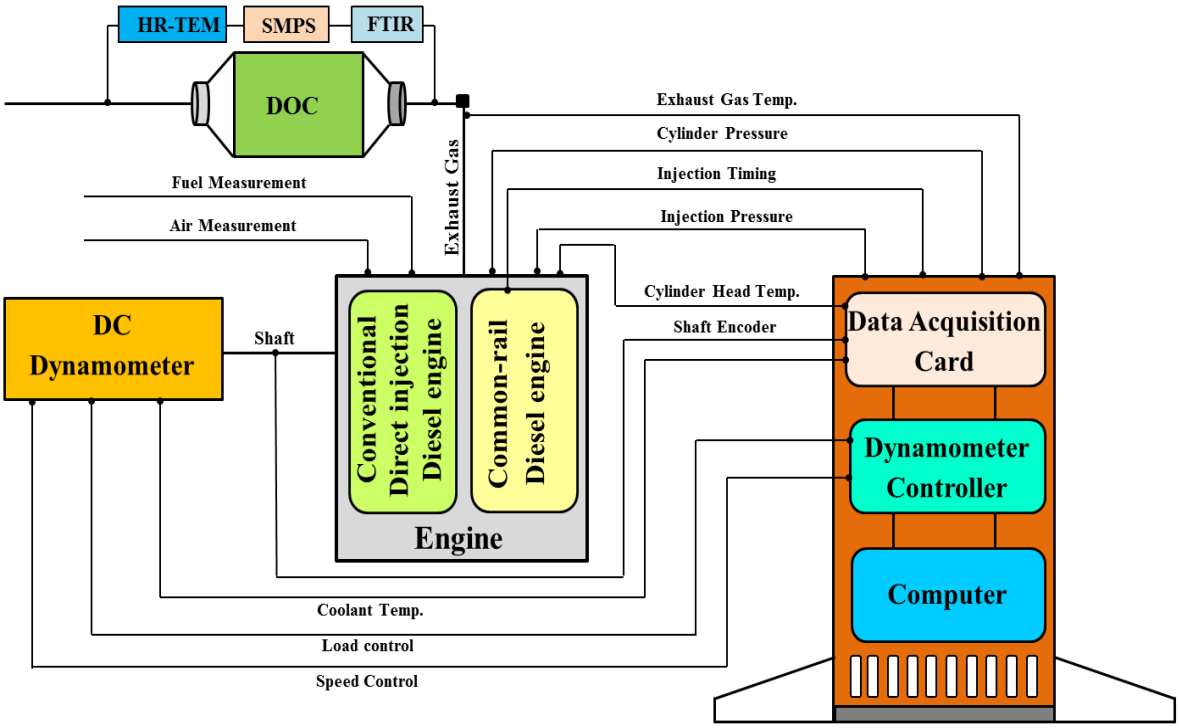

Figure 3.5: Schematic representation through overall experimental setup

3.3.2 Diesel Oxidation Catalyst and Particulate Filters

Johnson Matthey Plc developed the catalyst for a dual purpose: i) to adsorb hydrocarbons and oxidize CO at low exhaust temperatures; and ii) to release hydrocarbons and/or oxidize C-containing species (C, PM and some HC species) at high exhaust gas temperatures. The diesel oxidation catalyst (DOC) is sequentially connected with the diesel engine during this study. The DOC used in this research is a 120 g/ft^3 Platinum: Palladium (weight ratio 1:1) with alumina and zeolite washcoat (2.6 g/in^3 loading). The diameter, length and wall thickness of the DOC are 25.4 mm, 91.4 mm and 4.3 mil respectively, as shown in Figure 3.7. The monolithic catalyst substrates are made ceramics material with

square cells (see Appendix A). The DOC used in this thesis was supplied by Johnson Matthey Plc, and more details about catalyst are provided in Chapter 2. The temperature upstream and downstream of the DOC was monitored using K-type thermocouples. The diesel particulate filter (DPF) used for the aftertreatment throughout this study was also supplied by Johnson Matthey Plc. As a part of the research, the DPF was installed downstream of the DOC and linked directly to the exhaust gas of the engine. The diameter and length of the DPF that was used in this research was 24.2 mm and 75.2 mm respectively, with a channel density of 289 channels/si (Figure 3.7).

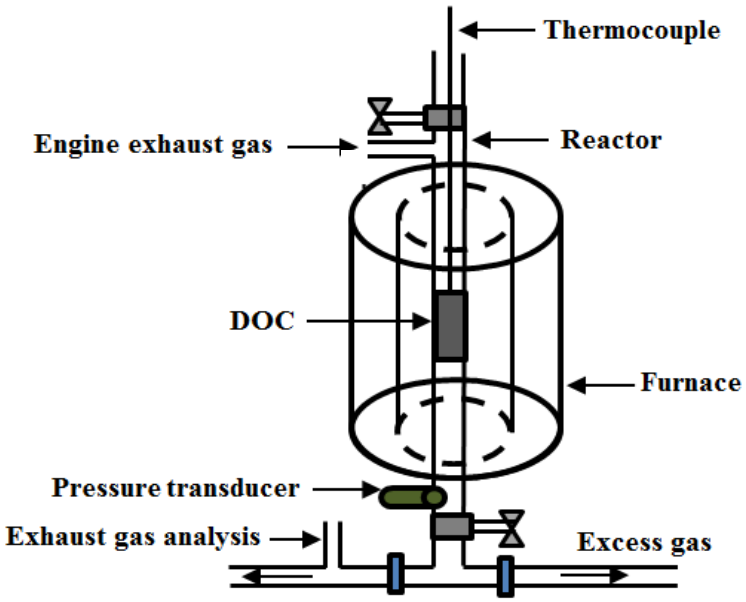

Figure 3.6: The mini reactor and furnace showing the main components of the system

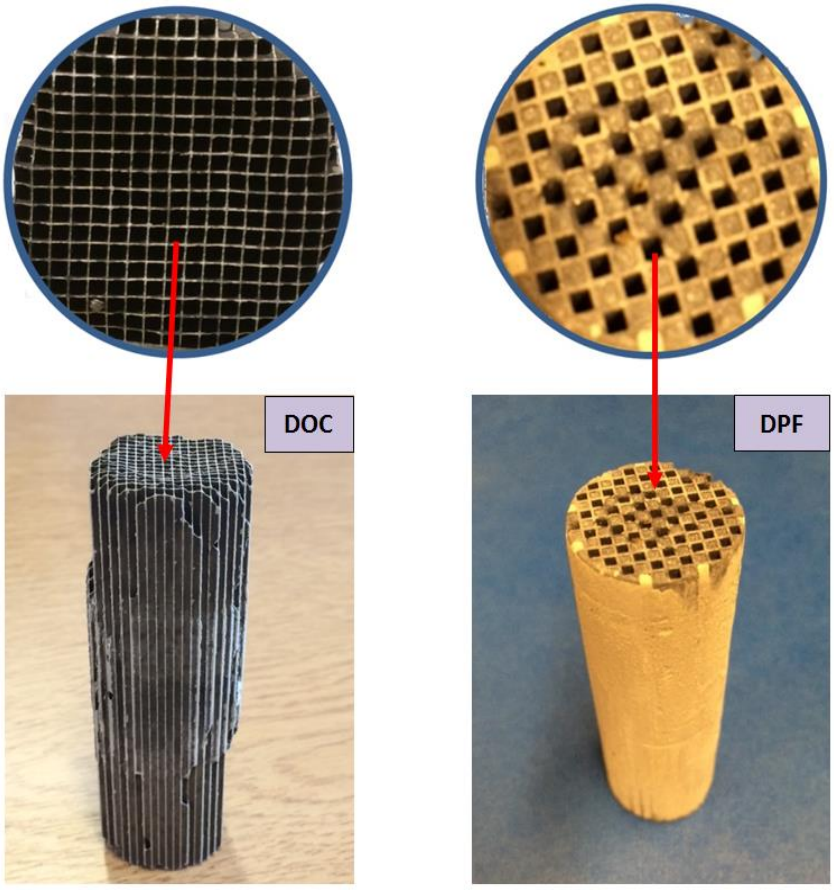

Figure 3.7: Pictures of the aftertreatment (DOC and DPF) components studied

3.4 EXHAUST GAS EMISSION ANALYSIS

3.4.1 Scanning Mobility Particle Sizer

A scanning mobility particle sizer (SMPS) was employed to measure the size of the particulate matter (PM) concentration and size distribution emitted from the diesel engine. A model TSI SMPS 3080 particle number and size classifier with thermodiluter was utilized to evaluate the two parameters of the PM emissions: the number of concentration and size. A rotating disk thermodiluter (TSI 379020A) was connected with the exhaust gas by small portion to dilute the air and control the dilution ratio. The principle measurement of particle size distribution within SMPS, based on the ability of the

particles to traverse an electric field, known as its electrical mobility, is directly related to the particle's size. The thermodiluter was fitted with an air dilution temperature of 150 °C in order to prevent hydrocarbon condensation and nucleation which occur during sampling and the dilution ratio was set at 1:100 for all tests. The range of particle size diameters was measured between 10.4 and 379 nm according to the sample and sheath flow rates. The number of particles for each size range was counted by the Condensation Particle Counter (CPC) eventually. The time required to measure the size distribution in SMPS is about 120 sec (upscan and downscan time) and then it waits another 120 sec to make another measurement. The following parameters were used to measure the particle size distribution:

Sheath Flow Rate: 6.00 L/min

Aerosol Flow Rate: 0.60 L/min

Lower Size: 10.4 nm

Upper Size: 378.6 nm

Scan Time: 120 sec

The particle size distribution of PM emitted from a diesel engine can be detected through employing the SMPS (Figure 3.8). The particulates obtained from diesel exhaust gas are divided into three groups (small, medium, and large particulates) based on the particles' size as shown in Figure 3.8.

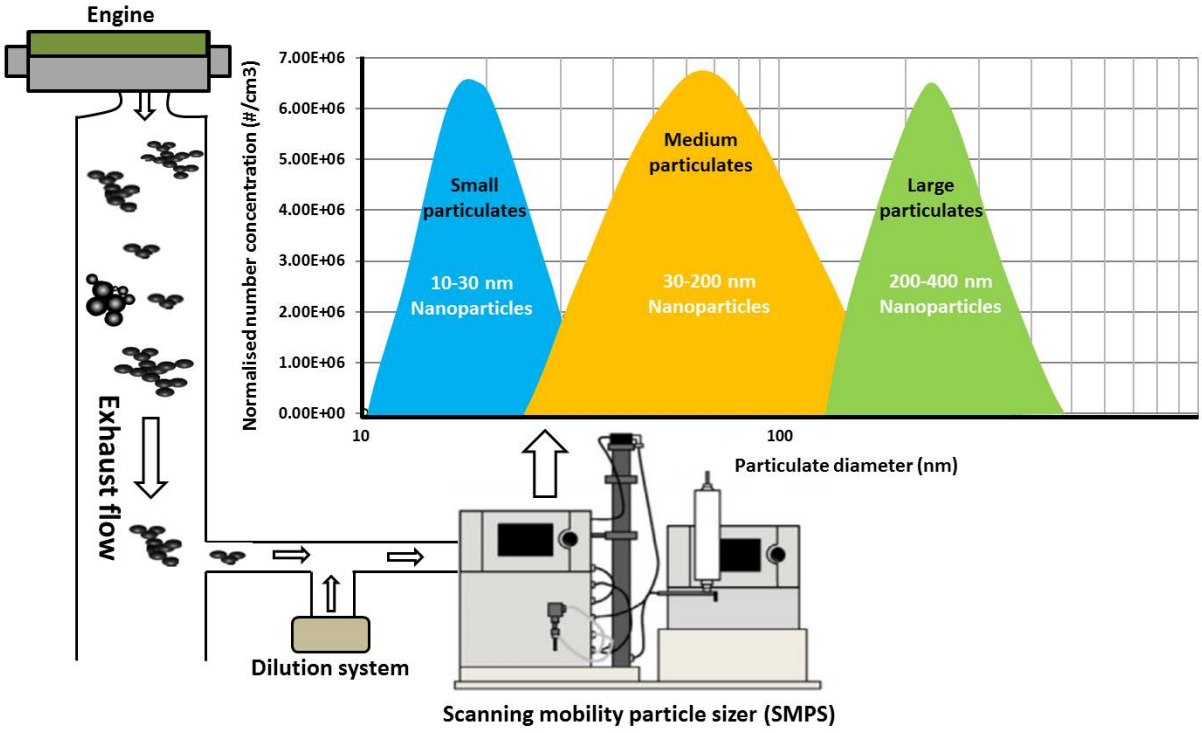

Figure 3.8: Particulate size distribution for the diesel engine

3.4.2 High-resolution Transmission Electron Microscopy (HR-TEM)

High-resolution transmission electron microscopy (HR-TEM) with a Philips CM-200 microscope is a sophisticated technique that can provide sufficient information on the morphological and microstructure parameters of the agglomerate, as shown in Figure 3.9. The soot particulate samples used in morphology studies have been collected from the exhaust gas stream at different points in 3-mm copper grids attached to a sampling probe for a short time. These soot particulates were analysed using HR-TEM with a Phillips CM-200 microscope which have high resolution about 2 Å at an accelerating voltage of 200 kV. The HR-TEM imaging and steps (1-4) of the image post processing of the soot particles are illustrated in Figure 3.10. The TEM image is formed from the interaction of the electrons' beam passing through the soot particles and the

carbon film, where the soot image form is magnified and focused onto a fluorescent screen. The soot particle images are detected by a sensor such as a CCD camera (11 mega pixels) with high resolution. The HR-TEM allows for two-dimensional images of extended grids up a million times over the original size (see Appendix C). Therefore, this technique allows the agglomerates' structure of soot to be seen as well as the microstructure of the primary particles and subsequently, obtains the different morphological characteristics of the soot agglomerates. The morphological parameters of the soot agglomerates (radius of gyration, number of primary particles and fractal dimension) and microstructural parameters (interlayer spacing and thickness of the graphene layer) were obtained from the TEM micrographs using homemade MATLAB software (digital image analysis software) [117, 240].

Figure 3.9: A picture of high-resolution transmission electron microscopy (HR-TEM)

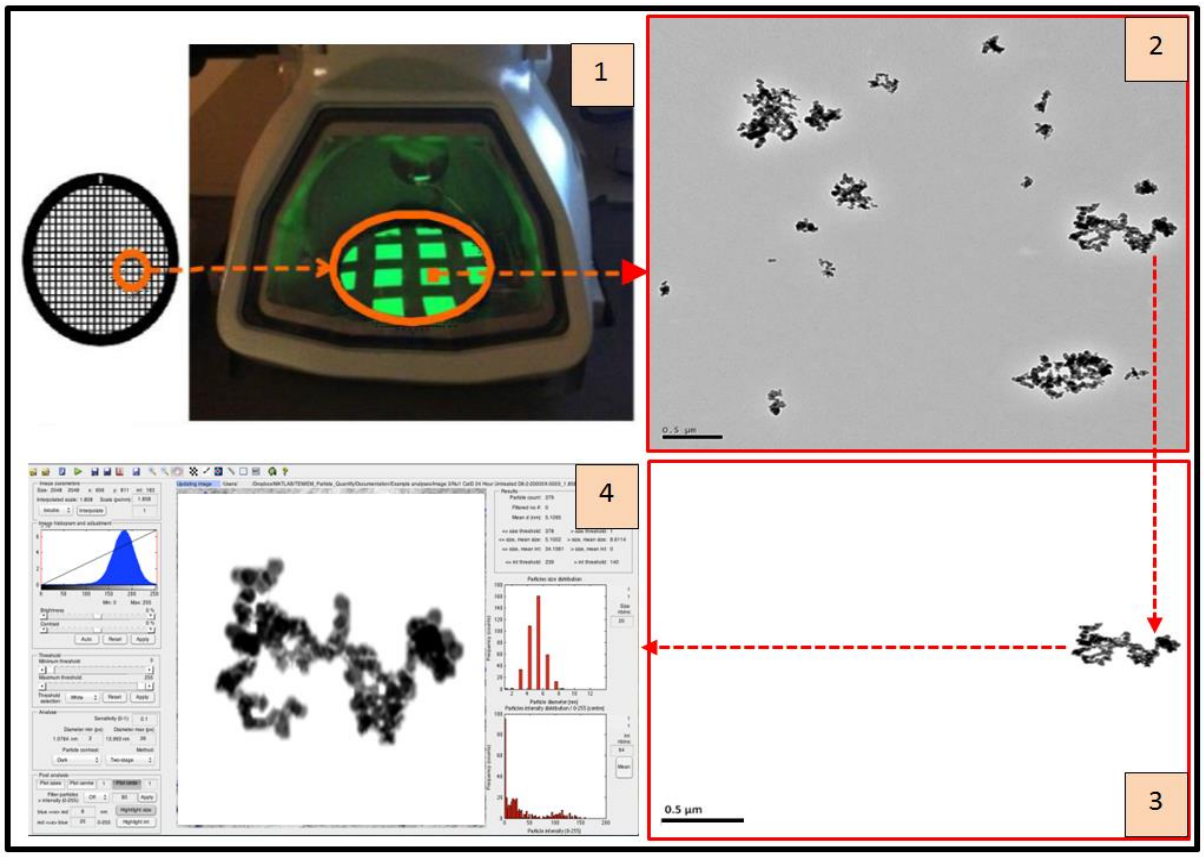

Figure 3.10: Image post processing steps (1-4) from HR-Transmission electron microscope imaging and analysing with MATLAB code

Figure 3.11 shows the TEM image for different ranges of magnification in order to reveal the morphological features and the soot particles' sizes. To observe the morphological features for TEM images, the applied magnification range is 125000 at the accelerating voltage of 120 kV; while for the case of the microstructure, the range of magnification is between (800000 - 1200000) at an accelerating voltage of 200 - 300 kV (see Appendix C). To calculate the statistical morphological results it is necessary to have at least 30 images for each soot sample and for the microstructure around 4 images for each soot sample are needed; three seconds were used to take each TEM image. The results obtained from the photographs showed at least 20 agglomerates for each engine operating condition.

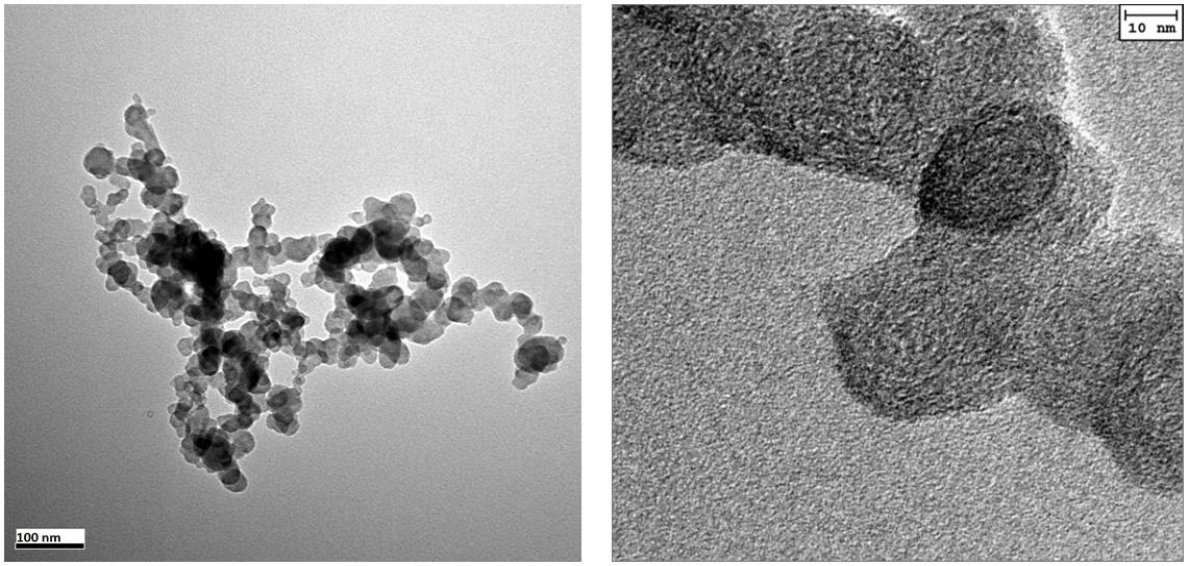

Figure 3.11: Different high magnifications of TEM micrographs of diesel soot agglomerate and the spherical primary soot particles

According to the method that is shown in Figure 3.12 [117], the fractal dimension can be calculated iteratively and then the number of primary particles and the bulk density of the agglomerates. The following assumptions of this method are summarized:

- It is assumed that the primary particles are spherical [241].
- There is an average size of primary particle agglomerates under the same conditions and fuel used [242].
- Primary particles have homogeneous density.
- Finally, neglect the moment of inertia of the mass enclosed in the image pixels.

There are two criteria that may cause the agglomerate image to be rejected by the program. The first is that the number of primary particles is less than five (the program rejects the particles which are too small) [243, 244]. The second criterion is that the fractal dimension is out of the theoretically acceptable range (D_f <1 or D_f >3). After calculating

the fractal dimension, the number of primary particles can be calculated by Equation 2.13. The calculation method is outlined in Figure 3.12.

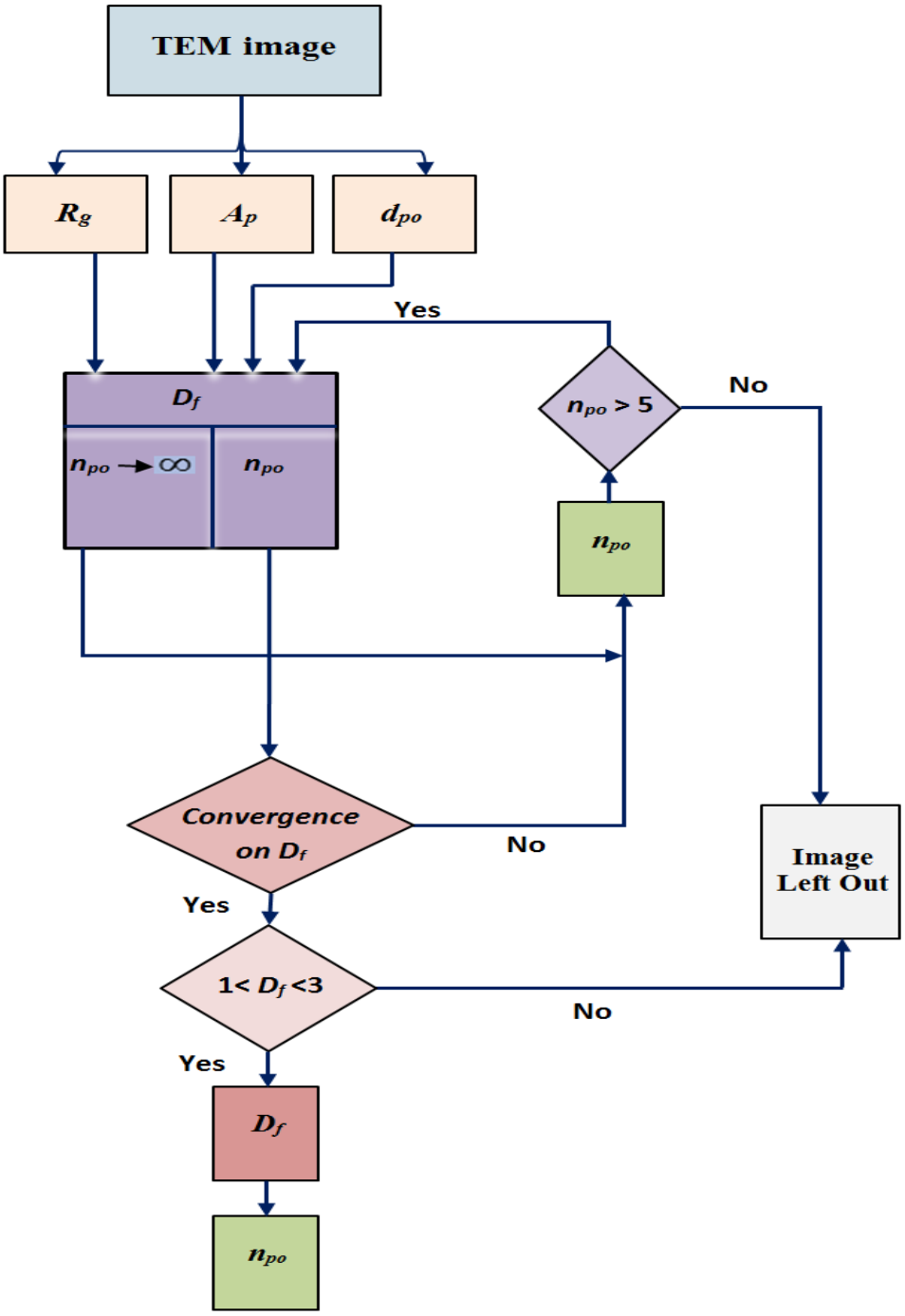

Figure 3.12: Block diagram of the method of calculation; adapted from [117]

3.4.3 Fourier Transform Infrared Spectrometry (FTIR)

The measurement starts when the sample is introduced in the FTIR gas analyser; the infrared beam is partially absorbed by the gas species present. The FTIR is capable of percent sensitivity for measuring multiple gases in a variety of the following applications:

- Catalysis and combustion process monitoring
- Stack and abatement system emission monitoring
- Process monitoring
- Ambient air monitoring
- Purity applications

The FTIR can perform analysis in gas streams containing up to 30% water and can simultaneously analyse and display more than 30 gases. When a gas sample is introduced in the gas cell, the infrared beam is partially absorbed by the gas species present. The absorption spectrum is unique for each infrared-active gas. The MultiGas analyser is equipped with a Helium Neon (HeNe) laser located along the side of the FTIR spectrometer, used for synchronizing the digitization of the measurement. For the measurement specifications refer to Appendix B: Table B-1.

Before taking measurements on a sample line, it is necessary to connect the gas cell to dry nitrogen gas. The FTIR requires a constant flow of dry nitrogen to purge the interferometer and transfer optics (Figure 3.13 (-c)). This will help to ensure optimal lifetime and operation of the instrument. The flow meter on the left controls the purge for the interferometer; while the flow meter on the right controls the purge for the transfer optics and detector chamber (see Figure 3.13 (-a)). Both flow meters are set between 0.2

and 0.3 LPM (litres per minute). The FTIR is equipped with a liquid-nitrogen-cooled detector (Figure 3.13 (-b)) and the detector should be completely filled with liquid nitrogen each time the instrument is used. Depending on the detector selected, it will operate for approximately eight or twelve hours on a single fill before the liquid nitrogen is exhausted.

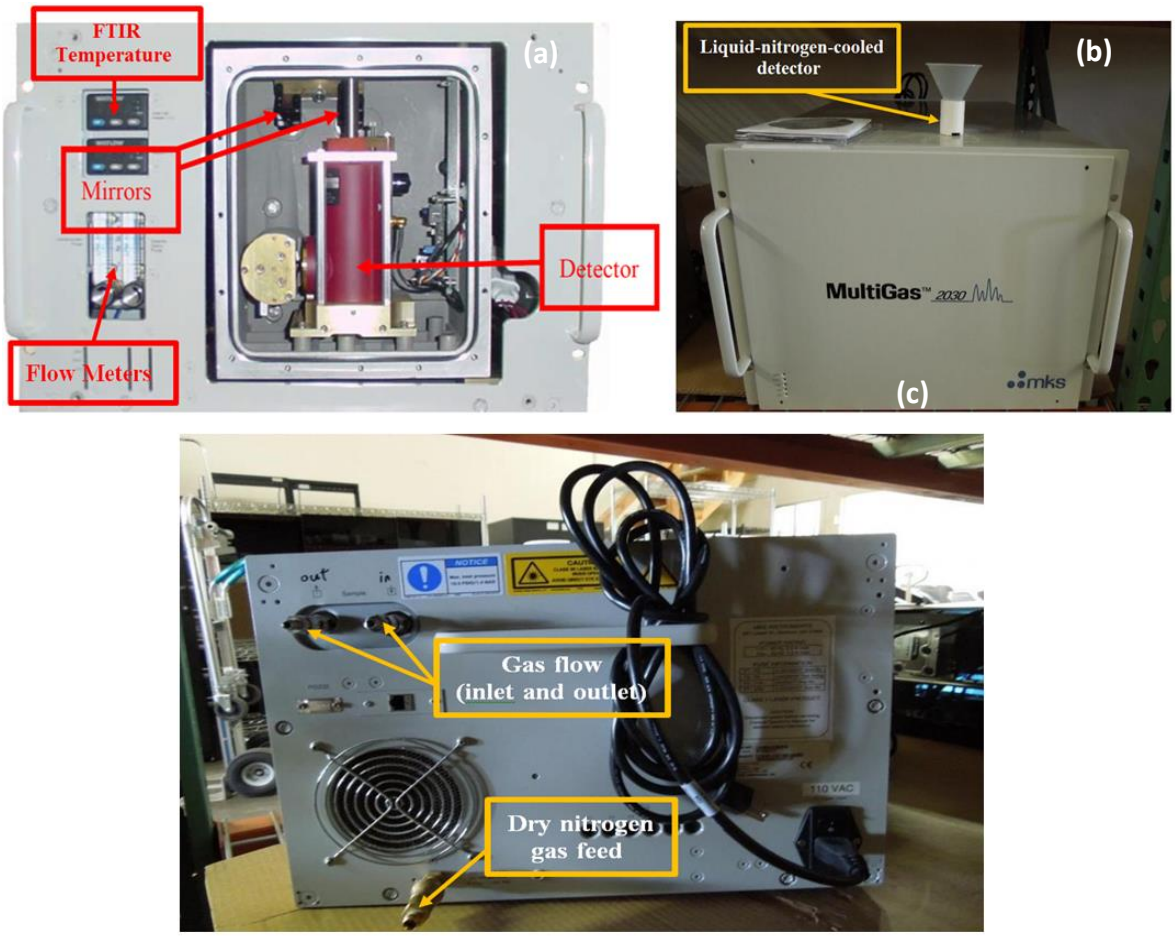

Figure 3.13: Different sides of the FTIR (MultiGas Model 2030)

The setup utility is used to configure the collection and processing data; for example which gases are selected for analysis, if and how the data are saved, where the data are stored. The collection and processing data are divided into four sections: gas analysis, data storage, gas cell, and external devices. The following table (Table 3.5) describes the functions of the four sections in the FTIR set-up:

Table 3.5: MG2030 set-up sections

Sections	Definition
Gas analysis	Displays the name of the currently used recipe
Data storage	Allows the system to store the computed gas concentration (as well as temperature, pressure) in one or several files. This can be read by spreadsheet programs such as Microsoft Excel
Gas cell	Specifies the gas cell temperature in degrees Celsius Specifies the gas cell pressure in atmospheres Specifies the gas cell path length in metres
External devices	External devices allow for additional functionality of the MG2030 software, such as: data output, external display, temperature and pressure measurements, and depend on the analyser type and configuration

After the software set-up is finished, then by selecting the run button from the MultiGas main tab, this allows the user to initiate the collection and automated data analysis. The run button should be used only after the set-up has been completed. The gas measurements can be viewed in the screens as illustrated in Figure 3.14.

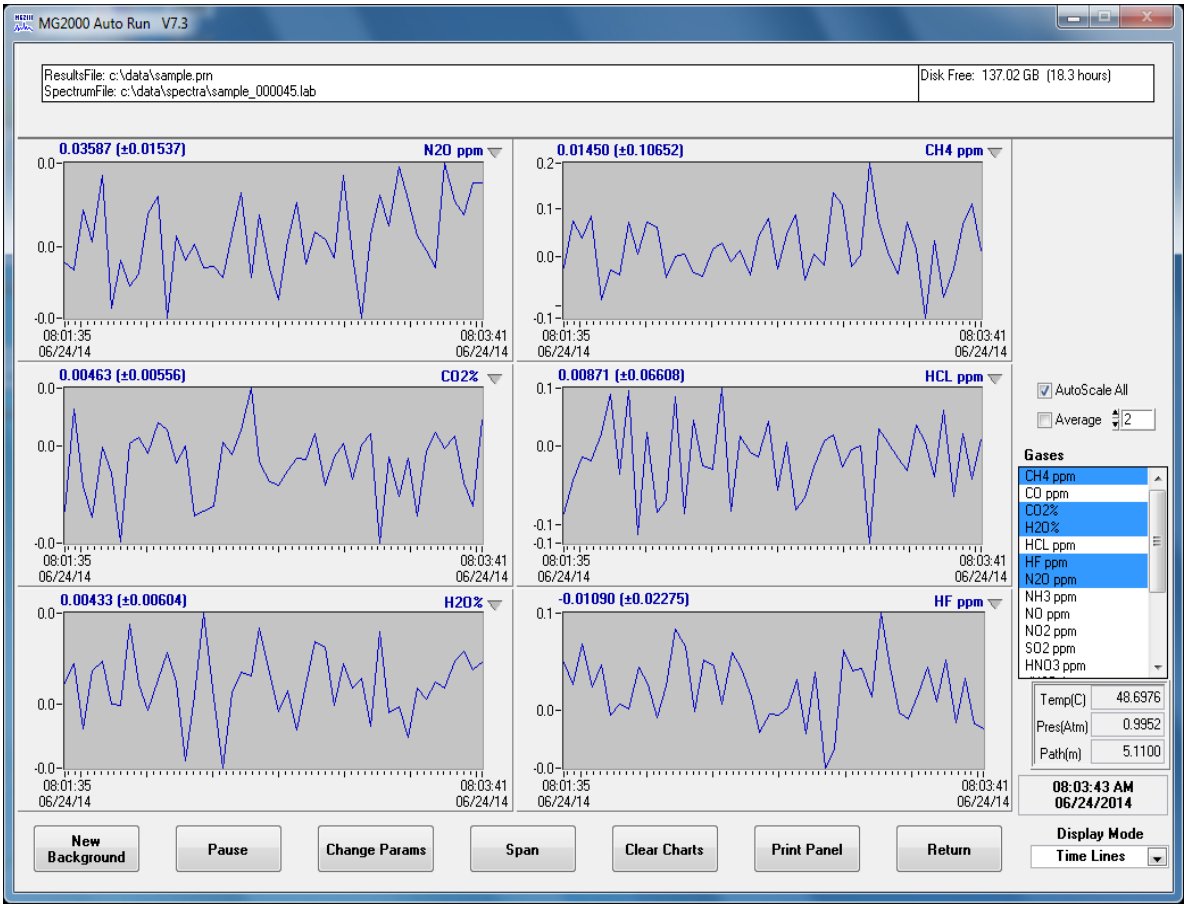

Figure 3.14: Gas measurements' screen

Gaseous emissions emitted from the diesel engine such as: carbon monoxide (CO), carbon dioxide (CO_2), nitrogen oxide (NO and NO_2), nitrous oxide (N_2O), and individual hydrocarbon species such as methane (CH_4), ethane (C_2H_6), ethylene (C_2H_4), ethylene (C_2H_4) and acetylene (C_2H_2) were measured using a MultiGas 2030 FTIR spectrometry based analyser. A filter was used in the FTIR to avoid any possible damage in the optical lenses by the PM from the exhaust gas. The FTIR was maintained at 190 °C to prevent the condensation of HCs and water in the heated lines. The relation between light absorption at a certain wavelength and species concentration was adopted in the measurement technique. Medium and long-chain hydrocarbon concentrations were measured as a single exhaust group due to spectrum interfernces

3.5 ANALYSIS OF THE UNCERTAINTIES IN THE RECORDED DATA

To ensure confident about the results, each test was repeated for two or three times. The data was averaged and then the standard deviation was determined. The error was defined according to the following equations:

$$x_{avg} = \frac{\sum_{i=1}^{N} x_i}{N} \quad (3.7)$$

Where, mean (x_{avg}) is the average of all values of x.

$$\Delta x = \sigma = \sqrt{\frac{\sum_{i=1}^{N}(x_i - x_{avg})^2}{N}} \quad (3.8)$$

Where, Δx is the uncertainty in a measurement of x. The vast majority of your data lies in the range $x_{avg \pm \sigma}$

$$\Delta x_{avg} = \frac{\sigma}{\sqrt{N}} \quad (3.9)$$

Where, x_{avg} is the uncertainty in the mean value of x. The actual value of x will be somewhere in a neighbourhood around x_{avg}. This neighbourhood of values is the uncertainty in the mean.

$$x_m = x_{avg} \pm \Delta x_{avg} \quad (3.10)$$

Where, x_m is the measured value.

The final presented value of a measurement of x contains both the average value and the uncertainty in the mean. The analysis of the uncertainties in the data recorded for this thesis, please refer to Appendix B.

CHAPTER 4

ROLE OF ALTERNATIVE FUELS ON PARTICULATE MATTER (PM) CHARACTERISTICS AND INFLUENCE OF THE DIESEL OXIDATION CATALYST

In this work, the influence of a Pt:Pd based diesel oxidation catalyst (DOC) on the engine out particulate matter (PM) emissions morphology and structure from the combustion of alternative fuels including alcohol-diesel blends and RME biodiesel (Rapeseed methyl ester) have been studied. PM size distribution was measured using a scanning mobility particulate spectrometer (SMPS) and the PM morphology and microstructure including size distribution, fractal geometry and number of primary particles was obtained using a high resolution transmission electron microscopy (TEM).

All tests were performed at a constant engine speed of 1500 rpm, 4 bar of indicated mean effective pressure (IMEP) and 180 bar of injection pressure. In order to study the effect of alternative fuels on particulate matter (PM) characteristics and gaseous emissions within a diesel oxidation catalyst and compared with reference fuels (diesel fuel).

4.1 METHODOLOGY

The schematic diagram of the engine and aftertreatment system set-up is shown in Figure 4.1. The catalyst activity studies have been carried-out using exhaust from a naturally aspirated single cylinder four stroke, direct injection diesel engine; the main specifications of diesel engine are presented in Table 3.1. Intake air flow, fuel

consumption, exhausts pressure, and exhaust temperature were also measured. The physical and chemical properties of the pure components of diesel fuel and fuel blends were presented Table 3.3. The details of DOC catalyst used in this research were explained in chapter 3. The DOC was loaded inside a furnace and exposed to the engine exhaust keeping a gas space velocity of 35000/h and a heating temperature of about 2 °C/min.

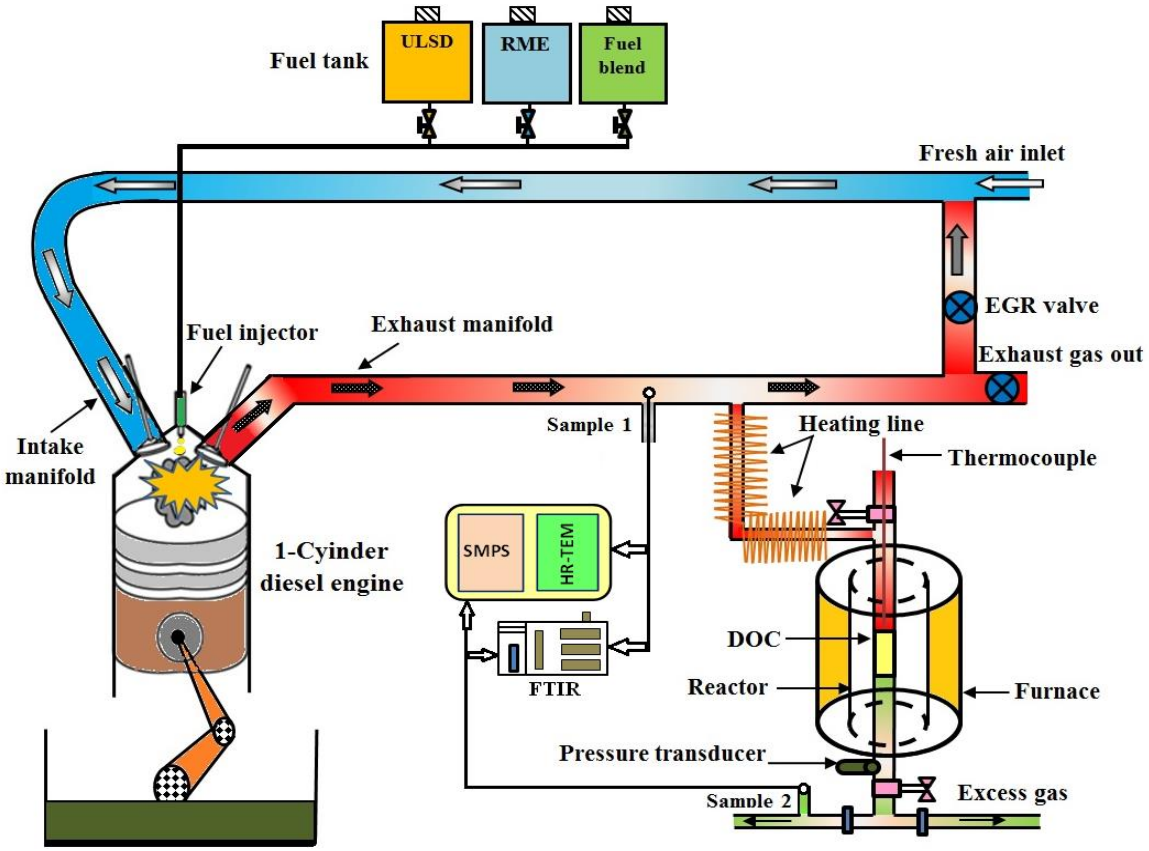

Figure 4.1: A simplified schematic diagram of Lister Petter diesel (single fuel injection) engine and DOC system

4.2 RESULTS AND DISCUSSION ON THE STUDY PARTICULATE MATTER (PM) CHARACTERISTICS

Particulate matter (PM) concentration and some exhaust gas species such as CO, HCs, and NO_X in the exhaust gas can effect on the catalyst oxidation efficiency. Analysis of PM emissions in terms of size, morphology and microstructure and their effect could support the correlation between soot emissions and aftertreatment system in reduction/oxidation. This study eventually gives understanding for the future design of environmental catalyst to trap and oxidise efficiently pollutant emissions including particulate matter agglomerates emitted from the combustion of alternative fuels.

4.2.1 DIESEL OXIDATION CATALYST (DOC) EFFECT ON PARTICULATE MATTER

Particulate matter size distributions and morphology from the combustion of the different fuels have been studied in order to identify the possible effects of the DOC on the (i) oxidation of gaseous hydrocarbons which can later be nucleate, adsorbed or condensed to form particulate matter, (ii) oxidation or desorption of the hydrocarbon already present onto the particulate matter, (iii) agglomeration of particulates increasing the number of particulates and increasing the size of the agglomerates, (iv) trapping effect due to the deposition by diffusion of particulates in the DOC channels and (v) oxidation of soot particulates.

The particulate number concentration in exhaust system for diesel combustion is significantly higher for all the particulate sizes compared to RME and the butanol blend as depicted in Figure 4.2. This lower particulate number concentration in the case of oxygenated fuels has been previously reported in the literature [142]. The oxygen content

in the ester group of RME and in the hydroxyl group of butanol are the main reasons to justify the lower engine output PM emissions.

It is reported that the number of rich regions in the combustion reduced due to the presence of oxygen in fuel molecules and this lead to diminishing particle precursors and formation and also enhancing the process of particle oxidation [182]. Furthermore, it is obtained that the combustion of oxygenated fuels shifted (in horizontal axis) the size distribution to smaller particles leading to a reduction in the mean particle diameter. This is due to reduction in the soot formation and also a reduction in the likelihood of collisions between particles thereby less chance to form the large particles through agglomeration.

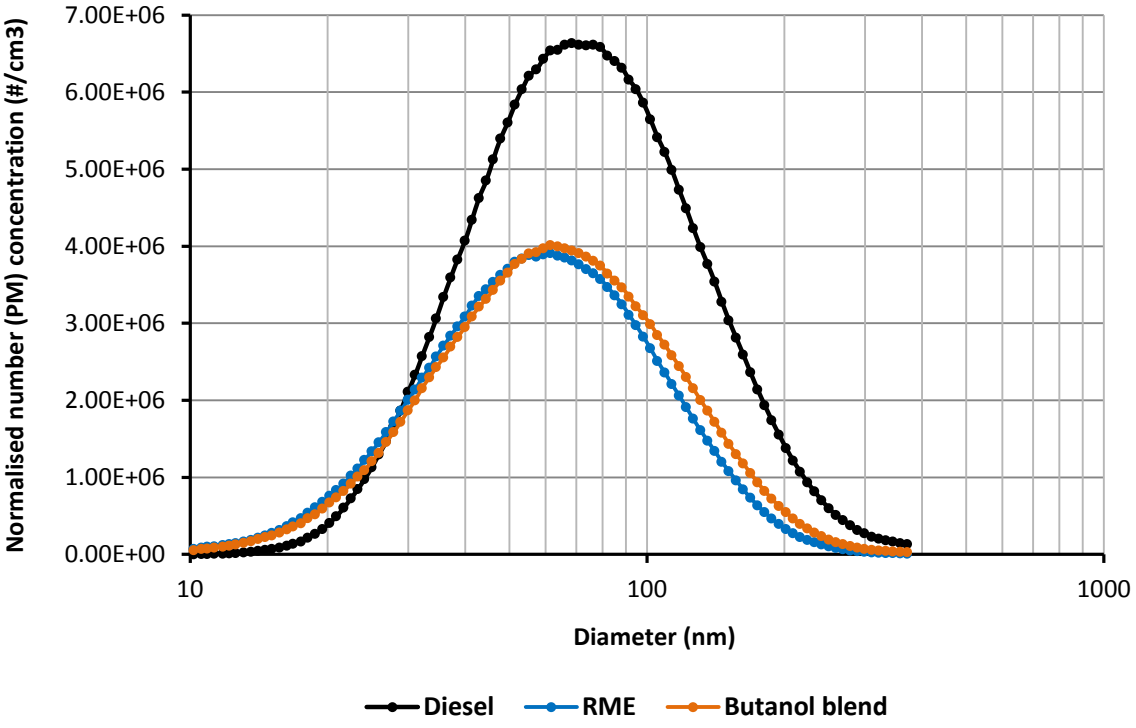

Figure 4.2: Particulate size distribution for different fuels

Figure 4.3 and Figure 4.4 show the number of particulate matter reduced in the DOC from the combustion of the four fuels when the catalyst inlet temperature is 400 and 500 °C, respectively. For temperatures lower than 400 °C (i.e., 100, 200, 300, °C) and the results are not shown to avoid duplication. The reduction in the number of particulates over the DOC reaches a constant level around 30% for particulates larger than 50 nm.

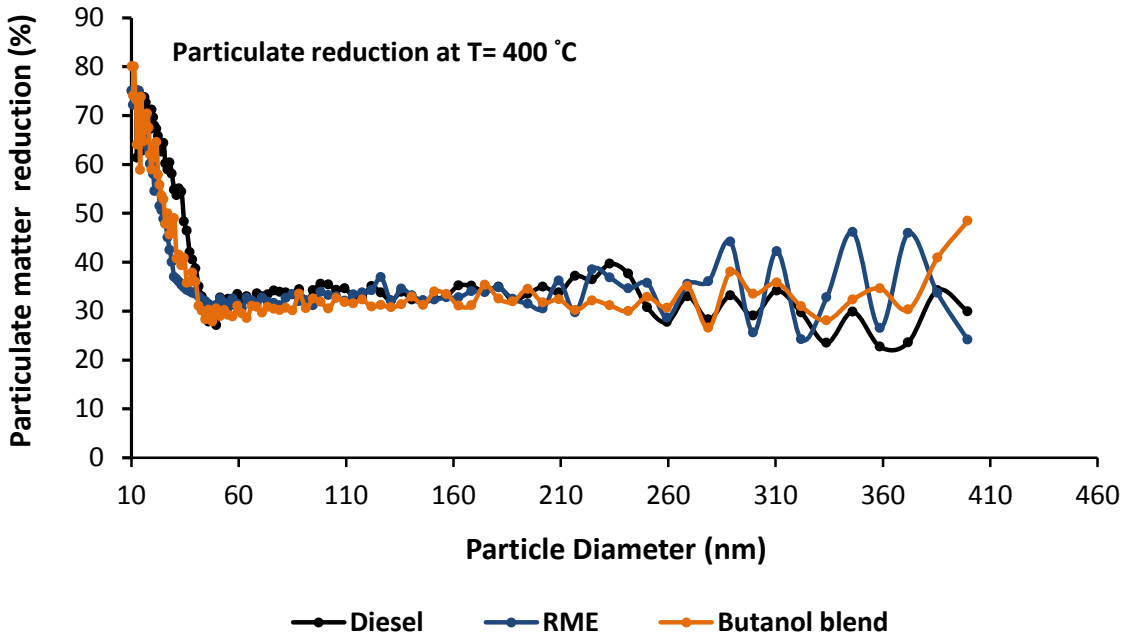

Figure 4.3: Particulate matter reduction in the DOC for different fuels at 400 °C

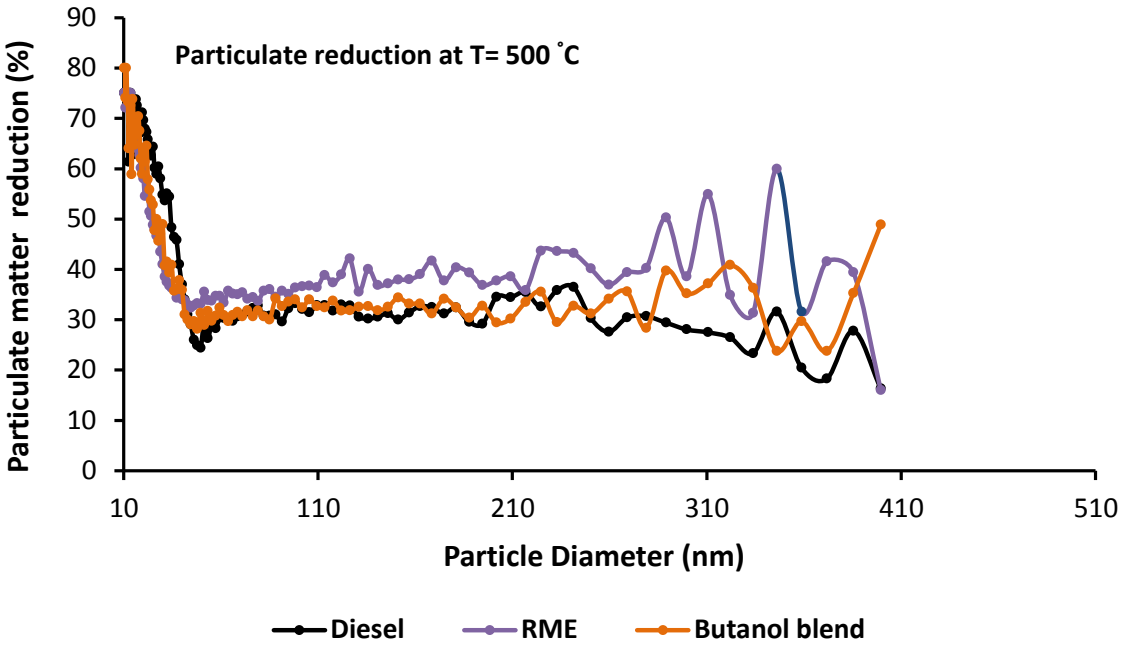

Figure 4.4: Particulate matter reduction in the DOC for different fuels at 500 °C

The average particulate electrical mobility diameter (obtained with SMPS) and average gyration radius (obtained from the TEM images, Figure 4.5) has been compared in Figure 4.6. Furthermore, the number of primary particulates that obtained from the TEM micrographs which compose the aggregates is also plotted in Figure 4.6. In all the cases (Figure 4.6) the values of the average mobility diameter and gyration diameter are similar and of the same rank, even though they are based on different measurement methods (e.g. mobility diameter is obtained from particulates after dilution, while TEM analysis is obtained directly from exhaust agglomerates). The average particulate size for butanol blend and RME is lower than in the case of diesel fuel combustion. However, the smaller average agglomerate size of the particulates emitted with RME and the butanol blend is not due to an increase in the number of small particulates but due to a significant reduction in the number of larger ones [5, 174].

There is also an increase in the average particulate size along the catalyst trend that is supported by the mobility diameter (SMPS) and to lesser extent by the radius of gyration results obtained by (TEM). This increase is obtained at both 400 and 500 °C temperatures for all the studied fuels. This increase in the mean particulate diameter is due to the higher diffusion losses associated to the particulates of smaller diameters (below 20 nm) as well as due to the collision of particulates in the DOC channels. This leads to the formation of larger size agglomerate from the high number of primary particles as it was also confirmed from the TEM results (Figure 4.6). The trapping effect of the small particulates is the major effect in the exhaust gas from the combustion of RME and butanol blends exhaust as the agglomerates analysed with TEM upstream and downstream the catalyst have similar size (Figure 4.6). However, the increase in the agglomerate size in the case of diesel is dominated by the collision and further aggregation between them as it is shown in the TEM results (Figure 4.6). The higher number of particulates in the case of diesel combustion increases the likelihood of collisions between them. The larger reduction in the number of particulate matter when the DOC temperature is 500 °C with respect to 400 °C in the case of RME cannot be due to the oxidation of gas phase hydrocarbon as the DOC oxidation efficiency was the same for both temperatures. It could be interpreted as an indication of the oxidation of organic material already contained in the particulates or an indication of soot oxidation activity due to the lower soot oxidation temperature from RME combustion as it has been previously reported [142, 168]. This should be confirmed by the morphological and microstructural results discussed below.

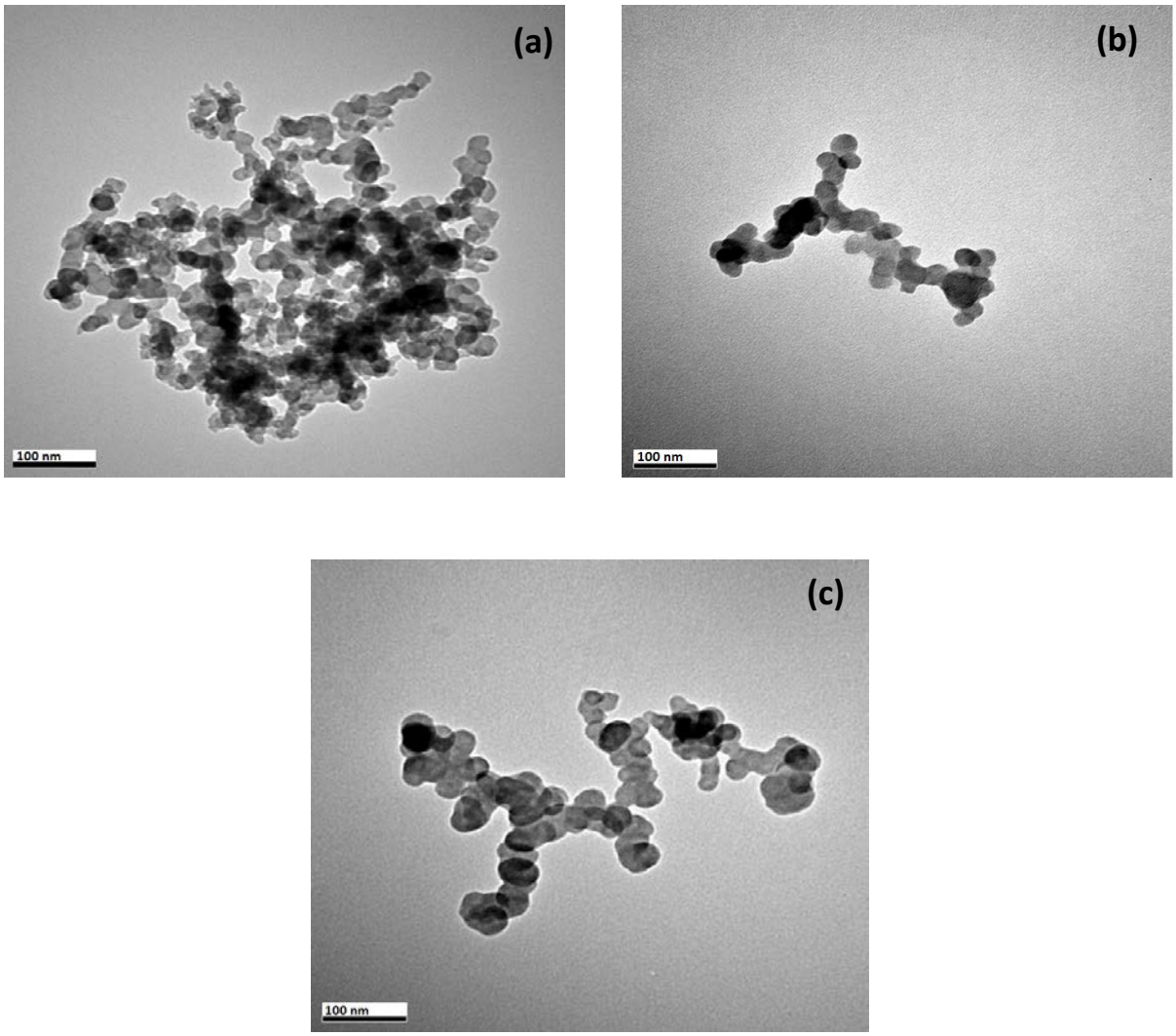

Figure 4.5: TEM micrograph of particulates matter collected at the exhaust gas (a) diesel, (b) RME, (c) butanol blend

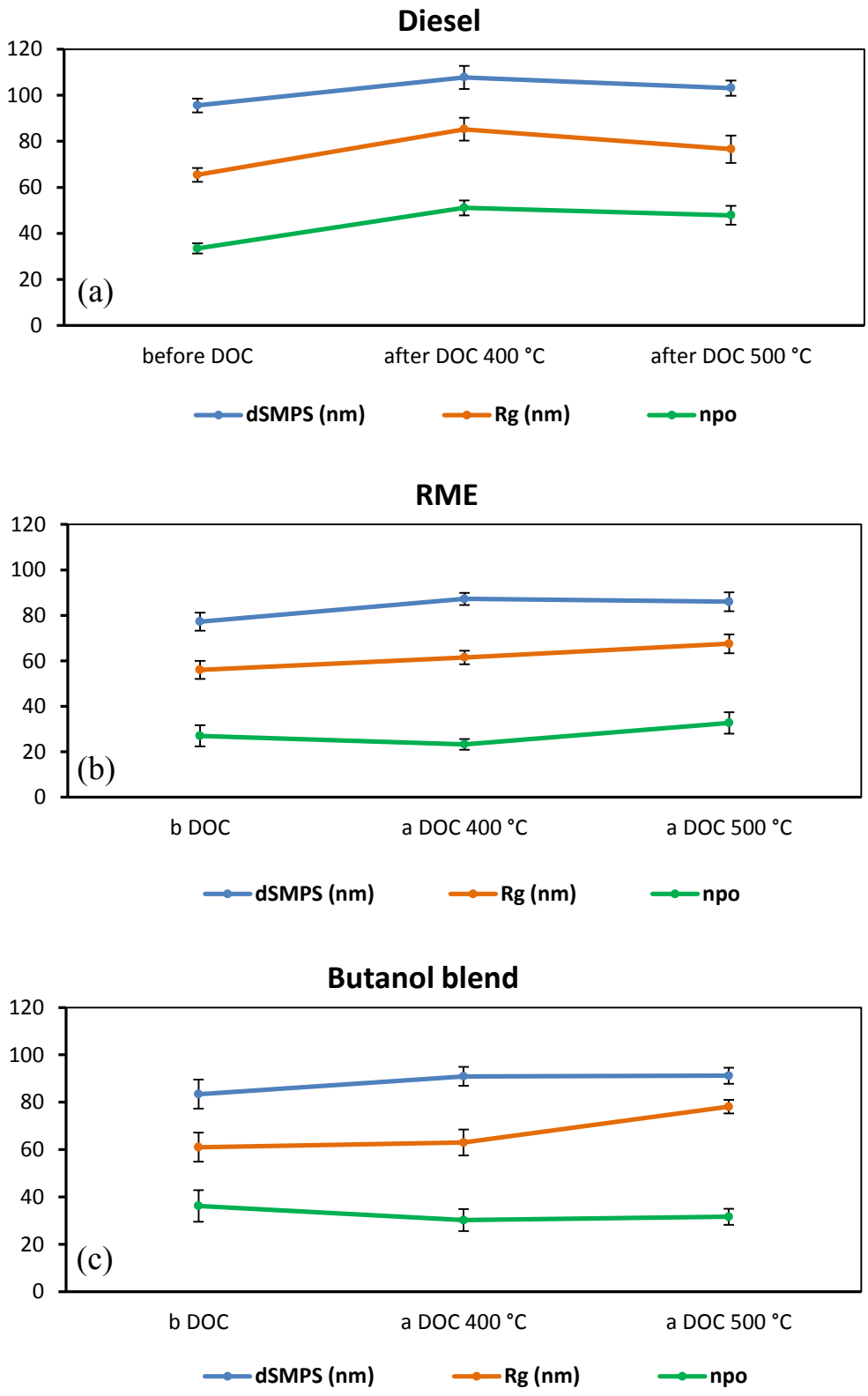

a DOC: after DOC, b DOC: before DOC

Figure 4.6: Particle size of SMPS results Vs. Gyration radius (R_g) and number of primary particles (n_{po}) for (a) diesel fuel, (b) RME, and (c) butanol blend

The fractal dimension (D_f) results obtained for all the conditions are in the typical range of diesel particulates (1.7-1.8) which is characteristic of diffusion-limited aggregation mechanism growth [245]. According to the results, the fractal dimension of the aggregates of particulates produced from the combustion of diesel is larger than those produced from the combustion of RME, and the butanol blend (Figure 4.7). Soot aggregates from the diesel combustion have a more pronounced spherical shape compared to the rest of the fuels [117, 245]. Therefore, it is expected that the particulates emitted from the alternative fuels would be more easily to be trapped in the filters due to their chain-shape morphology (e.g. Figure 4.5). The PM shape was also changed over the DOC due to the aggregation as well as thermal restructuration of the agglomerates resulting from the temperature increase within the catalyst. As a result, the particles downstream the DOC have slightly more spherical shape, especially in the case of those emitted from diesel fuel. It can be noted that the DOC has considerable reduction and a significant influence on the size and concentration of particulate emissions, which in turn enables to reduce tail pipe PM emission.

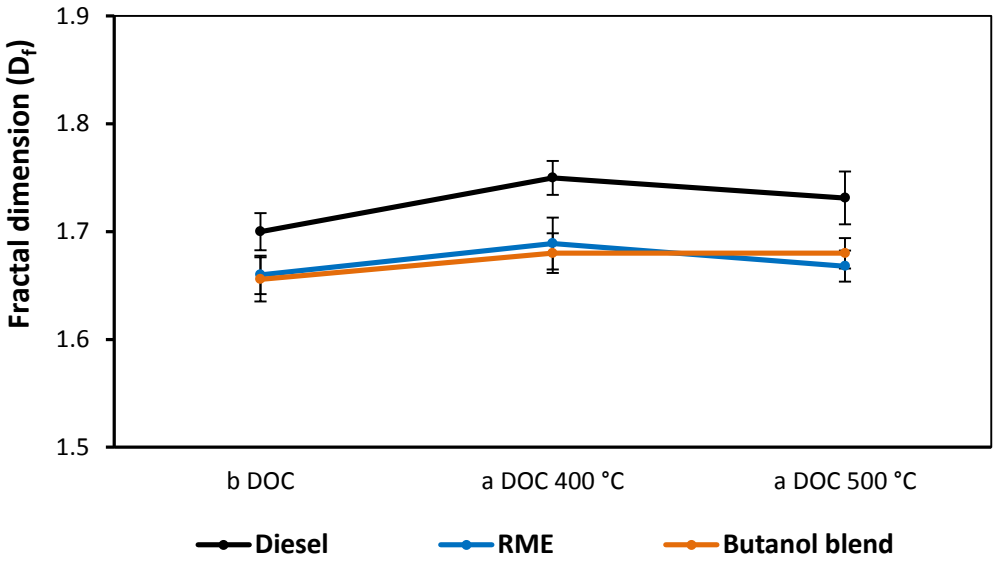

Figure 4.7: Fractal dimensions of particulates matter from TEM for all fuels tested

The size of primary particulates (d_{po}) and microstructural parameters for all the studied fuels has also been investigated. Figure 4.8 shows the primary particulate size distributions for all the fuels. A statistically significant number of primary particulates (around 150-200) for each fuel and condition (before and after the DOC) has been measured to produce the fitted log-normal/normal distribution (Figure 4.8) and calculate the mean primary particulate size (Figure 4.9). It can be obtained that the size of primary particulates is bigger in the case of diesel fuel, while the smallest primary particulate size is obtained from the combustion of butanol blend. This is a result of the lower rate of production of soot precursors, which limits the soot formation and the increased rate of soot oxidation during the combustion process of the oxygenated fuels. This result together with the morphology results demonstrates that the smaller size agglomerates in the case of oxygenated fuels is due to the lower number of primary particulates as well as the smaller size of the primary particulates which composed the agglomerates. It can also be concluded

that the DOC does not modify the primary particulate size in any of the fuels. This result supports the idea that the DOC only affects the particulate agglomerates rather than the primary particulates which would need higher temperatures and residence time in the catalyst to be oxidised.

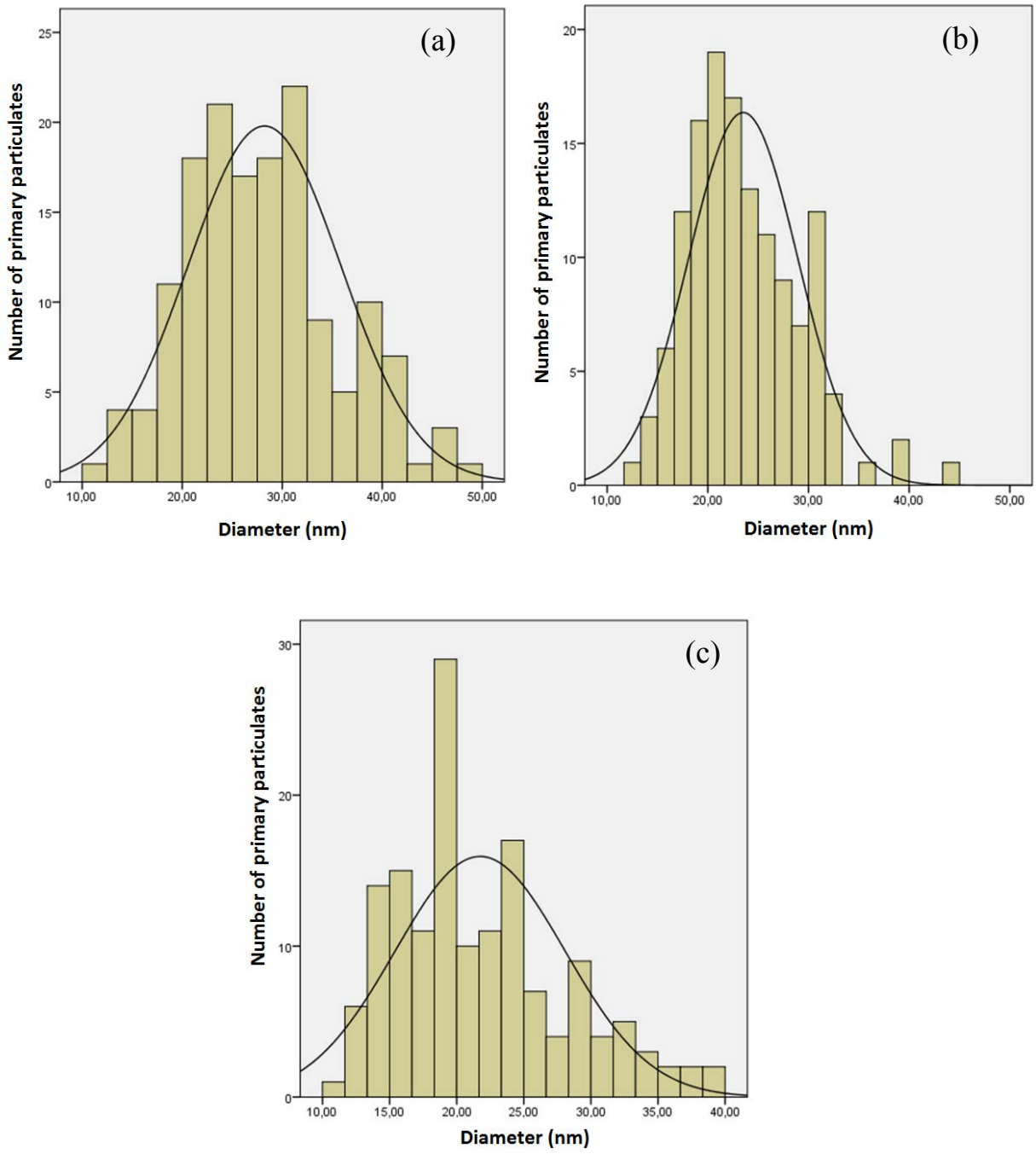

Figure 4.8: Primary particles size distributions for (a) diesel fuel, (b) RME(c) butanol blend

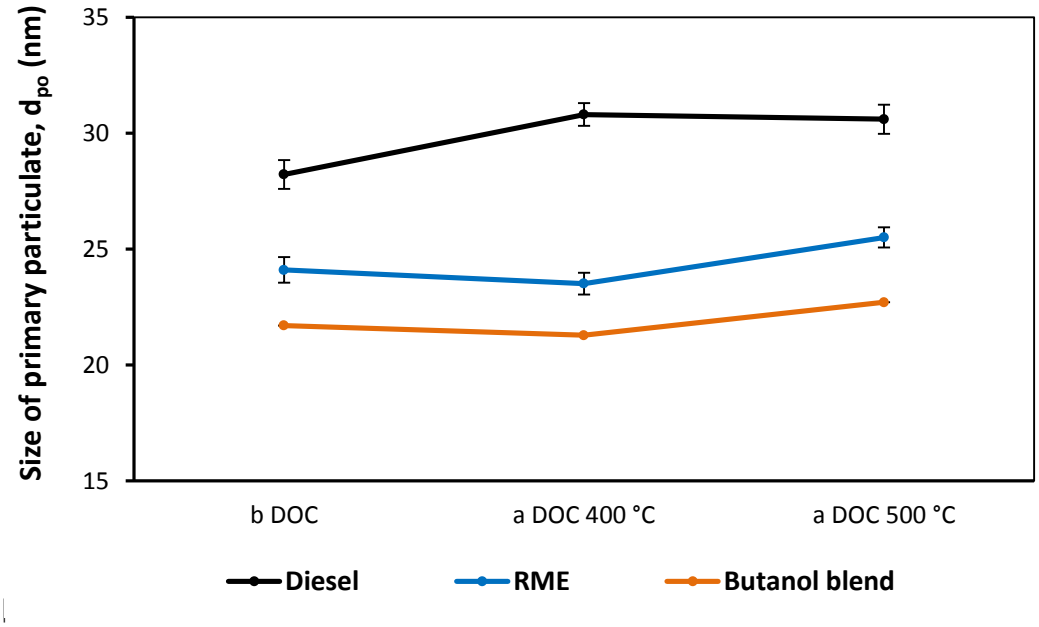

Figure 4.9: Size of primary particulate (d_{po}) for all fuel tested

PM microstructure (see a high resolution micrograph in Figure 4.10-a) has been quantified by the average interlayer spacing (d_{002}) and average thickness of the graphene layer which composed the soot primary particulates (Figure 4.10-b). It is shown that the interlayer spacing from the soot produced from RME and butanol blends combustion is smaller than those found in the soot produced from diesel combustion (Figure 4.10-b). However, there are no statistically significant differences between the average thicknesses of the graphene layer derived from the combustion of the studied fuels. The smaller interlayer spacing for the soot derived from oxygenated fuels is an indication of a more ordered structure, as supported by the literature [20, 130]. Figure 4.10-b also shows that the DOC does not produce any statistically significant effect on the microstructural parameters obtained from the PM of all the fuels. On the basis of the morphology and microstructural

results of particulate matter upstream and downstream of the diesel oxidation catalyst, it can be concluded that the influence of the DOC in the (i) oxidation of gaseous hydrocarbons which can later be nucleate, oxidizes the adsorbed hydrocarbons on PM (effect (ii)), leads to agglomeration of particulates (effect (iii)), and traps by diffusion some of the solid particulates (effect (iv)). However, the DOC is not able to oxidise the soot (effect (v)). It is proposed that the residence time between the soot and the catalysed active sites within the DOC is not enough to oxidise soot being only able to trap some particulates and oxidise the gas-phase volatile components irrespective of the fuel used.

(a)

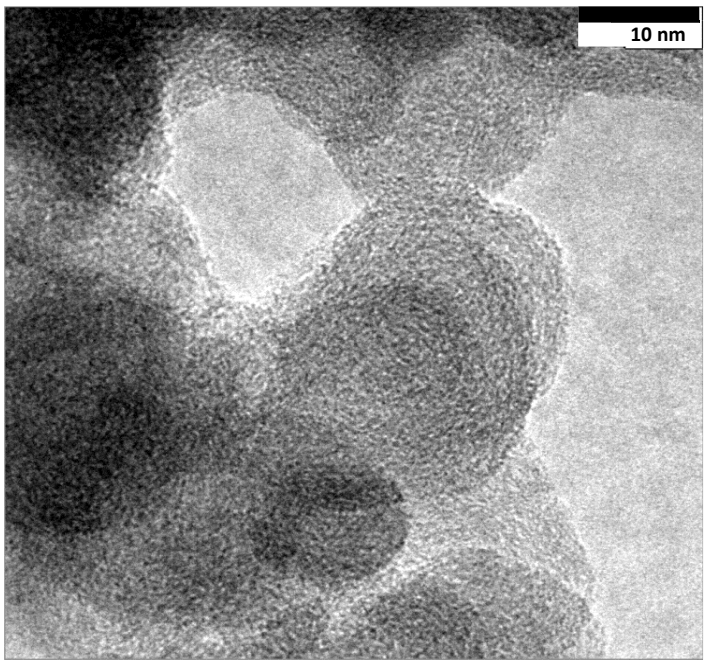

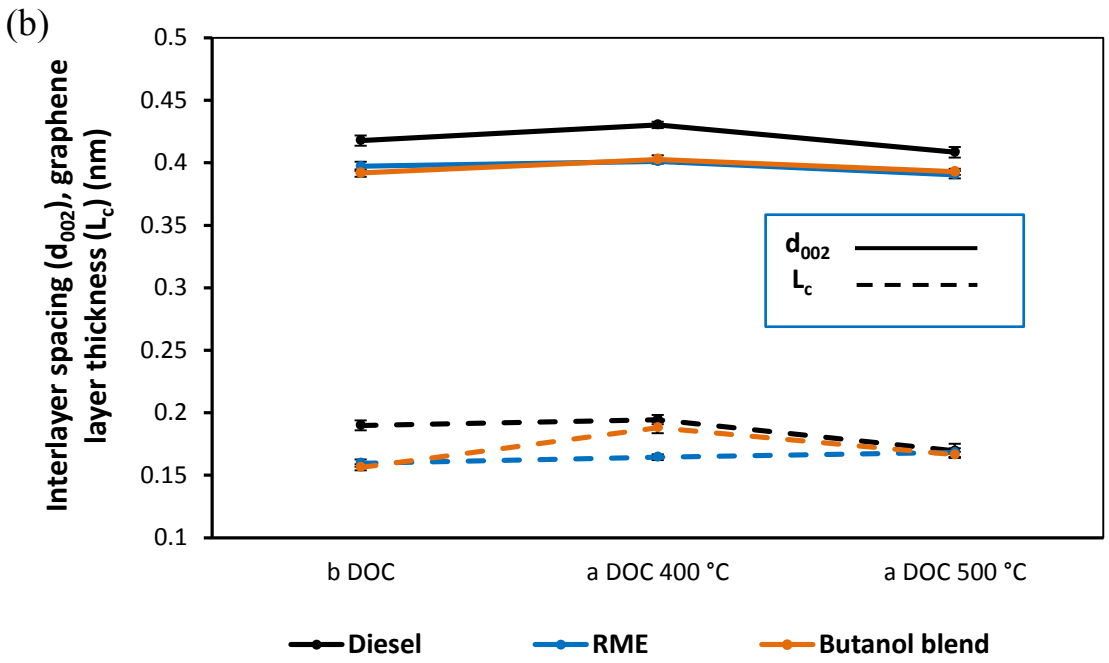

a DOC: after DOC, b DOC: before DOC

Figure 4.10: Particulate matter microstructure (a) High resolution TEM micrograph, (b) Interlayer spacing (d_{002}) and graphene layer thickness (L_c)

4.2.2 CARBON MONOXIDE (CO) REDUCTION IN THE DOC

It has been previously reported that the DOC performance depends on the exhaust temperature and composition [20] as some of the exhaust emissions are competing each other to be adsorbed into the active site of the catalyst. Therefore, by changing the exhaust temperature and composition by using different fuels for combustion will have an influence on the oxidation performance of the DOC catalyst. The CO and HCs engine output emissions from the combustion of conventional diesel fuel are higher compared to the rest of the tested fuels Figure 4.11.

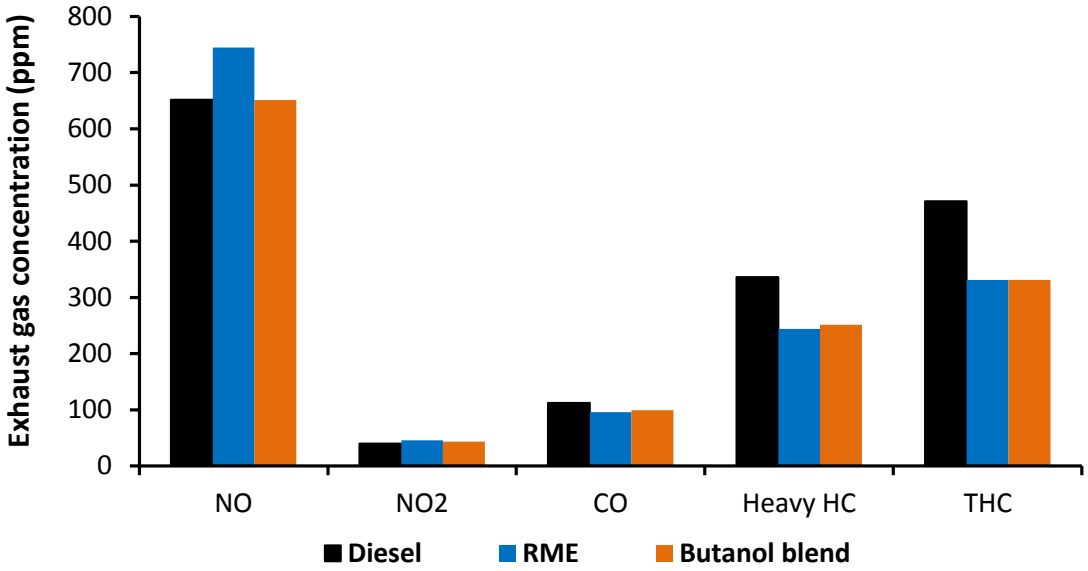

Figure 4.11: Engine gaseous emissions

The high level of CO and HCs for diesel combustion hampers the CO adsorption onto the catalyst (zeolites) at low exhaust gas temperatures [20] leading to a delay in the start of CO light-off compared to the other fuels (Figure 4.12). In contrast, the lower engine output HC and CO concentration from the combustion of RME and alcohol blend (Figure 4.11) reduces the possibility for obstruction from CO and HC competition and improved the catalyst CO light-off. At low temperatures, the CO oxidation in the DOC is kinetically limited (poor accessibility to active sites by other component inhibition) [246].

Once the oxidation has started, there are some plateaus in the CO light-off curves for most of the fuels (around 100 - 150 °C). At high exhaust temperatures, CO is not thermodynamically limited and the heat release from its oxidation increases the local temperature of the catalyst. This higher active site temperature helps the oxidation of CO (Figure 4.12), especially in the case of diesel combustion where the level of CO emission is higher. Moreover, this higher rate of CO oxidation for the case of diesel at this temperature

could be due to high medium-heavy hydrocarbon depletion as shown in Figure 4.13. At higher temperatures (approximately 180 °C), the CO oxidation in the DOC catalyst for diesel combustion reaches 100 % at lower temperature compares to the rest of the fuels, especially for RME (Figure 4.12). The exhaust from the RME combustion has the lowest level of CO and the highest levels of NO_x leading to reduced exothermic and increased competition for active sites between CO and NO [87].

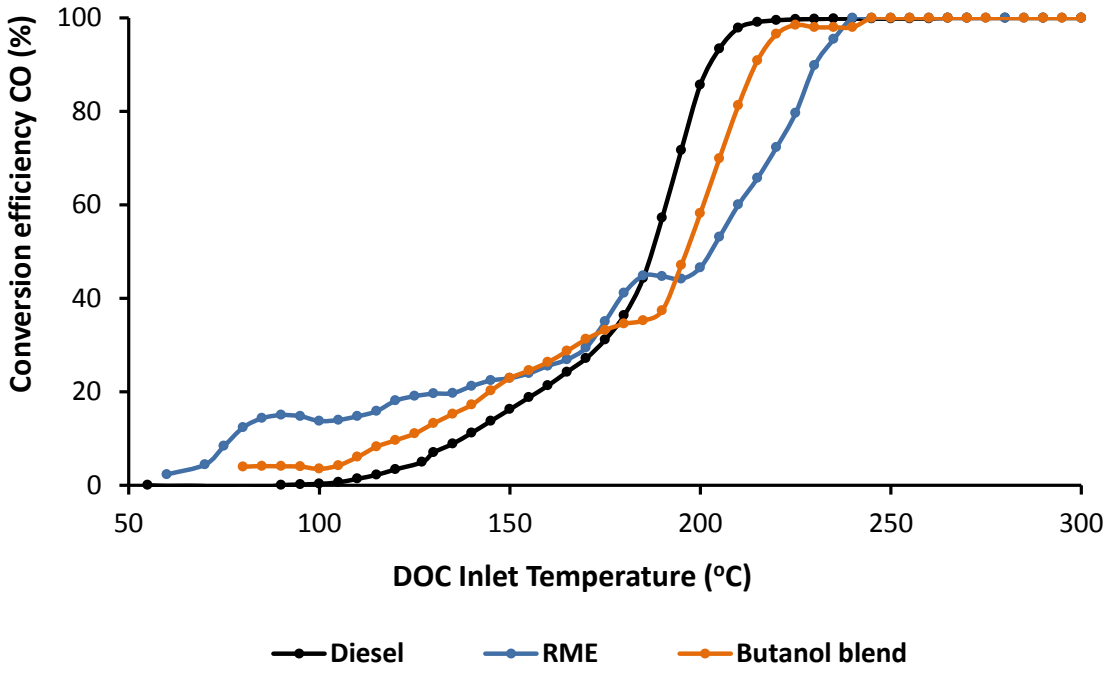

Figure 4.12: CO light-off curves from exhaust gas produced for different fuels

4.2.3 HYDROCARBONS (HCs) REDUCTION IN THE DOC

The low temperature hydrocarbon conversion seen in the DOC is due to the trapping effect by the zeolites ('virtual conversion') [87]. When temperature increases and the conversion efficiency for CO is high, the catalyst active sites become available for HCs adsorption and oxidation. It can be seen that HCs oxidation for all the fuels increased once CO was fully oxidised (Figure 4.12 and Figure 4.13-a).

The lowest HCs conversion efficiency over the DOC occurs for the case of diesel combustion. This is due to the higher upstream concentration of engine out aromatic hydrocarbons which have been reported to be more difficult to be adsorbed and oxidised [87, 174, 247, 248]. Meanwhile, higher HC conversion in the DOC was noted when exhaust gas from the combustion of the RME was used and this is due to the absence of aromatic hydrocarbons in the fuel structure. Moderate HC conversion is obtained when exhaust gas from for the combustion alcohol blends was used and this is due to the large presence of diesel in the fuel blend, partially compensated by the presence of the alcohol.

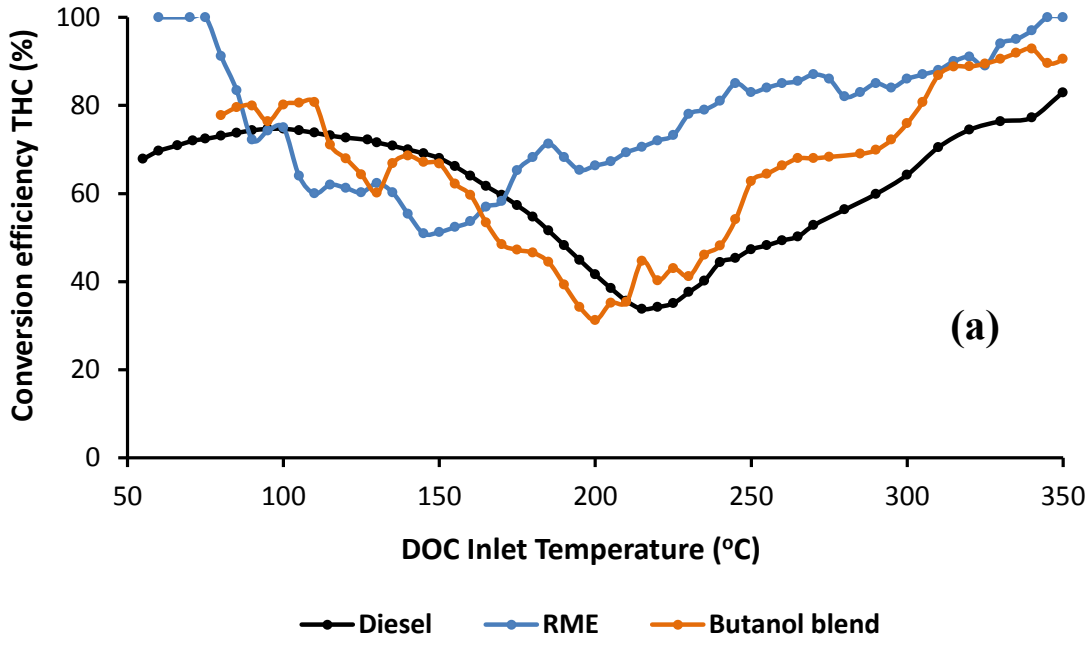

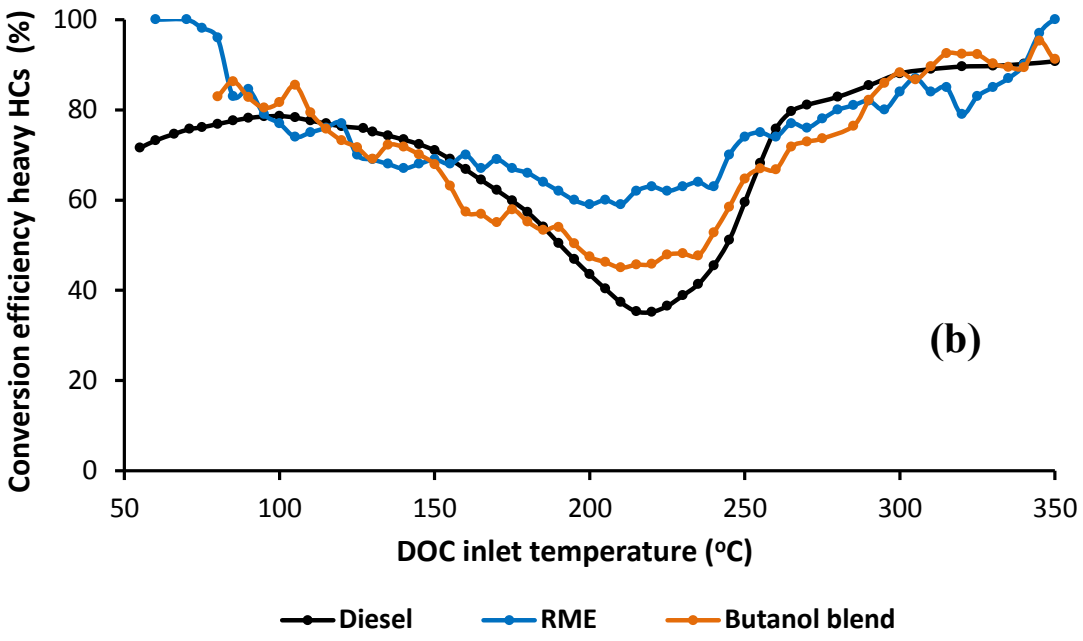

Figure 4.13: DOC conversion efficiency for a) THC and b) heavy HCs

4.2.4 NO TO NO_2 OXIDATION IN THE DOC

The oxidation of NO to produce NO_2 in the DOC (Figure 4.14) is influenced by the different concentrations of CO, NO and by the concentration and type of HCs. It can be observed that at low temperature the NO_2 concentration downstream the DOC is lower than the engine output NO_2. This is the effect of NO_2 reacting with CO and HC in the DOC catalyst. The increase in the NO_2 concentration downstream the catalyst starts around the same temperatures (approximately 220 °C) for all the studied cases, once the CO has been completely oxidised by oxygen in the catalyst active sites. Hence, it is evident the inhibition of CO on NO_2 production occupying the catalyst active sites as well as the consumption of any NO_2 created by reaction with CO and HCs to form CO_2.

It is noticeable the higher NO_2 concentration downstream the catalyst at temperatures below 350 °C was seen in the case of butanol combustion. The formation of some very active oxygenated hydrocarbon components which could be formed in the catalyst can enhance NO_2 production. A similar effect has been already reported in the case of Ag/Al_2O_3 catalyst where the formation of NO_2 is highly promoted under the addition of alcohol fuels [249, 250]. At temperatures higher than 350 °C the NO_2 production is not further increasing forming a plateau as the NO_2 production from NO oxidation is thermodynamic limited [251].

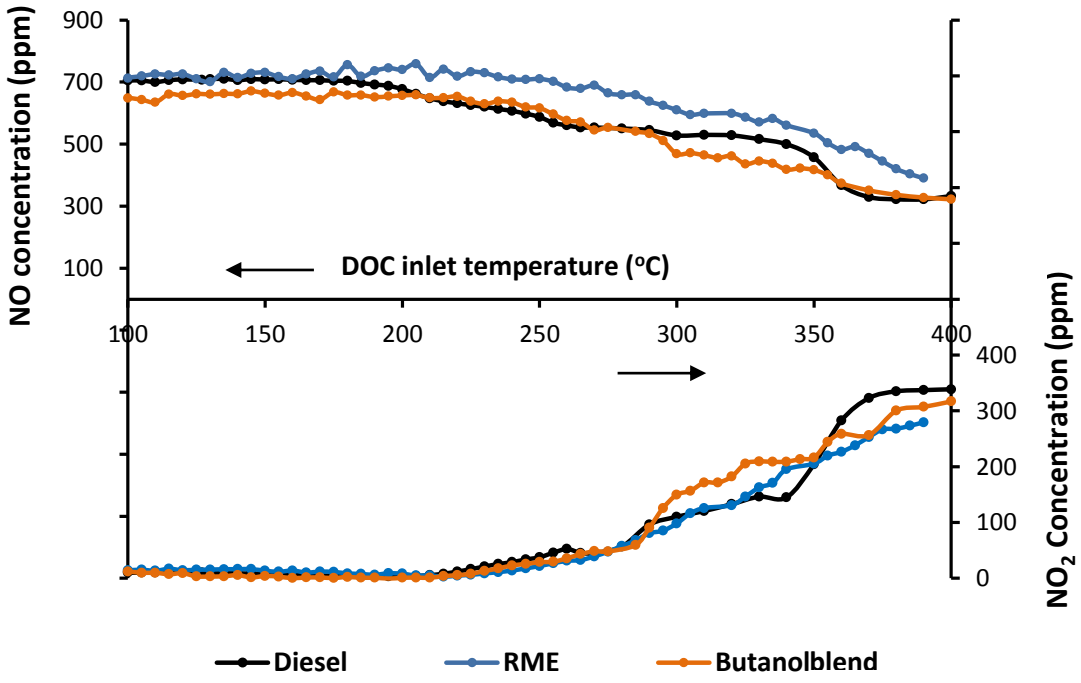

Figure 4.14: NO and NO_2 catalyst outlet concentration from engine operation

4.2.5 SUMMARY

The purpose of the present work was to investigate the effects of a diesel oxidation catalyst on particulate matter characteristics and gaseous emissions from the combustion of alternative fuels. This study gives an insight regarding of the effects of alternative fuels on the DOC performance over (i) particulate matter reduction/modification, (ii) pollutant emissions oxidation such as CO and THCs to CO_2 and H_2O and (iii) NO oxidation to NO_2 which can be further used in the catalytic reduction of NO_x in the SCR or in the DPFs passive regeneration.

The combustion of alternative fuels produces lower emissions of unburnt hydrocarbons, CO, and PM number concentration which enhances the catalyst activity at lower temperatures by limiting the CO and HCs inhibition effect and DOC performance in long-term operation by reducing the PM accumulation effect. PM agglomerates and their primary particles emitted from the combustion of alternative fuels are on average smaller and with a lower fractal dimension, thus more easily trapped or oxidised. It has to be noticed that the average smaller size of the agglomerates emitted from the combustion of alternative fuels is due to the production of lower number of large particulates rather than a high number of small particulates, being less detrimental for the environment and/or downstream diesel particulate filter.

Analysis revealed that results from SMPS and TEM support the larger size of particulates downstream the DOC catalyst for all fuels due to the higher filtration efficiency for small particulates as well as the aggregation taken place within the DOC. Furthermore, the SMPS and TEM analysis revealed that the PM filtration efficiency in the DOC is higher for the small particles and that there is a PM aggregation process that takes

place within the DOC. Furthermore, DOC does not modify the primary particulates size and microstructural parameters for any of the studied fuels. Therefore, it is thought that the DOC only has a trapping effect on soot and oxidises the PM volatile components, while a longer residence time is needed to oxidise the soot. The combustion process proved that when using alternative fuels are most effective, not only creating lower gaseous and PM emission levels in the exhaust gas which enhances the low temperature DOC performance but also PM with characteristics being easier to be trapped or oxidised.

CHAPTER 5

MANIPULATING MODERN DIESEL ENGINE PARTICULATE EMISSION CHARACTERISTICS THROUGH BUTANOL FUEL BLENDING AND FUEL INJECTION STRATEGIES FOR EFFICIENT DIESEL OXIDATION CATALYSTS

Decoupling the dependences between emission reduction technologies and engine fuel economy in order to improve them both simultaneously has been proven a major challenge for the vehicle research communities. Additionally, the lower exhaust gas temperatures associated with the modern and future generation internal combustion engines are challenging the performance of road transport environmental catalysts. In this work the effect of fuel properties and fuel injection strategies on the combustion characteristics, emissions formation, and catalysts performance has been studied. The impact of the fuel post-injection strategy that is commonly used as part of the aftertreatment system function (i.e. regeneration of diesel particulate filters or activity in hydrocarbon selective reduction of NO_X), combined with butanol-diesel fuel blend (B20) combustion on engine emissions formation, particulate matter characteristics (size distribution, morphology and structure) and oxidation catalyst activity were studied.

This experimental study focuses on the role of the fuel post-injection and diesel-butanol fuel blends combustion on PM characteristics (number, size, morphology) and the impact on the DOC activity at exhaust gas temperature (300 °C). The DOC catalyst activity

was assessed under the same temperature, space velocity and pressure conditions with the only comparative parameter being the exhaust gas composition.

5.1 METHODOLOGY

For this study, a modern single-cylinder, water-cooled, common rail fuel injection system, four-stroke experimental diesel engine equipped with a diesel oxidation catalyst (DOC) were employed in this investigation. A schematic diagram of the experimental set up is shown in Figure 5.1. The physical and chemical properties of diesel, butanol and fuel blend properties are presented in Table 3.4 (in chapter 3). The particular diesel fuel used in this research as reference fuel was selected without any biodiesel (thereby with zero oxygen content) in its composition, in order to study the effect of the oxygen in the combustion process when diesel fuel is blended with butanol.

All tests were performed under a constant engine speed of 1800 rpm with an engine load of 3 bar IMEP (Indicated Mean Effective Pressure). The injection was split in pre, main, and post fuel injection with injection timing of 15 and 3 deg bTDC and 60 deg aTDC, injection pressure of 650 bar, and post-injection duration of 0.1 ms. The pre and main injection for this test were set at 0.15 ms and 0.48 ms respectively. The temperature of the reactor inside a tubular furnace was set at 300 °C while maintaining constant gas hourly space velocity (GHSV) of 35000 h^{-1}. The details of diesel oxidation catalyst (DOC) and instruments are presented in Chapter 3.

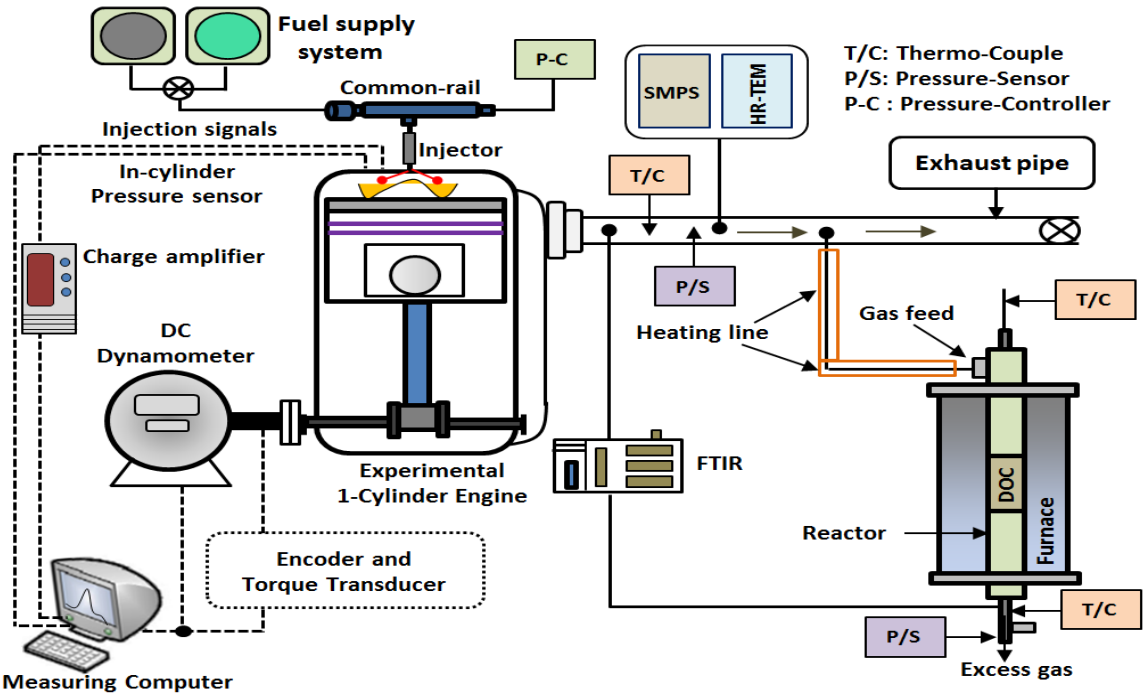

Figure 5.1: Schematic diagram of test platform and sampling system

5.2 RESULTS AND DISSCUSSION

Most of modern diesel engines in Europe countries operate at lower cylinder pressure and thus lower temperature to comply with stringent NOx emissions requirements. In addition, lower load operations of diesel engines cause lower cylinder pressure and thus lower temperature. Therefore, low temperature can lead to ignition problems and poor combustion which causes increased soot formation and aggregation of unburned fuel in the cylinder, and intuitively presenting a significant challenge to DOCs.

The influence of fuel and post injection effects on catalysts activity is minimal. This experimental study is conducted with various injection strategies for diesel fuel and butanol blend (B20) at exhaust gas temperature (300 °C). This work focuses on

how these parameters effect on the morphological parameters of soot particles and diesel catalyst performance under the same temperature.

5.2.1 COMBUSTION CHARACTERISTICS

Figure 5.2 shows the effects of the injection strategy on the in-cylinder pressure and the rate of heat release (ROHR) versus crank angle degree (CAD) for the combustion of diesel and B20. It has to be noted that neither the post-injection nor the fuel properties notably affected the combustion events. It is though that this is due to the effect of the pre-injection which thermally conditioned the in-cylinder, thus minimizing the effect of the worse autoignition properties (Table 3.4) of the B20 blend with respect to diesel fuel. Small increase of the in-cylinder pressure and heat release was obtained from the combustion of B20 that may also explain the changes in emissions later on.

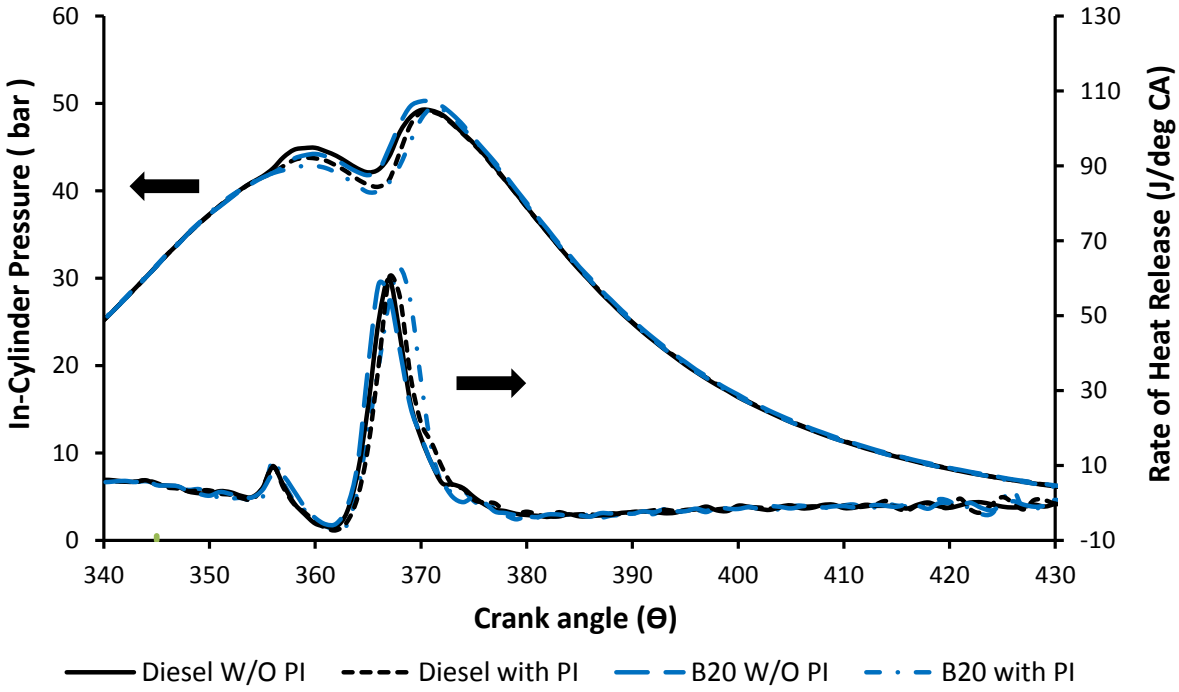

Figure 5.2: Effect of fuel post-injection strategy and fuels structure on combustion characteristics

5.2.2 INFLUENCE OF FUEL POST-INJECTION AND FUEL STRUCTURE ON ENGINE OUT PM (SIZE DISTRIBUTION AND CHARACTERISTICS)

The PSDs were obtained upstream the DOC in order to understand the influence of B20 and post-injection on the particle formation and oxidation processes. The combustion of the alcohol blend (B20) reduced the number of particles along the whole distribution with respect to combustion of the diesel fuel with and without post-injection (Figure 5.3). A slight reduction is observed in the average particle diameter, from 94 nm for diesel down to 64 nm for B20 in the absence of post-injection. These results are in agreement with previous studies of butanol-diesel blends combustion [33, 77] justified by the presence of the hydroxyl group in the butanol molecule [77] leading to lower rates of

PM formation [5, 77] and to enhanced PM oxidation rates [77, 252]. Reductions of the soot in the exhaust are often reported when post-injection is introduced due to increased expansion temperature and enhanced mixing within the cylinder that increases oxidation of soot produced from the main injection [44, 225-227].

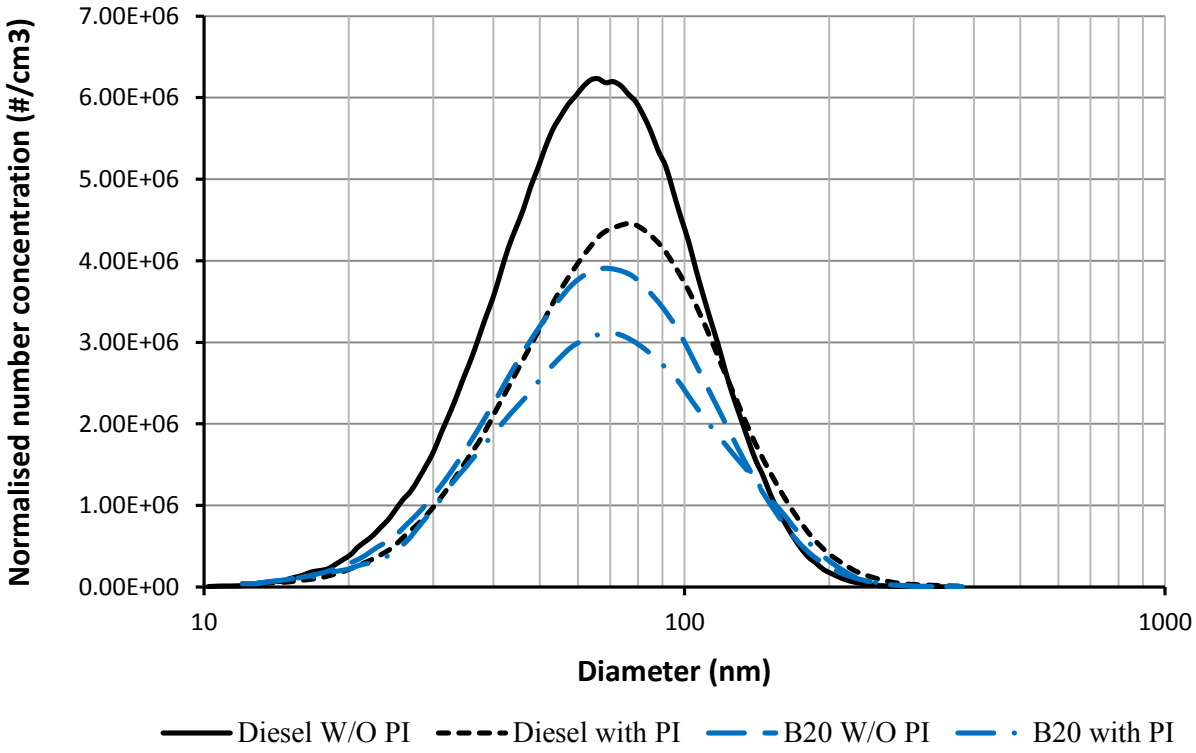

Figure 5.3: Effect of post-injection on particle size distribution for diesel and B20 fuels.

The particles emitted from diesel engine have a variety of shapes and sizes and consist of tens to hundreds of primary particles agglomerated together, forming irregular clusters [114, 135]. Figure 5.4 depicts representative examples of HR-TEM micrographs from particles sampled from the exhaust gas at the different conditions studied in this research. PM morphological parameters (radius of gyration (R_g), number of primary particles (n_{po}) and fractal dimension (D_f)) for Diesel and B20 are calculated from the obtained HR-TEM images (Figure 5.4). Trends observed in these representative examples

are in agreement with the statistical trends discussed below. Figure 5.5 shows the results of the average particles electrical mobility diameter obtained with SMPS jointly with soot's average radius of gyration and number of primary particles. According to these results the average agglomerate size (quantified by radius of gyration and mobility diameter) and the number of primary particles are lower for B20 than for diesel fuel independently of the injection strategy. It is believed that for diesel combustion the enhanced net formation rate of particles increases the likelihood of collisions and further aggregation leading to higher number of primary particles. It is thought that oxygen content in butanol blend (B20) improves the soot oxidation [160] while the incorporation of the post-injection leads to enhanced oxidation resulting in the disappearance of a fraction of the primary particles already formed (Figure 5.5). The reduction in number of particles as measured by the SMPS and the reduction in number of primary particles in the particle aggregate for B20 are also associated with the reduction in the formation of soot precursors due to the chemical structure of butanol and the lack of PAH in butanol, besides the effect of the oxygen content of butanol.

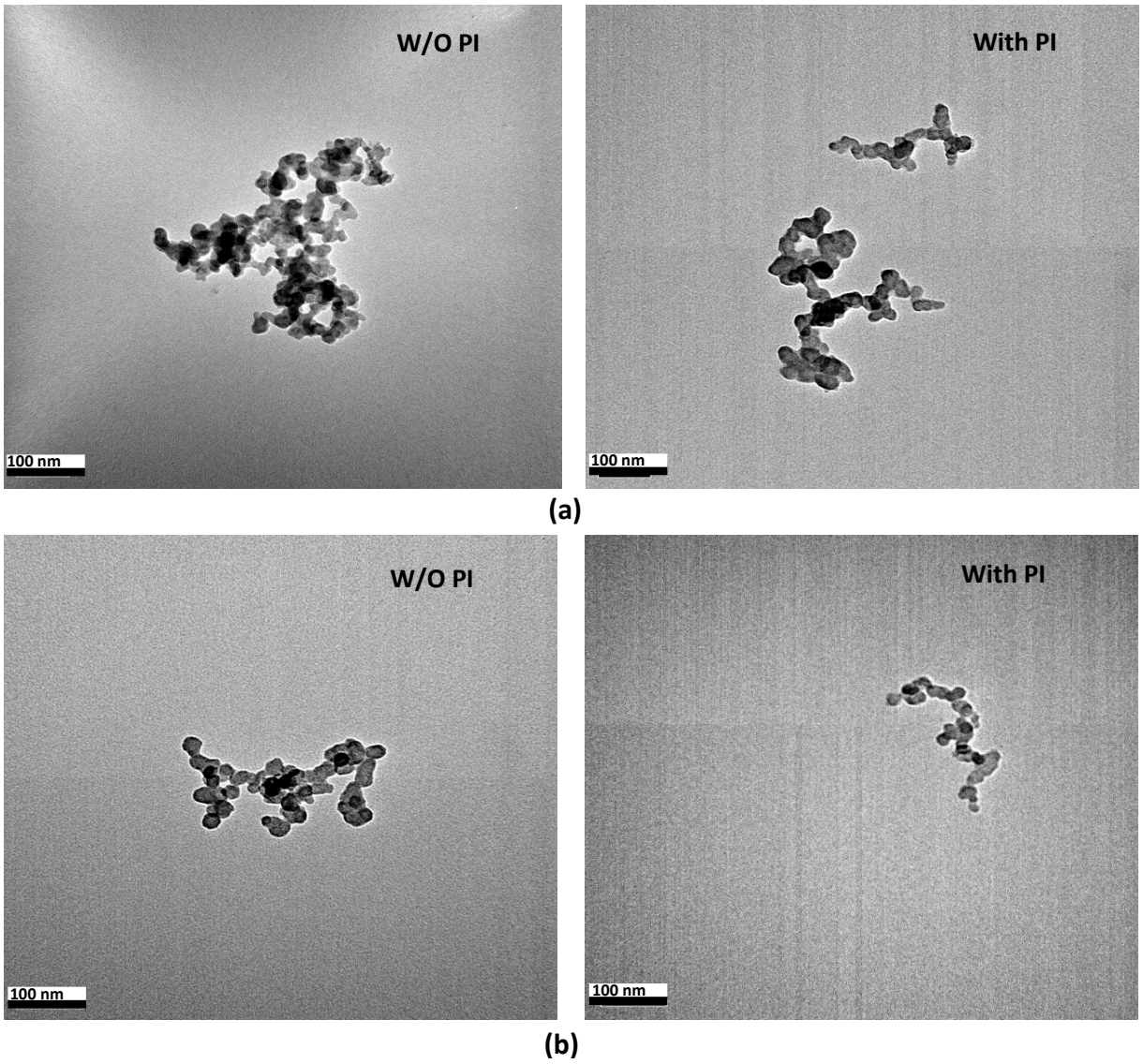

Figure 5.4: Typical examples of HR-TEM micrograph of particles matter collected at the exhaust gas for (a) diesel fuel, and (b) B20

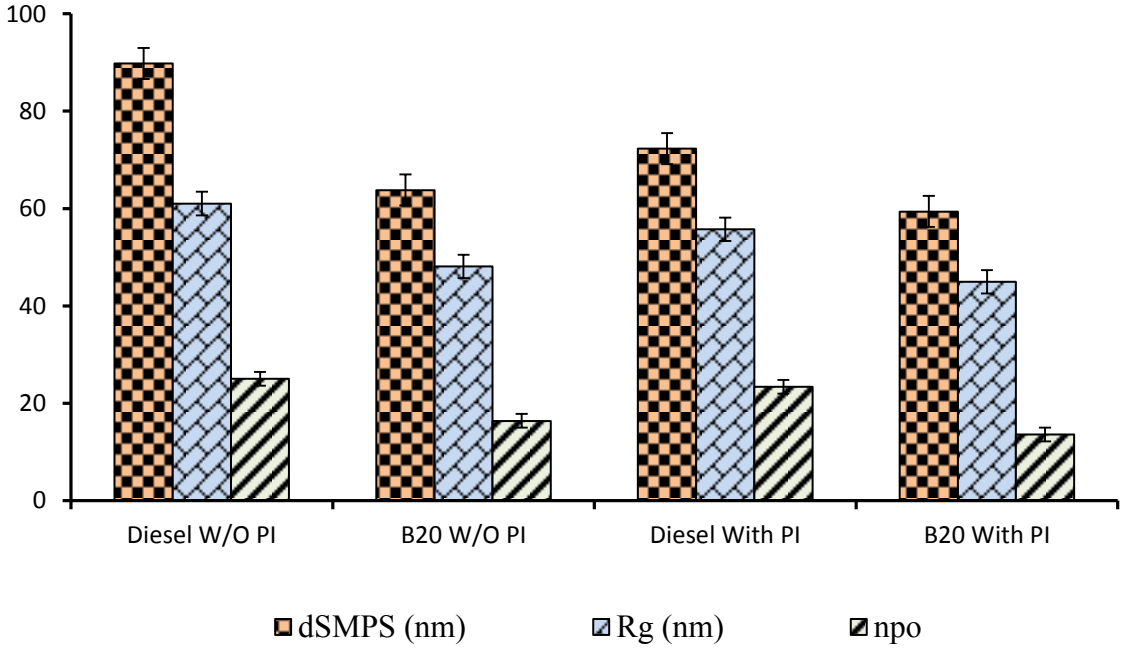

Figure 5.5: Effect of fuel injection strategy and fuel characteristics on particle size from SMPS, radius of gyration (R_g) and number of primary particles (n_{po})

The influence of the fuel and injection strategy (with and without post-injection) on the fractal dimension (D_f) is shown in Figure 5.6. The fractal dimension of the agglomerates produced from the diesel fuel is higher (by 1.62-1.66) than that from B20 for both injection strategies (Figure 5.6) and this is in agreement with the work described by both Fayad et al. [77] and Choi et al. [253]. As a general rule [216] a reduction of the fractal dimension should be expected when there is a high concentration of particles as a result of the increased likelihood of collisions between agglomerates. However, in the case of agglomerates from oxygenated fuels, despite the lower particle concentration (and the consequent reduced likelihood of collisions) fractal dimensions were not found to be higher, but were systematically lower instead, probably due to some internal oxidation of agglomerates occurring after being formed. Similarly, the fractal dimension is also lower

when post-injection was introduced for both fuels, despite the higher particle concentration also in this case (Figure 5.6). A conceptual model is suggested here to justify these trends. In the early stage of nuclei and primary particle formation fractal dimension is close to 3 and the primary particle size continuously increases (spherical nuclei and spherical primary particles). Collisions between particles and agglomerates and between agglomerates and agglomerates will increase the size of the agglomerate and reduce their fractal dimension (particle growth dominant over particle oxidation). This phenomenon will be more intense in the case of diesel without post injection conditions due to the higher rate of particle formation. Afterwards, the oxidation of particles will become dominant over the particle formation and the size of both primary particles and agglomerates could decrease, while the fractal dimension will deeply decrease, for the reason pointed out above. In this case, the decrease in fractal dimension will be more intense for the case of oxygenated fuels and post-injection conditions. Therefore, it is speculated that the resultant agglomerates from oxygenate fuels and post-injection conditions will have lower fractal dimension as the oxidation will remain being the dominant mechanism in front of particle formation and growth for longer time, as a consequence of the enhanced reactivity of soot particles (in the case of oxygenated fuels) or of the enhanced temperature conditions in the exhaust flow (in the case of post-injection). More research and some in-cylinder sampling techniques should be used for a more comprehensive justification.

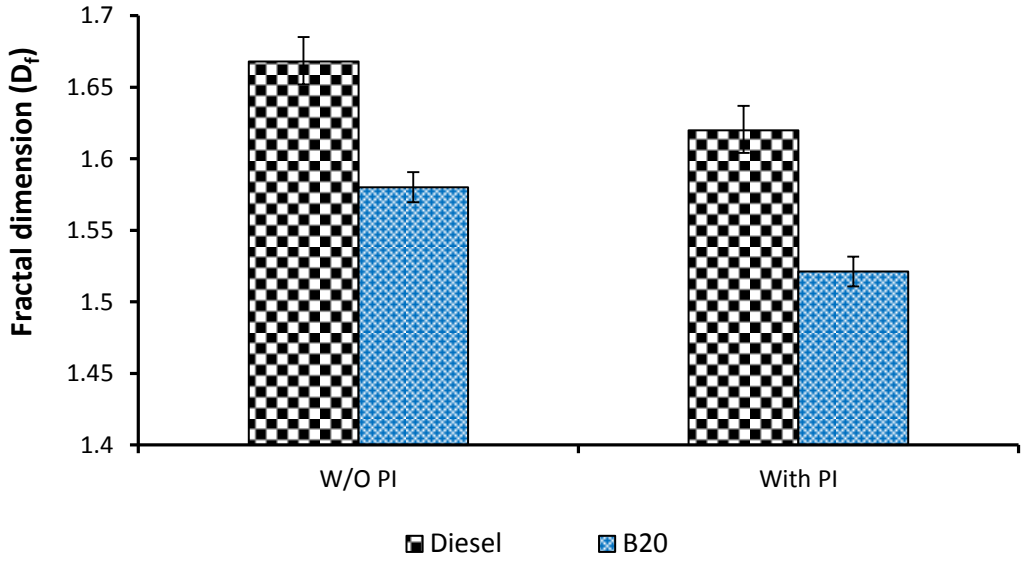

Figure 5.6: Fractal dimensions of particulate matter from the HR-TEM images

The primary particle diameter (d_{po}) size distribution for both fuels with or without post-injection has been measured by selecting around 200 primary particles (more than 33 HR-TEM photographs for each condition and fuel) in order to fit normal distribution as shown in Figure 5.7. Figure 5.8 shows smaller size primary particles from the combustion of B20 for both injection setting (with and without post-injection) compared to diesel primary particles due to lower rate of production of soot precursors, soot formation and soot growth, and to the increase soot oxidation during the combustion of oxygenated fuel [77]. This result is in agreement with results obtained from biodiesel fuel [254] and butanol [77, 119] fuel blends without post-injection using other engine technologies [77, 119]. The size of primary particles is slightly reduced when post-injection was used for both fuels (Figure 5.8). It is believed this is due to an enhancement in the soot oxidation rate in the expansion stroke under post-injection conditions.

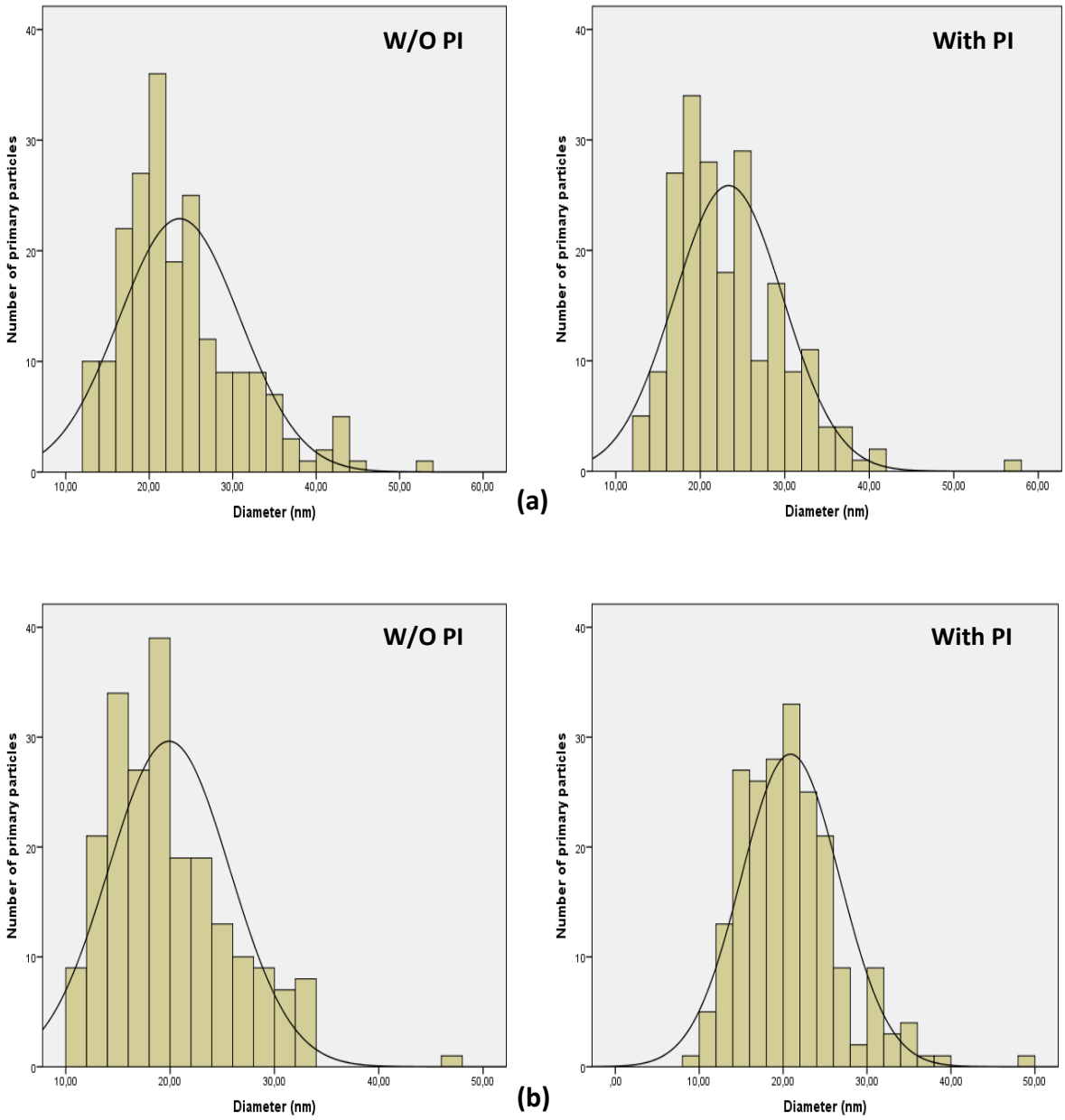

Figure 5.7: Primary particles size distributions for (a) diesel fuel, and (b) B20

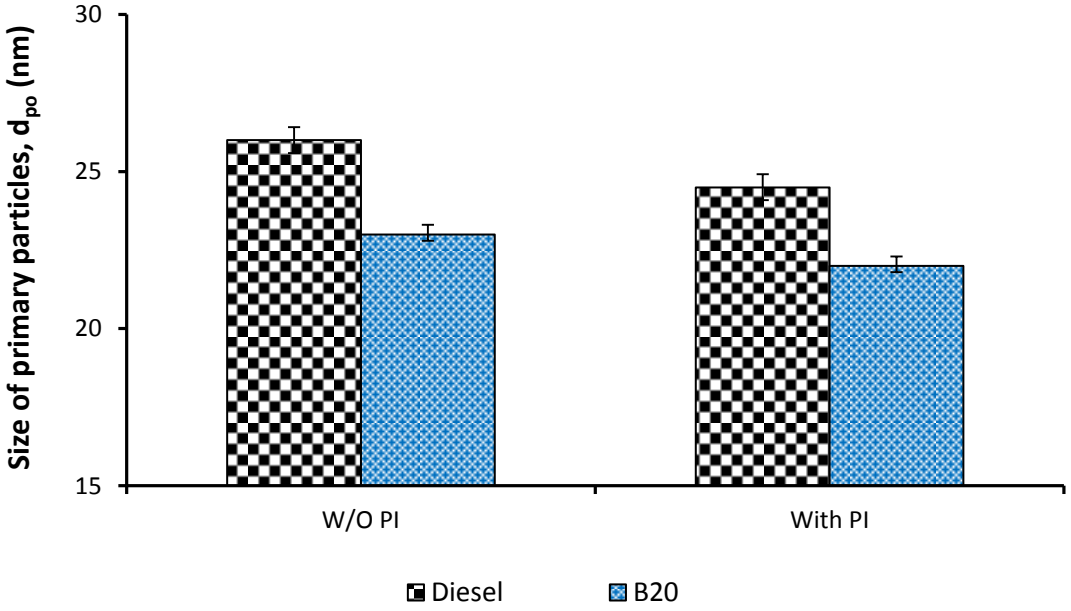

Figure 5.8: Average size of primary particles (d_{po}) for diesel and B20

5.2.3 INFLUENCE OF FUEL POST-INJECTION AND FUEL STRUCTURE ON ENGINE GASEOUS EMISSIONS

Figure 5.9 shows the CO, heavy HC, and THC engine-out emissions for the two studied fuels at both injection strategies. It can be noticed that THC emissions were lower from the combustion of the alcohol blend (B20) for both injection strategies. The higher HC emissions observed with diesel can be attributed to several reasons including absence of oxygen in the fuel molecule, and less efficient oxidation. The THC emissions in the case of post-injection are much higher compared to the case without post-injection. This confirms that the quantity and timing chosen for the post-injection allows to keep most of them unburnt and available to be oxidised in the DOC. Yamamoto, et al. and Chen, [41, 44] reported that the late post-injection lead to high level of THC emissions. It is reported that the reason of the increase in CO emissions observed for B20, especially without post-injection, can be attributed to the expected lower local in-cylinder temperature (Figure 5.2)

and less CO oxidation during the combustion process due to the higher enthalpy of vaporisation of butanol with respect to diesel fuel [42]. Therefore, it seems that at this engine load operation the oxygen content and high reactivity of the butanol molecule enables to partially oxidise most of the HC species to CO, but the colder in-cylinder conditions due to the enthalpy of vaporization of butanol hinders the complete oxidation from CO to CO_2.

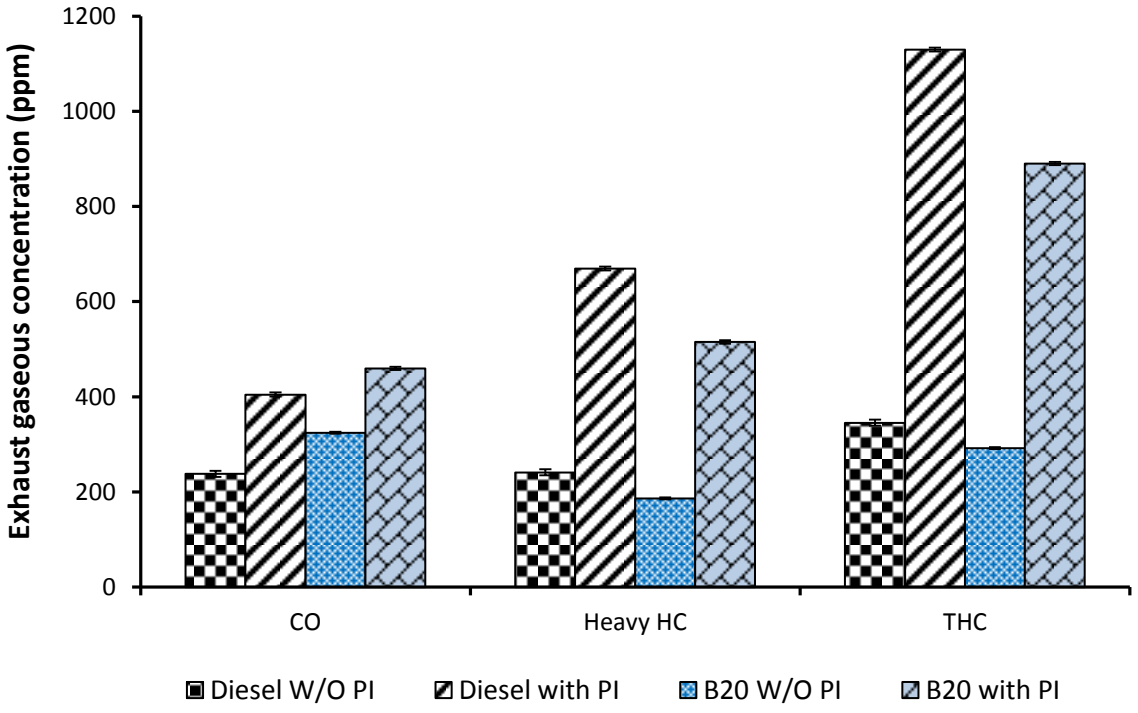

Figure 5.9: Engine exhaust gaseous emissions

The concentration of HC species in the engine exhaust upstream the catalyst differs for diesel and B20 engine fuelling (Figure 5.10). The concentration of the light HC species studied including saturated (methane, ethane) and unsaturated (ethylene) species is higher for B20 with respect to diesel fuel combustion, conversely to the THC emissions presented earlier. It is thought that this is due to the thermal decomposition of the butanol component to light HC species and CO rather than forming heavy HC components as in the

case of diesel fuel combustion. The level of HC emissions was lower from the combustion of B20 compared to the diesel fuel combustion. This can be due to improved combustion efficiency of the fuel in the presence of oxygen in the fuel as has also been described in [119] and due to the combustion patterns described in Figure 5.2, where a small increase in the in-cylinder pressure was obtained. From the results it can be also observed that with the incorporation of the fuel post-injection, higher concentration of the total and selected HC species were measured for both fuels due to the late timing of the post-injection [41].

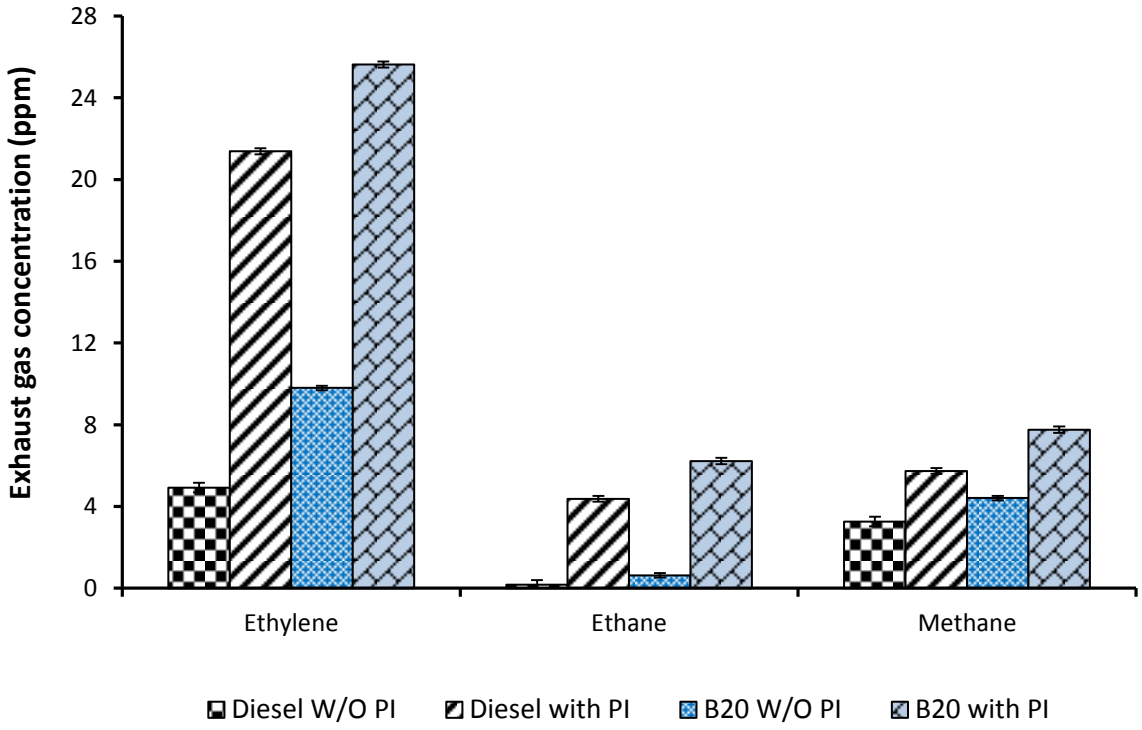

Figure 5.10: Engine exhaust hydrocarbon species measured upstream the DOC

A slight increase in NO_X ($NO+NO_2$) was measured for the B20 combustion with respect to diesel combustion for both injection strategies (Figure 5.11). This can be due to the slight increase of in-cylinder pressure as seen in Figure 5.2 and the presence of the chemically bound oxygen content in B20 as it has been previously reported in the case of

oxygenated fuels [119]. In addition, the oxygen content and lower cetane number of butanol enhanced the burning rate (faster burning). Chen et al [255] reported similar trends in NOx emissions from the combustion of n-butanol-diesel blends and suggested that this was a result of the increased ignition delay that was then led to wider high-temperature combustion region. In addition, the oxygen content and lower cetane number of butanol enhanced the burning rate (faster burning). Although both fuels have similar NO concentration, it seems that B20 blend has higher oxidation from NO to NO_2 than diesel fuel due to the oxygen in the molecule. When post-injection was utilised the emissions of NO were decreased with simultaneously increasing in NO_2 for both fuels (Figure 5.11). This is can be explained because a portion of NO was oxidised to NO_2 by hydroperoxy radical (HO_2) formed during post combustion [256] and because of the reduction of NO_X with some of the HCs post-injected. It was noted that the engine out NO_X emissions decreased under post-injection due to the possible formation of nitrated-hydrocarbon by reacting NO_X with radical HC [256].

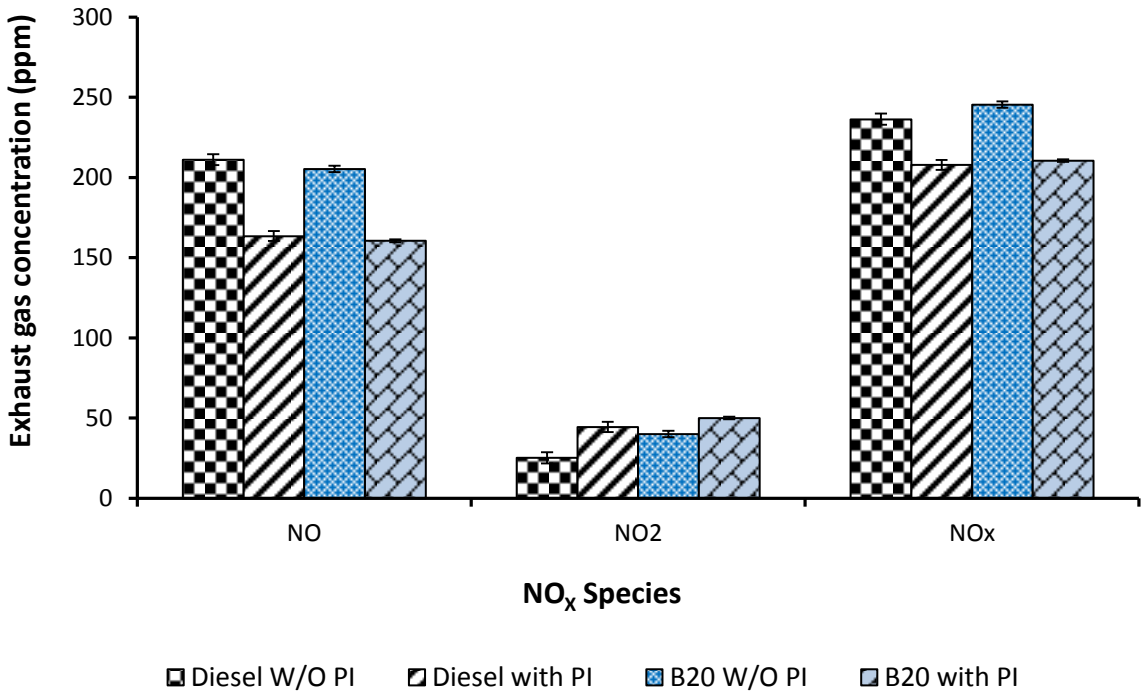

Figure 5.11: NO_X species concentrations of each gas species for with and without post-injection

5.2.4 BRAKE SPECIFIC FUEL CONSUMPTION AND BRAKE THERMAL EFFICIENCY

The brake specific fuel consumption (BSFC) and brake thermal efficiency (BTE) for both diesel and butanol blends are summarized in Table 5.1. It was noticed that post injection strategy increased the brake specific fuel consumption (BSFC) compared to that of main injection for both fuels. Moreover, BSFC slightly increased with B20 for both injection strategies when compared to the diesel fuel. The mean increase in BSFC for B20 when compared to the diesel under the same condition is 0.02811 and 0.02903 kg/kWh for without post-injection and with post-injection respectively. This is due to the lower calorific value recorded for B20 (see Table 3.4 in chapter 3) compared to the diesel fuel. Lapuerta et al. [6] and Hajbabaei et al. [257] reported that the oxygenated fuels increases

the BSFC mainly due to the reduced calorific value when compared to the diesel. Furthermore, the smaller increase in BSFC for B20 its compensated by its lower calorific value resulting in an increase in brake thermal efficiency. This could be due to the oxygen content in the B20 that improves the combustion efficiency and this is consistent with other researchers cited in introduction. It is clear from Table 5.1 that the post-injection reduce brake thermal efficiency and increase the exhaust gas temperature (EGT) for both fuels.

Table 5.1: Brake specific fuel consumption and thermal efficiency

Fuel	**Diesel fuel**		**B20**	
Parameters	W/O PI	With PI	W/O PI	With PI
Brake specific fuel consumption, BSFC (kg/kWh)	0.3484	0.3645	0.3765	0.3935
Exhaust gas temperature, EGT (°C)	283	291	272	284
Brake thermal efficiency (BTE)	23.97	23.25	25.44	24.83

5.2.5 INFLUENCE OF FUEL POST-INJECTION AND FUEL PROPERTIES ON DOC ACTIVITY

Combustion by-products in the exhaust gas are competing with each other to be adsorbed into the active sites of the catalyst [20, 77], effects that is highly depends on the temperature, flow conditions, space velocity and concentration and nature of the exhaust species. In active control aftertreatments such as diesel particulate filters (DPFs) the ability of the DOC to effectively oxidise the fuel and hydrocarbons and provide the required heat

is important for the efficient operation of the engine system (including aftertreatment and engine fuel economy and emissions). The gas hourly space velocity (GHSV) and temperature of the DOC in this study were controlled and set at 35000 h^{-1} and 300 °C, respectively in order to isolate the effect of exhaust gas composition.

The DOC is very effective in reducing CO in the engine exhaust from the combustion of both fuels, with the catalyst's CO conversion efficiency being higher for B20 blend. In the case of post-injection, the catalyst's CO oxidation efficiency was reduced (Figure 5.12), this is due to increased concentration of species that are now competing for the same number of active sites. The HC species presented in Figure 5.12 are light saturated (methane, ethane), light unsaturated (ethylene) and heavy HCs. The results confirm the differences in reactivity of the hydrocarbon species. Methane (CH_4) as a short chain saturated hydrocarbon was the most difficult component to oxidise in the catalyst due to its low oxidation reactivity [21, 81]. Particularly, it can be observed that the conversion efficiency of methane over the catalyst was even lower than 10% at 300 °C for all the conditions studied. In addition, the increased concentration of heavier HCs and fuel in the exhaust that reaches the DOC leads to its non-selective poisoning (i.e. fouling or masking).

The catalyst active sites are now occupied by the increased concentration of HCs and fuel that are interfering with the reactants transport phenomena to the catalyst active sites. This non-selective poisoning limits the catalytic surface area and obstructs access of the reactants to the pores. In this case the effect is reversible as for the B20 fuel combustion, the catalyst has the highest HC conversion efficiency at 300 °C compared with diesel fuel (Figure 5.12). This could be due to several reasons such as lower concentration of HC upstream the catalyst, higher reactivity of butanol and its derivatives, higher level of

NO_2 emissions to catalytically oxidise the HC species [77, 187], lower PM/soot levels that can be responsible for blocking the active sites.

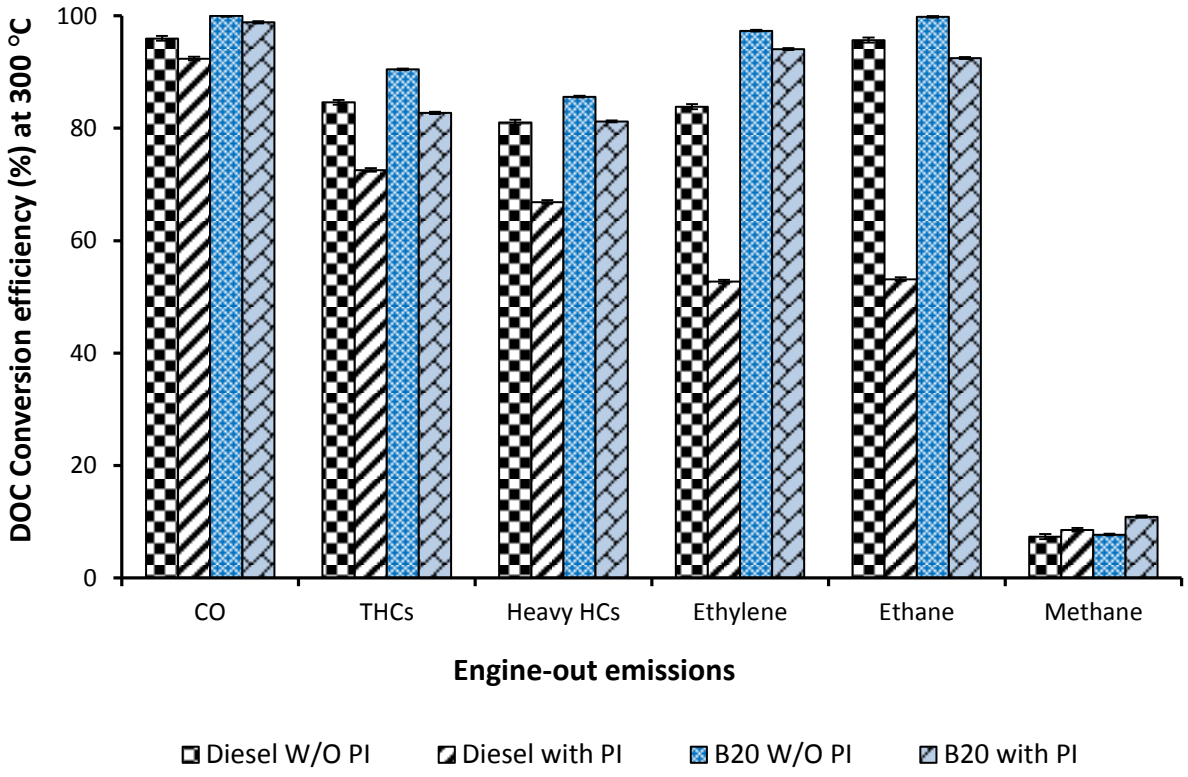

Figure 5.12: Diesel oxidation catalyst (DOC) activity at 300 °C

5.2.6 SUMMARY

The effect of fuel post-injection and butanol-diesel fuel blends (B20) on PM characteristics (including size, fractal dimension, radius of gyration, and size of primary particles) and gaseous emissions were analysed and their influence on DOC activity was investigated at exhaust temperature of 300 °C. Due to reduced PM number concentration and HC emissions from the combustion of B20 the catalyst activity was improved. The HR -TEM analysis showed that the number of primary particles of PM agglomerates emitted

from B20 combustion was lower than that from the combustion of diesel fuel. As B20 has oxygen-containing compounds, they contribute to inhibit the rate of soot formation and to increase the rate of oxidation, resulting in particles with smaller average size and fractal dimension. It is observed that the fuel post-injection has more clear benefits on PM reduction, resulting in enhanced soot oxidation with similar trends on the morphology of agglomerates as the presence of oxygenated compounds. HR-TEM analysis supports the results from SMPS and revealed that B20 produces particles with smaller average size compared to diesel fuel.

The fuel components as has been highlighted from the use of primary alcohols in this study, can improve engine systems performance by providing a chain of beneficial effects; from the combustion process to emissions formation processes to their abatement processes in the aftertreatment systems. In this case the changes in fuels properties from the incorporation of butanol into diesel fuel, led to cleaner combustion that eased species (i.e. HCs/fuel and engine out emissions) oxidation in the DOC. These trends will favour the active control strategies in the aftertreatment systems and will positively impact on their performance (i.e. increase activity, improve durability) and overall engine fuel economy.

CHAPTER 6

INTERACTIONS BETWEEN AFTERTREATMENT SYSTEMS ARCHITECTURE AND COMBUSTION OF OXYGENATED FUELS IN DIESEL FOR IMPROVED LOW TEMPERATURE CATALYSTS ACTIVITY

Diesel engine vehicles, despite their good fuel economy and reduced CO_2, are receiving significant attention and negative publicity in recent years due to their inability in achieving the emissions regulations. This has widely been linked to undesirable environmental impact and premature deaths. In addition, the lower exhaust gas temperatures associated with modern more efficient hybrid powertrain and diesel engines makes current technology catalytic aftertreatment systems inactive under range of vehicle operating conditions. It is possible to optimise the mechanisms that enhance the lower temperatures of catalyst activity by understanding the interactions (promotion/inhibition) between exhaust gas species from oxygenated fuel and catalyst performance.

In the current chapter, the engine is operated with alternative fuel (butanol blend) and diesel fuel as a reference fuel to produce a variety of exhaust gases such as CO, HC, NOx, and PM. In this test examine three main dominant parameters of the diesel engine exhaust gas, the composition, temperature and reactant residence time on catalyst light-off performance using butanol-diesel blend (B20). Furthermore, the combination of a filtration unit (DPF) upstream an oxidation catalyst (DOC) at various space velocities is

also studied. The combination of cleaner combustion (i.e. butanol blend) and unconventional aftertreatment architecture allows to study the impact of carbon species accumulation within the catalyst and the effect on its catalytic activity.

6.1 METHODOLOGY

The details of diesel engine used in this chapter are explained in chapter 3 (see Table 3.2). A simplified schematic layout of the representative experimental set-up is detailed and illustrated in Figure 6.1. The engine exhaust is linked to a bespoke catalyst research and development test rig that allows catalyst activity and characterisation studies. The set-up of mini reactor and catalyst position inside furnace were explained in chapter 3. The combined arrangement of DPF and DOC aftertreatment systems inside furnace are also shown (see Figure 6.1).

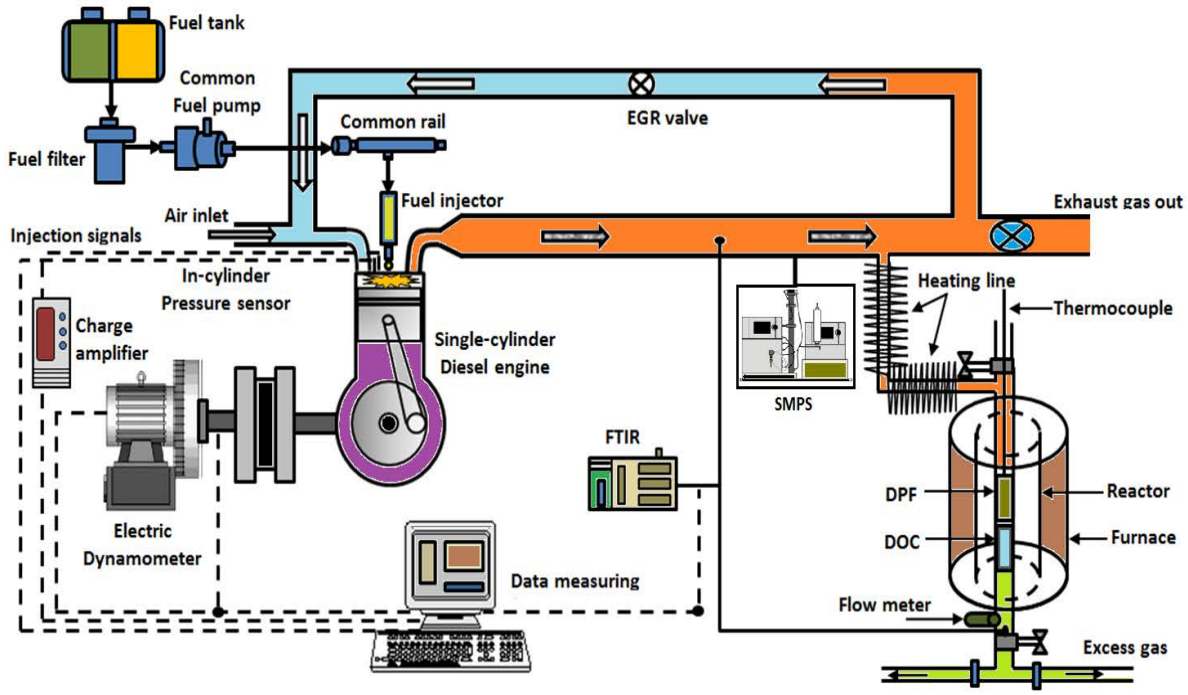

Figure 6.1: Schematic diagram of experimental test and sampling point

The other details of engine operating parameters, including injection strategy (i.e. post injection timing, main/post injection ratio, and injection pressure) were controlled by using an in-house developed LabVIEW programme and these conditions are listed in Table 6.1. During this work, the engine was running under post-injection and speed was controlled at 1800 rpm for all tests with an engine load of 3 bar indicated mean effective pressure (IMEP) which representing approximately 50% of the maximum load. The oxidation catalyst was subjected for two exhaust gas space velocity of 25,000 h^{-1} and 50,000 h^{-1} and heating temperature ramp of around 2 °C/min during every test. The ratio between the volumetric gas flow rate and the reference volume of the aftertreatment system is called the space velocity (SV) and is given in s^{-1} [258].

Table 6.1: Injection system characteristics.

Injection parameters	Specifications
Injection system	Common rail
Pre, main injection timing	15, and 3 deg bTDC
Pre, main, and post injection quantity	0.15, 0.48, and 0.1 ms
Injection duration	0.250 ms
Injection pressure	650 bar
Post-injection timing	60 aTDC

The conversion efficiency calculated according to the continuously recorded of exhaust gas concentration at the catalyst. In order to remove any remaining fuel from the previous experiment, the test fuel was changed as well as the fuel tank and fuel lines were

cleaned through run the engine was running for a period of time (30 min) with the same test fuel. During the test the engine exhaust gas concentration were measured at the beginning of engine outlet and at the beginning of the reactor (before DOC) at each test with a view to compare any changes in the exhaust gas concentration. The outlet exhaust gas concentration of DOC was continuously recorded throughout the experiment to calculate the conversion efficiency. The experiments engine research was carried out to explore the post-injection activation aptitude to produce hydrocarbons at the exhaust which are needed by DOC and for the regeneration DPF. The details of DOC and DPF used for the aftertreatment throughout this study were presented in chapter 3.

6.2 RESULTS AND DISCUSSION

The presence particulate matter (PM) in the exhaust gas can affect the catalyst oxidation activity by accumulate soot particles in the catalyst channels. This is could be effect the interactions of some exhaust gas species (CO, HCs, NO_X) with each other over catalyst and delay the light-off catalyst. Understanding this effect could eventually support the design of the aftertreatment system to enhance the removal pollutants at low temperatures and improve the catalyst activity. The combined effect of oxygenated fuels and changes in the commonly used aftertreatment position has been studied. In this chapter, the effect of butanol blending on particulate matter size distribution and gaseous emissions in the engine exhaust was analysed under post-injection strategy.

6.2.1 INFLUENCE OF FUEL ON PM AND GASEOUS EMISSIONS AT LOW SPACE VELOCITY (25,000 h^{-1})

6.2.1.1 Particulate Size Distribution (PSD)

Figure 6.2 shows particle number concentrations and particle size distributions for ULSD and B20 measured from the engine exhaust. Lower particle number concentrations are observed when B20 was used, as well as a lower mean particle diameter. The average particle diameters were 79.71 nm for diesel and 74.81 nm for B20, respectively. The main reason for the reduction in the particulate number is the oxygen content in the butanol molecule, which promotes soot oxidation from the internal bond-oxygen, leading to the elimination of most of the soot particles previously formed, and to the reduced size of the remaining particles [66, 259]. In addition, the reduction in the particle concentration contributes to reduce the probability of collisions between particles, thus further producing smaller agglomerates compared to the diesel fuel, in agreement with previous studies with alcohol blends [225, 259, 260]. The use of fuel post-injection it is also reduces the production of soot emissions due to better air/fuel mixing within the cylinder and as a result enhances the soot oxidation process [225, 227, 259].

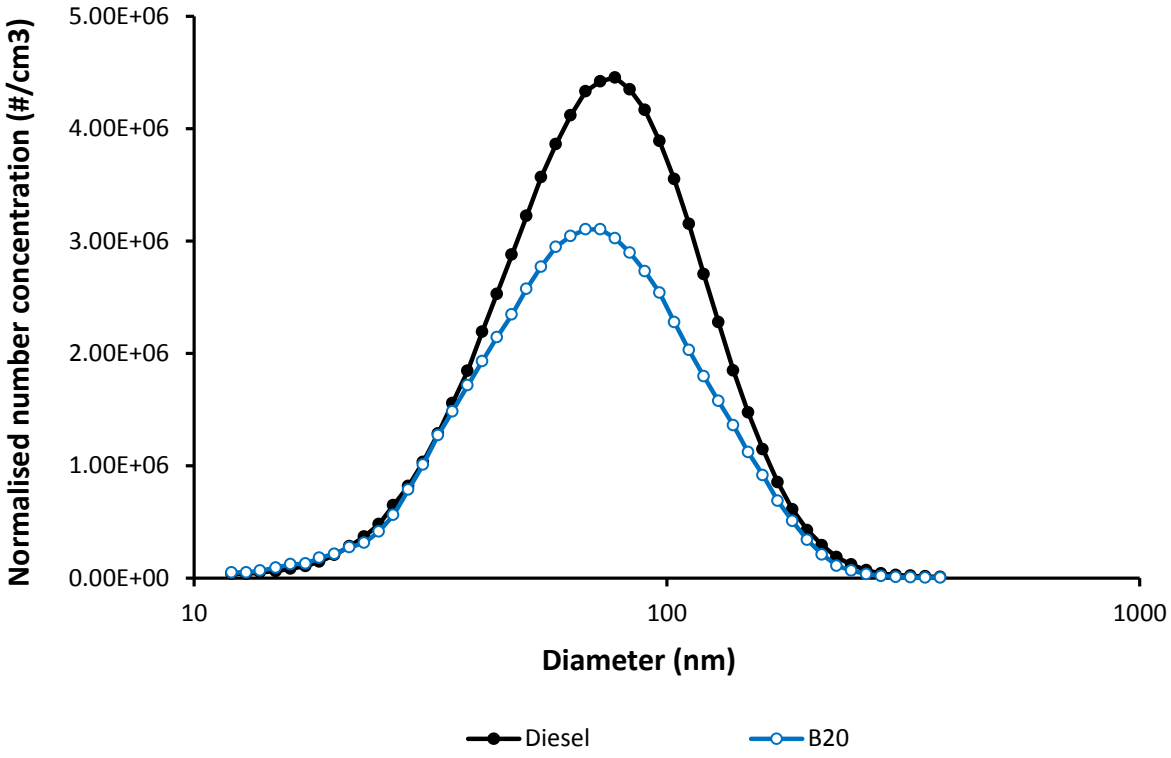

Figure 6.2: Effect of fuel on particulate size distribution

6.2.1.2 Engine Output Gaseous Emissions

The effect of fuel properties on gaseous emissions for diesel and butanol blend are shown in Table 6.2. The NO_X emissions remain constant independently of the fuel used. It is thought that the potential increase of NO_X due to the lower cetane number and presence of the internal oxygen in the butanol molecule is compensated by a reduction in local temperature because of butanol's higher enthalpy of vaporization. However, an increase in the NO_2 emissions from the combustion of B20 was observed [261] as compared to the diesel fuel combustion, effect that has been also described by Chen et al. [255] and Fayad et al. [259]. CO emissions increase slightly and THC emissions decrease when B20 is used instead of diesel fuel. The presence of butanol in the blend has a twofold

effect: on the one side, internal oxygen enhances combustion efficiency and as a consequence THC emissions decrease with respect to diesel fuel combustion. However, these THC emissions could not be completely oxidised to CO_2, leading to partially oxidised CO, because of the higher vaporization enthalpy of the alcohol. For a more comprehensive analysis of the THC, some relevant light saturated hydrocarbons ((methane and ethane) and unsaturated hydrocarbons (ethylene, propylene, acetylene) species have been analysed independently, while the rest of species have been grouped as heavy hydrocarbons (HCs). Table 6.2 shows that HCs, which represent around 65% of THCs for both fuels, have the same tendency as THC. However, a higher level of light HCs species (saturated and unsaturated) can be observed from the combustion of the butanol blend (B20) compare to diesel fuel, which could influence the DOC light-off [255]. This is likely to be a result of the butanol's thermal decomposition to light HC species and CO while in case of diesel fuel combustion it produces heavier HC components.

Table 6.2: Engine output emissions at 1800 rpm and 3 bar IMEP

Engine output concentration (ppm)	Diesel (100%)	Butanol blend B20
Nitric oxide (NO)	163.512	160.126
Nitric dioxide (NO_2)	44.421	50.754
Nitrogen oxides NO_X	207.933	210.881
Carbone monoxide (CO)	391.215	475.142
Total hydrocarbons (THCs)	1129.232	890.251
Heavy hydrocarbons (HCs)	757.621	570.614
Methane (CH_4)	5.814	8.324
Ethane (C_2H_6)	4.7124	6.231
Acetylene (C_2H_2)	3.581	4.681
Ethylene (C_2H_4)	21.921	26.532
Propylene (C_3H_6)	8.241	8.732
Formaldehyde (HCHO)	23.942	25.542

6.2.2 EFFECT OF FUEL COMBUSTION AND DPF INCORPORATION ON THE DOC LIGHT-OFF

In this section the effect of B20 and diesel fuel combustion on the DOC light-off performance has been analysed with and without a DPF under 25,000 h^{-1} of space velocity. The incorporation of an upstream DPF to the DOC implies removing or not large

part of the soot and heavy hydrocarbons from the exhaust before they reach the oxidation catalyst. As it has been previously reported the DPF can trap more than 99% of solid PM by mass and number from a diesel engine exhaust derived from diesel and oxygenated fuel combustion [18]. The prevention of soot and those heavy HC reaching the DOC could improve transport limitations of the reactants to the active sites and will allow a better study of the adsorption of gaseous emissions in the active sites of the DOC. Furthermore, these tests add further understanding to identify and evaluate the different factors which contributed to the improved catalyst oxidation activity previously reported with B20 engine fuelling with respect to diesel fuel combustion.

6.2.2.1 DOC Ability to Oxidise CO and HCs

Figure 6.3 and Figure 6.4 show that the DOC is more efficient in oxidising CO and THC, respectively when the DPF is introduced upstream the DOC for both fuels studied. Particularly, the placement of the DPF in front of the DOC and the incorporation of B20 improved the CO catalyst light-off by up to around 70 °C (temperature are compared when catalyst reach 50% conversion efficiency) when compared to diesel fuel combustion. It can be noticed that the oxidation of the THC wasn't complete over the catalyst and their oxidation started at higher temperature than the CO, especially for the combustion of diesel fuel without the use of an upstream DPF. It is thought this is due to incomplete conversion for some of HC species, which are difficult to oxidise over the catalyst. Potential condensation of heavy hydrocarbons enhanced through the presence of zeolite within the catalyst's washcoat enable to trap medium-heavy hydrocarbons at low temperature, being released at higher temperature [20, 21].

Therefore, the DOC's light-off temperature is highly dependent on the exhaust gas composition, as the cleaner combustion of B20 and the filtering of the exhaust gas with the DPF shifted CO and THC light-off towards lower temperatures. The results have shown in Figure 6.3 and Figure 6.4 (at low space velocity) enable to differentiate the effects of active sites availability (e.g. different particle and HC concentration level upstream DOC) with respect to the effect of the different diffusivity and reactivity between the combustion products. It is obtained that the negative effect of particle and heavy hydrocarbons blocking the active sites influence the catalyst activity for both fuels, but being more influential for diesel exhaust with respect to B20. From the comparison between the DOC catalytic activity with the DPF for both fuels, it is found the contributions to DOC'c improved activity are (i) the higher reactivity and diffusivity of butanol and its combustion derivatives [77, 187], (ii) the lower HC concentration upstream the catalyst and (iii) the higher NO_2 concentration in the butanol exhaust gas [187, 259]. Therefore, it is confirmed the combined effect of the enhanced active site aavailability reducing the competition for actives sites [41, 259] and higher reactivity and diffusivity of butanol combustion products to obtained an improved and steeper catalyst light-off conversion efficiency.

It can be noticed that CO has steeper light-off trends from the combustion of B20 at different light-off conditions than to the diesel fuel combustion. This is due to higher reactivity of CO with respect to some hydrocarbon species [262] and the oxygen content in the fuel blend reduced HC concentration upstream catalyst hence increases the catalytic surface area and encourage access of the reactants to the pores (reduce the competition for the same number of active sites).

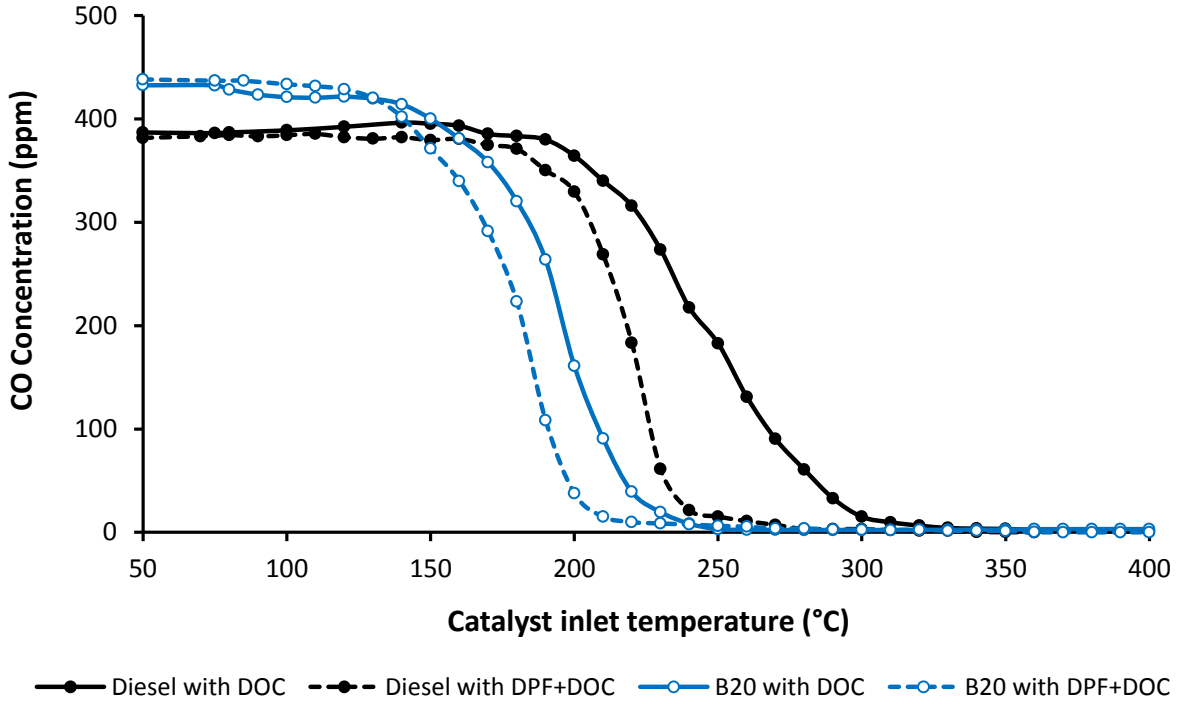

Figure 6.3: CO oxidation light-off temperature in the DOC (with and without DPF) for diesel and B20 fuels

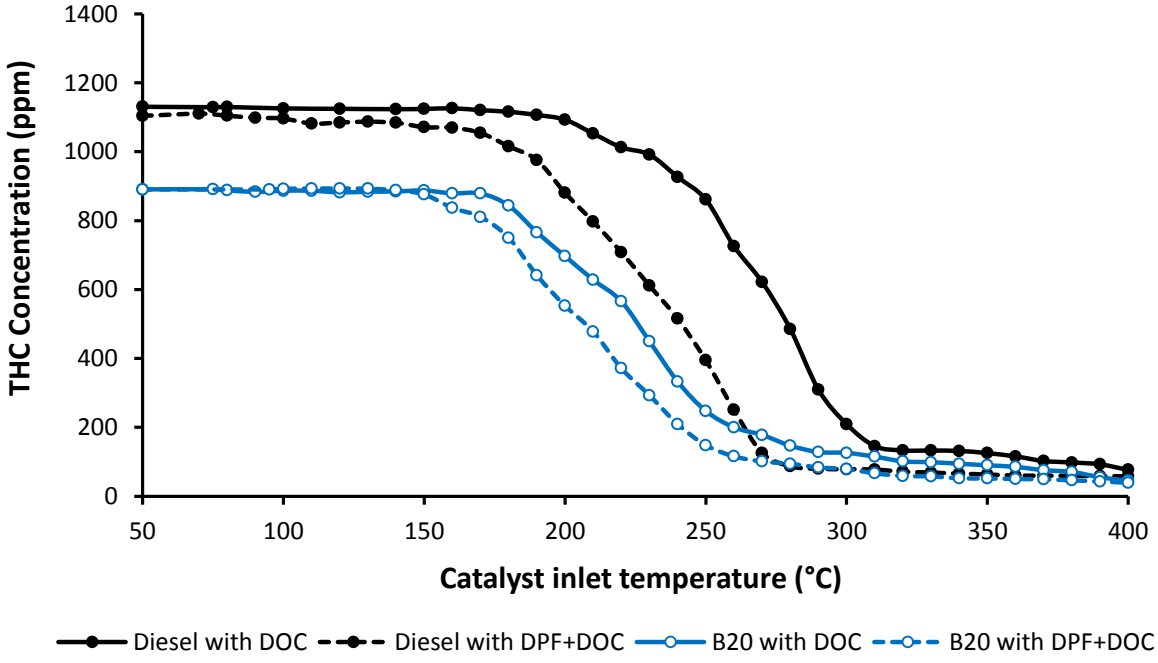

Figure 6.4: THC oxidation (light-off) temperature in the DOC (with and without DPF) for diesel and B20 fuels

6.2.2.2 DOC Ability to Reduce the Individual HCs Species

The conversion of the individual HC species in the DOC from the combustion of diesel and B20 are presented in Figures started from Figure 6.5 to Figure 6.11. The incorporation of the DPF upstream the DOC, also reduces it's light-off temperature for the individual HC species (Figure 6.6 to Figure 6.11). The individual hydrocarbon species light-off form the combustion of B20 started earlier than those obtained for diesel fuel. The oxidation process of the individual HC species in the DOC started with acetylene, followed by propylene and then the rest of HC species (Figure 6.6 to Figure 6.11). In the studied temperature range methane was not oxidised or affected by the differences in the exhaust gas composition, higher exhaust gas temperature are required (Figure 6.5). Furthermore, the presence of some long chain hydrocarbons classified as "heavy HC" contribute to the incomplete conversion of THC, resulting from their reduced diffusivity to reach the catalyst active sites [20]. This sequence in hydrocarbon oxidation, with short chain saturated hydrocarbons being the most difficult to control agrees with the results found to Diel et al. and Herreros et al. [21, 81]. From the results, it can be concluded that the same factors and contributions to the case of CO and THC emissions also apply to the oxidation of the individual hydrocarbon species [81].

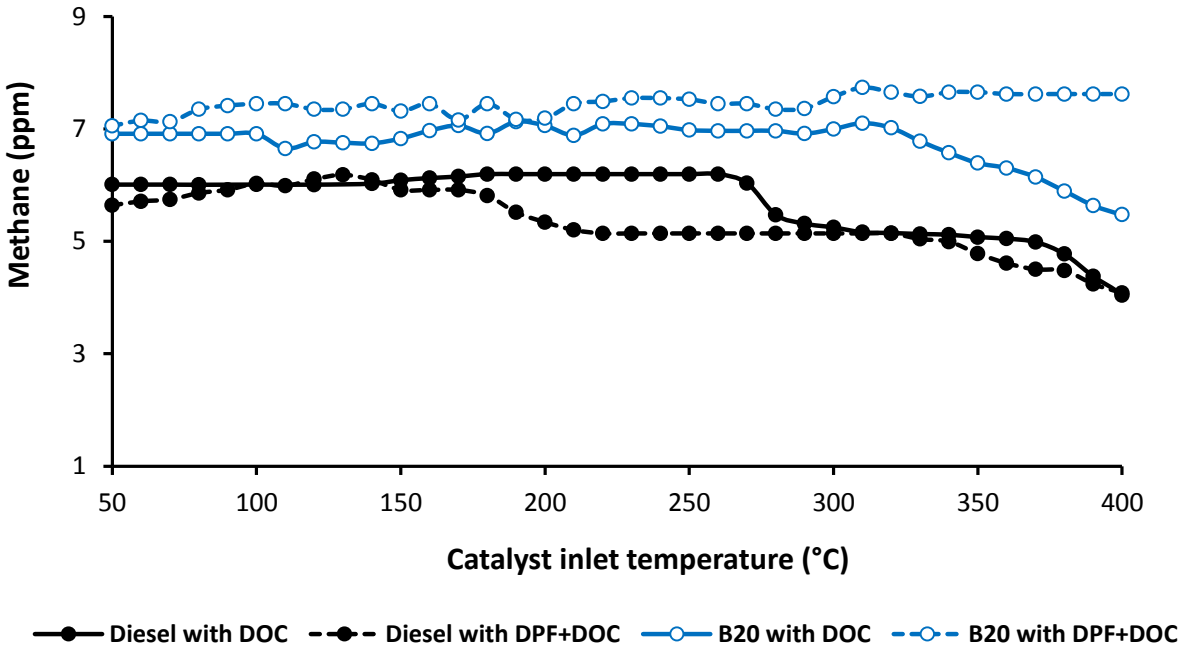

Figure 6.5: Methane light-off temperature in the DOC (with and without DPF) for diesel and B20 fuels

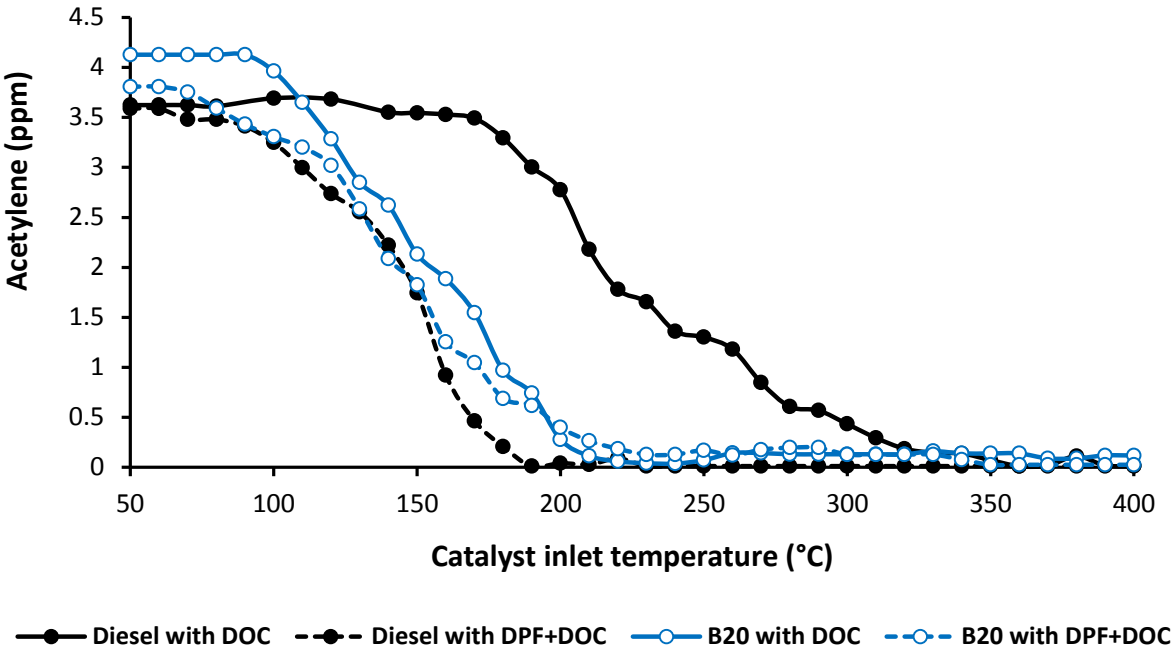

Figure 6.6: Acetylene light-off temperature in the DOC (with and without DPF) for diesel and B20 fuels

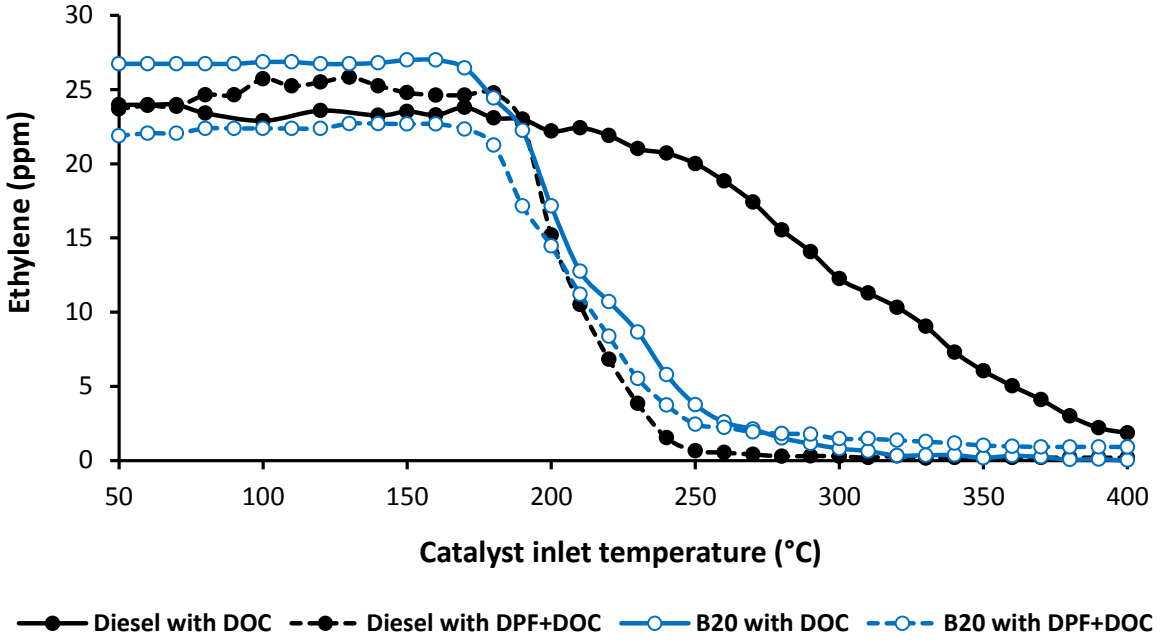

Figure 6.7: Ethylene light-off temperature in the DOC (with and without DPF) for diesel and B20 fuels

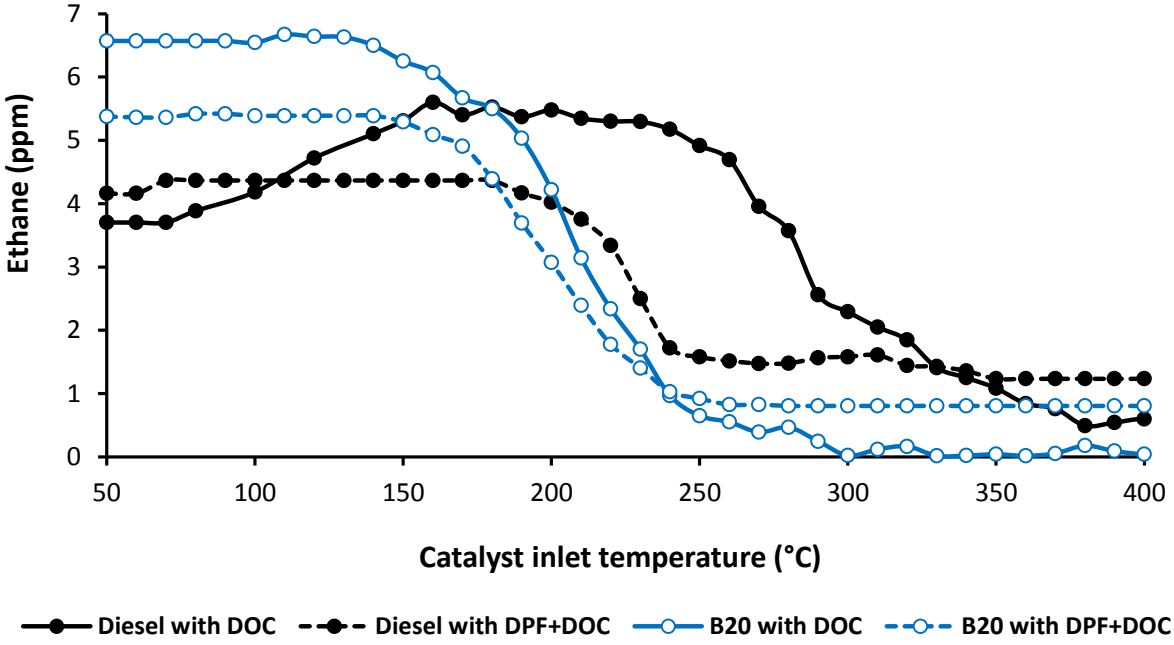

Figure 6.8: Ethane light-off temperature in the DOC (with and without DPF) for diesel and B20 fuels

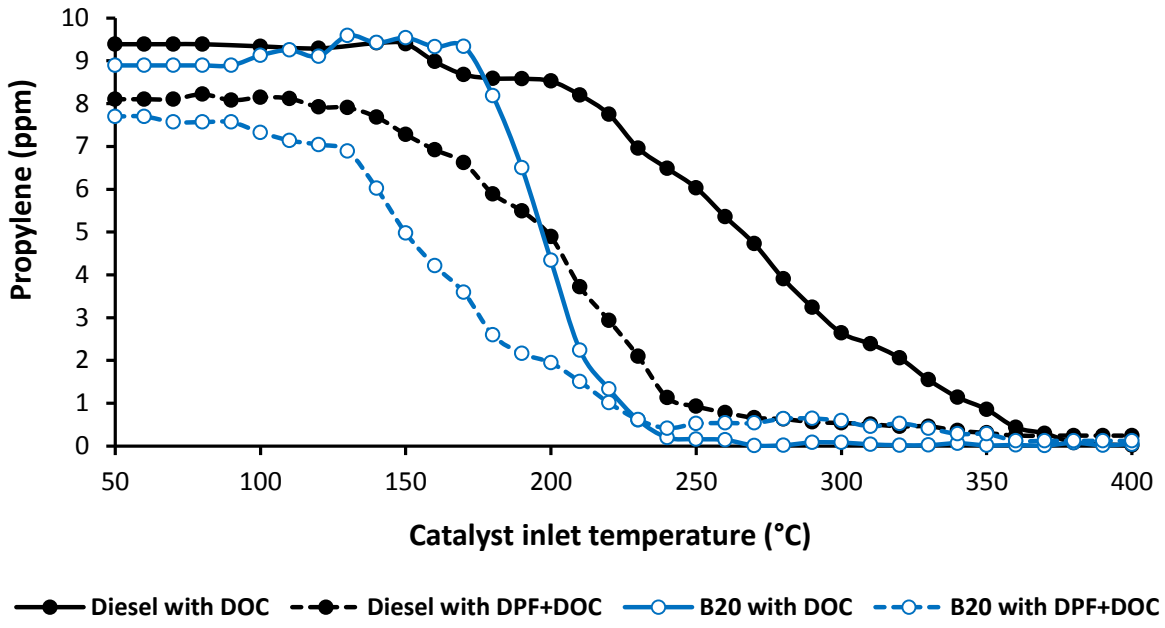

Figure 6.9: Propylene light-off temperature in the DOC (with and without DPF) for diesel and B20 fuels

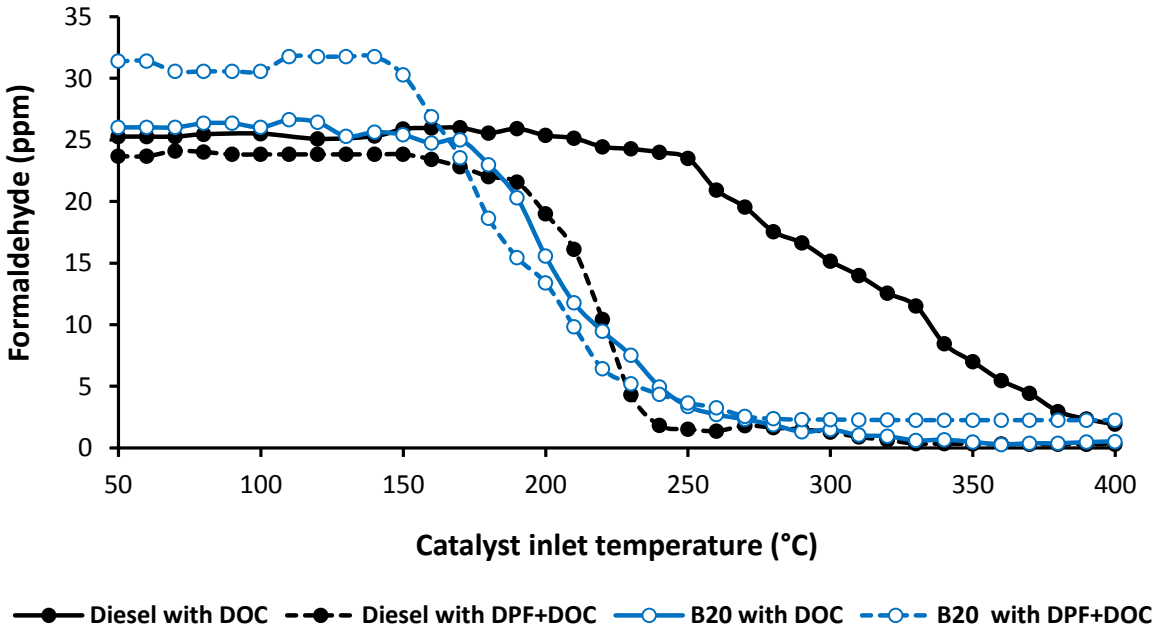

Figure 6.10: Formaldehyde light-off temperature in the DOC (with and without DPF) for diesel and B20 fuels

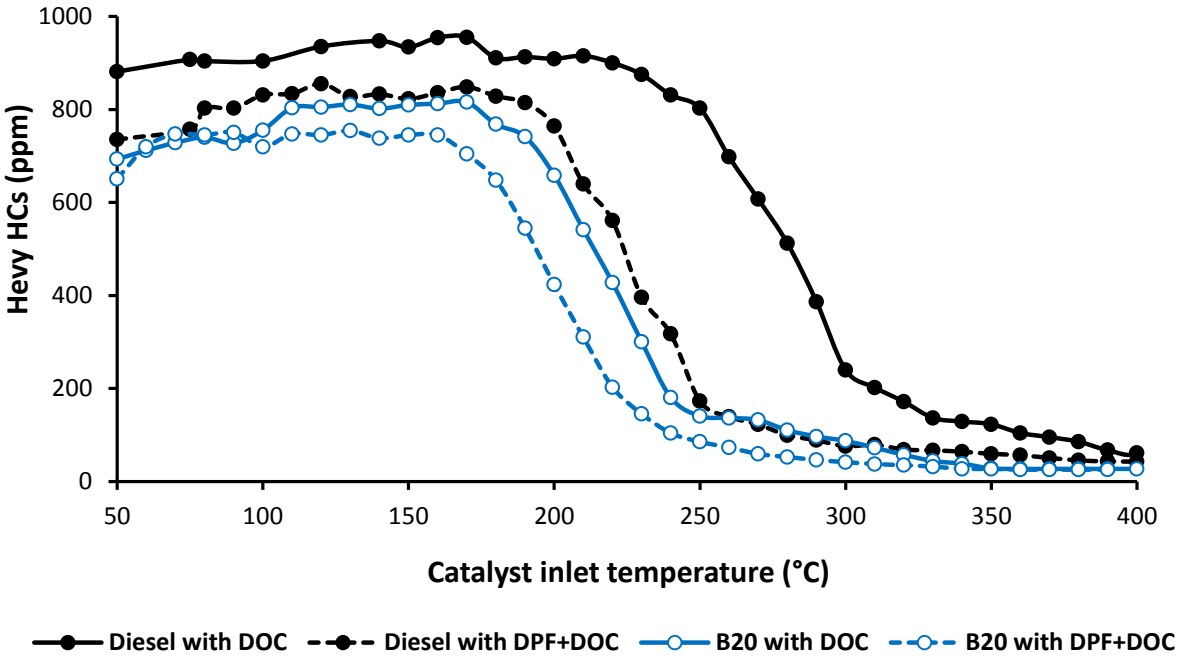

Figure 6.11: Heavy HCs light-off temperature in the DOC (with and without DPF) for diesel and B20 fuels

6.2.2.3 DOC Ability to Oxidise NO/NO_2

NO_2 concentration in the untreated exhaust is dependent on the fuel used and engine operation (i.e. load, air/fuel ratio and fuel injection strategies). A higher ratio of NO_2/NO upstream the DOC can be observed from the combustion of B20 (Table 6.2), trend that was also reported in [21]. Pioneering work by Murakami et at. 1982 [263, 264] investigated several additives as promotes, including CH_3OH, H_2, H_2O_2, CH_2O, CH_4, and they found that the degree of NO to NO_2 conversion was dependant on the production rate of peroxyl (HO_2) radicals during the combustion process of the additives. Hjuler et al. [265] using a laboratory scale reactor, proved that at a specific temperature window a simultaneous oxidation of the organic compounds and NO to NO_2 occurs, results that we

amongst other have observed in catalytic processes in vehicle pollutants reduction [266, 267]. The oxygenated organic compounds such as methanol, methylamine, acetaldehyde, acetone and ethane were found to affect the rate of NO to NO_2 conversion but also the width of the temperature window for oxidation. They reported that the efficiency of a given compound in oxidizing NO could be attributed to its oxidation mechanism as it depends on the production of peroxyl radicals, HO_2. Parameters such as the ratio of organic compounds to NO, reaction temperate, reaction time, and presence of water are all found to influence the NO to NO_2 oxidation [265]. For example methanol/NO ratio of around 1 provided high NO to NO_2 promotion efficiencies i.e. (80% to 90%), at lower molar ratios the conversion was reduced.

A CFD investigation by Zhang *et al*. [268] and Lilik et al. [269] confirmed that combustion temperature changes alone are not sufficient to explain the increase in NO_2 with increasing H_2. Their CFD results are also consistent with the hypothesis that in-cylinder HO_2 enhances the conversion of NO to NO_2 in the diesel engine exhaust. The same trend was noticed in this work with the introduction of butanol in diesel combustion, where the OH in the oxygenated fuels can increase the OH_2 radicals in the combustion process and thus promote the formation of NO_2.

The DOC catalyst can be designed to promote the NO to NO_2 [270-272] in order to enhance the low temperature passive soot oxidation, and reaction that it is also influenced by the concentration of CO and the type of THC in the catalyst [20, 21]. The production of NO_2 is also temperature dependant, with approximately 250 °C being the starting for the DOC under investigation for both fuels. It has to be emphasised that at low temperature, the engine out NO_2 of approximately 44 and 50 ppm from the diesel and B20 combustion (see Table 6.2) is preferentially used to oxidize HCs in the DOC. The

presence of the DPF upstream the DOC also enhances the NO_2 production in the DOC for both fuels. This is can be attributed to a) the reduced reaction rates of the produced NO_2 with carbon contained species and b) the enhanced catalyst oxidation activity, as evidenced from the earlier CO and HC light-off curves, due to improved reactant and products transport to and from the active sides, respectively due to the reduction in carbon species reaching the DOC [272, 273]. On the other hand, it can be noticed from Figure 6.22 that B20 slightly increased in NO production after 250 °C without DPF than to the with DPF. The improved CO and THC oxidation with the incorporation of the DPF, does not promote the increase in the NO_2 emitted to the atmosphere. The higher CO and THC oxidation when the DPF is introduced, consumed more O_2 and NO_2, therefore, as higher NO_2 concentration has been utilised in the carbonaceous species oxidation [265].

Higher values of NO_2 downstream the catalyst from B20 combustion with increasing catalyst temperatures due to a higher oxidation of NO to NO_2, while NO level was reduced downstream the catalyst with respect to the inlet value as shown in Figure 6.12. This is due to a higher NO to NO_2 oxidation as there is lower competition between the different exhaust component as well as NO reacting preferably with molecular oxygen and lower rate of NO_2 consumption over the catalyst through reaction with HC species as the HC level from B20 combustion is lower than for diesel fuel (Figure 6.12). In case of using Ag/Al_2O_3 catalyst, a similar effect has been already reported by Fayad et al. [77] where the formation of NO_2 is highly promoted under the addition of alcohol fuels.

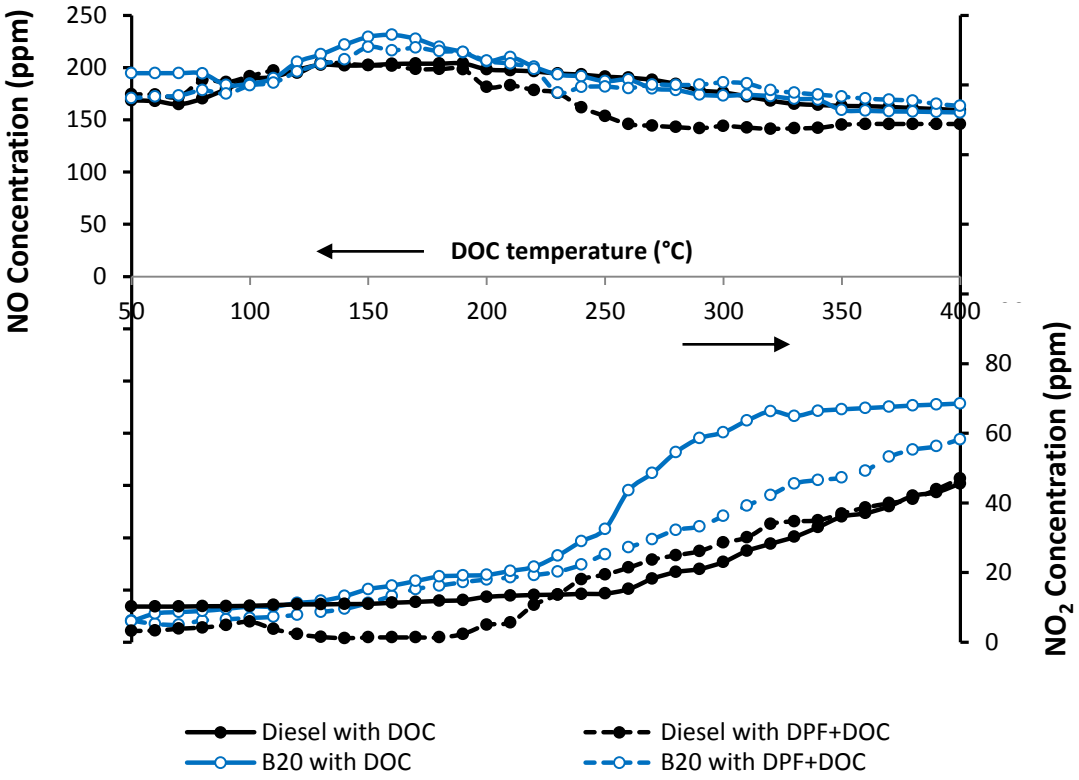

Figure 6.12: NO to NO_2 oxidation light-off temperature in the DOC (with and without DPF) for diesel and B20 fuels

6.2.3 EFFECT OF FUEL AND FLOW RATE OVER DOC PERFORMANCE LIGHT-OFF

In this section the effects of B20 and diesel fuel combustion over the DOC light-off performance with an upstream DPF have been analysed with different flow rates (i.e. space velocities of 25,000 h^{-1} and 50,000 h^{-1}) (Figure 6.13). This allows to investigate the effect of the residence time of the exhaust products on their adsorption and oxidation in the DOC active sites, while the temperature in the DOC inlet was varied from 50 °C to 400 °C.

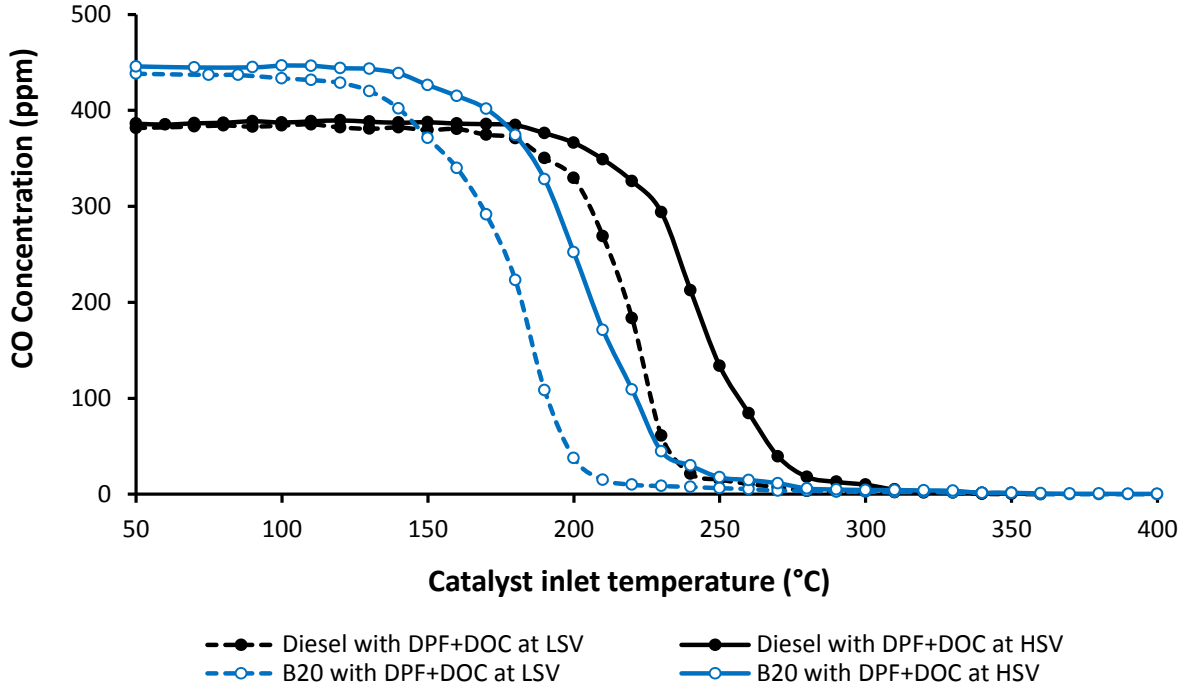

Figure 6.13: CO oxidation light-off temperature in the DOC at different space velocities for diesel and B20 fuels

6.2.3.1 CO and THC Oxidation over DOC at Different Space Velocity (SV)

Comparing between different space velocities, Figure 6.13 and Figure 6.14 show that light-off temperatures for CO and THC oxidation start at higher temperature (with a difference of around 30 °C for CO and 40 °C for THC) in the DOC catalyst when the space velocity (SV) was increased from 25,000 h^{-1} to 50,000 h^{-1} (HSV) for both fuels [274]. The difference is likely to be a consequence of the lower available time between the catalyst active sites and exhaust species [84, 272, 273, 275] to diffuse and undergo the oxidation reactions in the active sites. B20 still maintains an earlier CO and THC light-off with respect to those obtained with diesel fuel combustion. As it was discussed in the previous section, the low level of THC emissions derived from B20 combustion as well as the higher diffusivity and reactivity and presence of oxygen in the butanol molecule and

their combustion products favour the accessibility and reaction of CO and THC in the catalyst active sites [233].

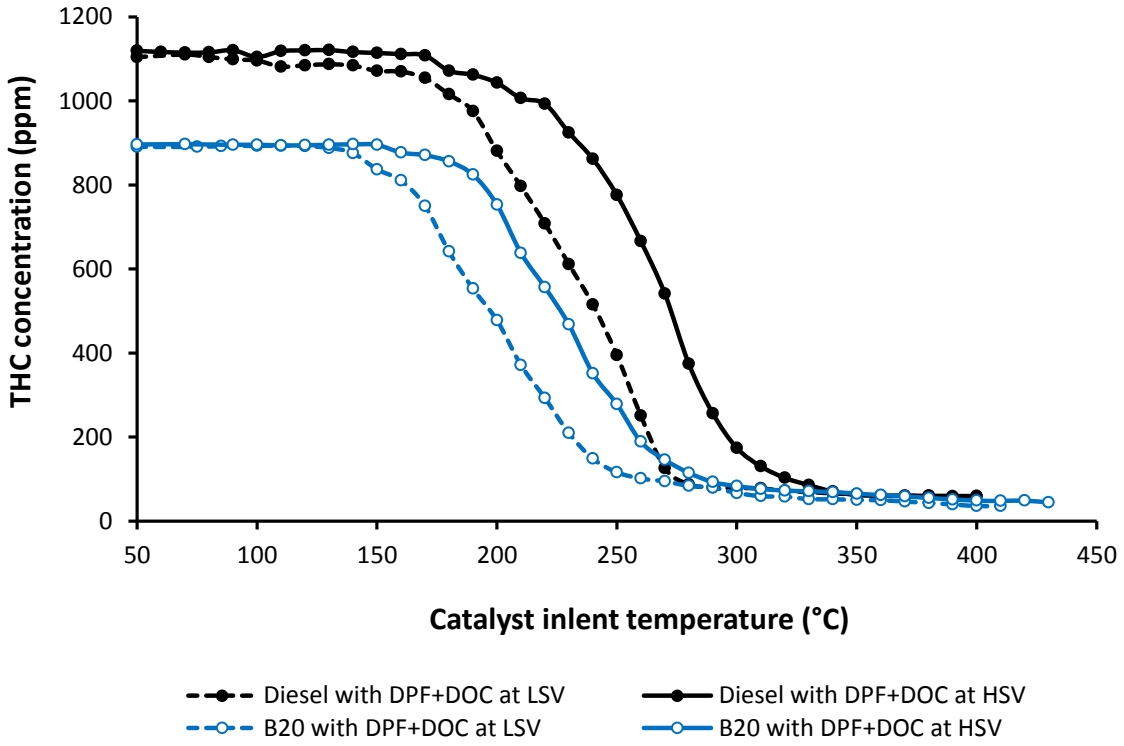

Figure 6.14: THC oxidation light-off temperature in the DOC at different space velocities for diesel and B20 fuels

6.2.3.2 HCs Species Oxidation over DOC at Different SV

The concentration of the individual of the HC species and heavy HCs downstream the DOC at both space velocities is shown in figures from Figure 6.15 to Figure 6.21. According to the catalyst light-off temperatures, the oxidation rate of HC species was slower at HSV compared to LSV for both fuels as a result of limited residence time of the exhaust gas within the catalyst. For both SV, the unsaturated HCs are oxidised at lower temperatures than saturated ones a results that agrees with [227]. Eventually, at both space velocities the DOC oxidised those light HC species except for CH_4. At high

space velocity, the conversion efficiencies in the case of B20 operation are similar to those obtained with diesel for most of the HC species. Therefore, with the exception of acetylene, it seems that the earlier catalyst light-off for B20 with respect to diesel fuel does not happen at high space velocity, with the exception of acetylene (see Figure 6.15 to Figure 6.21).

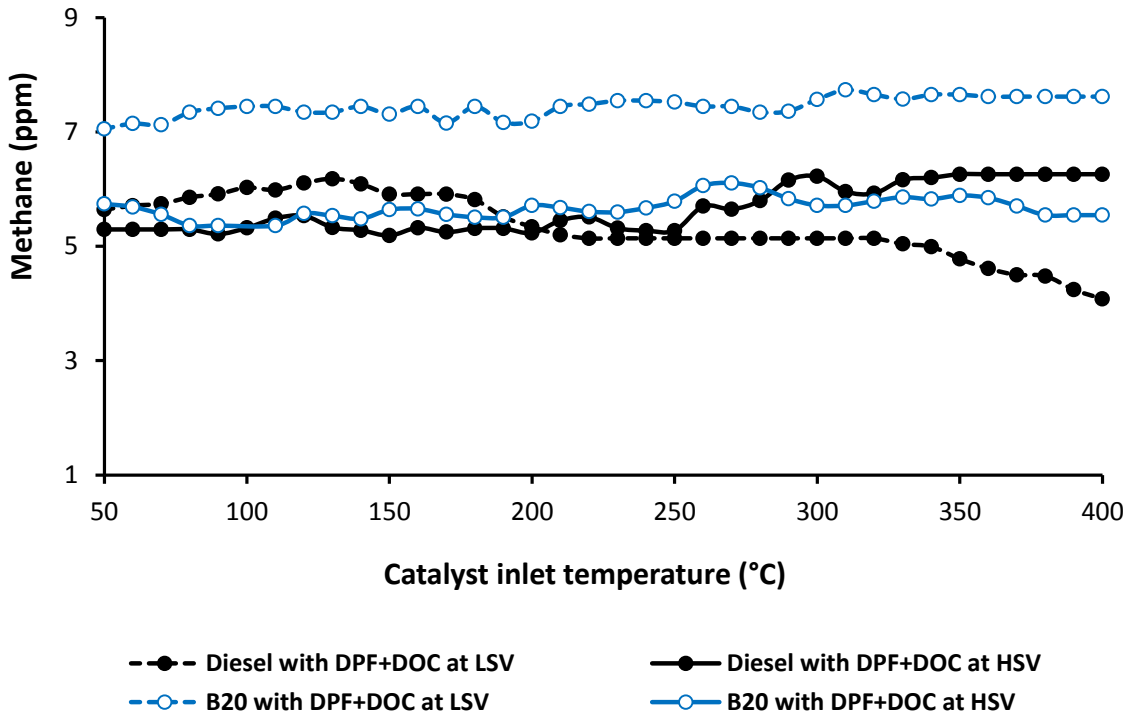

Figure 6.15: Methane light-off temperature in the DOC at different space velocities for diesel and B20 fuels

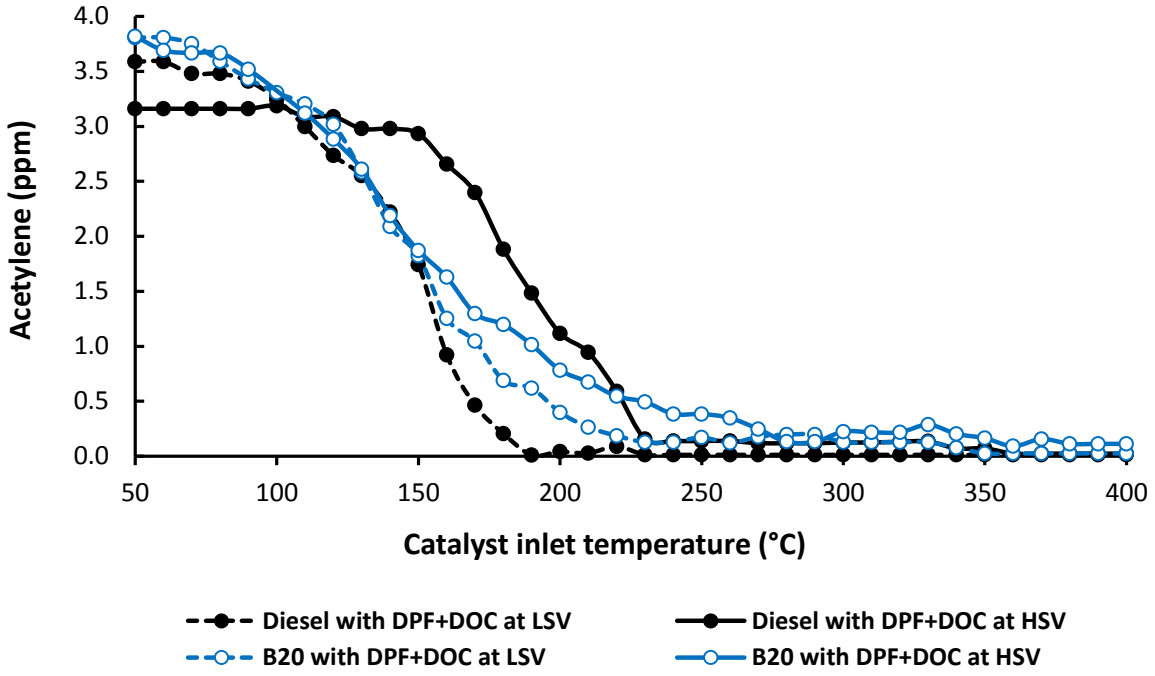

Figure 6.16: Acetylene light-off temperature in the DOC at different space velocities for diesel and B20 fuels

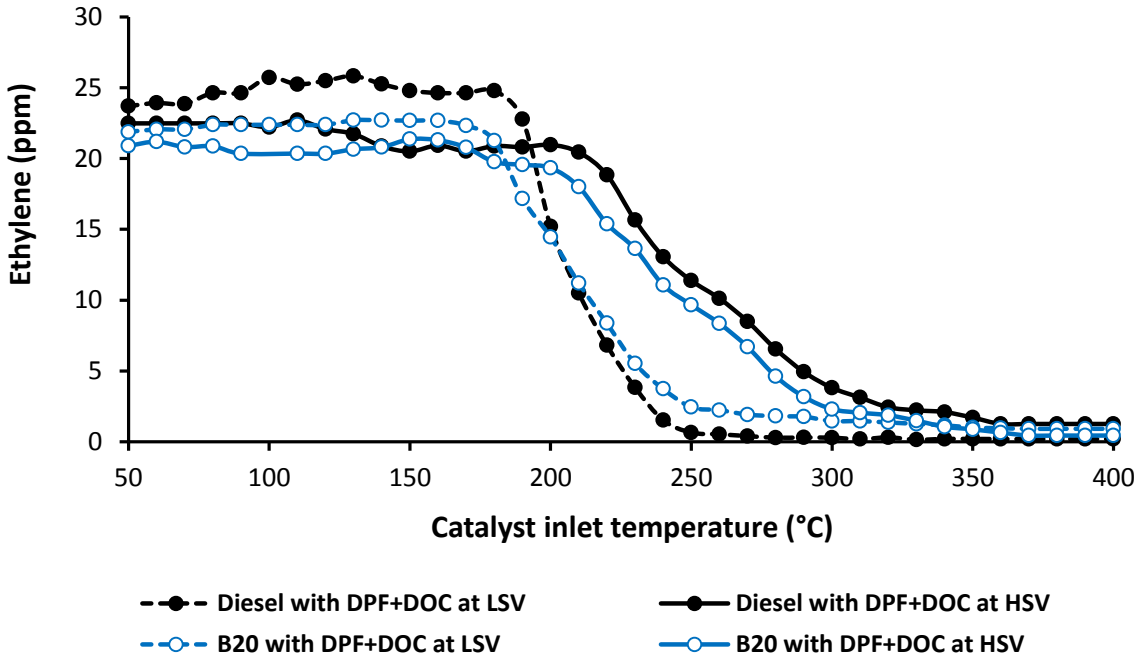

Figure 6.17: Ethylene light-off temperature in the DOC at different space velocities for diesel and B20 fuels

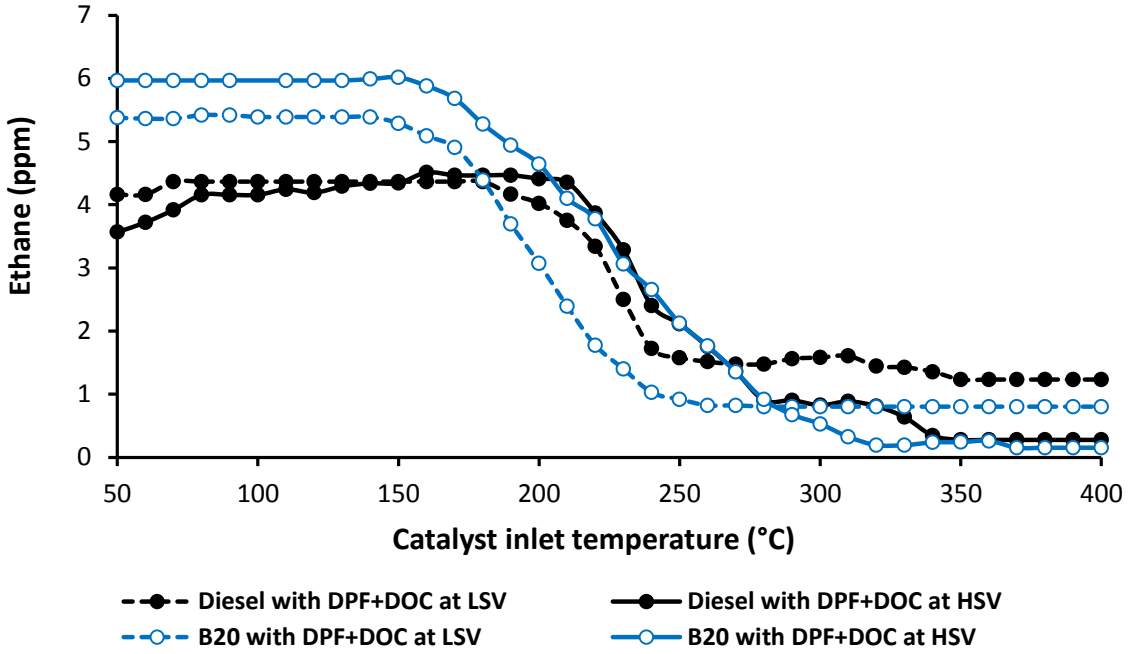

Figure 6.18: Ethane light-off temperature in the DOC at different space velocities for diesel and B20 fuels

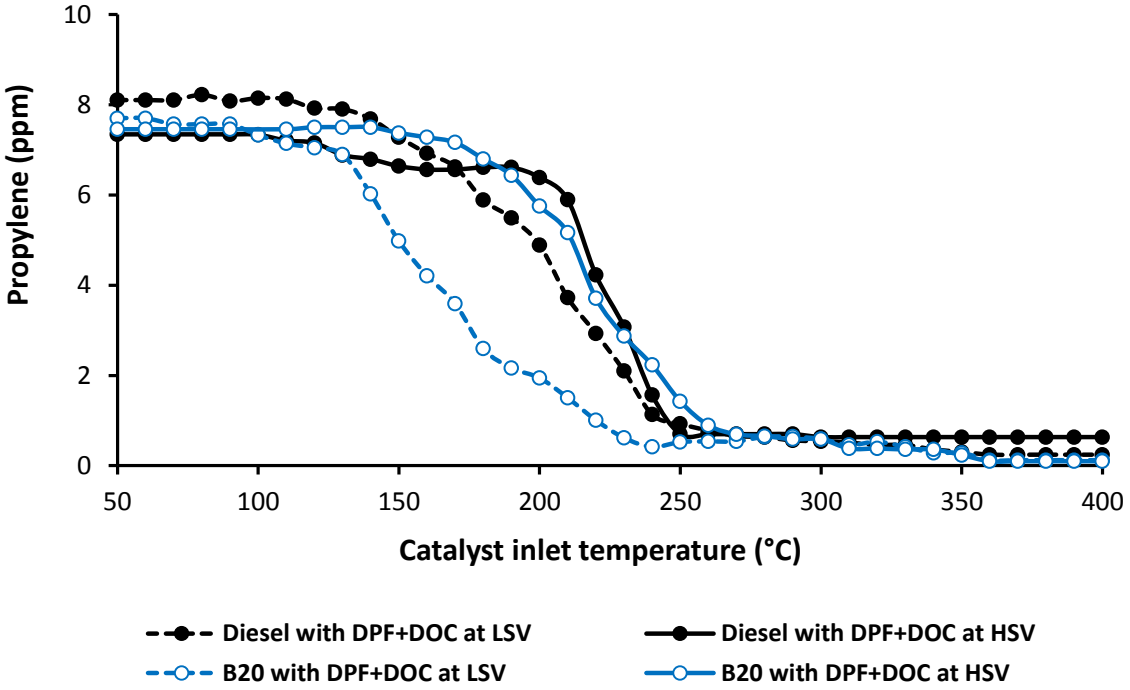

Figure 6.19: Propylene light-off temperature in the DOC at different space velocities for diesel and B20 fuels

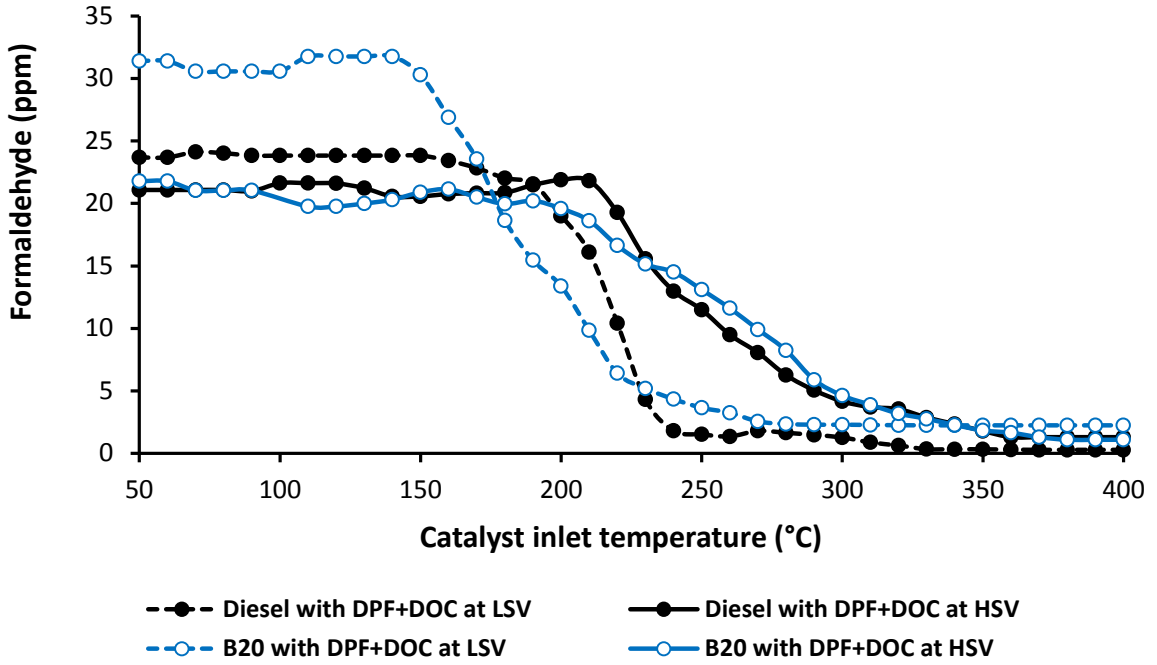

Figure 6.20: Formaldehyde light-off temperature in the DOC at different space velocities for diesel and B20 fuels

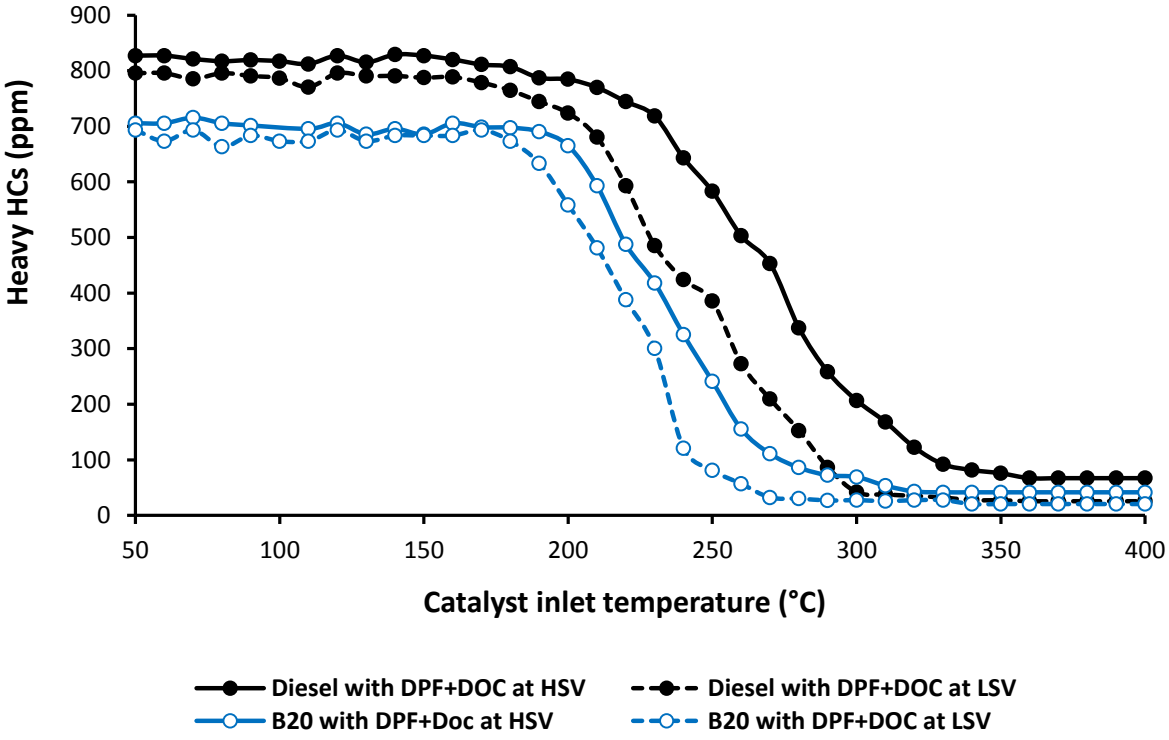

Figure 6.21: Heavy HCs light-off temperature in the DOC at different space velocities for diesel and B20 fuels

6.2.2.3 NO/NO_2 Oxidation over DOC at Different SV

For both fuels the NO_2 production was promoted at low space velocity (Figure 6.22), which is in accordance with the oxidation of the carbon containing species. This trend confirms the findings that oxidation of the organic compounds and NO to NO_2 occurs simultaneously [265]. They have also suggested that reduced reaction time (i.e. increased space velocity) also reduces the production of OH_2 radicals and hence NO_2 production. The effect of space velocity is even more pronounced at high temperature when the concentration of NO_2 increases as the formed NO_2 is not consumed in THC oxidation, which reacts preferably with molecular oxygen when the temperature increases [77, 256, 276]. Furthermore, for both SV's the NO to NO_2 oxidation over DOC is slightly higher for B20 than for diesel fuel due to the higher reactivity and diffusivity of the combustion products of B20 in comparison to diesel fuelling which enhance the oxidation rate over catalyst [277].

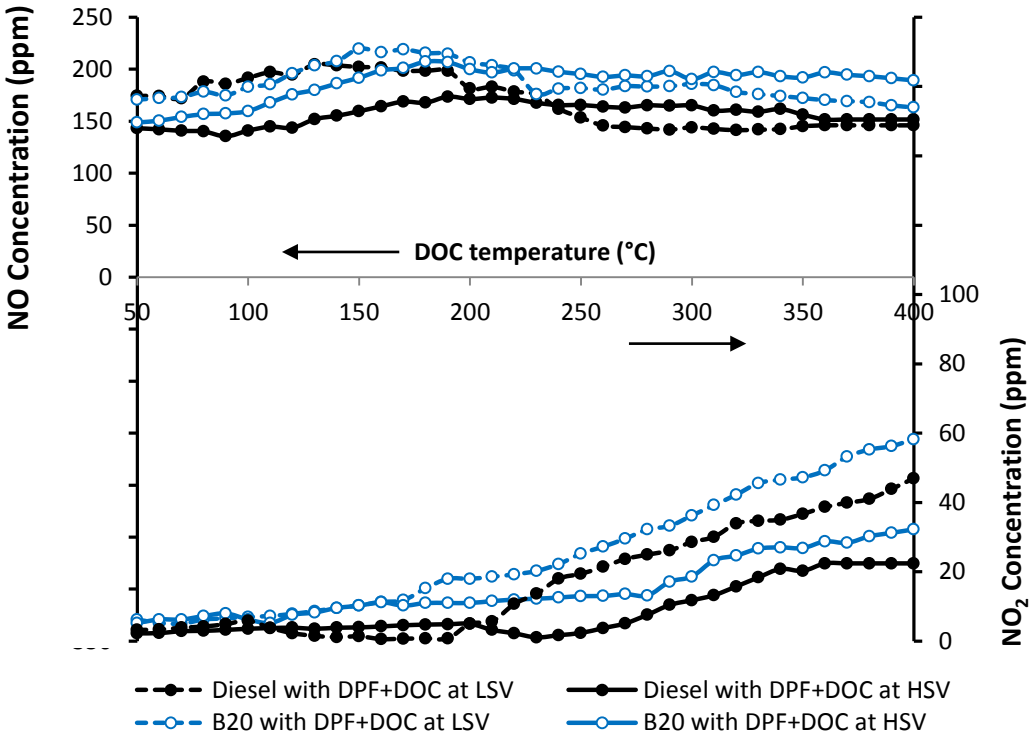

Figure 6.22: NO/NO_2 oxidation light-off temperature in the DOC at different space velocities for diesel and B20 fuels

6.3 SUMMARY

This study reports the effects of butanol blends (B20) properties and soot particles on diesel oxidation catalyst performance; by investigating the effect of soot accumulation on the channels of a high cell density catalyst. The research also covered the effect of different space velocities (SV) on conversion efficiency (light-off) of engine emissions such as CO, THC, HC species and NOx.

Through fuel blending and aftertreatment systems architecture the engine exhaust gas composition can be manipulated in order to improve the catalysts activity especially at low temperatures. Our finding can be used to guide the design of both more efficient

compact aftertreatment systems architecture and cleaner fuels. By identifying the role of the individual species (i.e. reaction promoter, spectators or distractor) during the combustion process and catalytic processes, fuels composition, engine operation and catalyst design can be optimised. Improved catalyst activity can also be translated in the design of catalytic technologies and overall cost.

The absence of solid particles in the exhaust gas played a key role in improved the catalyst light-off temperature and enhances the oxidation rate of CO, THC, and HC species at low temperatures by eases accessibility to the coated material and active sites (without soot) in the catalyst. Therefore, positioning DPF upstream DOC leads to a great benefit on CO and HCs light-off temperature, starting their oxidation at lower temperatures than without DPF. This work has shown that B20 has favourable synergetic effect in promoting CO and HCs oxidation over catalyst and enhancing the catalyst light-off temperature by providing a chain of beneficial effects at both SV. In general, CO and HCs species emitted from the combustion of B20 were easier oxidized over catalyst compared with diesel fuel over different condition tested. A higher ratio of NO_2/NO upstream the DOC can be observed from B20 combustion with DPF+DOC because as the THC concentration is lower for B20, less NO_2 is needed to their oxidation.

The catalyst activity was affected by the space velocity. Light-off temperatures for CO and THC oxidation start at higher temperature in the catalyst (DPF upstream DOC) with high space velocity for both fuels. This is because of the reduction of the exhaust gas residence time of the in the catalyst which leads to lower contact time between the active sites and exhaust species in the catalyst. NO_2 concentration at HSV is lower than the concentration at LSV for both fuels studied because at high temperature, THC reacts preferably with O_2 and consequently, as NO is oxidised to NO_2 in the catalyst

but NO_2 is not used to oxidise THC, NO_2 concentration increases. It can be concluded that B20 has higher oxidation rate than diesel at LSV and HSV, also the rate oxidation of CO, THC, and HC species with high space velocity are slightly higher in B20 than to the diesel fuel. It is suggested that using oxygenated fuel blends can promote the DOC activity by reducing the soot formation in the exhaust and enhanced the emissions oxidation with low catalyst temperatures.

CHAPTER 7

CONCLUSIONS AND RECOMMENDATIONS FOR FUTURE WORK

7.1 INTRODUCTION

The summary and details of the main research results are provided in this chapter in an attempt to understand the role of alternative fuels (butanol-diesel blend) on particulate matter (PM) characteristics and on a diesel catalys't performance in a compression ignition diesel engine. The soot particles generated from the combustion of the oxygenated fuels were of a smaller size and lower number compared to thos produced from diesel fuel combustion. The oxygenated fuel exerts a strong influence on soot morphology and nanostructure parameters. The catalyst light-off temperatures shifted towards lower temperatures with the addition of butanol fuel to the diesel fuel (butanol blend) compared to the conventional diesel fuel. The outcome from these results encourages further investigation of PM's characteristics. More study has been performed on the oxygenated fuel and the incorporation of a post-injection strategy which helps in reducing PM and simultaneously modifies the soot's morphology characteristics. The recommendations for future work are also presented in this chapter.

7.2 CONCLUDING REMARKS

In this research thesis, the results from the experimental investigation into the reduction and understanding of PM emissions' characteristics (from a diesel engine's exhaust) have been presented and discussed. Various types of fuels (diesel, RME, butanol blend) and combustion modes were used in this experimental investigation to produce a variety of exhaust gases (including PM) and show the adsorption competition between the exhaust gas pollutants and PM onto the same catalytic sites. Understanding the PM characteristics in the exhaust and over the catalyst were the singularity point in this investigation to reduce the inhibitions effect and improve the catalyst's activity at low temperatures. This study also gives an insight regarding the effect of alternative fuels on the DOC's performance on PM reduction/modification and pollutant emissions' oxidation, which can help identify synergies between fuel specifications and catalyst efficiency. It can be concluded that the use of oxygenated fuels is a very effective way to improve the engine output emissions, combustion, and conversion efficiency of a diesel oxidation catalyst at low temperatures. Ultimately, this will lead to achieving levels of emissions' legislation limits. The soot HR-TEM imaging results are consistent with the SMPS results; where the combustion of oxygenated fuels produces a lower level of PM emissions (number and size) than the diesel fuel combustion.

The soot particles collected from the exhaust system in a diesel engine have shown that the butanol blend and biodiesel (RME) have produced a lower number of primary particles (n_{po}) and smaller sized (d_{po}) soot agglomerate. It can be concluded that when the oxygen content increases in the fuel (also reducing the number of aromatic compounds) it leads to a reduction in the average mobility diameter and the total number concentration of the PM. In addition, it enhances the soot particle oxidation and reduces the

soot particle formation. For the same oxygen content (around 5 %) in the fuel, it was found that a butanol blend reduces the number of primary soot particles, the size of the primary particles, and produces smaller fractal dimension of soot agglomerate compared to the biodiesel (RME). Also, the butanol blend was very beneficial for light-off catalyst temperatures compared to the other fuels used in this research. In the case of the primary particulates' size and microstructure parameters, the diesel oxidation catalyst does not show any clear effect on these parameters at different catalyst temperatures for all the fuel studies. Regarding the PM, the main role of the diesel catalyst was the reduction of the total PM to 30% (trapping effect) and oxidization of the PM volatile components; while the DOC needed a longer residence time to oxidize the soot.

Further studies on the effect of injection strategies and oxygenated fuel were conducted on a common rail modern diesel engine to understand how the post-injection and butanol blend (B20) affected the PM's characteristics (size of primary particles and fractal dimension). Thorough further investigation on the particulate emissions of the oxygenated fuel reported that the presence of the oxygen content in the fuel blend incorporated with post-injection was more effective in restraining the rate of soot formation (lower PM) and increasing the rate of soot oxidation, which resulted in particles with a smaller average size and fractal dimension. It can be concluded that the use of primary alcohol in the fuel blend can improve the combustion process and lead to cleaner combustion that eases the species' (HCs/fuel and engine out emissions) oxidation in the diesel catalyst (DOC). Additionally, these trends will positively impact on the catalyst's performance and favour active control strategies in the aftertreatment systems. Another conclusion from this work is that the soot accumulation in the catalyst's 'active' site' channels can reduce the diesel oxidation catalyst's activity. The catalyst's activity can be improved at low temperatures by the addition of fuel blending and a change of the position

of the aftertreatment systems. This thesis has provided a guide to the design for both compact aftertreatment systems' architecture and cleaner fuels, with the aim of improving combustion performance and reducing the particulate emissions.

Finally, the conclusions include consideration of some relationships among several of the dependent variables used in this thesis. The characteristics of PM have been described in this thesis from the combustion of various oxygenated fuels in a diesel engine, with the aim to understand the soot particles' size and structure. It was found that the oxygenated fuel had a positive effect on PM reduction and a favourable synergetic effect on the diesel oxidation catalyst. The lower PM emissions' levels with oxygenated fuels are consistent with less soot formation in the combustion chamber and the increase of oxygen radicals that favour oxidation, as explained throughout the literature review. The post-injection strategy has also alleviated the impact of the increase of PM by increasing the soot oxidation inside the engine. The implementation of a DPF upstream of the DOC with oxygenated fuel is an attractive approach to improve the catalyst light-off at lower temperatures, as it removes the soot accumulation from the exhaust system.

7.3 RECOMMENDATIONS FOR FUTURE WORK

There are some potential topics which are worth further study and may act as a continuation and extension to this thesis. According to the research results presented in this thesis, to expand the study of PM's characteristics (size and structure) to other interesting fuels and other equipment, the following recommendations are suggested:

- For further work, it would be desirable to extend the current study and develop a strategy to collect fresh soot from an exhaust system in an appreciable amount to analyse the chemical structure parameters of soot particles. Understanding the

nanostructure changes from the oxidation process is a key to gain knowledge about soot oxidation behaviour. Application of Raman spectroscopy and XRD techniques can be used for such a study and can provide information about nanostructure changes in soot particles with oxidation. The data from the analyses of the chemical properties of soot agglomerates could support the results from the physical properties to find confident results. Limited methods available to collect fresh soot samples from exhaust systems were the obstacle towards continuing with this measurement.

- It is also suggested that the impact of different levels of exhaust gas recirculation (EGR) with the use of post-injection strategy on the soot particles' characteristics could be establised. The use of aftertreatment systems is recommended to investigate a diesel catalyst's performance with active regeneration. Furthermore, the level of nitrogen increased in the combustion process from reforming (by applying high level of EGR) and it will be interesting to study how the nitrogen percentage affects the size and shape of soot particles' agglomerates. The results from this test would be a great contribution to the engine research and emissions' community.
- Fuels produced from new raw materials (those not destined for food) and mixtures with a higher percentage of biobutanol could be studied. These fuels allow an independent effect from different properties such as oxygen content, amount of aromatics, volatility. This can probably improve the combustion characteristics, emissions, catalyst activity, and an increase of fuel economy.
- In the present thesis, a common rail fuel injection system was available that allows the control of the injection parameters (injection timings, pressures, duration); therefore, it would be interesting to carry out tests on all the injection

parameters and try to see the effect of injection characteristics (timing, duration, quantity, and pressure) on the size, shape and nanostructure of the soot particles' agglomerates.

- It is advised to make a mathematical model (simulation model) that studies the collisions between the particles' agglomerates in the exhaust system, based on measurements of size distributions in different locations. It would need the ability to predict and identify changes of the final shape of the soot agglomerates in the tailpipe from the user specified fuel injection strategy and combustion characteristics.
- Additional engine tests are also recommended to measure the size and shape of soot agglomerates in engine oils with different fuels. Post-injection can be applied to increase the level of unburned hydrocarbons and fuel dilution in the engine sump.

LIST OF AUTHOR PUBLICATIONS AND CONFERENCES ATTENDED

Publications:

1. **Fayad M.A.**, Herreros J.M., Martos F.J., Tsolakis A. Role of Alternative Fuels on Particulate Matter (PM) Characteristics and Influence of the Diesel Oxidation Catalyst. Environmental Science & Technology. 2015; 49(19): p. 11967-11973.

2. **Fayad M.A.**, Tsolakis A., Fernández-Rodríguez D., Herreros J.M., Martos F.J., Lapuerta M. Manipulating modern diesel engine particulate emission characteristics through butanol fuel blending and fuel injection strategies for efficient diesel oxidation catalysts. Applied Energy. 2017; 190: p. 490-500.

3. Bogarra M., Doustdar O., **Fayad M.A.**, Wyszynski M., Tsolakis A., Ding P., Pacek A., Martin P., Overend R., Leary S. Performance of a drop-in biofuel emulsion on a single-cylinder research diesel engine. Combustion Engines PTNSS Journal. 2016; 166 (3): P. 9-16, doi:10.19206/CE-2016-324.

4. **Fayad M.A.**, Fernández-Rodríguez D., Herreros J.M., Lapuerta M., Tsolakis A., Interactions Between Aftertreatment Systems Architecture and Combustion of Oxygenated Fuels in Diesel for Improved Low Temperature Catalysts Activity. Submitted to the Applied Catalysis Journal.

Contribution to Conferences:

1. **Fayad M.A.**, Herreros J.M., Martos F.J., Tsolakis A. Influence of Current Aftertreatment Technology on Emissions Control From the Next Generation Fuels. Future Powertrain Conference 2015 (FPC2015). 2015; 19/20 February, Solihull.

2. **Fayad M.A.**, Dearn K.D., Tsolakis A. Influence of Alternative Fuels on Lubricant Properties in Diesel Engines, 2015, University of Birmingham's Research Poster Conference 2015.

3. **Fayad M.A.**, Tsolakis A. Understanding the Combined Impact of Renewable Fuel and Injection Strategy on Particulate Emission Characteristics in Modern Diesel Engine, 2016, EPS Research Conference, University of Birmingham.

4. **Fayad M.A.**, Tsolakis A. Effect of Injection Strategy on Gaseous Emissions within Diesel Oxidation Catalyst in Diesel Engine Fuelled with Renewable Fuel, 2016, University of Birmingham's Research Poster Conference 2016.

AWARDS

1. Runner-up for the College of Engineering and Physical Science's best paper award (September 2015) for the paper entitled "the role of alternative fuels on particulate matter (PM) characteristics and influence of the diesel oxidation catalyst" published in Environmental Science & Technology Journal, 2015, 49, 11967-11973.
2. Third best poster at the 4th Mechanical Engineering Symposium, University of Birmingham, May 2015.

LIST OF REFERENCES

[1] Heywood, J.B., *Internal combustion engines fundamentals.* USA: McGraw-Hill, 1988: p. ISBN 0-07-100499-8.

[2] Bouchez, M., Dementhon, J.B., *Strategies for the control of particulate trap regeneration*. 2000, SAE Technical Paper. p. 01-0472, doi:10.4271/2000-01-0472.

[3] Gill, S.S., Chatha, G.S., Tsolakis, A., *Analysis of reformed EGR on the performance of a diesel particulate filter.* International Journal of Hydrogen Energy, 2011. 36(16): p. 10089-10099.

[4] Zhu, L., Z. Huang, and J. Fang, *The Effects of Diesel Oxidation Catalyst on Particulate Emission of Ethanol-Biodiesel Blend Fuel*. 2014, SAE Technical Paper, doi:10.4271/2014-01-2730.

[5] Sukjit, E., Herreros, J.M., Dearn, K.D., Garcia-Contreras, R., Tsolakis, A., *The effect of the addition of individual methyl esters on the combustion and emissions of ethanol and butanol -diesel blends.* Energy, 2012. 42(1): p. 364-374.

[6] Lapuerta, M., Armas, O., Rodríguez-Fernández, J., *Effect of biodiesel fuels on diesel engine emissions.* Progress in Energy and Combustion Science, 2008. 34: p. 198-223.

[7] Lapuerta, M., Armas, O., Herreros, J.M., *Emissions from a diesel-bioethanol blend in an automotive diesel engine.* Fuel, 2008. 87: p. 25-31.

[8] Hellier, P., Ladommatos, N., Allan, R., Rogerson, J., *The Influence of Fatty Acid Ester Alcohol Moiety Molecular Structure on Diesel Combustion and Emissions.* Energy & fuels, 2012. 26: p. 1912-1927.

[9] Eveleigh, A., Ladommatos, N., Hellier, P., Jourdan, A., *An investigation into the conversion of specific carbon atoms in oleic acid and methyl oleate to particulate matter in a diesel engine and tube reactor.* Fuel, 2015. 153: p. 604-611.

[10] Xing-cai, L., Jian-Guang, Y., Wu-Gao, Z., Zhen, H., *Effect of cetane number improver on heat release rate and emissions of high speed diesel engine fueled with ethanol–diesel blend fuel.* Fuel, 2004. 83(14): p. 2013-2020.

[11] Rakopoulos, D.C., Rakopoulos, C. D., Giakoumis, E. G., Dimaratos, A. M., Kyritsis, D. C., *Effects of butanol–diesel fuel blends on the performance and emissions of a high-speed DI diesel engine.* Energ. Convers. Manage., 2010. 51(10): p. 1989-1997.

[12] Rakopoulos, D.C., Rakopoulos, C. D., Papagiannakis, R. G., Kyritsis, D. C., *Combustion heat release analysis of ethanol or n-butanol diesel fuel blends in heavy-duty DI diesel engine.* Fuel, 2011. 90(5): p. 1855-1867.

[13] Kittelson, D.B., *Engines and nanoparticles: a review.* Journal of Aerosol Science, 1998. 29: p. 575-588.

[14] Tree, D.R. and K.I. Svensson, *Soot processes in compression ignition engines.* Progress in Energy and Combustion Science, 2007. 33(3): p. 272-309.

[15] Broday, D.M.a.R., R., *Deposition of fractal-like soot aggregates in the human respiratory tract.* Journal of Aerosol Science, 2011. 42(6): p. 372-386.

[16] Lighty, J.S.V., J. M. and Sarofim A. F., *Combustion aerosols: Factors governing their size and composition and implications to human health.* Journal of the Air and Waste Management Association, 2000. 50: p. 1565-1618.

[17] Muzyka, V.V., S. and Schmidt, N., *On the carcinogenic risk evaluation of diesel exhaust: Benzene in airborne particles and alterations of heme metabolism in lymphocytes as markers of exposure.* Science of The Total Environment, 1998. 217(1-2): p. 103-111.

[18] Rounce, P., Tsolakis, A., York, A.P.E., *Speciation of particulate matter and hydrocarbon emissions from biodiesel combustion and its reduction by aftertreatment.* Fuel, 2012. 96: p. 90-99.

[19] Ye, S., Yap, Y. H., Kolaczkowski, S. T., Robinson, K., Lukyanov, D., *Catalyst 'light-off' experiments on a diesel oxidation catalyst connected to a diesel engine-*

Methodology and techniques. Chemical Engineering Research and Design, 2012. 90(6): p. 834-845.

[20] Lefort, I., Herreros, J. M., Tsolakis, A., *Reduction of low temperature engine pollutants by understanding the exhaust species interactions in a diesel oxidation catalyst.* Environmental Science & Technology, 2014. 48(4): p. 2361-2367.

[21] Herreros, J.M., Gill, S.S., Lefort, I., Tsolakis, A., Millington, P., Moss, E., *Enhancing the low temperature oxidation performance over a Pt and a Pt–Pd diesel oxidation catalyst.* Applied Catalysis B: Environmental, 2014. 147: p. 835-841.

[22] Mittendorfer, F., Thomazeau, C., Raybaud, P., Toulhoat, H., *Adsorption of unsaturated hydrocarbons on Pd (111) and Pt (111): A DFT study.* The Journal of Physical Chemistry B, 2003. 107(44): p. 12287-12295.

[23] Meakin, P., Donn, B., Mulholland, G. W., *Collisions between point masses and fractal aggregates.* Langmuir, 1989. 5(2): p. 510-518.

[24] Prasad, R., Bella, R. V. , *A Review on Diesel Soot Emission, its Effect and Control.* Chemical Reaction Engineering & Catalysis, 2010. 5(2): p. 69-86.

[25] Geiser, M., and Kreyling, W., *Deposition and Biokinetics of Inhaled Nanoparticles.* Particle and Fibre Toxicology, 2010. 7(1): p. 1-17.

[26] McCormick, R.L.R., J. D.; Graboski, M. S., *Effect of Several Oxygenates on Regulated Emissions from Heavy-Duty Diesel Engines.* Environmental Science & Technology, 1997. 4: p. 1144-1150.

[27] Gonzales, D.M.A., Piel, W., Asmus, T., Clark, W., Garbak, J., Liney, E., Natarajan, M., Naegeli, D. W., Yost, D., Frame, E. A., Wallace III., J. P., *Oxygenates for Advanced Petroleum-Based Diesel Fuels: Part 2. The Effect of Oxygenate Blending Compounds on Exhaust Emissions.* SAE Technical Paper, 2001: p. 01-3632.

[28] Sendzikiene, E.M., V.; Janulis, P., *Influence of Fuel Oxygen Content on Diesel Engine Exhaust Emissions.* Renewable Energy, 2006. 31: p. 2505-2512.

[29] Ren, Y., et al., *Combustion and emissions of a DI diesel engine fuelled with diesel-oxygenate blends.* Fuel, 2008. 87(12): p. 2691-2697.

[30] Kim, H., Choi, B., *The Effect of Biodiesel and Bioethanol Blended Diesel Fuel on Nanoparticles and Exhaust Emissions from CRDI diesel Engine.* Renewable Energy, 2010. 35: p. 157-163.

[31] Rakopoulos, D.C., Rakopoulos, C. D., Giakoumis, E. G., Dimaratos, A. M., Kyritsis, D. C., *Effects of butanol-diesel fuel blends on the performance and emissions of a high-speed DI diesel engine.* Energy Conversion and Management, 2010. 51: p. 1989-1997.

[32] Mueller, C.J., Pitz, W. J., Pickett, L. M., Martin, G. C., Siebers, D. L., Westbrook, C. K., *Effects of oxygenates on soot processes in DI diesel engines: Experiments and numerical simulations.* SAE Technical Paper, 2003: p. 01-1791.

[33] Westbrook, C.K., W.J. Pitz, and H.J. Curran, *Chemical kinetic modeling study of the effects of oxygenated hydrocarbons on soot emissions from diesel engines.* J. Phys. Chem. A, 2006. 110(21): p. 6912-6922.

[34] Koivisto, E., Ladommatos, N., Gold, M., *Systematic study of the effect of the hydroxyl functional group in alcohol molecules on compression ignition and exhaust gas emissions.* Fuel, 2015. 153: p. 650-663.

[35] Zhang, Z., Balasubramanian, R., *Investigation of particulate emission characteristics of a diesel engine fueled with higher alcohols/biodiesel blends.* Applied Energy, 2016. 163: p. 71-80.

[36] Feng, Q.J., A.; Fincham, A. M.; Wang, Y. L.; Tsotsis, T. T.; Egolfopoulos, F. N., *Soot Formation in Flames of Model Biodiesel Fuels.* Combustion and Flame, 2012. 159(5): p. 1876-1893.

[37] López, A.F., Cadrazco, M., Agudelo, A.F., Corredor, L.A., Vélez, J.A., Agudelo, J.R, *Impact of n-butanol and hydrous ethanol fumigation on the performance and pollutant emissions of an automotive diesel engine.* Fuel, 2015. 153: p. 483-491.

[38] Parks, J., James, E., Huff, S. P., Kass, M. D., Storey, J. M., *Characterization of in-cylinder techniques for thermal management of diesel aftertreatment*. 2007, Oak Ridge National Laboratory (ORNL); Fuels, Engines and Emissions Research Center.

[39] Ko, A.K., J.; Choi, K.; et al., *Experimental study of particle emission characteristics of a heavy-duty diesel engine and effects of aftertreatment systems: Selective catalytic reduction, diesel particulate filter, and diesel particulate and NOx reduction.* Proc. Inst. Mech. Eng., Part D., 2012. 12: p. 1689-1696.

[40] Katare, S., Patterson, J., Laing, P., *Aged DOC is a Net Consumer of NO2: Analyses of Vehicle, Engine-dynamometer and Reactor Data.* SAE Technical Paper Ser., 2007: p. 01-3984.

[41] Yamamoto, K., Takada, K., Kusaka, J., Kanno, Y., Nagata, M. *Influence of diesel post injection timing on HC emissions and catalytic oxidation performance*. in *Powertrain and Fluid Systems Conference and Exhibition*. 2006.

[42] Chen, P., Ibrahim, U., Wang, J., *Experimental investigation of diesel and biodiesel post injections during active diesel particulate filter regenerations.* Fuel, 2014. 130: p. 286-295.

[43] Li, X., Guan, C., Luo, Y., Huang, Z., *Effect of multiple-injection strategies on diesel engine exhaust particle size and nanostructure.* Journal of Aerosol Science, 2015. 89: p. 69-76.

[44] Chen, S.K., *Simultaneous reduction of NOx and particulate emissions by using multiple injections in a small diesel engine*. 2000, SAE Technical Paper.

[45] Zhang, R.e.a., *Variability in morphology, hygroscopicity, and optical properties of soot aerosols during atmospheric processing.* Proceedings of the National Academy of Sciences, 2008. 105(30): p. 10291-10296.

[46] Dec, J., *A Conceptual Model of DI Diesel Combustion Based on Laser-Sheet Imaging.* SAE Technical Paper, 1997. 970873: p. doi:10.4271/970873.

[47] Stone, R., *"Introduction to Internal Combustion Engines (third edition),"*. Society of Automotive Engineers, Inc., Warrendale, PA, ISBN, 1999: p. 0-978 and 7680-0495-3.

[48] Musculus, M.P., Dec, John E. and Tree, Dale R.,, *Effects of Fuel Parameters and Diffusion Flame Lift-Off on Soot Formation in a Heavy-Duty DI Diesel Engine In-Cylinder Diesel Particulates and NOx Control.* SAE International, 2002: p. 01-0889.

[49] Flynn, P.F., Durrett, Russell P., Hunter, Gary L., zur Loye, Axel O., Akinyemi, O.C., Dec, John E. and Westbrook, Charles K., *Diesel Combustion : An Integrated View Combining Laser Diagnostics , Chemical Kinetics , And Empirical Validation.* ASAE Techinal Paper, 1999: p. 01-0509.

[50] Argachoy, C.a.P., A.P., *Phenomenological Model of Particulate Matter Emission from Direct Injection Diesel Engines.* Journal of the Brazilian Socity of Mechanical Sciences and Engineering, 2005, 27(3): p. 266-273.

[51] Gülder, O., Glavincevski, B., & Burton, G., *Ignition quality rating methods for diesel fuels - a critical appraisal.* Society of Automotive Engineers, 1985. Technical Paper 852080, doi:10.4271/852080.

[52] Rodríguez-Fernández, J., Tsolakis, A., Ahmadinejad, M. & Sitshebo, S., *Investigation of the deactivation of a NOx-reducing hydrocarbon-selective catalytic reduction (HC-SCR) catalyst by thermogravimetric analysis: effect of the fuel and prototype catalyst.* Energy & Fuels, 2009. 24: p. 992-1000.

[53] Emission Standards, C.a.L.T., Available at:http://www.dieselnet.com/standards/eu/ld.php (Accessed: 10 August 2016).

[54] Karl, T.R., Trenberth, K.E., *Global Climate Change. Science.* Science, 2003. 302: p. 1719-1723.

[55] Lapuerta, M., Martos, F. J., Herreros, J. M., *Effect of engine operating conditions on the size of primary particles composing diesel soot agglomerates.* Aerosol science, 2007. 38: p. 455-466.

[56] Kennedy, I.M., *Models of Soot Formation and Oxidation.* Progress in Energy and Combustion Science, 1997. 23(2): p. 95-132.

[57] Aldajah, S., Ajayi, O.O., Fenske, G.R., Goldblatt, I.L., *Effect of exhaust gas recirculation (EGR) contamination of diesel engine oil on wear*, Wear, 2007. 263: p. 93-98.

[58] Bowman, C.T., *Kinetics of pollutant formation and destruction in combustion*, Progress in Energy and Combustion Science, 1975. 1: p. 33-45.

[59] Miles, P., *Sources and Mitigation of CO and UHC Emissions in Low-temperature Diesel Combustion Regimes: Insights Obtained via Homogeneous Reactor Modeling.* US DOE. 13th Diesel Engine-Efficiency and Emissions Research (DEER) Conference. Detroit, Michigan. http://www1.eere.energy.gov/vehiclesandfuels/pdfs/deer_2007/session8/deer07_miles.pdf Accessed 15/9/2016, 2007.

[60] Strauss, S., Wasil, J. R. & Earnest, G. S., *Carbon monoxide emisions from marine outboard engines.* ASAE Techinal Paper, 2004: p. 01-320011.

[61] Yu, R.C., Shahed, S> M., *Effects of injection timing and exhaust gas recirculation on emissions from a DI diesel engine.* SAE Paper, 1981. 90(4): p. 3873-3883, doi:10.4271/811234.

[62] Burtscher, H., Stefan, S., Huglin, C., *Characterization of particles in combustion engine exhaust.* Journal of Aerosol Science, 1998. 29(4): p. 389-296.

[63] Majewski, W.A.a.K., M.K., *Diesel emissions and their control.* SAE International, 2006: p. ISBN-10-7680-0674.

[64] Ferguson, C.R., *Internal Combustion Engines.* Applied Thermosciences, 1986. NEW York, Wiley.

[65] Lavoie, G.A., Heywood, J. B. & Keck, J. C., *Experimental and theoretical study of nitric oxide formation in internal combustion engines.* Combustion Science and Technology, 1970. 1: p. 313-326.

[66] Eastwood, P., *Particle Emissions from Vehicles.* John Wiley & Sons Ltd. UK., 2008.

[67] Bacha, J., Blondis, L., Freel, J., Hemighaus, G., Hoekman, K., Hogue, N., Horn, J., Lesnini, D., McDonald, C., Nikanjam, M., Olsen, E., Scott, B. and Sztenderowic, M., *Diesel fuels technical review (FTR-2).* Chervron products company, a division of Chevron USA, Inc, 1998.

[68] Lapuerta, M.B., R.; Martos, F. J., *The effect of diesel engine conditions on the size and morphology of soot particles.* Int. J. Vehicle Design, 2009. 50(3): p. 91-106.

[69] Kittelson, D.B., Watts, W.F., Johnson, J.P., *Nanoparticle emissions on Minnesota highways.* Atmospheric Environment, 2004. 38(1): p. 9-19.

[70] Maricq, M.M., *Chemical characterization of particulate emissions from diesel engines: A review.* Journal of Aerosol Science, 2007. 38(11): p. 1079-1118.

[71] Ullman, T.L., *Investigation of the effects of fuel composition on heavy-duty diesel engine emissions.* JSAE international journal1989: p. 892072.

[72] Arai, M., Amagai, K., Nakaji, T., & Hayashi, S., *Primary and aggregate size distributions of PM in tail pipe emissions from diesel engines.* JSME International Journal, Series B Fluid and Thermal Engineering, 2005. 48: p. 639-647.

[73] Chen, Y., Shah, N., Braun, A., Huggins, F. E., & Huffman, G. P., *Electron microscopy investigation of carbonaceous particulate matter generated by combustion of fossil fuels.* Energy & Fuels, 2005. 19: p. 1644-1651.

[74] Krahl, J., Munack, A., Schroder, O., Stein, H. and Bunger, J., *Influence of biodiesel and different designed diesel fuels on the exhaust gas emissions and health effects.* SAE Technical Paper, 2003: p. 01-3199.

[75] Smith, O.I., *Fundamentals of soot formation in flames with application to diesel engine particulate emissions.* Progress in Energy and Combustion Science, 1981. 7: p. 275-91.

[76] Lakkireddy, V.R., Mohammed, H., Johnson, J.H., *The effect of a diesel oxidation catalyst and a catalyzed particulate filter on particle size distribution from a heavy duty diesel engine*. SAE Technical Paper , 2006: p. 0148-7191, doi: 10.4271/2006-01-0877.

[77] Fayad, M.A., Herreros, J. M., Martos, F. J., Tsolakis, A., *Role of Alternative Fuels on Particulate Matter (PM) Characteristics and Influence of the Diesel Oxidation Catalyst.* Environmental Science & Techology, 2015. 49(19): p. 11967-11973.

[78] Majewski, A., *Diesel particulate matter.* http://www.dieselnet.com. [Accessed 21 January 2017]. 2002.

[79] Johnson, J.H., Bagley, S.T., Gratz, L.D., Leddy, D.G., *A review of diesel particulate control technology and emissions effects. 1992 horning memorial award lecture*. 1994, SAE Technical Paper. p. doi:10.4271/940233.

[80] Eastwood, P., *Critical topics in exhaust gas aftertreatment*. Herts: Research Studies Press., 2000: p. ISBN 0-86380-242-7.

[81] Diehl, F., Barbier, J., Duprez, D., Guibard, I., Mabilon, G., *Catalytic oxidation of heavy hydrocarbons over Pt/Al2O3. Influence of the structure of the molecule on its reactivity.* Applied Catalysis B: Environmental, 2010. 95(3): p. 217-227.

[82] Al-Harbi, M., Hayes, R., Votsmeier, M., et al., *Competitive NO, CO and Hydrocarbon Oxidation Reactions Over a Diesel Oxidation Catalyst.* The Canadian Journal of Chemical Engineering, 2012. 90(6): p. 1527-1538.

[83] Patterson, M.J., Angove, D.E. and Cant, N.W., *The Effect of Carbon Monoxide on the Oxidation of Four C6 to C8 Hydrocarbons over Platinum, Palladium and Rhodium.* Applied Catalysis B: Environmental, 2000. 26: p. 47-57.

[84] Voltz, S.E., Morgan, C. R., Liederman, D.,, *Kinetic Study of Carbon Monoxide and Propylene Oxidation on Platinum Catalysts.* Product R&D, 1973. 12(4): p. 294-301.

[85] Yao, Y.-F.Y., *The Oxidation of CO and Hydrocarbons over Noble Metal Catalysts.* Journal of Catalysis, 1984. 87(1): p. 152-162.

[86] Katare, S.R.L., P. M., *Hydrogen in diesel exhaust: effect on diesel oxidation catalyst flow reactor experiments and model predictions.* SAE International Journal Fuels Lubricity, 2009. 2: p. 605-611.

[87] Lafossas, F., Matsuda, Y., Mohammadi, A., Morishima, A., Inoue, M., Kalogirou, M., Koltsakis, G., Samaras, Z., *Calibration and validation of a diesel oxidation catalyst model: From synthetic gas testing to driving cycle applications.* SAE International Journal of Engines, 2011. 4(1): p. 1586-1606, doi:10.4271/2011-01-1244.

[88] Blakeman, P.G., Chiffey, A.F., Philips, P.R., Twigg, M.V., and Walker, A.P., *Developments In Diesel Emission Aftertreatment Technology.* SAE Technical Paper, 2003: p. 01-3753, doi:10.4271/2003-01-3753.

[89] Neeft, J.P.A., van Pruissen, O.P., Makkee, M., Moulijn, J.A., *Catalysts for the oxidation of soot from diesel exhaust gases II. Contact between soot and catalyst under practical conditions.* Applied Catalysis B: Environmental, 1997. 12: p. 21-31.

[90] Watanabe, T., Kawashima, K., Tagawa, Y., Tashiro, K., Anoda, H., Ichioka, K., Sumiya, S. and Zhang, G., *New DOC for light duty diesel DPF system*, SAE Technical Paper, 2007: p. 01-1920, doi:10.4271/2007-01-1920.

[91] Heck, R.M., R.J. Farrauto., *Catalytic Air Pollution Control: Commercial Technology.* Van Nostrand Reinhold, New York., 1995.

[92] Diesel Filter System, Online Source: https://www.dieselnet.com/tech/dpf_cat.php. [Accessed 26 January 2017]. 2008.

[93] Turns, S.R., *An Introduction to Combustion: Concepts and Applications.* Singapore: McGraw-Hill, 2000: p. 550.

[94] Richter, H., Howard, J., *Formation of polycyclic aromatic hydrocarbons and their growth to soot - a review of chemical reaction pathways.* Progress in Energy and Combustion Science, 2000. 25: p. 565-608.

[95] Choi, M.Y., Hamins, A., Mulholland, G.W., Kashiwagi, T., *Simultaneous optical measurement of soot volume fraction and temperature in premixed flames.* Combust. Flame, 1994. 99: p. 174-86.

[96] Haynes, B.S., Wagner, H.GG., *"Soot formation",* *Progress in Energy and Combustion Science SCI*, 1981. 7: p. 229-73.

[97] Glassman, I., Yetter, R.A., *Combustion* San Diego: Academic Press, 4th Edition, 1996.

[98] Dobbins, R.A., Fletcher, R.A., and Lu, W., *Laser Microprobe Analysis of Soot Precursor Particles and Carbonaceous Soot.* Combustion and Flame, 1995. 100: p. 301-309.

[99] Dobbins, R.A., Govatzidakis, G.J., Lu, W., Schwartzman, A.F., and Fletcher, R.A., *Carbonization Rate of Soot Precursor Particles.* Combustion Science and Technology, 1996. 121: p. 103-121.

[100] Westmoreland, P.R., Dean, A. M., Howard J. B., Longwell, J. P., *Forming Benzene in Flames by Chemically Activated Isomerization.* Journal of Physical Chemistry, 1989. 93: p. 8171-8180.

[101] Cheng, A.S., Dibble, R.W., Buchholz, B.A., *The effect of oxygenates on diesel engine particulate matter.* SAE Technical Paper, 2002: p. 01-1705, doi:10.4271/2002-01-1705.

[102] Rakopoulos, C.D., Hountalas, D.T., Zannis, T.C., *Operational and environmental evaluation of diesel engines burning oxygen-enriched intake air or oxygen-enriched fuels: a review.* SAE Technical Paper, 2004: p. 01-2924, doi:10.4271/2004-01-2924.

[103] Pepiot-Desjardins, P., Pistch, H., Malhotra, R., Kirby, S.R., Boehman, A.L., *Structural group analysis for soot reduction tendency of oxygenated fuels.* Combustion and Flame, 2008. 154: p. 191-205.

[104] Bartok, W., Sarofim, A. F., *Fossil fuel combustion.* John Wiley and Sons Inc., New York NY, 1990.

[105] D'Anna, A., Violi, A., *A Kinetic Model for the Formation of Aromatic Hydrocarbons in Premixed Laminar Flames.* 27, 1998: p. 425-433.

[106] Harris, S.J., Weiner, A. M., *Surface Growth of Soot Particles in Premixed Ethylene/Air Flames.* Combustion Science and Technology, 1983. 31: p. 155-167.

[107] Frenklach, M., Harris, S.J., *Aerosol dynamics modeling using the method of moments.* Journal of Colloid and Interface Science, 1987. 118: p. 252-261.

[108] Frenklach, M., Clary, D. W., Gardiner, W. C. Jr., Stein S. E., *Detailed Kinetic Modeling of Soot Formation in Shock-Tube Pyrolysis of Acetylene.* Proceedings of the Combustion Institute, 1985. 20: p. 887.

[109] Glassman, I., Yetter, R. A., *Combustion, 4th edition.* San Diego: Academic Press, 2008: p. ISBN: 9780120885732.

[110] Bergman, M., Golovitchev, V. I., *Application of Transient Temperature vs. Equivalence Ratio Emission Maps to Engine Simulations.* SAE Technical Paper, 2007: p. 01-1086, doi:10.4271/2007-01-1086.

[111] Puri, R., Santoro, R.J., *The oxidation of soot and carbon monoxide in hydrocarbon diffusion flames.* Combustion and Flame, 1994. 97: p. 125-144.

[112] Virtanen, A.K.K., Ristimäki, J.M., Vaaraslahti, K.M., Keskinen, J., *Effect of engine load on diesel soot particles.* Environmental science & technology, 2004. 38: p. 2551-2556.

[113] Amann, C.A.a.S., D.C., *Diesel Particulates - What They Are and Why.* Aerosol science and technology, 1982. 1: p. 73-101.

[114] Lee, K.O., Cole, R., Sekar, R., Choi, M. Y., Z., J., Kang, J., Bae, C., *Detailed characterization of morphology and dimensions of diesel particulates via thermophoretic sampling*. 2001, SAE Technical Paper, doi:10.4271/201-01-3572.

[115] Bruce, C.W., Stromberg, T.F., Gurton, K.P., Mozer, J.B., *Transspectral absorption and scattering of electromagnetic radiation by diesel soot.* Applied Optics, 1991. 30(12): p. 1537-46.

[116] Ladommatos, N., Zhao, H., *A guide to measurement of flame temperature and soot concentration in diesel engines using the two-colour method. Part 1: principles.* SAE Technical Paper, 1994: p. 01-941956, doi:10.4271/941956.

[117] Lapuerta, M.B., R.; Martos, F. J., *A method to determine the fractal dimension of diesel soot agglomerates.* J. Colloid Interface Sci., 2006. 303: p. 149-158.

[118] Neer, A., Koylu, U. O., *Effect of operating conditions on the size, morphology, and concentration of submicrometer particulates emitted from a diesel engine.* Combustion and Flame, 2006. 14**6**(1-2): p. 142-154.

[119] Qu, L., Wang, Z., Hu, H., Li, X., Zhao, Y. , *Effects of butanol on components and morphology of particles emitted by diesel engines.* Researh of Environmental Sciences, 2015. 28(10): p. 1518-1523.

[120] Bockhorn, H., *Soot Formation in Combustion, Mechanisms and Models.* Springer Series in Chemical Physics, Springer-Verlag: Berlin., 1994.

[121] Kazakov, A.a.F., D.E., *Modeling of soot formation during DI diesel combustion using a multi-step phenomenological model.* ASAE Techinal Paper, 1998: p. 01-982463, doi:10.4271/982463.

[122] Tree, D.R., and Foster, D.E., *Optical measurements of soot particle size, number density, and temperature in a direct injection diesel engine as a function of speed and load.* SAE Technical Paper, 1994: p. 01-940270, doi:10.4271/94270.

[123] Bougie, B., Ganippa, L.C., van Vliet, A.P., Meerts, W.L., Dam, N.J., ter Muelen, J..J., *Soot particulate size characterization in a heavy-duty diesel engine for*

different engine loads by laser-induced incandescence. Proceedings of the Combustion Institute, 2007. 31: p. 685-691.

[124] Kock, B.F., Tribalet, B., Schulz, C., Roth, P., *Two-color time-resolved LII applied to soot particle sizing in the cylinder of a Diesel engine.* Combustion and Flame, 2006. 147: p. 79-92.

[125] Mathis, U., Mohr, M., Kaegi, R., *Influence of diesel engine combustion parameters on primary soot particle diameter.* Environmental science & technology, 2005. 39: p. 1887-1892.

[126] Kolodziej, C., Wirojsakunchai, E., Foster, D.E., Schmidt, N., Kamimoto, T., Kawai, T., Akard, M., Yoshimura, T., *Comprehensive characterization of particulate emissions from advanced diesel combustion.* SAE Technical Paper, 2007: p. 01-1945, doi:10.4271/2007-01-1945.

[127] Furuhata, T., Arai, M., Yaga, M., Lee, J.H., Chun, K.M., *Effect of fuel properties on diesel PM components.* SAE Technical Paper, 2007: p. 01-1941, doi:10.4271/2007-01-1941.

[128] Collings, N.a.G., B.R., *Particles from internal combustion engines - what we need to know.* Philosophical Transaction of Royal Society London, 2000. A358: p. 2611-2623.

[129] Burtscher, H., *Physical characterization of particulate emissions from diesel engines: A review.* Journal of Aerosol Science, 2005. 36: p. 896-932.

[130] Al-Qurashi, K., Boehman, A. L., *Impact of exhaust gas recirculation (EGR) on the oxidative reactivity of diesel engine soot.* combustion and Flame, 2008. 155: p. 675-695.

[131] Medalia, A.I., Heckman, F.A. , *Morphology of aggregates—II. Size and shape factors of carbon black aggregates from electron microscopy.* Carbon, 1969. 7: p. 567-568.

[132] Megaridis, C.M., Dobbins, R.A. , *Morphological description of flame-generated materials.* Combustion Science and Technology, 1990. 71: p. 95-109.

[133] Köylü, Ü.Ö., Faeth, G.M., Farias, T.L., Carvalho, M.G. , *Fractal and Projected Structure Properties of Soot Aggregates* . Combustion and Flame, 1995. 100: p. 621-633.

[134] Cai, J., Lu, N., Sorensen, C.M. , *Comparison of Size and Morphology of Soot Aggregates As Determined by Light Scattering and Electron Microscope Analysis* Langmuir, 1993. 9: p. 2861-2867.

[135] Lee, K.O., Sekar, R., Choi, M. Y., Kang, J. S., Bae, C. S., Shin, H. D., *Morphological investigation of the microstructure, dimensions, and fractal geometry of diesel particulates.* Proceedings of the Combustion Institute, 2002. 29(1): p. 647-653.

[136] Zhu, J., Lee, K.O., Yozgatligil, A., Choi, M.Y., *Effects of engine operating conditions on morphology, microstructure, and fractal geometry of light-duty diesel engine particulates.* Proceedings of the Combustion Institute, 2005. 30: p. 2781-2789.

[137] Ishiguro, T., Suzuki, N., Fujitani, Y., Morimoto, H., *Microstructural Changes of Diesel Soot during Oxidation.* Combustion and Flame, 1991. 85(1-2): p. 1-6.

[138] Fang, H.L.a.L., M.J., *Influence of Soot Surface Changes on DPF Regeneration.* SAE Technical Paper, 2004: p. 01-3043, doi:10.4271/2004-01-3043.

[139] Luo, C.H., Lee, W.M., Lai, Y.C., Wen, C.Y., Liaw, J.J., *Measuring the fractal dimension of diesel soot agglomerates by fractional Brownian motion processor.* Atmospheric Environment, 2005. 39: p. 3565-3572.

[140] Park, K., Cao, F., Kittelson, D.B., McMurry, P.H., *Relationship between particle mass and mobility for diesel exhaust particles.* Environmental science & technology, 2003. 37(3): p. 577-583.

[141] Maricq, M.M., Xu, N., *The effective density and fractal dimension of soot particles from premixed flames and motor vehicle exhaust.* Journal of Aerosol Science, 2004. 35: p. 1251-1274.

[142] Song, J., Alam, M., Boehman, A. L., Kim, U., *Examination of the oxidation behaviour of biodiesel soot.* Combustion and Flame, 2006. 146: p. 589-604.

[143] Hurt, R.H., Crawford, G.P., and Shim, H.S., *Equilibrium nanostructure of primary soot particles.* Proceedings of the Combustion Institute, 2000. 28: p. 2539-2546.

[144] Zhu, R.M., H.; Wang, X.; Huang, Z., *Effects of fuel constituents and injection timing on combustion and emission characteristics of a compression-ignition engine fueled with diesel-DMM blends.* Proc. Combust. Inst., 2013. 34(2): p. 3013-3020.

[145] Zhu, J., Lee, K.O., Sekar, R., *Morphological study of the particulate matter from a light-duty diesel engine.* Proceedings of the Third Joint Meeting of the U.S. Sections of the Combustion Institute, 2003.

[146] Lipkea, W.H., Johnson, J.H., Vuk, C.T., *The physical and chemical character of diesel particulate emissions- measurement techniques and fundamental considerations.* SAE Technical Paper, 1978: p. 01-780108, doi:10.4271/780108.

[147] Kawaguchi, A., Sato, Y., Yanagihara, H.L., Ishiguro, T., *A study of soot formation processes in dual fueled compression ignition engine.* SAE Technical Paper, 1992: p. 01-922304, doi:10.4271/922304.

[148] Heidenreich, R.D., *A Test Object and Criteria for High Resolution Electron Microscopy.* Journal of Applied Crystallography, 1968. 1: p. 1-19.

[149] Walker, P.L., *Complications introduced from gasification-induced densification of disordered carbons.* Carbon, 1996. 34(12): p. 1603.

[150] Al-Qurashi, K., *The impact of carbon dioxide and exhaust gas recirculation on the oxidative reactivity of soot from ethylene flames and diesel engines.* Ph.D. Thesis, Energy and Geo-Environmental Engineering. University Park: The Pennsylvania University., 2007.

[151] Chen, H.X., Dobbins, R.A., *Crystallogenesis of particles formed in hydrocarbon combustion.* Combustion Science and Technology, 2000. 159: p. 109-28.

[152] Iwashita, N., Park, C.R., Fujimoto, H., Shiraishi, M., Inagaki, M., *Specification for a standard procedure of X-ray diffraction measurements on carbon materials.* Carbon, 2004. 42(4): p. 701-14.

[153] Fujimoto, H., Mabuchi, A., Tokumitsu, K., Kasuh, T., Akuzawa, N., *Effect of crystallite size on the chemical compositions of the stage 1 alkali metal-graphite intercalation compounds.* Carbon, 1994. 32(2): p. 193-8.

[154] Vander, W., R.L, Tomasek, A.J, Street, K., Hull, D.R., Thompson, W.K., *Carbon nanostructure examined by lattice fringe analysis of high-resolution transmission electron microscopy images.* Applied Spectroscopy, 2004a. 58(2): p. 230-7.

[155] Vander, W., R.L., Tomasek, A.J., Pamphlet, M.I., Taylor, CD, Thompson, W.K., *Analysis of HRTEM images for carbon nanostructure quantification.* Journal of Nanoparticle Research, 2004b. 6(6): p. 555-68.

[156] Braun, A., Huggins, F.E., Seifert, S., Ilavsky, J., Shah, N., Kelly, K.E., Sarofim, A., Huffman, G.P., *Size- range analysis of diesel soot with ultra-small angle Xray scattering.* Combustion and Flame, 2004. 137: p. 63-72.

[157] Vander Wal, R., Tomasek, A.J., *Soot nanostructure: dependence upon synthesis conditions.* Combustion and Flame, 2004. 136: p. 129-140.

[158] Su, D.S., Jentoft, R.E., Müller, J.-O., Rothe, D., Jacob, E., Simpson, C.D., Tomovic, Z., Müllen, K., Messerer, A., Pöschl, U., Niessner, R., Schlögl, R., *Microstructure and oxidation behaviour of Euro IV diesel engine soot: a comparative study with synthetic model soot substances.* Catalyst Today, 2004. 90: p. 127-132.

[159] Wentzel, M., Gorzawski, H., Naumann, K.-H., Saathoff, H., Weinbruch, S., *Transmission electron microscopical and aerosol dynamical characterization of soot aerosols.* Journal of Aerosol Science, 2003. 34: p. 1347-1370.

[160] Crookes, R.J., Sivalingam, G., Nazha, M. A. A, Rajakaruna, H., *Prediction and measurement of soot particulate formation in a confined diesel fuel spray-flame at 2.1 MPa.* International journal of thermal sciences, 2003. 42(7): p. 639-646.

[161] Zhu, J., Lee, K.O., Yozgatligil, A., Choi, M.Y., *Effects of engine operating onditions on morphology, microstructure, and fractal geometry of light-duty diesel ngine particulates.* Proceedings of the Combustion Institute, 2005. 30: p. 2781-2789.

[162] Ishiguro, T., Takatori, Y., Akihama, K., *Microstructure of diesel soot particles probed by electron microscopy: first observation of inner core and outer shell.* Combustion and Flame, 1997. 108: p. 231-234.

[163] Vander Wal, R.L., Yezerets, A., Currier, N.W., Kim, D.H., Wang, C.M., *HRTEM study of diesel soot collected from diesel particulate filters.* Carbon, 2007. 45: p. 70-77.

[164] Hays, M.D., Vander Wal, R.L., *Heterogeneous soot nanostructure in atmospheric and combustion source aerosols.* Energy & fuels, 2007. 21: p. 801-811.

[165] Zhang, L., Michelangeli, D.V., Taylor, P.A., *Influence of aerosol concentration on precipitation formation in low-level, warm stratiform clouds.* Journal of Aerosol Science, 2006. 37: p. 203-217.

[166] Merola, S.S., Gambi, G., Allouis, C., Beretta, F., Borghese, A., D'Alessio, A., *Analysis of exhausts emitted by I.C. engines and stationary burners, by means of U.V. extinction and fluorescence spectroscopy.* Chemosphere, 2001. 42: p. 827-834.

[167] Müller, J.-O., Su, D.S., Jenthoft, R.E., Kröhnert, J., Jenthoft, .Schlögl, R., *Morphology-controlled reactivity of carbonaceous materials towards oxidation.* Catalyst Today, 2005. 102-103: p. 259-265.

[168] Boehman, A.L., Song, J., Alam, M., *Impact of Biodiesel Blending on Biodiesel Soot and the Regeneration of Particulate Filters.* Energy Fuels, 2005. 19: p. 1857-1864.

[169] Vander Wal, R.L., Tomasek, A. J., *Soot Oxidation: Dependence upon Initial Nanostructure.* Combustion and Flame, 2003. 134: p. 1-9.

[170] Demirbas, A., *"Political, Economic and Environmental Impacts of Biofuels: A Review"*. Applied Energy, 2009. 86: p. S108-S117.

[171] Biodiesel production, *http://www.biofuels-platform.ch/en/infos/production.php, [Cited 20 October 2016]*. 2014.

[172] Moon, G., Lee, Y., Choi, K., Jeong, D., *Emission characteristics of diesel, gas to liquid, and biodiesel-blended fuels in a diesel engine for passenger cars.* Fuel, 2010. 89(12): p. 3840-3846.

[173] Armas, O., García-Contreras, R., Ramos, Á., *Pollutant emissions from New European Driving Cycle with ethanol and butanol diesel blends.* Fuel Processing Technology, 2014. 122: p. 64-71.

[174] Aydin, H., Ikilic, C., *Effect of ethanol blending with biodiesel on engine performance and exhaust emissions in a CI engine.* Applied Thermal Engineering, 2010. 30(10): p. 1199-1204.

[175] Selvan, T., Nagarajan, G., *Combustion and Emission Characteristics of a Diesel Engine Fuelled with Biodiesel Having Varying Saturated Fatty Acid Composition.* International Journal of Green Energy, 2013. 10(9): p. 952-965.

[176] Zhang, Z., Balasubramanian, R., *Effects of oxygenated fuel blends on carbonaceous particulate composition and particle size distributions from a stationary diesel engine.* Fuel, 2015. 141: p. 1-8.

[177] Yao, M.F., Wang, H., Zheng, Z.Q., Yue, Y., *Experimental study of n-butanol additive and multi-injection on HD diesel engine performance and emissions.* Fuel, 2010. 89: p. 2191-201.

[178] Dogan, O., *The influence of n-butanol/diesel fuel blends utilization on a small diesel engine performance and emissions.* Fuel, 2011. 90: p. 2467-2472.

[179] Karabektas, M.H., M., *Performance and emission characteristics of a diesel engine using isobutanol-diesel fuel blends.* Renewable Energy, 2009. 34: p. 1554-1559.

[180] Lujaji, F., Kristof, L., Bereczky, A. & Mbarawa, M.⁋ *Experimental investigation of fuel properties, engine performance, combustion and emissions of blends containing croton oil, butanol, and diesel on a CI engine.* Fuel, 2011. 90: p. 505-510.

[181] Can, Ö., Çelikten, Ï. & Usta, N.⁋ *Effects of ethanol addition on performance and emissions of a turbocharged indirect injection Diesel engine running at different injection pressures.* Energy Conversion and Management, 2004. 45: p. 2429-2440.

[182] Sukjit, E., Herreros, JM, Piaszyk, J, Dearn, KD, Tsolakis, A, *Finding synergies in fuels properties for the design of renewable fuels–Hydroxylated biodiesel effects on butanol-diesel blends.* Environmental Science & Technology, 2013. 47(7): p. 3535-3542.

[183] He, B.Q., Shuai, S.J., Wang, J.X. & He, H.⁋ *The effect of ethanol blended diesel fuels on emissions from a diesel engine.* Atmospheric Environment, 2003. 37: p. 4965-4971.

[184] Li, D.-G., Zhen, H., Xingcai, L., Wu-Gao, Z. & Jian-Guang, Y., *Physicochemical properties of ethanol-diesel blend fuel and its effect on performance and emissions of diesel engines.* Renewable Energy, 2005. 30: p. 967-976.

[185] Harvey, B., and Meylemans, H., *The role of butanol in the development of sustainable fuel technologies.* Journal of Chemical Technology and Biotechnology, 2011. 86(1): p. 1097-4660.

[186] Cairns, A., Stansfield, P., Fraser, N., Blaxill, H. et al., *A Study of Gasoline-Alcohol Blended Fuels in an Advanced Turbocharged DISI Engine.* SAE International journal Fuels Lubricity, 2009. 2(1): p. 41-57.

[187] Lapuerta, M., García-Contreras, R., Campos-Fernández, J., Dorado, M.P., *Stability, lubricity, viscosity, and cold-flow properties of alcohol-diesel blends.* Energy Fuels, 2010. 24(8): p. 4497-4502.

[188.] European Biodiesel Board (EBB), a.E.F.p., *EU Biofuels Annual 2015.* 2015: p. http://www.ebb-eu.org/stats.php.

[189] Szybist, J.P., Boehman, A. L., Taylor, J. D. & Mccormick, R. L. , *Evaluation of formulation strategies to eliminate the biodiesel NOx effect.* fuel Processing Technology, 2005. 86: p. 1109-1126.

[190.] Kim, H., Kang, B., Kim, M., Park, Y., Kim, D., Lee, J., Lee, K., *Transesterification of vegetable oil to biodiesel using heterogeneous base catalyst.* Catalysis Today, 2004. 93: p. 315-320.

[191] Siddappa, S.B., and M. K. Gajendra Babu, J.P.S., *Studies on Performance and Exhaust Emissions of a CI Engine Operating on Diesel and Diesel Biodiesel Blends at Different Injection Pressures and Injection Timings.* SAE Techinal Paper, 2007: p. 01-0613, doi:10.4271/2007-01-0613.

[192] Pinzi, S., Rounce, P., Herreros, J.M., Tsolakis, A., Dorado P., *The effect of biodiesel fatty acid composition on combustion and diesel engine exhaust emissions.* Fuel, 2013. 104: p. 170-182.

[193] Glaude, P., Fournet, R., Bounaceur, R., Molière, M., *Adiabatic Flame Temperature from Biofuels and Fossil Fuels and Derived Effect on NOx Emissions.* Fuel Processing Technology, 2010. 91: p. 229-235.

[194] Chuck, C.J., Bannister, C.D., Hawley, J.G., Davidson, M.G., *Spectroscopic Sensor Techniques Applicable to Real-time Biodiesel Determination.* Fuel, 2010. 89: p. 457-461.

[195] Karavalakis, G., Stournas, S., Bakeas, E., *Light Vehicle Regulated and Unregulated Emissions from Different Biodiesels.* Science of The Total Environment, 2009. 407: p. 3338-3346.

[196] Staat, F., Gateau, P., *The Effects of Rapeseed Oil Methyl Ester on Diesel Engine Performance, Exhaust Emissions and Long Term Behaviour-a Summary of Three Years of Experimentation.* SAE Technical Paper, 1995: p. 950053, doi:10.4271/95003.

[197] Yamane, K., Ueta, A., Shimamoto, Y., *Influence of Physical and Chemical Properties of Biodiesel Fuels on Injection, Combustion and Exhaust Emission*

Characteristics in a Direct Injection Compression Ignition Engine. International Journal of Engine Research, 2001. 42: p. 249-261.

[198] Tsolakis, A., Megaritis, A., Wyszynski, M.L. Theinnoi, K., *Engine Performance and Emissions of a Diesel Engine Operating on Diesel-RME (Rapeseed Methyl Ester) Blends with EGR (Exhaust Gas Recirculation).* Energy, 2007. 32: p. 2072-2080.

[199] Lapuerta, M., Rodríguez-Fernández, J., Oliva, F. & Canoira, L.‚ *Biodiesel from low-grade animal fats: Diesel engine performance and emissions.* Energy & Fuels, 2009. 23: p. 121-129.

[200] Haas, M.J., Scott, K. M., Alleman, T. L. & Mccormick, R. L.‚ *Engine performance of biodiesel fuel prepared from soybean soapstock: A high quality renewable fuel produced from a waste feedstock.* . Energy & Fuels 2001 15: p. 1207-1212.

[201] Monyem, A., Van Gerpen, J. H. & Canakci, M.‚ *The effect of timing and oxidation on emissions from biodiesel-fueled engines.* Transactions of the ASAE (American Society of Agricultural Engineering), 2001. 44: p. 44.

[202] Tat, M.E., Wang, P. S., Gerpen, J. H., Clemente, T. E., *Exhaust emissions from an engine fueled with biodiesel from high-oleic soybeans.* journal of the Americal Oil Chemists' Society, 2007. 84: p. 865-869.

[203] Graboski, M.S.M., R. L.‚ *Combustion of fat and vegetable oil derived fuels in diesel engines.* Progress in Energy and Combustion Science, 1998. 24: p. 125-164.

[204] Labeckas, G.S., S.‚ *The effect of rapeseed oil methyl ester on direct injection diesel engine performance and exhaust emissions.* Energy Conversion and Management 2006. 47(1954-1967): p. 1954-1967.

[205] Serdari, A., Fragioudakis, K., Teas, C., Zannikos, F., Stournas, S. & Lois, E.‚ *Effect of biodiesel addition to diesel fuel on engine performance and emissions.* Journal of Propulsion and Power, 1995. 15: p. 224-231.

[206] Tsolakis, A., *Effects on particulate size distribution from the diesel engine operating in RME-biodiesel with EGR.* Energy & Fuels, 2006. 20: p. 1418-1424.

[207] Szybist, J.P., Kirby, S. R., Boehman, A. L.. *NOx emissions of alternative diesel fuels: a comparative analysis of biodiesel and FT diesel.* . Energy & Fuels, 2005. 19: p. 1484-1492.

[208] Zhang, Y., Boehman, A. L., *Impact of biodiesel on NOx emissions in a common rail direct injection diesel engine.* Energy & Fuels, 2007. 21: p. 2003-2012.

[209] Guerrassi, N., and Dupraz, P., *A Common Rail Injection System for High Speed Direct Injection Diesel Engines.* SAE Technical Paper ‎, 1998: p. 0148-7191, doi:10.4271/980803.

[210] Pickett, L.M.a.S., D. L., *Soot in diesel fuel jets: Effects of ambient temperature, ambient density, and injection pressure.* Combustion and Flame‎, 2004. 138(1-2): p. 114-135.

[211] Agarwal, A.K.D., A.; Srivastava, D. K.; Maurya, R. K.; Singh, A. P., *Effect of fuel injection pressure on diesel particulate size and number distribution in a CRDI single cylinder research engine.* Fuel, 2013. 107(0): p. 84-89.

[212] Sugiyama, G., Ryu, H., Kobayashi, S., *Computational simulation of diesel combustion with high pressure fuel injection.* International Symposium COMODIA, 1994.

[213] Bakar, R.A., Ismail, A. R., *Fuel injection pressure effect on performance of direct injection diesel engines based on experiment.* American Journal of Applied Sciences, 2008. 5(3): p. 197-202.

[214] Qi, D., Leick, M., Liu, Y., and Lee, C. f. F., *Effect of EGR and injection timing on combustion and emission characteristics of split injection strategy DI-diesel engine fueled with biodiesel.* Fuel 2011. 90(5): p. 1884-1891.

[215] Li, Z.S., C.; Song, J.; Lv, G.; Dong, S.; Zhao, Z., *Evolution of the nanostructure, fractal dimension and size of in-cylinder soot during diesel combustion process.* Combustion and Flame, 2011. 158(8): p. 1624-1630.

[216] Park, K.K., D. B.; McMurry, P. H., *Structural properties of diesel exhaust particles measured by transmission electron microscopy (TEM): Relationships to particle mass and mobility.* Aerosol Science and Technology, 2004. 38(9): p. 881-889.

[217] Zhang, R., and Kook, S., *Influence of Fuel Injection Timing and Pressure on In-Flame Soot Particles in an Automotive-Size Diesel Engine.* Environmental Science & Technology, 2014. 48: p. 8243-8250.

[218] Kong, Y., Kozakiewicz,T., Johnson, R., Huffmeyer, C., Huckaby, J., Abel, J., Baurley, J., and Duffield, K., *Active DPF Regeneration for 2007 Diesel Engines.* SAE Technical Paper, 2005: p. 01-3509, doi:10.4271/2005-01-3509.

[219] Mendez, S., Thirouard, B., *Using Multiple Injection Strategies in Diesel Combustion: Potential to Improve Emissions, Noise and Fuel Economy Trade-Off in Low CR Engines.* SAE Technical Paper, 2008. 1: p. 662-674, doi:10.4271/2008-01-1329.

[220] Benajes, J., Malina, S., Garcia, J.M., *Influence of Pre- and Post-Injection on the Performance and Pollutant Emissions in a HD Diesel Engine.* SAE Paper, 2001: p. 01-0526, doi:10.4271/2001-01-0526.

[221] Mohan, B., Yang, W., Chou, S.K., *Fuel injection strategies for performance improvment and emissions reduction in compression ignition engines - A review.* Renewable and Sustainable Energy Reviews, 2013. 28: p. 664-676.

[222] Desantes, J., Bermúdez, V, Pastor, JV, Fuentes, E, *Investigation of the influence of post-injection on diesel exhaust aerosol particle size distributions.* Aerosol Science and Technology, 2006. 40(1): p. 80-96.

[223] O'Connor, J., and Musculus, M., *Post Injections for Soot Reduction in Diesel Engines - A Review of Current Understanding.* SAE Technical Paper, 2013: p. 01-0917, doi:10.4271/2013-01-0917.

[224] Sperl, A., *The Influence of Post-Injection Strategies on the Emissions of Soot and Particulate Matter in Heavy Euro V Diesel Engine*, SAE Technical Paper , 2011: 36(0350): p. 0336-0350, doi: 10.4271/2011-36-0350.

[225] Bobba, M., Musculus, M., Neel, W., *Effect of post injections on in-cylinder and exhaust soot for low-temperature combustion in a heavy-duty diesel engine.* SAE International Journal of Engines, 2010. 3(1): p. 496-516, doi:10.4271/2010-01-0612.

[226] Yun, H., Reitz, R. D., *An experimental investigation on the effect of post-injection strategies on combustion and emissions in the low-temperature diesel combustion regime.* Journal of Engineering for Gas Turbines and Power, 2007. 129(1): p. 279-286.

[227] Barro C., T.F., Obrecht P., Boulouchos K. *Influence of post-injection parameters on soot formation and oxidation in a common-rail-diesel engine using multi-color-pyrometry*. in *Conference: ASME 2012 internal combustion engine division fall technical conference*. 2012. doi: 10.1115/ICEF2012-92075.

[228] Desantes, J.M., Arrègle, J., López, J. J., García, A., *A comprehensive study of diesel combustion and emissions with post-injection*. 2007, SAE Technical Paper, doi:10.4271/2007-01-0915.

[229] Poorghasemi, K., Ommi, F., Yaghmaei, H., Namaki, A., *An investigation on effect of high pressure post injection on soot and NO emissions in a DI diesel engine.* Journal of mechanical science and technology, 2012. 26(1): p. 269-281.

[230] Valentino, G., Iannuzzi, S. E., Marchitto, L., Merola, S. S., Tornatore, C., *Optical Investigation of Postinjection Strategy Effect at the Exhaust Line of a Light-Duty Diesel Engine Supplied with Diesel/Butanol and Biodiesel Blends.* Journal of Energy Engineering, 2013. 140(3): p. 0148-7191.

[231] Fino, D., *Diesel emission control: Catalytic filters for particulate removal.* Science and Technology of Advanced Materials, 2007. 8(1): p. 93-100.

[232] Yehliu, K., Armas, O., Vander W., Randy L., Boehman, A. L., *Impact of engine operating modes and combustion phasing on the reactivity of diesel soot.* Combustion and Flame, 2013. 160(3): p. 682-691.

[233] Storey, J.M., Lewis Sr., S.A., West, B.H., Huff, S.P., sluder, C.S., Wagner, R.M., Domingo, N., Thomas, J., Kass, M., *Hydrocarbon Species in the Exhaust of*

Diesel Engines Equipped with Advanced Emission Control Devices. Final Report CRC Project No. AVFL-10b-2, 2005: p. 01-19.

[234] Badami, M., Mallamo, F., Millo, F., Rossi, E.E., *Experimental Investigation on the Effect of Multiple Injection Strategies on Emissions, Noise and Brake Specific Fuel Consumption of an Automotive Direct Injection Common-Rail Diesel Engine.* International Journal of Engine Research, 2003. 4: p. 299-314.

[235] Merola, S.S., De Filippo, A., Valentino, G., Tornatore, C., Marchitto, L., Iannuzzi, S., *Optical Investigation of Post-Injection Strategy Impact on the Fuel Vapor within the Exhaust Line of a Light Duty Diesel Engine Supplied with Biodiesel Blends.* SAE Paper, 2013: p. 01-1127, doi:10.4271/2013-01-1127.

[236] AVL, *Pressure Sensor for Combustion Analysis – Data Sheet GH13P [Internet]. [Cited 3 November 2015].* Available from URL: https://www.avl.com/documents/10138//885983//AT3368E_GH13P.pdf., 2011.

[237] AVL, *Microifem Piezo 4th Generation – Piezo Amplifier [Internet] [Cited 3 November 2015].* Available from URL: https://www.avl.com/documents/10138//0//MicroIFEM+4P4+Piezo., 2013.

[238] Flaig, U., Polach, W., Ziegler, G. , *Common rail system (CR-system) for passenger car DI diesel engines: experiences with applications for series production projects.* SAE Technical Paper, 1999: p. 01-0191, doi:10.4271/1999-01-0191.

[239] Russell, M.F., Greeves, G., Guerrassi, N., *More torque, less emissions and less noise.* SAE Technical Paper, 2000: p. 01-0942, doi:10.4271/2000-01-0942.

[240] Lapuerta, M., Martos, F. J., Martín-González, G., *Geometrical determination of the lacunarity of agglomerates with integer fractal dimension.* Journal of Colloid and Interface Science, 2010. 346(1): p. 23-31.

[241] Lehtinen, K.E.J., Zachariah, M.R., *Energy accumulation in nanoparticles collision and coalescence processes.* Journal of Aerosol Science, 2002. 33: p. 357-368.

[242] Lee, K.O., Zhu, J., *Evolution in size and morphology of diesel particulates along the exhaust system.* SAE Technical Paper, 2004: p. 01-1981, doi:10.4271/2004-01-1981.

[243] Samson, R.J., Mulholland, G.W., Gentry, J.W., *Structural analysis of soot agglomerates.* Langmuir, 1987. 3: p. 272-281.

[244] Wu, M.K., Friedlander, S.K., *Note on the power law equation fro fractal-like aerosol agglomerates.* Journal of Colloid and Interface Science, 1993. 159: p. 246-248.

[245] Meakin, P., *Computer simulation of growth and aggregation processes.* In On Growth and Form, Stanley, G., Ostrowsky, N., Eds., Martinus-Nijhoff Publishers: Boston, MA, 1986: p. 11-135.

[246] Stevanovic, S., Miljevic, B., Surawski, N. C., Fairfull-Smith, K. E., Bottle, S. E., Brown, R., Ristovski, Z. D., *Influence of Oxygenated Organic Aerosols (OOAs) on the Oxidative Potential of Diesel and Biodiesel Particulate Matter.* Environmental Science & Technology, 2013. 47(14): p. 7655-7662.

[247] Hori, M., *Experimental study of nitrogen dioxide formation in combustion systems.* Symp. (Int.) Combust, [Proc.], 1988. 21(1): p. 1181-1188.

[248] Ladommatos, N., Abdelhalim, S. M., Zhao, H., *Effects of exhaust gas recirculation temperature on diesel engine combustion and emissions.* Proceedings of the Institution of Mechanical Engineers, Part D, 1998. 212(6): p. 479-500.

[249] Herreros, J.M., George, P., Umar, M., Tsolakis, A., *Enhancing selective catalytic reduction of NOx with alternative reactants/promoters.* Chemical Engineering Journal, 2014. 252: p. 47-54.

[250] Johnson, W.L., Fisher, G. B., Toops, T. J., *Mechanistic investigation of ethanol SCR of NOx over Ag/Al2O3.* Catalyst Today, 2012. 184(1): p. 166-177.

[251] Cooper, B., Thoss, J., *Role of NO in Diesel Particulate Emission Control.* SAE Technical Paper Ser., 1989. 890404.

[252] Choi, B., Jiang, Xiaolong, *Individual hydrocarbons and particulate matter emission from a turbocharged CRDI diesel engine fueled with n-butanol/diesel blends*. Fuel, 2015. 154: p. 188-195.

[253] Choi, S.C.R., Hyun G. u., Lee, K. S., Lee, C. S., *Effects of fuel injection parameters on the morphological characteristics of soot particulates and exhaust emissions from a light-duty diesel engine.* Energy & Fuels, 2010. 24(5): p. 2875-2882.

[254] Hwang, J.J., Y., Bae, C. *Particulate morphology of waste cooking oil biodiesel and diesel in a heavy duty diesel engine*. in *International Conference on Optical Particle Characterization (OPC 2014)*. 2014. International Society for Optics and Photonics.

[255] Chen, Z., Wu, Z., Liu, J., Lee, C., *Combustion and emission characteristics of high n-butanol/diesel ratio blend in a heavy duty diesel engine and EGR impact.* Energy Conversion and Management, 2014. 78: p. 787-795.

[256] Richard K., L., J. Cole, A.. *"A reexamination of the Rapre NOx process"*. Combustion and Flame, 1990. 82(3-4): p. 435-443.

[257] Hajbabaei, M., Johnson, K.C., Okamoto, R., Durbin, T.D., *Evaluation of the Impacts of Biofuels on Emissions for a California Certified Diesel Fuel from Heavy-Duty Engines.* SAE Technical Paper, 2013: p. 01-1138, doi:10.4271/2013-01-1138.

[258] Stein, H.J., *Diesel oxidation catalysts for commercial vehicle engines: strategies on their application for controlling particulate emissions.* Applied Catalysis B: Environmental, 1996. 10: p. 69-82.

[259] Fayad, M.A., Tsolakis, A., Fernández-Rodríguez, D., Herreros, J.M., Martos, F.J., Lapuerta, M., *Manipulating modern diesel engine particulate emission characteristics through butanol fuel blending and fuel injection strategies for efficient diesel oxidation catalysts.* Applied Energy, 2017. 190: p. 490-500.

[260] Valentino, G., Iannuzzi, S., Corcione, F. E., *Experimental investigation on the combustion and emissions of a light duty diesel engine fuelled with butanol-diesel blend.* 2013, SAE Technical Paper. p. 01-0915, doi: 10.4271/2013-01-0915.

[261] Ozsezen, A.N., Canakci, M., Turkcan, A., Sayin, C., *Effects of Biodiesel from used frying palm oil on the performance, injection, and combustion characteristics of an indirect injection diesel engine.* Energy & Fuels, 2008. 22: p. 1297-305.

[262] Zervas, E., *Impact of different configurations of a Diesel oxidation catalyst on the CO and HC tail-pipe emissions of a Euro4 passenger car.* Applied Thermal Engineering, 2008. 28: p. 962-966.

[263] Murakami, N., Kojima, N., Hashiguchi, M., *Oxidation of NO to NO_2 in the Flue Gas (I) - Oxidation by Addition of CH_3OH.* Nenryo Kyokaishi, 1982. 61: p. 276-284.

[264] Murakami, N., I zumi, J., Shirakawa, S., *Oxidation of NO to NO_2 in the Flue Gas (11) - Oxidation by Addition of H_2, H_2O_2, CH_2O, CH.* Nenryo Kyokaishi, 1982. 61(329-336).

[265] Hjuler, K., Glarborg, Peter, Dam-Johansen, Kim, *Mutually promoted thermal oxidation of nitric oxide and organic compounds.* Industrial Engineering Chemistry Research, 1995. 34(5): p. 1882-1888.

[266] Chong, J.J., Tsolakis, A., Gill, S.S., Theinnoi, K., Golunski, Stanislaw, E., *Enhancing the NO 2/NOx ratio in compression ignition engines by hydrogen and reformate combustion, for improved aftertreatment performance.* International Journal of Hydrogen Energy, 2010. 35(16): p. 8723-8732.

[267] Wang, W., Herreros, J.M., Tsolakis, A., York, A.P.E., *Increased NO_2 concentration in the diesel engine exhaust for improved Ag/Al_2O_3 catalyst NH_3-SCR activity.* Chemical Engineering Journal, 2015. 270: p. 582-589.

[268] Zhang, H.L., G.K., Boehman, A.L., Haworth, D.C. *Effects of Hydrogen Addition on NOx Emissions in Hydrogen-Assisted Diesel Combustion*. in *International Multidimensional Engine Modeling Users Group Meeting Detroit*. 2009.

[269] Lilik, G.K., Zhang, H., Herreros, J.M., Haworth, D.C. and A.L. Boehman, *Hydrogen assisted diesel combustion.* International Journal of Hydrogen Energy, 2010. 35(9): p. 4382-4398.

[270] Sharma, H., Mhadeshwar, A., *A detailed microkinetic model for diesel engine emissions oxidation on platinum based diesel oxidation catalysts (DOC).* Applied Catalysis B: Environmental, 2012. 127: p. 190-204.

[271] Mudiyanselage, K., Yi, C., Szanyi, J., *Oxygen Coverage Dependence of NO Oxidation on Pt(111).* Journal of Physical Chemistry, 2009. 113: p. 5766-5776.

[272] Tighe, C.J., Twigg, M.V., Hayhurst, A.N., Dennis, J.S., *The kinetics of oxidation of diesel soots by NO*2. Combustion and Flame, 2012. 159(1): p. 77-90.

[273] Liu, S., Wu, X., Weng, D., Li, M., Ran, R., *Roles of acid sites on Pt/H-ZSM5 catalyst in catalytic oxidation of diesel soot.* ACS Catalysis, 2015. 5(2): p. 909-919.

[274] Jiao, P., Li, Z., Shen, B., Zhang, W., Kong, X., Jiang, R., *Research of DPF regeneration with NOx-PM coupled chemical reaction.* Applied Thermal Engineering, 2017. 110: p. 737-745.

[275] Dou, D., *Application of Diesel Oxidation Catalyst and Diesel Particulate Filter for Diesel Engine Powered Non-Road Machines.* Platinum Metals Review, 2012. 56(3): p. 144-154.

[276] Shrivastava, M., Nguyen, A., Zheng, Z., Wu, H.W., Jung, H.S., *Kinetics of soot oxidation by NO2* Environmental Science & Technology, 2010. 44: p. 4796-4801.

[277] Thomas, J.F., Lewis, S.A., Bunting, B.G., Storey, J.M., Graves, R.L., Park, P.W., *Hydrocarbon selective catalytic reduction using a silver-alumina catalyst light alcohols and other reductants.* SAE International Journal, 2005: p. 0148-7191, doi: 10.4271/2005-01-1082.

Appendix A

Appendix A: Diesel Oxidation Catalyst (DOC) Properties

Catalysts can be characterized by two fundamental properties:

- Activity, and
- Selectivity.

Activity relates to the catalyst's ability to enhance reaction rates. If two catalysts influence the rate of the same chemical reaction, the more active catalyst will produce higher reaction rates. Selectivity refers to the catalyst's ability to accelerate certain reactions in preference to others. This behaviour is illustrated by the influence of different catalysts upon the decomposition of ethyl alcohol. In the presence of an activated alumina (Al_2O_3) catalyst, ethylene and water are formed, whereas, with a copper (Cu) catalyst, acetaldehyde and hydrogen predominate

The catalytic converter is composed of three main constituents: the substrate, the washcoat and the catalytic component. The purpose of the substrate is to support and provide a surface area for the coated material. The most commonly used substrate shape is the cylindrical honeycomb monolith, composed of channels running along the length of the component onto which the catalytic material can be coated.

Catalyst Substrates:

The substrate is used to support and provide a surface area for the coated material. The cylindrical honeycomb monolith is the common substrate shape, composed of channels running along the length of the component onto which the catalytic material can be coated.

The catalytic component is responsible for reducing the temperature required for a reaction to take place. Different groups of materials can be found in automotive catalysts: precious metals (such as platinum (Pt), palladium (Pd), rhodium (Rh), iridium (Ir) and ruthenium (Ru)) or base metals (iron (Fe), cobalt (Co), nickel (Ni), silver (Ag) and cupper (Cu)). The choice of catalytic components depends on the nature of the reaction that needs promoting (oxidation or reduction), as different catalytic converters are used for the removal of specific exhaust pollutants.

Monolithic catalyst substrates (Figure A-1) are made of ceramics or metal. Ceramic substrates (honeycombs) usually have square cells, while most metallic substrates have sinusoidal channels. Other channel cross sections are possible, including triangular, hexagonal, trapezoidal and round. The number of cells can vary between 10 and over 1000 cells per square inch (cpsi). Parts that were commercially used for internal combustion engine applications in the 1990s had cell densities between 200 and 600 cpsi. With parts in excess of 1000 cpsi being available for both ceramic and metallic designs. Most substrates for diesel applications remain in the 300-400 cpsi range. Compared to materials used in catalysis, the walls of ceramic honeycombs have large pores and very low specific surface areas of about 0.3 m^2/g. Foils used for metal substrates have no porosity.

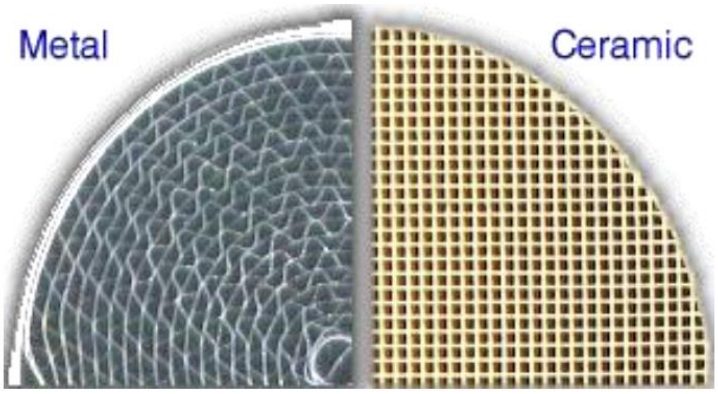

Figure A-1: Monolithic Catalyst Substrates

That coating, called the washcoat, is composed of porous, high surface area inorganic oxides such as gamma-Al_2O_3. The washcoat layer on a metallic foil and on a ceramic substrate is illustrated in Figure A-2. The thickness of the washcoat layer is 20-40 µm. Much thicker washcoat deposits ("fillets") are formed in the cell corners, especially in the sinusoidal channels of metallic substrates. In some technologies, the metal foil is washcoated prior to forming the honeycomb. These technologies produce clean channels with no fillets in the corners but tend to compromise the mechanical strength and durability of the substrate. The washcoat can increase the catalyst heating time by as much as 40% compared to an uncoated support.

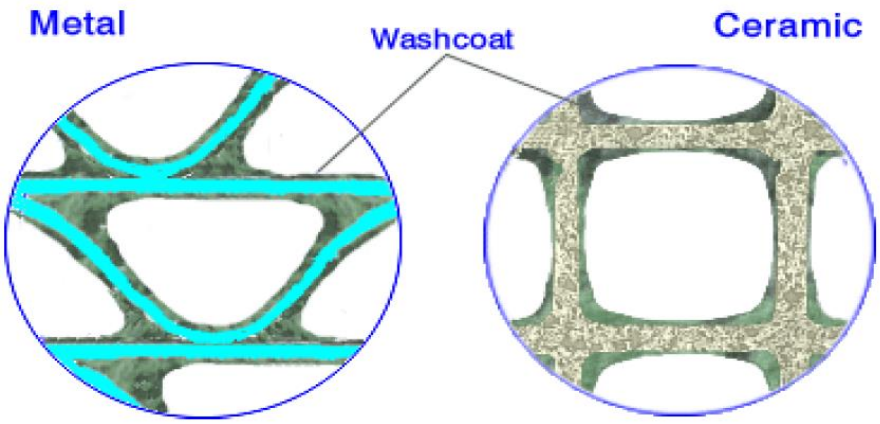

Figure A-2: Catalyst Washcoat

Appendix B

Appendix B: Measuring Equipment Technical Data

The data collected in this thesis is accurate and also the accuracy of the main components of the engine test rig and equipment that used for emissions measurements have been collected from the relevant manufacturer instruction manuals. Regarding to the gaseous emissions, the MultiGas Analyser (FTIR) was used to analyse these emissions were accurate to within ± 1% as shown in Table B-1. The SMPS system was used to measure the PM emission. The condensing particle counter (CPC 3775) had a particle count accuracy of ±20% for particle concentration lager than $5x10^4$ while ±10% for particle concentration lower than $5x10^4$ particles/cm^3 but smaller than $1x10^7$ particles/cm^3.

Table B-1: Measurements Specifications for MultiGas Analyser (FTIR)

Specification	Comment
Gas Analyser	MKS MG-2030
Measurement Technique	FT-IR Spectroscopy
Range	Concentrations between high ppb and 100% full scale
Spectral Resolution	0.5-128cm^{-1}
Scan Time/ Speed	1-300sec / 1 scans per sec @ 0.5cm^{-1}
Gas Cell	MKS 5.11 Meter fixed path length heated cell
Detector	Infrared Analysis 0.25mm Liquid Nitrogen cooled MCT, digitally linearised
Pressure Transducer	± 1% uncertainty

Table B-2: Technical data for the SMPS

Specification	Value
Particle Type	Solids and non-volatile liquids
Particle size range	10 – 1000 nm
Maximum input concentration	10^8 particles/cm^3 at 10 nm
Voltage	10 – 10000 VDC
Sheath Flow Rate	6.00 L/min
Aerosol Flow Rate	0.60 L/min
Time Measurement	120 Sec

Appendix C

Appendix C: HIGH-RESOLUTION TEM (HR-TEM) IMAGES

Table C-1: TEM Images from Different Fuels

Fuels	TEM Imaged Soot Agglomerates
Diesel Fuel (ULSD)[†]	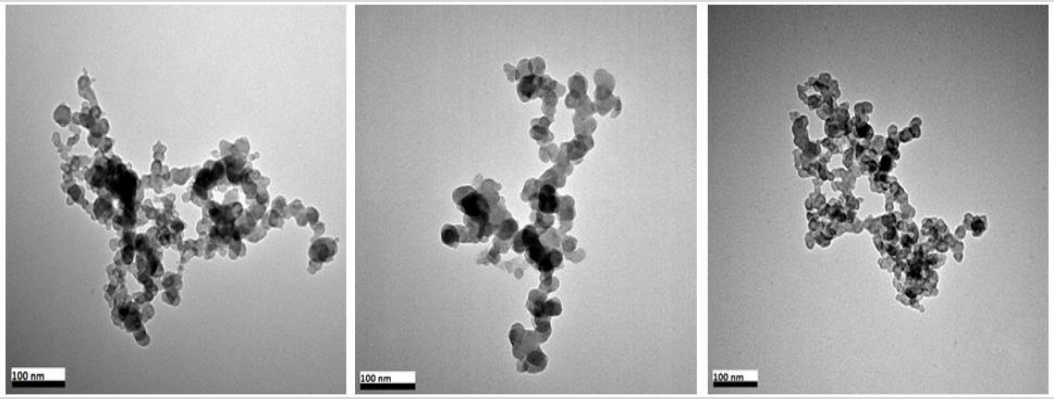
Biodiesel (RME)[†]	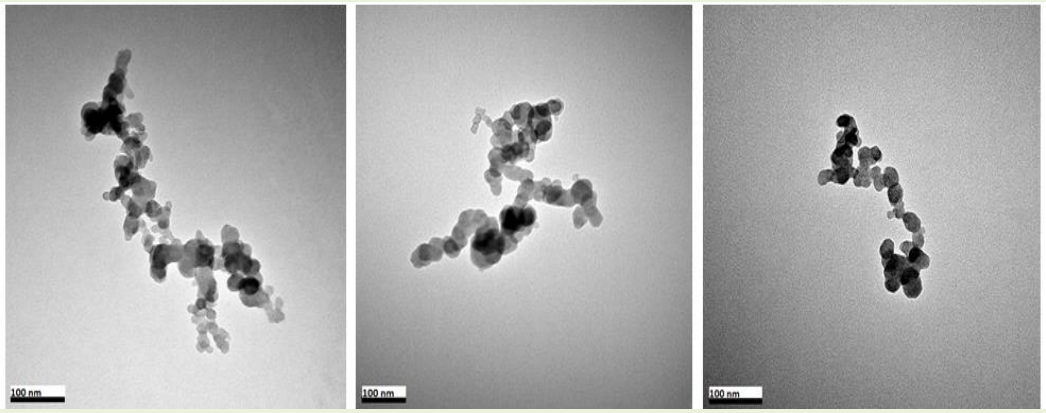

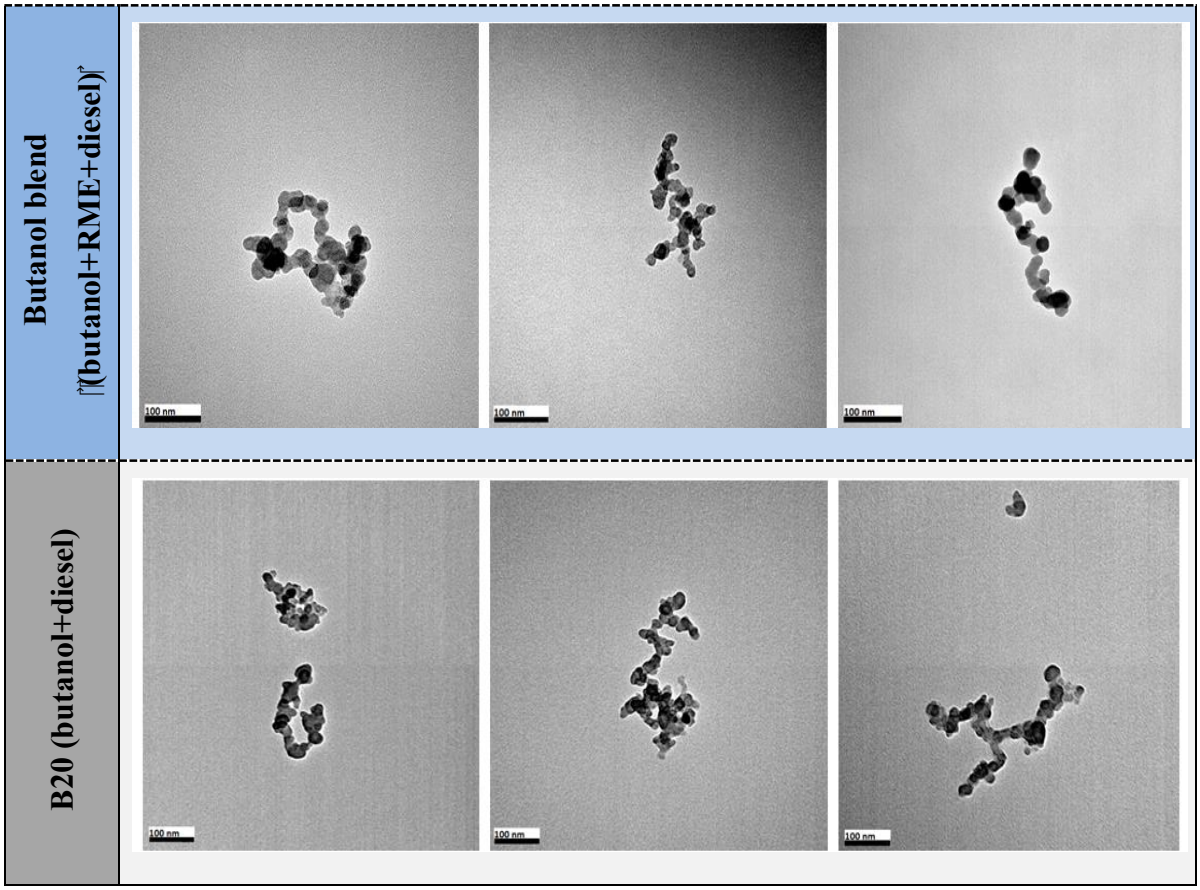

Table C-2: TEM Images with high resolution from Different Fuels

Fuels	TEM Imaged Soot Agglomerates With High Resolution
Diesel Fuel (ULSD)	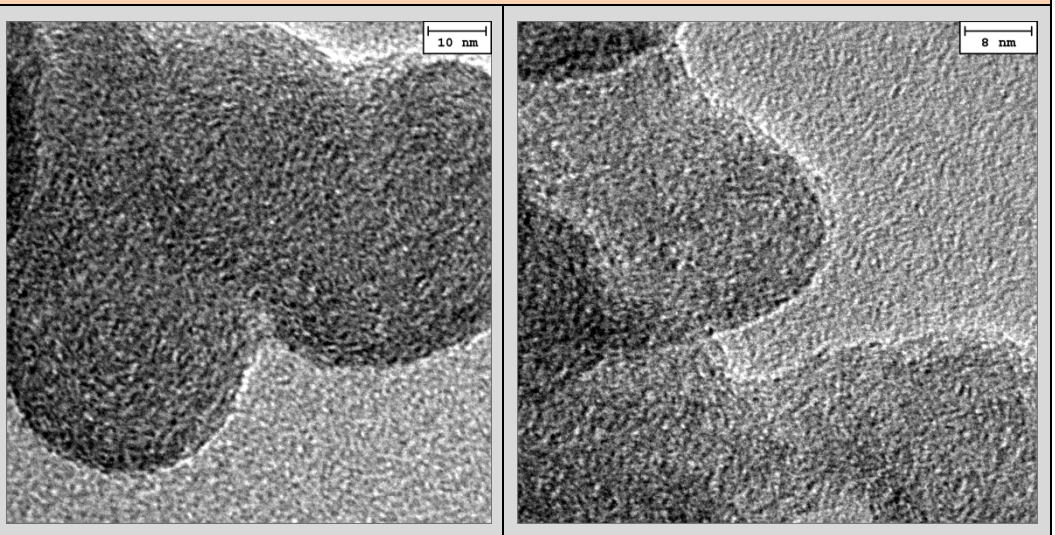

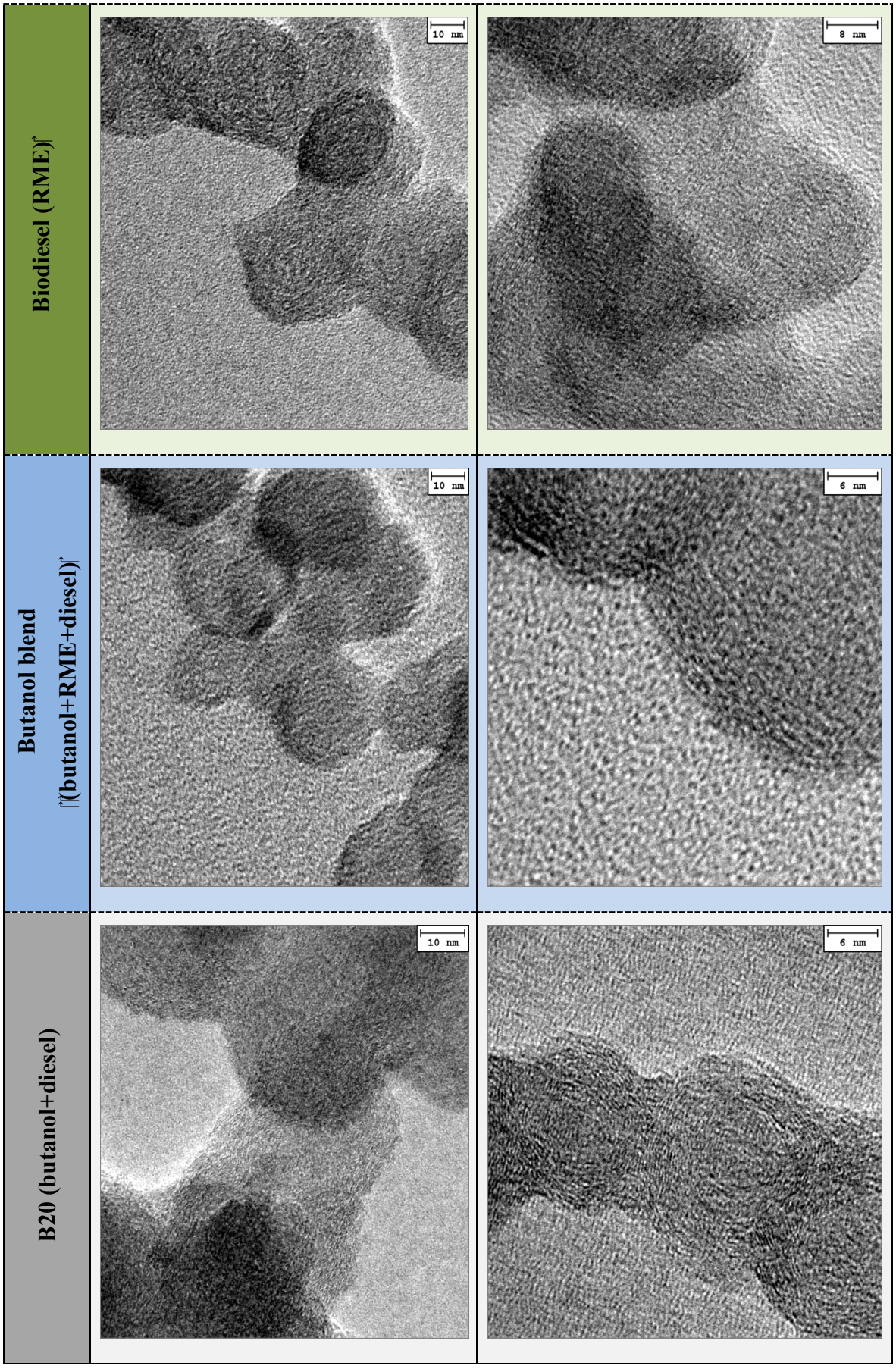
Biodiesel (RME)
Butanol blend
(butanol+RME+diesel)
B20 (butanol+diesel)
10 nm
8 nm
10 nm
6 nm
10 nm
6 nm